

**DEVELOPMENT OF ANALYTICAL
RELATIONSHIPS AND CRITERIA FOR
BLAST AND FIRE VULNERABILITY
OF
FALLOUT SHELTER OCCUPANTS**

Final Report

Contract No. DAHC20-67-C-0147
OCD Work Unit 1614B

October 1, 1968

Each transmittal of this document outside the agencies of the U. S. Government must have prior approval of THE OFFICE OF THE SECRETARY OF THE ARMY, OFFICE OF CIVIL DEFENSE, RESEARCH, The Pentagon, Washington, D. C. 20310

System Sciences

INCORPORATED



SYSTEM SCIENCES, INCORPORATED

4720 Montgomery Lane
Bethesda, Maryland 20014

DEVELOPMENT OF ANALYTICAL RELATIONSHIPS AND CRITERIA
FOR BLAST AND FIRE VULNERABILITY OF FALLOUT SHELTER
OCCUPANTS

Final Report

Contract No. DAHC20-67-C-0147

OCD Work Unit 1614B

by

J.W. Crowley, R.M. Hogue, H.J. Avise, E.H. Smith, W.G. Hiner

for
Office of Civil Defense
Office of the Secretary of the Army
Washington, D. C. 20310

October 1, 1968

OCD Review Notice

This report has been reviewed in the Office of Civil Defense and approved for publication. Approval does not signify that the contents necessarily reflect the views and policies of the Office of Civil Defense.

Each transmittal of this document outside the agencies of the U.S. Government must have prior approval of THE OFFICE OF THE SECRETARY OF THE ARMY, OFFICE OF CIVIL DEFENSE, RESEARCH, The Pentagon, Washington, D. C. 20310

ABSTRACT

The objective of this study is the development of improved methods and criteria for estimating blast casualties and for handling nuclear fire effects in order to determine means for improving survivability and injury avoidance for shelter occupants. The urban fire analysis model, FIREFLY, was developed to provide an automated method for assessing the potential damage to shelter buildings from fires which occur as a result of ignition from the thermal pulse of a nuclear weapon or fire spread from nearby buildings. Two promising approaches for classification of urban environments with regard to potential fire susceptibility were developed. Upon the basis of blast vulnerability analyses of structures including interior floors, walls and partitions, a set of blast fatality functions was produced which may be used to determine the survivability of personnel in shelters in various locations within three principal types of structures. Trial applications of improved methods and criteria served as a pilot sensitivity analysis for future shelter systems vulnerability analyses.

SYSTEM SCIENCES, INCORPORATED

4720 Montgomery Lane
Bethesda, Maryland 20014

SUMMARY
OF
RESEARCH REPORT

DEVELOPMENT OF ANALYTICAL RELATIONSHIPS AND CRITERIA
FOR BLAST AND FIRE VULNERABILITY OF FALLOUT SHELTER
OCCUPANTS

Final Report

Contract No. DAHC20-67-C-0147

OCD Work Unit 1614B

by

J.W. Crowley, R.M. Hogue, H.J. Avise, E.H. Smith, W.G. Hiner

for
Office of Civil Defense
Office of the Secretary of the Army
Washington, D. C. 20310

October 1, 1968

OCD Review Notice

This report has been reviewed in the Office of Civil Defense and approved for publication. Approval does not signify that the contents necessarily reflect the views and policies of the Office of Civil Defense.

Each transmittal of this document outside the agencies of the U.S. Government must have prior approval of THE OFFICE OF THE SECRETARY OF THE ARMY, OFFICE OF CIVIL DEFENSE, RESEARCH, The Pentagon, Washington, D. C. 20310

SUMMARY

DEVELOPMENT OF ANALYTICAL RELATIONSHIPS AND CRITERIA FOR BLAST AND FIRE VULNERABILITY OF FALLOUT SHELTER OCCUPANTS

The objective of this study is the development of improved methods and criteria for estimating blast casualties and for handling nuclear fire effects in order to determine means of improving survivability and injury avoidance for shelter occupants. The study produced the following results:

URBAN FIRE ANALYSIS MODEL

The urban fire analysis model, FIREFLY, has been developed to provide an automated method for assessing the potential damage to shelter buildings from fires which occur as a result of ignition from the thermal pulse of a nuclear weapon or fire spread from nearby buildings. The model considers a wide range of variables which may be modified as desired. These include:

- The degree of external shielding from thermal radiation as a function of physical environment; range from radiating source; weapon yield and height of burst; floor levels in building, the area of window openings and degree of window shading
- Fuel loadings for ignition and fire spread as a function of occupancy and use

- Specific building types and the separation distance of each building from neighboring buildings
- Meteorological conditions.

Extensive application of FIREFLY for analysis of different classes of urban environment will provide improved data inputs for the OCD DASH System and could provide the basis for an urban nuclear fire effects handbook.

BLAST FATALITY FUNCTIONS

Upon the basis of analyses of blast vulnerability of structures including interior floors, walls and partitions conducted under subcontract by E. H. Smith & Co., Inc., a set of blast fatality functions has been produced which may be used to determine the survivability of personnel in shelters in various locations within three principal types of structures. Table 1 summarizes these blast fatality functions. In addition, the blast fatality functions have been translated into a form suitable for computer assessment of blast effects by the OCD DASH System. These VN codes have been reported separately.

BLAST FATALITY FUNCTIONS

BUILDING TYPE	SHELTER LOCATION		
<p style="text-align: center;">Brick, wood frame not more than 2 stories</p>	<p style="text-align: center;">In above-grade rooms 6-8 psi</p>	<p style="text-align: center;">In basement without a prepared shelter ~ 10 psi</p>	<p style="text-align: center;">In basement with simple but well constructed shelter ~ 15 psi</p>
<p style="text-align: center;">Multistory wall bearing</p>	<p style="text-align: center;">Exposed rooms on above-grade floors (bldg collapse) ~ 7 psi</p>	<p style="text-align: center;">Core rooms on above-grade floors (bldg collapse) ~ 7 psi</p>	<p style="text-align: center;">In basement 15-20 psi</p>
<p style="text-align: center;">Commercial residential multistory steel frame 30-40% window area</p>	<p style="text-align: center;">Exposed rooms above grade 8-11 psi</p>	<p style="text-align: center;">Core rooms or corridor above grade 9-12 psi</p>	<p style="text-align: center;">In basement 20 psi</p>

NOTE: Where a range of psi values is shown, the lower value is associated with lower megaton yields while the high value is associated with lower kiloton yields. Stated values are approximately at the 50% fatality level.

TABLE 1

URBAN ENVIRONMENT CLASSIFICATION SCHEMES

To improve urban fire analysis in detailed assessments of the protection afforded by shelter systems from the hazards of nuclear attack upon the United States such as obtained by OCD's DASH System, relatively simple indices of fire susceptibility are necessary which will, nevertheless, accurately reflect, statistically at least, the probabilities of ignition and fire spread. These probabilities are based upon complicated mechanisms. To calculate them as is accomplished with the FIREFLY model involves myriad data inputs which are obtainable only with considerable effort. In addition, the data from which to derive fire susceptibility indices should be easily obtained and maintained for currency.

Two promising approaches for classification of Standard Location (SL's) were developed. In one approach, four factors relative to housing are averaged to obtain an index of potential fire susceptibility. For the total number of houses in an SL, the percent built before a given year, the percent deteriorating and dilapidated, the percent that are multi-family and the percent which are less than \$10,000 in value are the indicators utilized.

In the second approach, SL's are characterized by both population per square mile and the percentage of total housing units that are one-unit structures. In applications of this approach, SL's were found to group according to their basic class, e.g., single-family residential, multi-family residential, central business district and livelihood, suburbanizing, or nonurban. Experience to be gained from future applications of FIREFLY assessments may indicate the need for further subdivision of

these urban environment classes.

TRIAL APPLICATION OF IMPROVED METHODS AND CRITERIA

Using the existing shelter system of Peoria, Illinois, as the subject for comprehensive study, several analyses of the survivability of that city's projected 1975 population were conducted. These served to demonstrate the urban fire analysis model, FIREFLY, and the refined blast fatality functions. The relative value in terms of survivability of various alternative systems which might be projected for the subject shelter system was determined. Thus, the trial applications of improved methods and criteria served as a pilot demonstration for future shelter systems vulnerability analyses. Such analyses will be of great benefit in determining means of improving survivability and injury avoidance for shelter occupants.

TABLE OF CONTENTS

	<u>Page</u>
I. SHELTER SYSTEMS VULNERABILITY ANALYSIS	1
A. OBJECTIVE	1
B. APPROACH	1
1. Background	1
2. Requirements	3
C. ANALYTICAL EFFORTS	4
1. Fire Effects	4
2. Blast Effects	6
3. Combined Effects	6
4. Classification of Urban Environments	6
5. Classification of Shelter Facilities	7
II. HANDLING OF FIRE EFFECTS	8
A. NUCLEAR FIRE PHENOMENOLOGY	9
B. IGNITION OF INTERIOR FURNISHINGS	13
1. Criteria for Ignition	14
2. Probability of Ignition of Furnishings	20
C. ROOM IGNITION	24
1. Furniture Density	24
2. Probability of Ignition of an Exposed Room	25
3. Shielding by Nearby Structures	30
D. FIRE SPREAD WITHIN BUILDINGS	34
E. FIRE SPREAD THROUGH URBAN AREAS: The FIREFLY Model	49
F. SYNTHESIS AND APPLICATION	58
III. BLAST VULNERABILITY	63
A. BLAST CASUALTY PHENOMENOLOGY	63
B. LOADING OF BUILDINGS BY THE BLAST WAVE	66
1. Loading of the Front Face	66
2. Loading on the Side Walls and Roof	66
3. Loading on the Rear	66
4. Pressure Buildup Inside a Building	67
5. Computation of Building Loading	68

	<u>Page</u>
C. ANALYTICAL PROCEDURES	68
1. Dynamic Response of a Building When Treated as an Elastic Beam	69
2. Deflection of a Beam under Static Load	77
3. The Rayleigh-Ritz Principle	79
4. Simple One-Dimensional Theory of Building Deflection	84
D. COLLAPSE VULNERABILITY, WALL- BEARING BUILDINGS	86
1. Structural Characteristics of Wall-Bearing Buildings	86
2. Collapse of a Brick House in Nevada	90
3. Failure of a Multistory Load-Bearing Building	94
4. Some General Considerations on Load-Bearing Buildings	99
E. COLLAPSE VULNERABILITY, MULTISTORY FRAMED BUILDINGS	99
1. Column Response	99
2. Calculation of Building Resistance	106
3. Characteristics of a Twenty- Story Steel Frame Building	119
4. Failure of a Twenty-Story Steel Frame Building	122
F. VULNERABILITY OF CURTAIN WALLS AND PARTITIONS	126
1. Introduction	126
2. Static Strength	127
a. Effect of Wall Opening	127
b. Static Strength Data	130
c. FCDA Nevada Test Data	134
3. Response in Tests	139
G. FIRST-FLOOR FAILURE	149
1. Introduction	149
2. Methods	149
3. Structural Analysis Method	150
4. Response of Floor Slabs	151
5. Criteria for Analyzing Response	154
6. Ultimate Concrete Shears	156
7. Assumptions for Analyzing Steel Beam Connections	159
8. Alternate Floor Designs	160
9. Example: Collapse Calculations, R. C.-Framed Floors	162
10. Examples of Collapse Calculations, Steel-Framed Floors	164

	<u>Page</u>
11. Structural Analysis Method	
Results	166
H. SYNTHESIS AND APPLICATION	168
1. Residence Shelters	168
2. Shelters in Multistory Wall-	
Bearing Buildings	169
3. Shelters in Multistory Frame	
Buildings	170
4. Blast Fatality Summary	171
IV. INTERACTIVE AND COMBINED EFFECTS	174
A. INTERACTIVE EFFECTS	174
B. COMBINED EFFECTS	174
C. SUMMARY	181
V. CLASSIFICATION OF URBAN ENVIRONMENTS	183
A. ANALYSIS OF TWENTY-ONE SELECTED	
STANDARD LOCATIONS	183
1. Types of Data	183
2. Indicators of Potential Fire	
Susceptibility	184
3. Shelter Assessment	184
B. ANALYSIS OF PEORIA URBAN ENVIRONMENTS	184
1. Aim and Approach	184
2. Basic Indicators for	
Classification	187
3. Sources of Data	189
4. Discussion of Urban Classes	191
a. Livelihood	191
b. Residential	192
c. Suburbanizing	193
d. Nonurban	194
VI. TRIAL SHELTER SYSTEM ANALYSES	195
A. RELATIVE EFFECTIVENESS OF VARIOUS	
PEORIA SHELTER SYSTEMS	195
B. FIRE SUSCEPTIBILITY OF PEORIA	197
REFERENCES	202
APPENDICES	204
A. THERMAL PULSE AND ATMOSPHERIC	
TRANSMISSION	204
B. PROBABILITY CHARTS FOR EXPOSED	
ROOM IGNITION	221
C. FIREFLY RESULTS	229
D. BUILDING LOADING	245
DISTRIBUTION LIST	248

LIST OF FIGURES

	<u>Page</u>
1. Quintiles of Critical Ignition Energies - Upholstered Furniture	18
2. Quintiles of Critical Ignition Energies - Beds	19
3. Probability of Ignition - Divans	22
4. Probability of Ignition - Randomly Exposed Furniture Items	23
5. Range for 50% Probability of Sustained Room Ignition - Surface Burst Weapon	27
6. Range for 50% Probability of Sustained Room Ignition - Air Burst Weapon	28
7. Angles of Fireball Elevation vs. Ground Range for Surface Burst Weapons	32
8. Angles of Fireball Elevation vs. Ground Range for Air Burst Weapons	33
9. Expected Window Shielding of Three-Story Apartments by Other Structures	35
10. Expected Window Shielding of One- and Two-Family Dwellings and Small Apartments	36
11. Expected Window Shielding of Tenement Apartments in High Density Residential Areas	37
12. Expected Window Shielding of Commercial/Mercantile Buildings - Lower East Side, New York City	38
13. Expected Window Shielding of Commercial/Mercantile Buildings - Chicago	39
14. Expected Window Shielding of High Rise Apartments - New York City	40
15. The FIREFLY Model	54
16. Building Damage in One FIREFLY Run	55
17. Percentage of Buildings Burned by Thermal Pulse and by Thermal Pulse plus Spread versus Probability of Room Ignition for the Angles of Fireball Elevation Medium Class Residential Areas - Medium Wind	57

	<u>Page</u>
18. Schematic Plan Drawing for a Load-Bearing Structure	88
19. Column Response Schematic for Multistory Framed Buildings	100
20. Distributed Tensile and Compressive Forces on Columns	103
21. Interior Initial and Reflected Overpressure vs. "f", Outside Area Open Fraction	129
22. Critical Shear Stress vs. Ratio of Net Area to Gross Areas	133
23. Probability of Room Ignition with Superimposed Blast Curves--Wood Frame Dwelling	176
24. Probability of Room Ignition with Superimposed Blast Curves--Brick Dwelling	177
25. Probability of Room Ignition with Superimposed Blast Curves--One- and Two-Story Wall-Bearing Commercial.	178
26. Probability of Room Ignition with Superimposed Blast Curves--Multistory Steel Frame Office Building	179
27. Room Ignition Weapon Radius vs. Peak Overpressure - Surface Burst	182
28. Classification of the Urban Environment of Standard Location Areas of Peoria, Illinois	188
29. Map of Urban Environment of Peoria, Illinois	190
30. Aim Points, Peoria Attacks.	199
31. Figure 28 annotated	201
A1. Thermal Energy vs. Slant Range - Air Burst, Visibility <.5 mi.	209
A2. Thermal Energy vs. Slant Range - Air Burst, Visibility 0.6 mi.	210
A3. Thermal Energy vs. Slant Range - Air Burst, Visibility 1.2 mi.	211
A4. Thermal Energy vs. Slant Range - Air Burst, Visibility 3 mi.	212

	<u>Page</u>
A5. Thermal Energy vs. Slant Range - Air Burst, Visibility 6 mi.	213
A6. Thermal Energy vs. Slant Range - Air Burst, Visibility 12 mi.	214
A7. Thermal Energy vs. Slant Range - Surface Burst, Visibility <.5 mi.	215
A8. Thermal Energy vs. Slant Range - Surface Burst, Visibility .6 mi.	216
A9. Thermal Energy vs. Slant Range - Surface Burst, Visibility 1.2 mi.	217
A10. Thermal Energy vs. Slant Range - Surface Burst, Visibility 3 mi.	218
A11. Thermal Energy vs. Slant Range - Surface Burst, Visibility 6 mi.	219
A12. Thermal Energy vs. Slant Range - Surface Burst, Visibility 12 mi.	220
B1. Probability of Room Ignition - Surface Burst, Visibility 12 mi.	222
B2. Probability of Room Ignition - Surface Burst, 1.0 Megaton	223
B3. Probability of Room Ignition - Surface Burst, 10 Megatons.	224
B4. Probability of Room Ignition - Surface Burst, 30 Megatons.	225
B5. Probability of Room Ignition - Air Burst, 1.0 Megaton	226
B6. Probability of Room Ignition - Air Burst, 100 Megatons	227

LIST OF TABLES

	<u>Page</u>
1. Blast Fatality Functions	v, 172
2. Range of Critical Ignition Energies, Megaton Range	15
3. Range of Critical Ignition Energies, 20 KT	17
4. Constants for Determining RIWR for Surprise and Air Burst Weapons	29
5. Occupancy Fire Loading	43
6. Exterior Wall Construction	45
7. Floor Construction	46
8. Height Multipliers	47
9. Roof Construction	48
10. Example Summary of FIREFLY Results	56
11. Elastic Section Modulus Compared to Ultimate Section Modulus for Two Columns	108
12. Column Parameters for a Twenty-Story Building with 100-Foot Depth	115
13. Static Strength of Concrete Masonry and Composite Masonry Walls	132
14. Peak Shear Resistance for Nevada Wall Panel	136
15. Calculated Values of Velocity and Displacement for "c" Panels	140
16. Observed Response, FRONT Wall Panels, Structure 3.29c, 1953 FCDA Tests	142
17. Observed Response, REAR Wall Panels, Structure 3.29c, 1953 FCDA Tests	145
18. Calculated Values of Velocity and Displacement for "a" Panels	147
19. Observed Response, REAR Wall Panels, Structure 3.29a, 1953, FCDA Tests	148
20. Definition of Symbols	152

	<u>Page</u>
21. Collapse Pressures for Concrete Floors	167
22. RIWR Versus Peak Overpressure	180
23. Indicator Characteristics for Potential Fire Susceptibility	185
24. Shelter Assessment	186
25. Percent of Peoria Shelter Facilities Surviving Blast Effects From Various Nuclear Attacks	198
26. Fire Susceptibility of Five Urban Environments	200
A1. Optical Thickness of a Clear Atmosphere	207
A2. Effects of Atmospheric Conditions on Transmittance	208
B1. Standard Deviations (in miles)	228

I. SHELTER SYSTEMS VULNERABILITY ANALYSIS

A. OBJECTIVE

In conjunction with other OCD shelter system research activities, System Sciences, Incorporated, has been performing research on OCD Work Unit 1614B, Development of Analytical Relationships and Criteria for Blast and Fire Vulnerability of Fallout Shelter Occupants. The objective of this work has been to develop improved methods and criteria for estimating blast casualties and for handling nuclear fire effects in order to determine means of improving survivability and injury avoidance for shelter occupants.

B. APPROACH

1. Background

1

The OCD DASH System for providing detailed assessments of the hazards of nuclear attack considers the three principal categories of effects generated in a nuclear weapon explosion which may inflict damage and casualties upon personnel and facilities. These are:

- Prompt effects directly from blast pressures, immediate nuclear radiations, and thermal flash; and indirectly from collapsing buildings, structural components, and debris
- Building fires
- Radioactive fallout.

Initial nuclear radiations and radioactive fallout are beyond the scope of this work.

The DASH System utilizes the blast damage susceptibility classification for structures and personnel developed by physical vulnerability scientists and engineers of the Defense Intelligence Agency (DIA) Produc-

tion Center (formerly, AFIC). It is known as the Vulnerability Numbering (VN) System and is presented in Reference 2. This system and the computational procedures associated with it are completely flexible and able to accommodate additional damage and casualty functions as these are analyzed and determined. Hence, the OCD DASH System is capable of supporting quite sensitive shelter system vulnerability analysis if suitable inputs are available.

Normally, damage assessment systems concerned with weapon systems evaluation employ damage and casualty functions which permit no assumptions regarding the disposition of building occupants. Shelter system analysis, in distinct contrast, is directly concerned with specific dispositions of persons in present or possible future designated shelter space in a specific location within a known type of structure. To enhance the survivability potential of the population, the cost-effectiveness and feasibility of alternative shelter systems must be assessed. Measurement of the relative worth of simple expedients which a warned population might take involve the assumption of definite dispositions in buildings which subsequently sustain varying degrees of damage. The development of analytical relationships and criteria for a whole range of blast vulnerability situations which could then be transformed into appropriate VN's for use by DASH in support of sensitivity analyses of shelter systems constituted an important portion of the effort.

The development of methods for handling nuclear fire effects constituted the second major portion of the research. IITRI, Gage-Babcock,

URS, SRI, and others have done a great deal of developmental and applied work in the field of fire phenomenology. Attempts have been made to specify the parameters which have a bearing on the problem, define some of these parameters in terms of workable expressions, and to construct fire models. No single study, however, appeared to treat the problem in enough detail so that real city blocks under hypothetical attack conditions could be assessed rapidly for all possible conditions of nuclear threat. IITRI's model was by far the most complete attempt at solving the urban fire problem, and Gage-Babcock went furthest in classifying buildings and separation distances. Parts of both methods have been employed in this effort.

2. Requirements

In the blast portion of the study, the vulnerability of fallout shelters located in buildings has been a prime concern. Shelter spaces in upper floors of buildings could be subject to the hazards of curtain wall and partition failures at levels of blast loading insufficient to destroy the building, while at higher levels of blast loading these shelters would be eliminated with the collapse of the building. In addition, collapse of one floor into others from blast loading or rubble is another possible factor. The vulnerability of shelter spaces in the basement in the event of building collapse, or more particularly the possible collapse of the ground floor into the basement, is an important concern.

For that portion of the study devoted to development of methods for handling nuclear fire effects, it was necessary to examine a variety of built-up areas in detail. The development of an ignition model was

required, reflecting the influence of weapon size, height of burst, atmospheric visibility, building configuration, and the frequency and distribution of potential ignition points of various types. Fire spread relationships based upon occupancy types, building density, and type of construction were developed. Monte Carlo procedures for analyzing ignition and fire spread processes were deemed an essential part of this work. Accordingly, a computer model to assess the extent of nuclear fire damage in urbanized areas was developed.

It was necessary to collect considerable data on population housing, and shelter facilities in order to determine the statistical significance of the salient parameters bearing upon the research investigations of blast and fire effects.

C. ANALYTICAL EFFORTS

Within the scope of work, the following tasks were accomplished:

1. Fire Effects

- A review of nuclear fire phenomenology to provide the basis for determining potential ignitions.

- A review of criteria for ignition of interior furnishings and a determination of suitable means for handling critical ignition energy data.

- Analysis of the data available on representative urban areas as provided by the National Fallout Shelter Survey and U. S. Census to determine schemes for utilizing these data in nuclear fire spread assessments.

- Assessments of nuclear fire damage to selected urbanized areas utilizing developed techniques.
- Development of procedures for calculating probabilities of ignition of "standard" items of furniture.
- A determination of reasonable assumed distributions of "standard" items of furniture within rooms.
- The derivation of equations for calculating the probability of individual exposed room ignitions.
- The development of probabilistic schemes for determining the percentage of rooms in different types of buildings that will be shielded from thermal radiation as a function of elevation angle of the fireball and the surrounding environment.
- The derivation of equations for calculating the probability of fire spread within individual buildings of various types and construction. The determination of the range of values or ratings to be assigned for occupancy fire loading and construction of exterior walls, floors, and roofs.
- The development of procedures for calculating the probability of fire jump between buildings for various wind conditions and separation distance.
- The development of a computer model which will provide statistical data on the expected number of buildings destroyed by fire from the thermal pulse of a nuclear weapon and from any subsequent fire spread.

2. Blast Effects

- Analysis of the response of wall-bearing and multistory framed buildings to loading from the blast wave.
- Analysis of the vulnerability of curtain walls and partitions.
- Synthesis of damage and casualty functions and the transformation of the results into VN's suitable for computer assessment of blast effects.
- Analysis of the blast vulnerability of fallout shelters for a given location.

3. Combined Effects

- Analysis of the capabilities of an existing shelter system and possible desirable modifications thereto in terms of the protection afforded the population of the area considering various population postures.
- Analysis to characterize building types and environments into classifications facilitating overall assessments.

4. Classification of Urban Environments

- Analyses of data on selected standard locations.
- Detailed analysis of the data on a selected Standard Metropolitan Statistical Area (SMSA).

5. Classification of Shelter Facilities

- Development and application of an automated process for retrieving data from the National Fallout Shelter Survey Phase I file for analysis of shelter systems.

II. HANDLING OF FIRE EFFECTS

A nuclear attack may initiate building fires which may spread, depending upon a variety of circumstances. The fire aspects of Civil Defense have been elaborated by Strobe and Christian (Ref. 3), and other investigators are active in the field. However, no complete system for predicting nuclear fire initiation and spread has existed. The FLAME⁴ model, which deals with wildlands only, and the DASH model,¹ which applies IITRI data to indicate the fire risk in certain limited types of building blocks, handle part of the problem. A principal obstacle to obtaining a system for predicting urban fire effects has been the magnitude of the tasks of accumulating, analyzing, and classifying data on the real structural world in such a manner that those physical specifications which influence the fire problem can be integrated into an overall system of fire prediction.

The handling of the wide variety of buildings of all sizes, shapes, construction, and distributions presents a formidable problem. Recent strides, however, have been made in classifying buildings, shelters, and block types by IITRI, Gage-Babcock, Factory Mutual, and other OCD⁵ research contractors. A simple methodology has been developed for applying available techniques in a fire spread indexing system.

In succeeding parts of this section, this methodology is further developed and extended. Following a brief summary of nuclear fire phenomenology, an ignition model is derived which reflects the influence of weapon size, height of burst, atmospheric visibility, building configurations, and the frequency and distribution of potential ignition points of various types as derived from ignition surveys of metropolitan areas. Fire spread relationships are developed and applied, based upon

pertinent findings regarding occupancy types, building density, type of construction, and other factors which can be correlated with the structural classification and fire rating work being accomplished by Gage-Babcock, Factory Mutual, IITRI and others mentioned above. A Monte Carlo procedure is described which may be repeatedly applied to both the ignition and fire spread processes. Trial shelter system analyses utilizing this and other procedures are described in Section VI.

A. NUCLEAR FIRE PHENOMENOLOGY

Approximately one-third of the total energy of a nuclear weapon burst on the earth's surface or in the lower atmosphere is in the form of thermal radiations which are generated as a rapid, intense, pulse of heat from the fireball. This emission spectrum of thermal radiation is composed of ultraviolet, visible, and infrared light and is emitted by high-temperature air within the weapon fireball which has been heated to incandescence by the absorption of soft x-rays. The radiation travels outward from the fireball through the atmosphere at the speed of light and spreads over ever-larger areas with increasing distance in all directions, thereby losing intensity. The radiations are also attenuated by the molecules and particles encountered in the atmosphere. The atmospheric transmissivity is related to a quality of the atmosphere known as visibility, an index of the degree of light penetration through the dust, precipitation, fog, low clouds, and other material which impede the passage of light and heat radiations. Although very low visibility (poor penetration) can almost eliminate the nuclear fire hazard on foggy days, the area of potential ignition from a large weapon on a clear day may be substantially greater than the area of important

blast effects.

The height of weapon burst has a significant influence upon the amount of thermal radiation impinging on a potential ignition point. Thermal energies reaching targets at specified ranges from the point of detonation are appreciably less for surface bursts than for air bursts of the same total yield. Among the various phenomena contributing to this effect, absorption by atmosphere and earth is the most predominant.

Radiations from surface bursts traverse the lower strata of the atmosphere where increased air densities, moisture, and dust generally produce greater absorption and scattering than occur at the higher levels traversed by air burst radiations. Generally a fireball which intersects the earth's surface also delivers less thermal radiation to a point on the surface than an air burst because of surface absorption and reflection, obscuration by the dust cloud and geometry. A more detailed discussion of the thermal pulse and atmospheric transmission is contained in Appendix A.

The thermal energy radiated by the fireball that survives the passage through the atmosphere may be of sufficient intensity to ignite combustible material found in urban and rural areas. For the ignition process to occur, the impinging thermal energy must be of sufficient intensity to raise the surface temperature of a cellulosic substance to about 500°C, at which level the irradiated surface and its decomposition gases will generally burst into flame.

The mechanisms of raising the temperature of an object to the point of ignition are quite complex. The absorptive properties of the material,

its bulk and density, moisture content, configuration, and chemical reaction to heat are all important considerations. Generally, dark-colored, thin, low-density objects will be brought to ignition temperature with a lesser total amount of heat energy than would be required to ignite a light-colored, thicker, high-density object. The period of time over which a given amount of heat energy is supplied is especially important because the heat dissipating processes within or over an object have longer time to operate during a longer delivery period. The thermal pulse duration may vary from less than a second for a small yield weapon to more than 30 seconds for a very large weapon. Thus a typical kindling material which may be ignited by 10 cal/cm^2 delivered in a very short pulse from a small weapon may not ignite until 50 cal/cm^2 or more have been delivered over a much longer period by the large weapon. It does not follow, of course, that small weapons constitute a greater fire hazard than larger ones. Since the total thermal energy generated is nearly proportional to weapon yield, a large weapon will cause ignitions at greater distances.

There are a wide variety and substantial numbers of potential ignition points in most built-up areas. Although many of these will be readily ignited by the thermal pulse of a nuclear weapon, a large proportion of such ignitions will not lead to continuing fires. They are not near or in contact with other, heavier combustible material, or they are consumed before the heavier material becomes ignited. This category includes most outdoor ignition points such as loose papers, leaves, litter, and trash piles. Interior furnishings, on the other hand, represent a significant fire threat. These items are upholstered chairs, sofas, beds, rugs,

drapes, and piles of cloth or papers. Critical incident thermal energy required for their ignition ranges from 10 to 60 cal/cm² for most yields. The probability of an interior ignition depends on weapon yield and height of burst, distance of building from the burst point, its orientation to the fireball, the number and size of windows, and the number and distribution of potential ignition points in the room. Ignited interior furnishings are often of such bulk and so distributed that they lead, if uncontrolled, to rapid involvement of all combustibles and flashover of the room.

The blast wave itself may generate some fires by overturning stoves, breaking gas pipes, shorting electric lines, and similar indirect effects. Such secondary fires may occur in regions of significant blast overpressures, but their effects are generally thought to be overshadowed by the blast damage and casualties within the region and by the high frequency of direct fires caused by the thermal pulse and the subsequent spread of fire. However, the effects of these secondary fires on survivors in basement shelters have not been adequately considered. For those cases where the atmospheric visibility may be low, indirect ignitions may be a principal (although limited) source of room fires.

If uncontrolled, an initial room fire in a combustible building will penetrate doors, walls, ceiling, and floor, thus spreading in a series of room-to-room flashovers until the entire building is consumed. The heat generated by a burning building is substantial. Transfer of this energy to the exterior environment is effected by radiation from flames streaming out of windows, openings, and roof; by sparks and flying fire-

brands; and by convection of the heated air and gases. One or more of these heat-transfer mechanisms is involved in spreading fire from a burning building to nearby exposed structures. The fire spread process depends on the size of the flames radiating from the burning building; the speed and direction of the surface wind which may incline the flames toward the exposed structure and transport firebrands and hot gases to it; the orientation of the exposed structure; the number and size of windows and openings; the combustibility of its construction (wood siding, window sash, ignitable roof, combustible contents); and, most important, the separation distance between burning buildings and nearby structures.

Mass fires may occur where there are large numbers of burning buildings in a given area. In this case, the rising columns of flames and hot gases from individual fires may coalesce into a single large column. The intruding surface air prevents the fire storm from spreading outward while creating a furnace-like interior that consumes almost everything combustible within its periphery. If the prevailing winds are of flagration velocity, the mass fire may take the form of a moving configuration, the burning canopy of which may engulf almost everything in its path until it runs out of fuel or the wind changes.

B. IGNITION OF INTERIOR FURNISHINGS

1. Criteria for Ignition

The Critical Ignition Energy (CIE) is the lowest level of thermal energy in calories per square centimeter (or comparable units of measurement) that will cause combustion of a given ignitable substance. Potential ignition points relating to fires in urban residential areas have been limited to beds and deeply upholstered furniture. These

furniture items are large, substantial items in which the thermal radiation will penetrate to such a depth that a subsequent ignition will not be extinguished or "blown out" by the dynamic segment of the blast wave. Also, these items contain enough fuel to provide a source for room flashover in a reasonably short time--10 to 15 minutes.⁶ The items chosen are found in all residential areas, and their physical characteristics and distributions may be reasonably predicted.

⁷
Recent test investigations indicate that CIE's for upholstered items vary greatly with the type of fabric and padding material. An upholstery fabric will generally ignite with less energy when backed by cotton padding than when exposed by itself. Additionally, a state of "glowing" ignition and a smouldering condition which will eventually produce a sustained fire may be induced at an even lower thermal energy level. On the other hand, polyurethane foam padding material requires larger amounts of thermal energy to produce ignition. Foam padding is generally not as susceptible to the glowing or smouldering fire involvement as is cotton. Foam padding tends to decompose at lower radiation intensities than are required to produce sustained fire, and the voluminous smoke and decomposition products cool the fabric surface. There is evidence to indicate that upholstered items of either type will ignite at lower radiation intensities when in contact with more flammable materials, such as newspapers, light cotton materials, etc. The condition of the upholstery itself must be a consideration, worn materials being more apt to split or rupture and thus expose more flammable padding material. Table 2 illustrates the large range of critical ignition energies that may be associated with various upholstery or bedding materials.

TABLE 2

Range of Critical Ignition Energies, Megaton Range

<u>LOMT</u>	<u>Material</u>	<u>100MT</u>
--	White wool--foam padded	136 cal/cm ²
--	Green nylon upholstery--unpadded	120 cal/cm ²
--	Brown nylon upholstery--foam padded	115 cal/cm ²
58 cal/cm ²	Brown nylon upholstery--unpadded	114 cal/cm ²
--	Brown nylon upholstery--cotton padded Rapid fire involvement	112 cal/cm ²
77 cal/cm ²	White wool--unpadded	103 cal/cm ²
--	White wool--cotton padded--rapid fire involvement	96 cal/cm ²
--	Natural burlap--foam padded	87 cal/cm ²
47 cal/cm ²	Natural burlap--unpadded	69 cal/cm ²
--	Natural burlap--cotton padded	66 cal/cm ²
40 cal/cm ²	White tufted bedspread, 84% cotton, 16% rayon	62 cal/cm ²
--	White wool--cotton padded--smouldering fire involvement	59 cal/cm ²
--	Red broadcloth	58 cal/cm ²
28 cal/cm ²	White broadcloth	51 cal/cm ²
--	Brown nylon upholstery--cotton padded-- smouldering fire involvement	44 cal/cm ²
--	Brown nylon--cotton padded--paper covered--rapid fire involvement	44 cal/cm ²
--	Brown nylon--cotton padded--paper covered--possible fire involvement	32 cal/cm ²

Although laboratory test samples such as those shown in Table 2 must be subject to some uncertainty, the existence of a fairly wide range of possible ignition energies centered approximately at 75 cal/cm² for a 100-MT burst seems certain. In the absence of more definitive information, even a gross approximation of a normal distribution seems a better solution than attempting to select one CIE to simulate all materials. However, as the samplings shown in Table 2 result from the thermal pulse durations associated with very large yield weapons, some further brief review of other test results is appropriate.

8

The experiments of Upshot-Knothole illustrate the variance in ignition potential among different furniture materials. A block house furnished with an abundance of cotton-covered upholstered items, some in close proximity to newspapers, burst into flames immediately, and the house was rapidly consumed. A second identical structure with wool pile-covered furnishings, etc., free from newspapers, suffered some ignitions, but the fire spread so slowly that it was readily extinguished an hour after the blast. While these structures represent extreme cases, a vast variety of combinations are possible. Critical ignition energies, 20KT yield, as given by "The Effects of Nuclear Weapons"⁹ and summarized in part in Table 3 seem to place quite adequate numerical limits upon expected ignition ranges for lower yields.

A normal (Gaussian) distribution of critical ignition energies has been arbitrarily selected as a means of giving some reasonable cognizance to variances noted. These distributions, broken into quintiles to expedite further processing, are shown in Figures 1 and 2. It is noted that

TABLE 3

Range of Critical Ignition Energies, 20KT

Cotton chenille bedspread	4 cal/cm ²
Cotton corduroy, brown	6 cal/cm ²
Burlap, heavy woven brown	8 cal/cm ²
Cotton auto seat upholstery	9 cal/cm ²
Cotton sheeting, unbleached	14 cal/cm ²
Cotton tapestry, tight weave	16 cal/cm ²
Wool pile chair upholstery	above 16 cal/cm ²

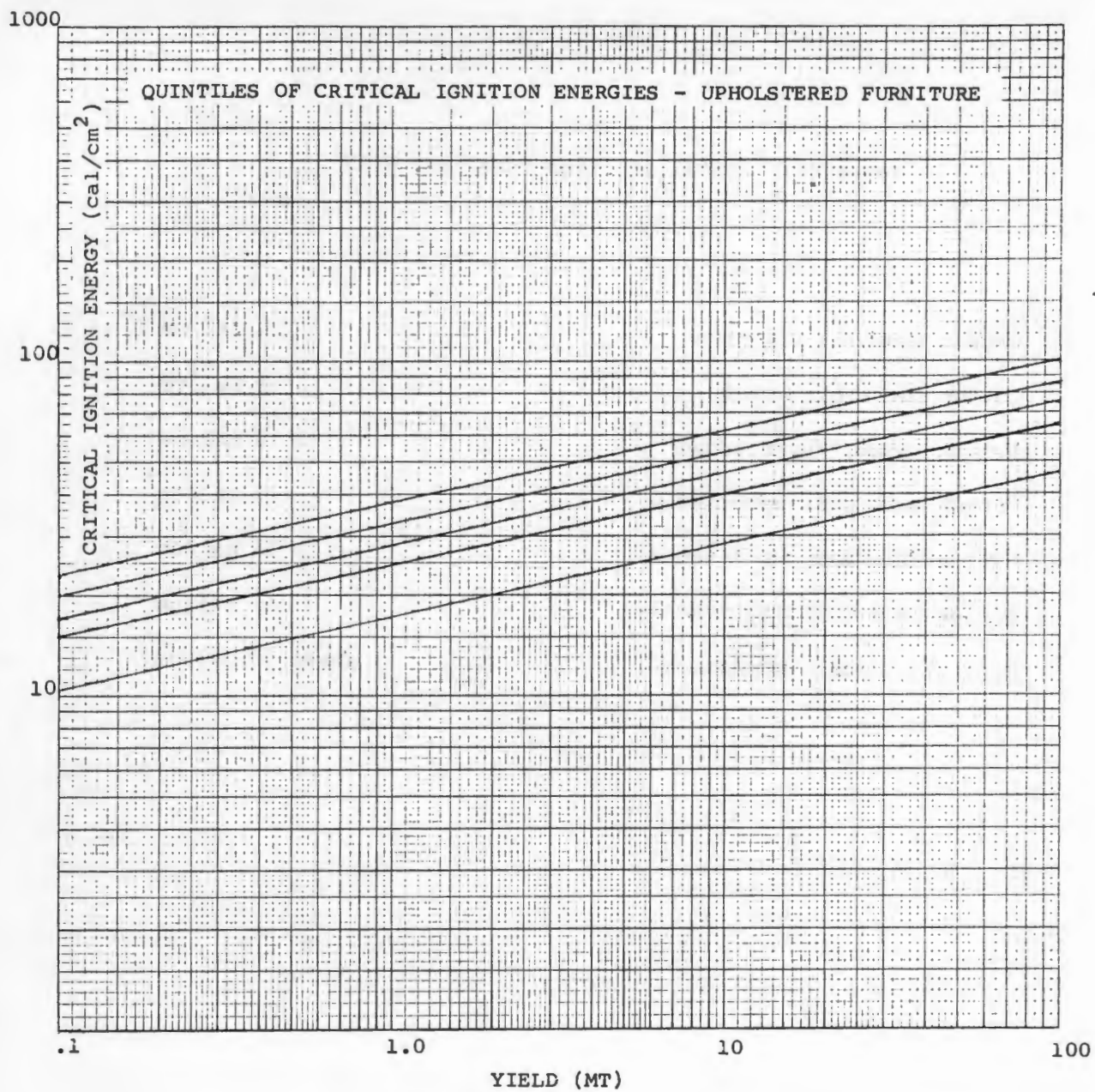


FIGURE 1

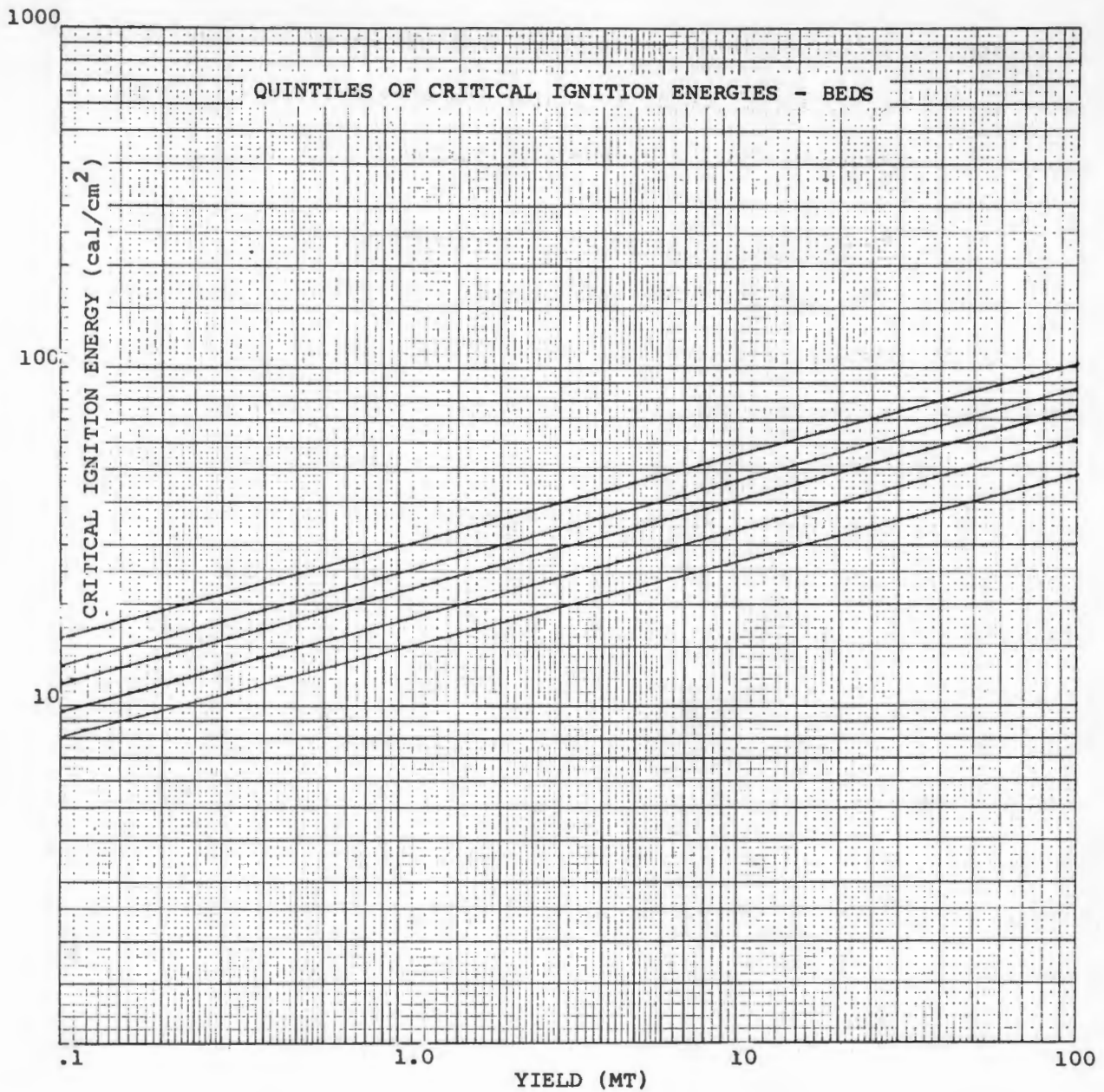


FIGURE 2

the range of values selected encompasses some of the most current estimates in the midranges of yield, excluding the extrapolations to 10MT given by Reference 9, which are generally believed to be too low.

2. Probability of Ignition of Furnishings

The concept of an ignition model described in Reference 6 is used to calculate room ignition* probability, with some modifications made to calculate the fireball diameter and the effective center of the surface burst radiating source. Parameters analyzed include room dimensions, window size, slant range, orientation of the burst (0° to 45°) and CIE for as many different types of furniture items as described. The CIE necessary to create ignitions within a room was multiplied by a factor of 2.0 to account for an overall window glass transmission factor of 0.50. ¹⁰ NASL has experimental data which suggest that the transmission factor may be closer to 0.70 for random selections of window types, angle of orientation and degree of cleanliness although Hoover of Corning Glass is inclined to accept the value of 0.50 as a standard for practical applications.

For any given set of parameters, the ignition model calculates the pattern of irradiation on a plane 2 feet above the floor. Thus at any one range with constant weapon parameters, a family of patterns relating to various critical ignition energies is computed, each individual pattern representing an irradiated "patch" which is produced by the thermal energy.

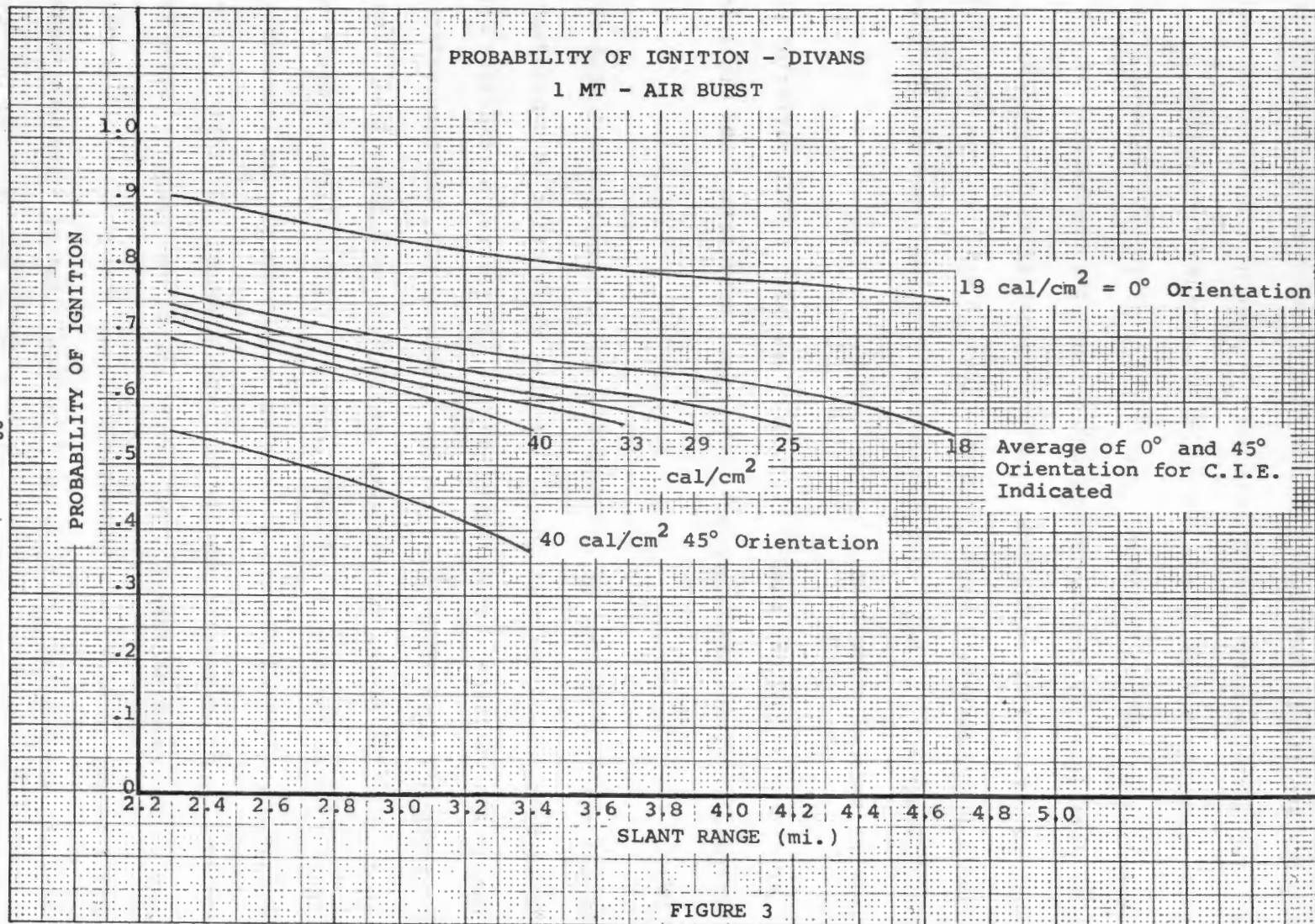
* In all usage, "room ignition" shall be the ignition of items within a room which, if uncontrolled, will be subsequently followed by a buildup to room flashover.

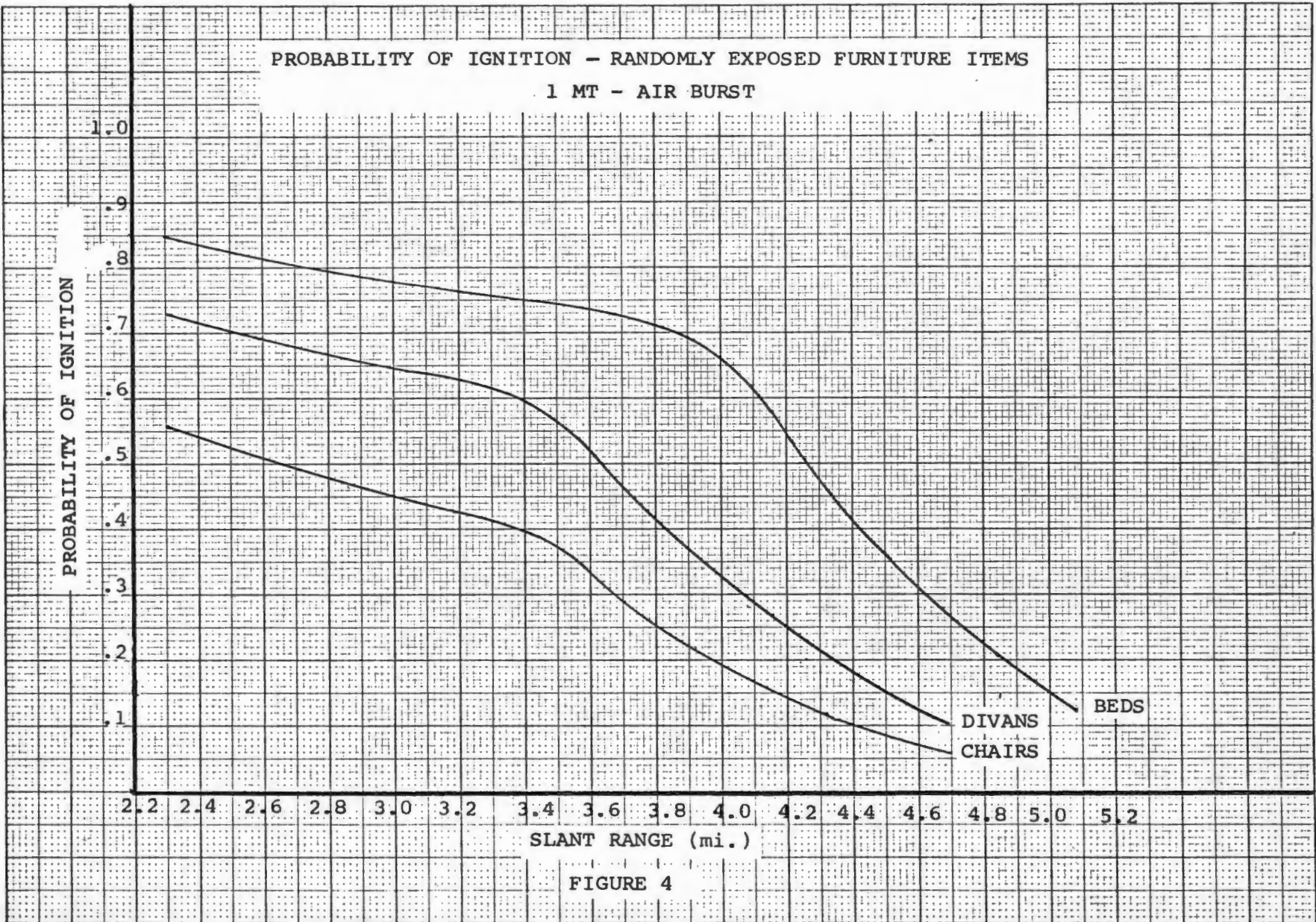
Patterns are larger for lower CIE's as the penumbra effect is considered. For these, another area is calculated--that described by the loci of all possible points of the center of a furniture item placed randomly about within the room. The fraction of this "furniture area" irradiated by the energy "patch" becomes the probability of ignition. With like conditions, then, the probability of igniting a small item which will normally have a low CIE will be less than that for a larger one; a chair will have many more places in which to "hide" from the thermal pulse than a bed will have.

Figure 3 for a 1-MT air burst illustrates the rather wide variation of response for divans which depends upon weapon orientation and CIE selection.

The selection of any one of the possible sets of ignition criteria displayed by Figure 3 would be unrealistically restrictive in consideration of the variance that actually exists. Therefore, a composite curve of Figure 3's five divans, each with a different CIE, has been calculated. Similar curves for beds and chairs have been determined. Thus Figure 4, also for a 1-MT air burst, shows the probability of ignition of randomly selected furniture items at various ranges and introduces the probability of increasing numbers of items becoming vulnerable to ignition as the range decreases. The curves extend the range in which some ignitions may be expected considerably beyond that which would be calculated for any arbitrarily selected "standard" item of furniture because adjustments for the estimated spread of items at the high and low limits have been provided by the Gaussian distribution.

It is necessary to estimate the relative frequency distribution of these items.





C. ROOM IGNITION

1. Furniture Density

An assumption of a Poisson distribution for the random arrangement of all furniture items permits a combined treatment of the various types in computing probability of ignition. This method was employed by the IITRI model.⁶ The convenience of such an assumption is quite obvious since with the establishment of a mean value for each group, the prediction of ignition of any randomly selected grouping from among all 15 items (chairs, divans, and beds--each item duplicated with five different CIE's) is readily calculated as the summation of the mean number of items for each group times the previously computed probability of ignition of a randomly selected item from within the group.

A further brief review of the numerical propriety of assuming a Poisson distribution of furniture articles was conducted. Values of .5, .25, and .5 were tentatively selected as the mean number of chairs, divans, and beds per room, respectively, for an average household, and a three-dimensional matrix was calculated giving the odds of all possible random arrangements according to a Poisson distribution. The most frequent occurrence, 27 percent, was the case of no flammable object in a room. The majority of the other arrangements seemed fairly reasonable although some 5 to 10 percent of the furniture combinations seemed physically improbable. Errors arising from double counting of multiple ignitions in a single room were estimated. Double counting errors which would increase predicted single room ignitions by 10 to 37 percent can occur although the higher increase would never occur outside of very high overpressure ranges.

Calculations of the probability of room ignitions involving double counting should be counteracted to some extent by uncalculated probabilities of ignition of items other than those considered in the sample. Thus, the error should not be appreciable in calculating total probability of room ignitions on the assumption of Poisson distributions. There is the necessity of being somewhat cautious in setting upper limits of mean values, however.

2. Probability of Ignition of an Exposed Room

Values of the probability of room ignition as a function of the random orientation of the mean number of furniture items shown below were established as follows:

Low Density Occupancy: 0.5 persons/room
 .5 chairs, .25 divans, .40 beds/room

Medium Density Occupancy: 0.70 persons/room
 .5 chairs, .25 divans, .40 beds/room

High Density Occupancy: 1.00 or more persons/room
 .5 chairs, .25 divans, .70 beds/room

The expected number of ignitions was calculated using the expression

$$p = \sum_{j=1}^{N_f} M_j P_j \quad (1)$$

where

P = probability of ignition
 in a randomly selected
 room

M_j = the mean number of furni-
 ture items of the j th type

P_j = the probability of ignition
 of a furniture item of the
 j th type

N_f = the number of furniture
 types.

The potential room ignition rates are based on a clear atmosphere.

The calculations using equation (1) may be presented in a form such as Figures 5 and 6 which show the room ignition weapon radius (RIWR) for 50 percent probability of exposed room ignition as a function of weapon yield, height of burst, and atmospheric visibility. The RIWR (in miles) may be given by the general expression

$$\text{RIWR} = a \left(\frac{W}{0.1} \right)^b \quad (2)$$

where W is in megatons and a and b are constants which depend upon visibility and height of burst (surface or 640-foot scaled). Values for a and b are given in Table 4 for both surface and air bursts.

Graphs of the probability of exposed room ignition for various visibilities are shown in Appendix B.

The probability of room ignition, p, is

$$p = \Phi \left(\frac{\text{RIWR} - d}{\sigma} \right) \quad (3)$$

where

d = distance in miles

Φ = standard cumulative normal function.

Values for p in Appendix B and in Figures 5 and 6 have been derived assuming a range of typical interior furnishings for occupancy of 0.7 persons per room. Data from the National Resource Analysis Center (NRAC) housing files provide room occupancy data for each Standard

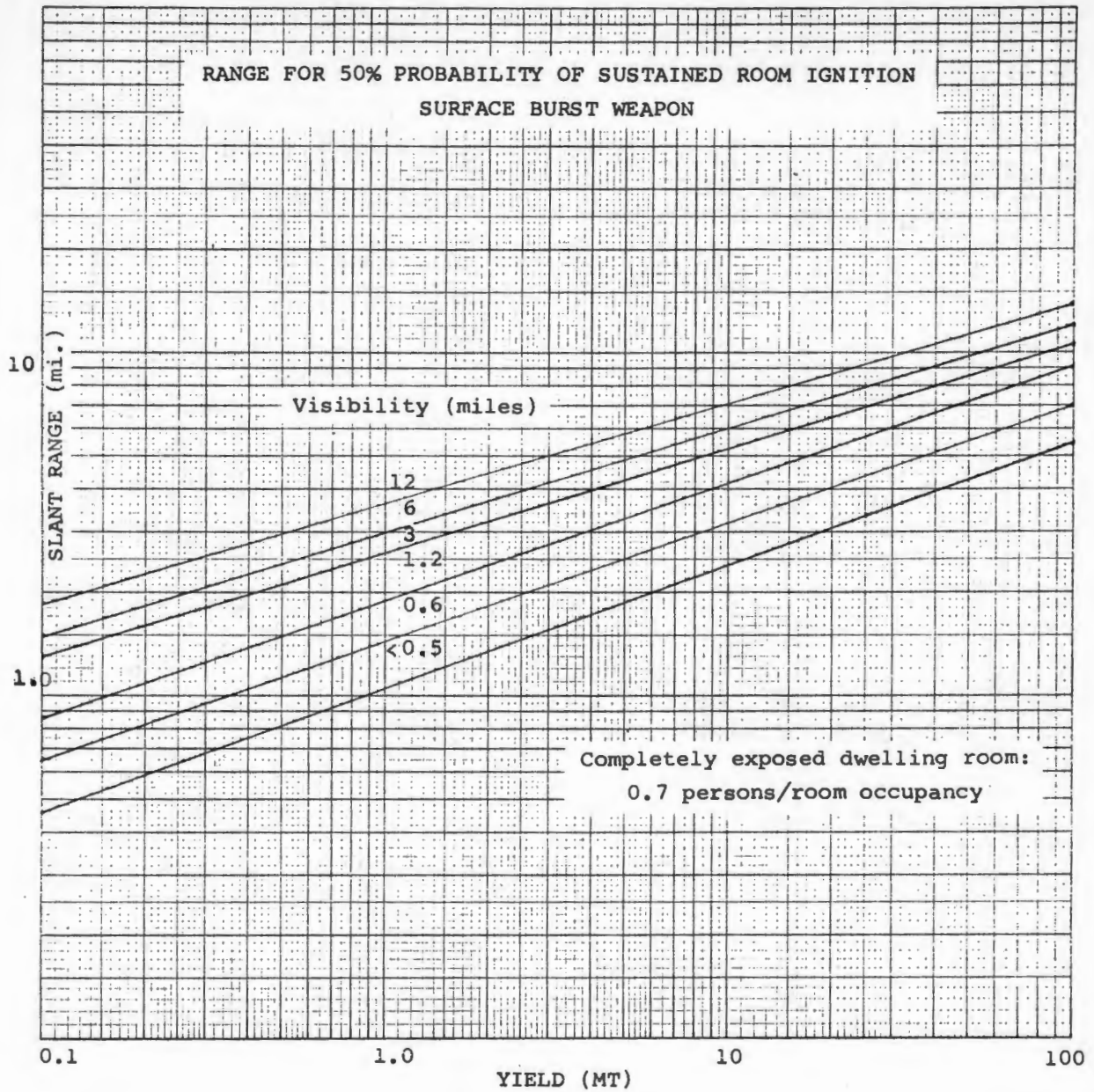


FIGURE 5

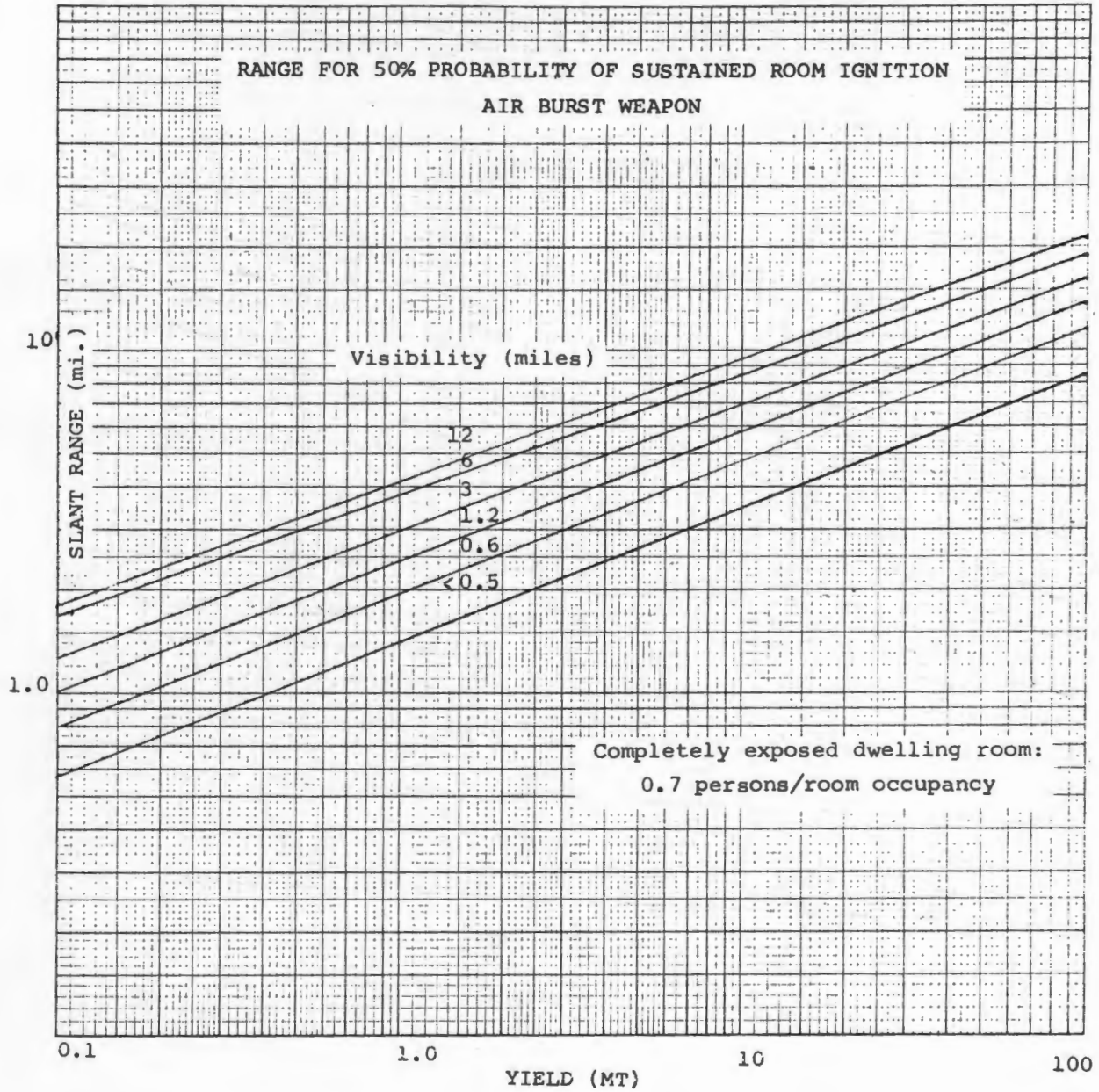


FIGURE 6

TABLE 4

CONSTANTS FOR DETERMINING RIWR

SURFACE BURST WEAPONS

Visibility (mi.)	<u>a</u>	<u>b</u>
< 0.5	0.45	0.362
0.6	0.63	0.349
1.2	0.88	0.335
3.0	1.22	0.307
6.0	1.48	0.297
12.0	1.80	0.286

AIR BURST WEAPONS

Visibility (mi.)	<u>a</u>	<u>b</u>
< 0.5	0.58	0.387
0.6	0.80	0.387
1.2	1.01	0.387
3.0	1.28	0.366
6.0	1.62	0.355
12.0	1.82	0.354

Location (SL). For other room occupancies, p may be adjusted to higher or lower values; p_n will be defined as this adjusted probability and defined as this adjusted probability and

$$p_n = \left[1.0 + \left(\frac{\text{persons/room} - 0.7}{0.2} \right) (0.232 - 0.108p) \right] p. \quad (4)$$

The value of p_n cannot, of course, exceed 1.0.

It is to be noted that the foregoing equations represent analytical derivations from a sampling of more than 5000 computer solutions of individual room ignition problems. The range of the samplings were designed to simulate the actual variances which might be expected.

3. Shielding by Nearby Structures

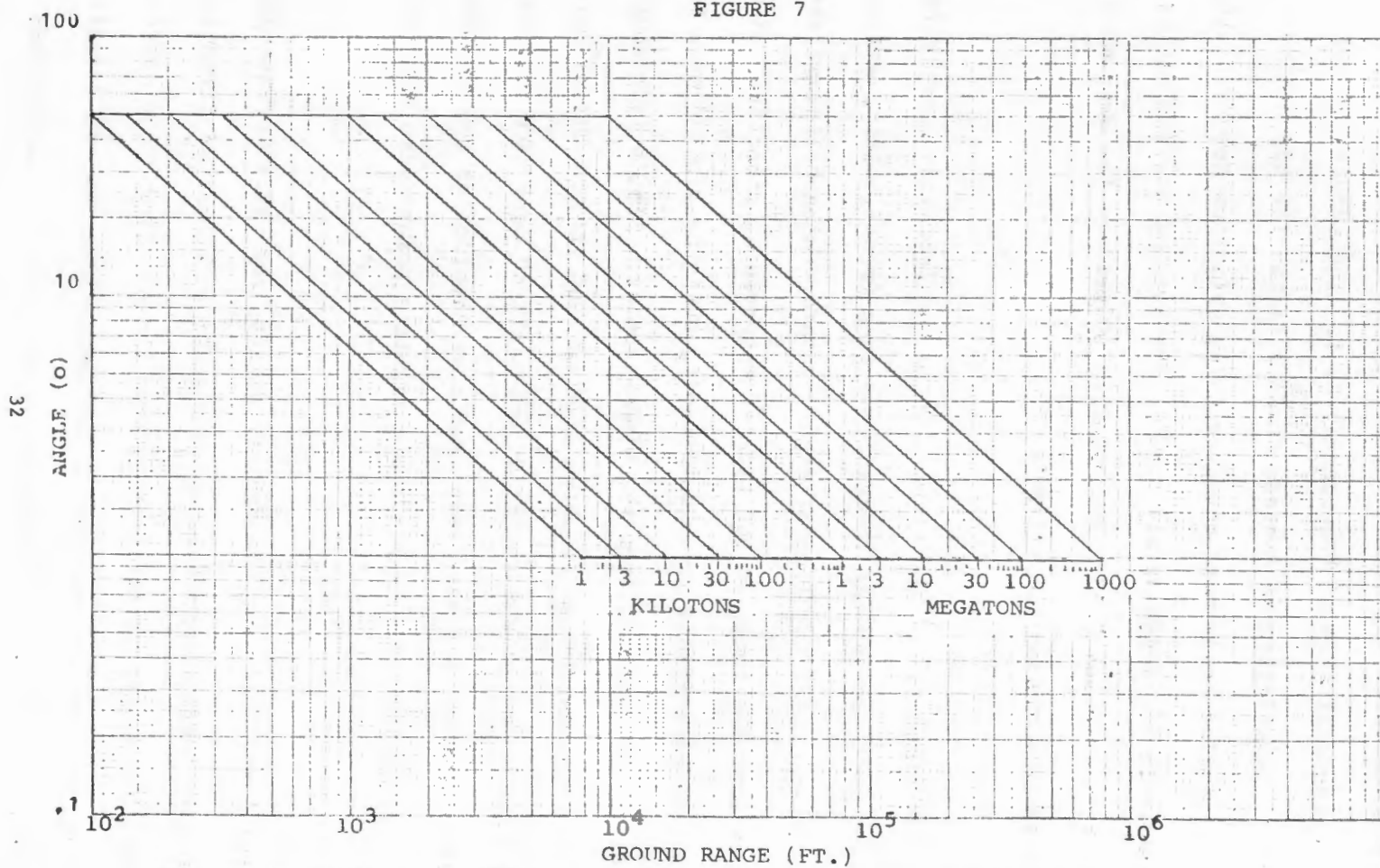
In the preceding paragraphs of this section, the discussion has been developed to the point of the exposed room concept. Such a room may be thought of as being placed on a smooth plane with no physical interference between the source of radiation and the room itself. In actuality, the thermal pulse may be blocked, and flammable objects within a room may safely escape ignition with the presence of such a barrier. These barriers may take the form of hills, trees, window shades, and other structures. It is nearly impossible in a general model to assess the effects of hills and other terrain features since maps that are detailed enough to give actual parameters about buildings themselves (Sanborn maps, for example) do not give elevation data. Also, trees do not appear to pose a significant barrier because of their lack of continuous appearance, sparseness in urban areas, and limited height.

NASL¹⁰ has conducted a survey of window shielding from shades and blinds in the residential area of Providence, R. I. The results of this survey in terms of calculating an average shading factor for 433 windows is 0.514. A similar study was conducted using data from New York City for 332 windows in buildings of all types. The average shading factor in the New York case was 0.55. The value of 50 percent for average shading appears to be a reasonable estimate.

ings. Sightings 45° to the right, 45° to the left and directly forward (0°) were made for several thousand building fronts, sides, and rears. The interception of the line of sight by intervening buildings was noted together with the range to and type of intervening structure. A window was considered shielded if an intervening building blocked more than 50 percent of the fireball from the window center. Simple trigonometric relations between "range at which sighted" and "height difference between sighting point and top of object sighted" were used with various elevation angles to assess each sample as shielded or not shielded. First and subsequently higher story sighting points were processed separately.

Figures 7 and 8 for surface and air bursts, respectively, are graphs which permit easy calculation of the angle of center of fireball elevation as a function of yield and ground range. It will be noted that the area enclosed by the envelope of the family of curves is identical in both figures; the area is shifted to the right for the 640-foot scaled height of burst.

FIGURE 7



ANGLES OF CENTER OF FIREBALL ELEVATION VS. GROUND RANGE FOR SURFACE BURST WEAPONS

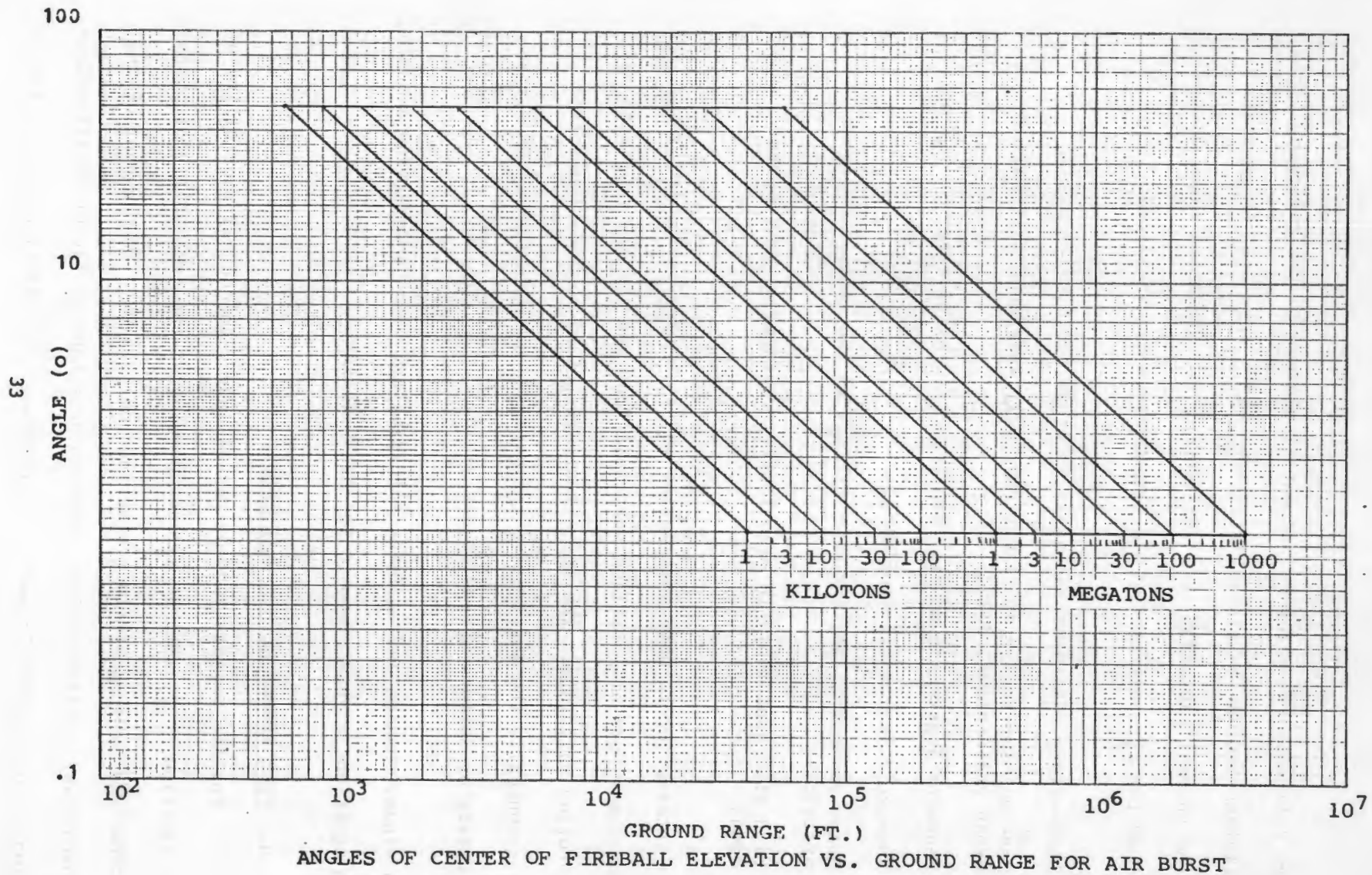


FIGURE 8

Figures 9-14 show the expected percent of windows in the following types of buildings facing the fireball (within $\pm 45^\circ$) that will be shielded from the thermal radiation as a function of the elevation angle of the center of the fireball as derived from Sanborn map samplings:

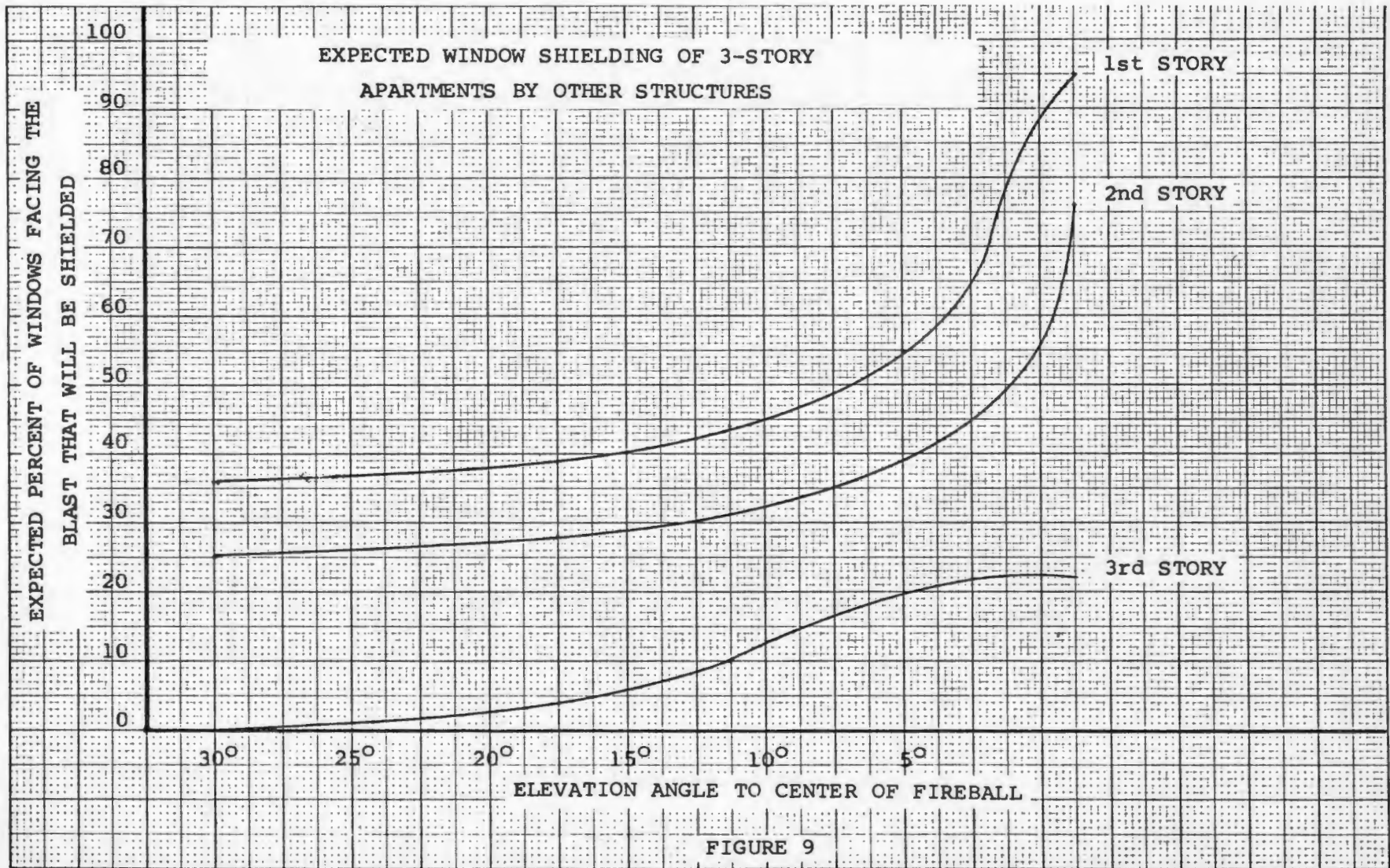
- a. Three-story apartment buildings in urban residential areas
- b. One- and two-family dwellings and small apartment buildings in urban residential areas
- c. Tenement apartments in high density residential areas
- d. Commercial/mercantile buildings
- e. Heavy commercial/mercantile buildings in the central business district
- f. High rise apartments in high density residential development areas.

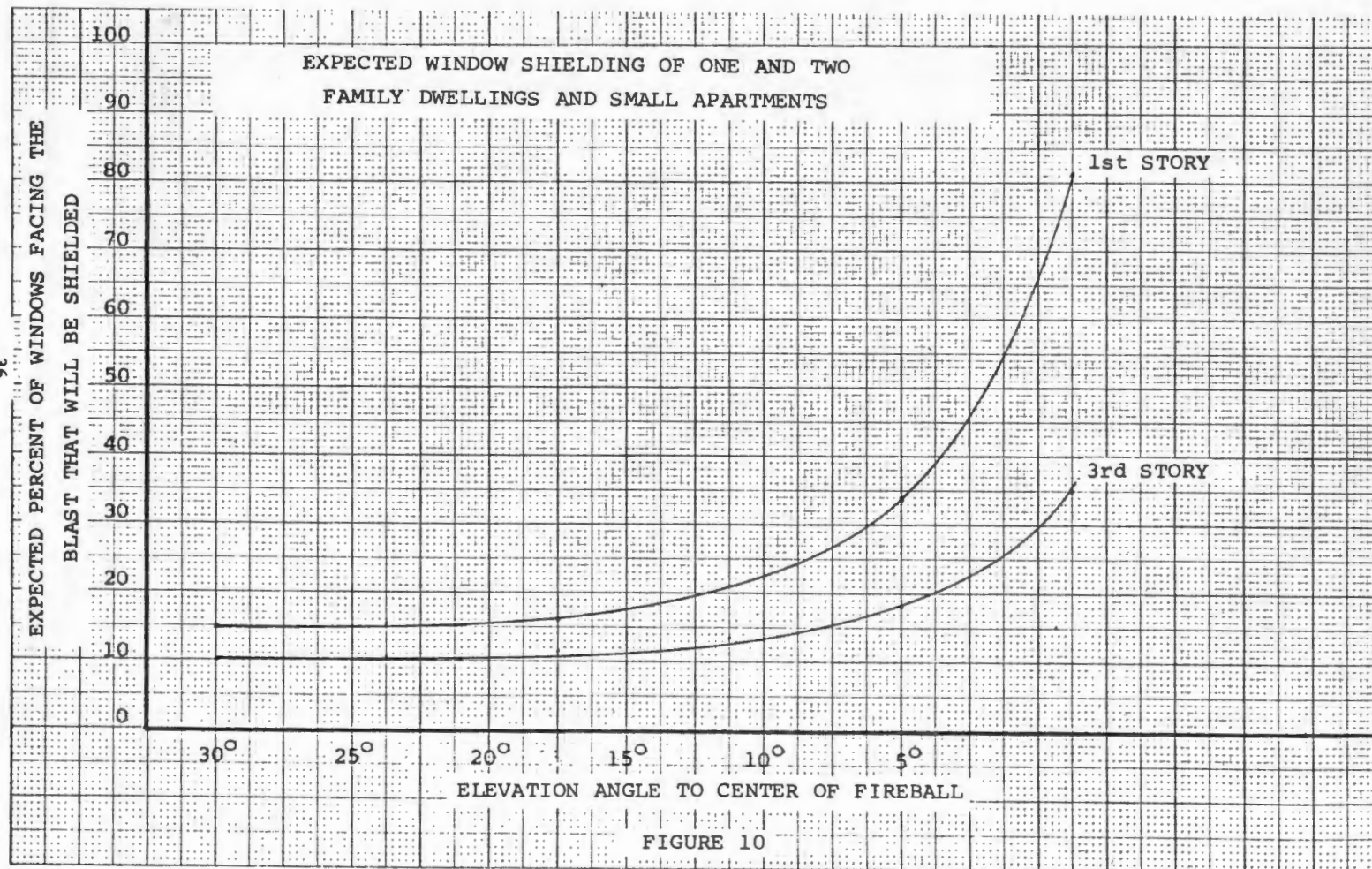
It is interesting to note that in the cases of most taller buildings, the bottom floors are shielded very well from the thermal radiation by neighboring buildings. The approximate ranges of application scales show graphically the sections of the curves applying to 640-foot scaled air bursts or surface bursts of any yield.

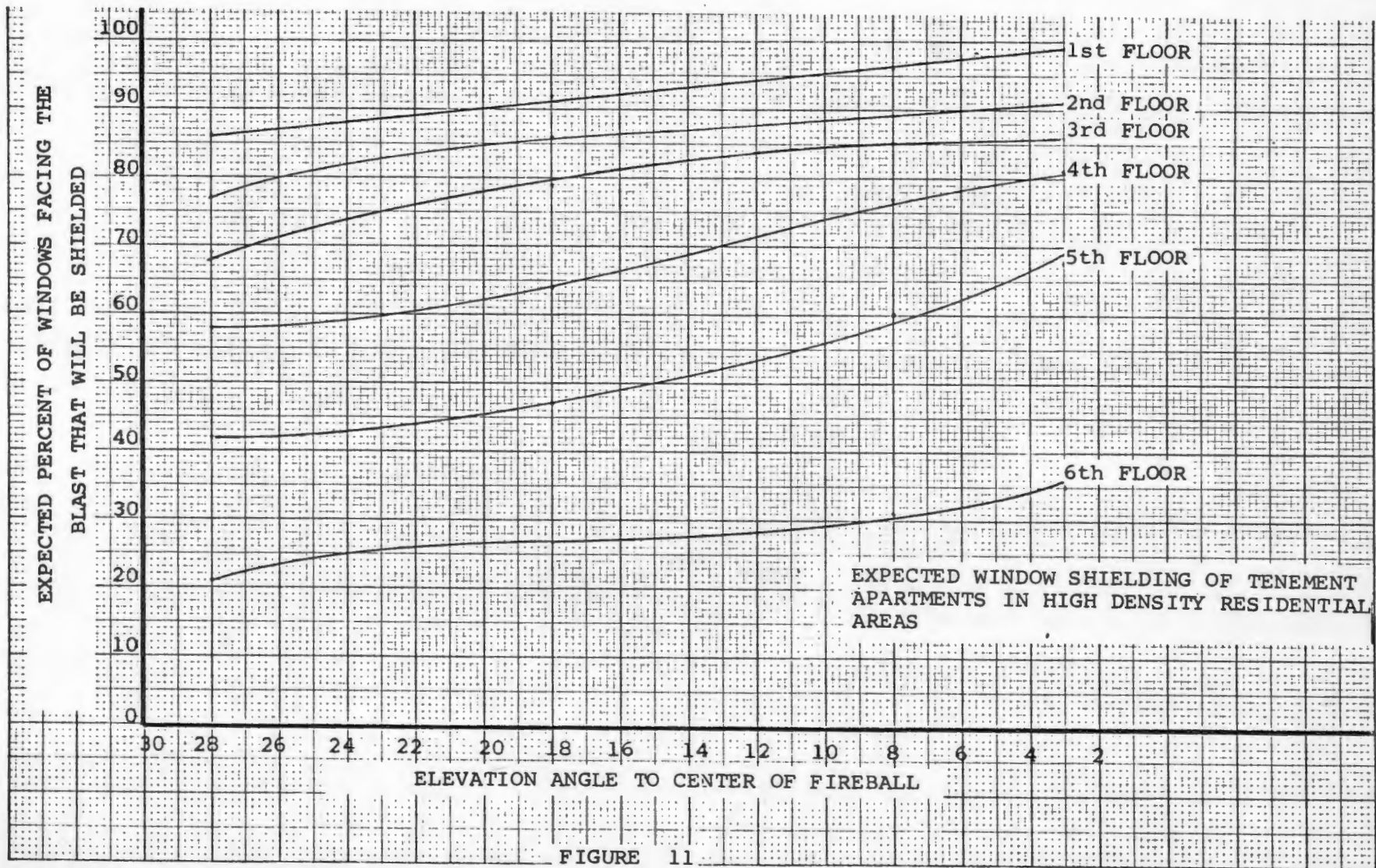
Both window shading and building shielding are used to determine actual room ignitions as explained in the next section.

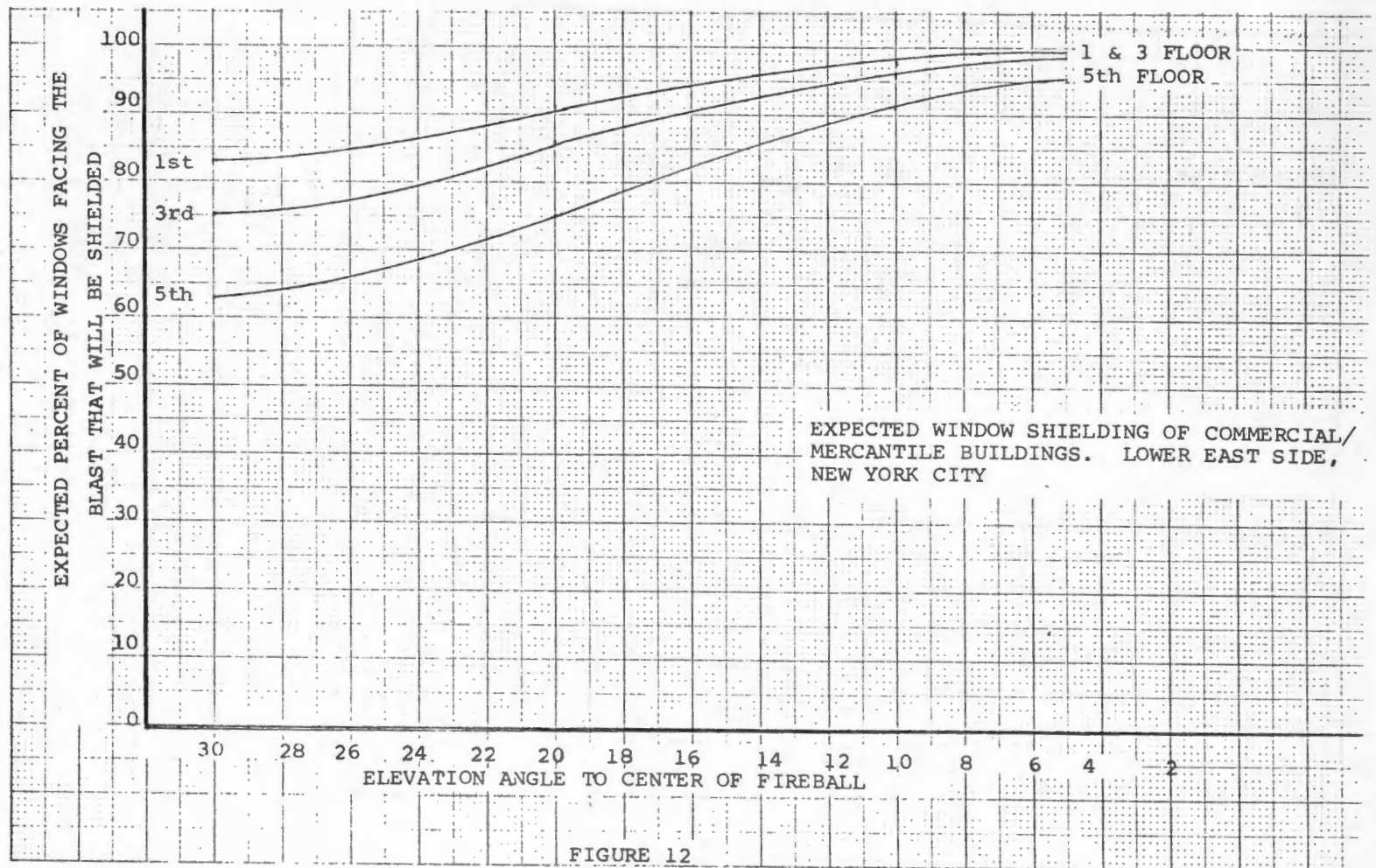
D. FIRE SPREAD WITHIN BUILDINGS

For the reasons just discussed above, the actual probability of room ignition, P_{ri} , will be a reduced value of the probability of exposed room ignition, p_n previously defined on page 30. The concept of the exposed room ignition will be retained as a central factor in all calculations since it will become the springboard for all fire effects calcu-









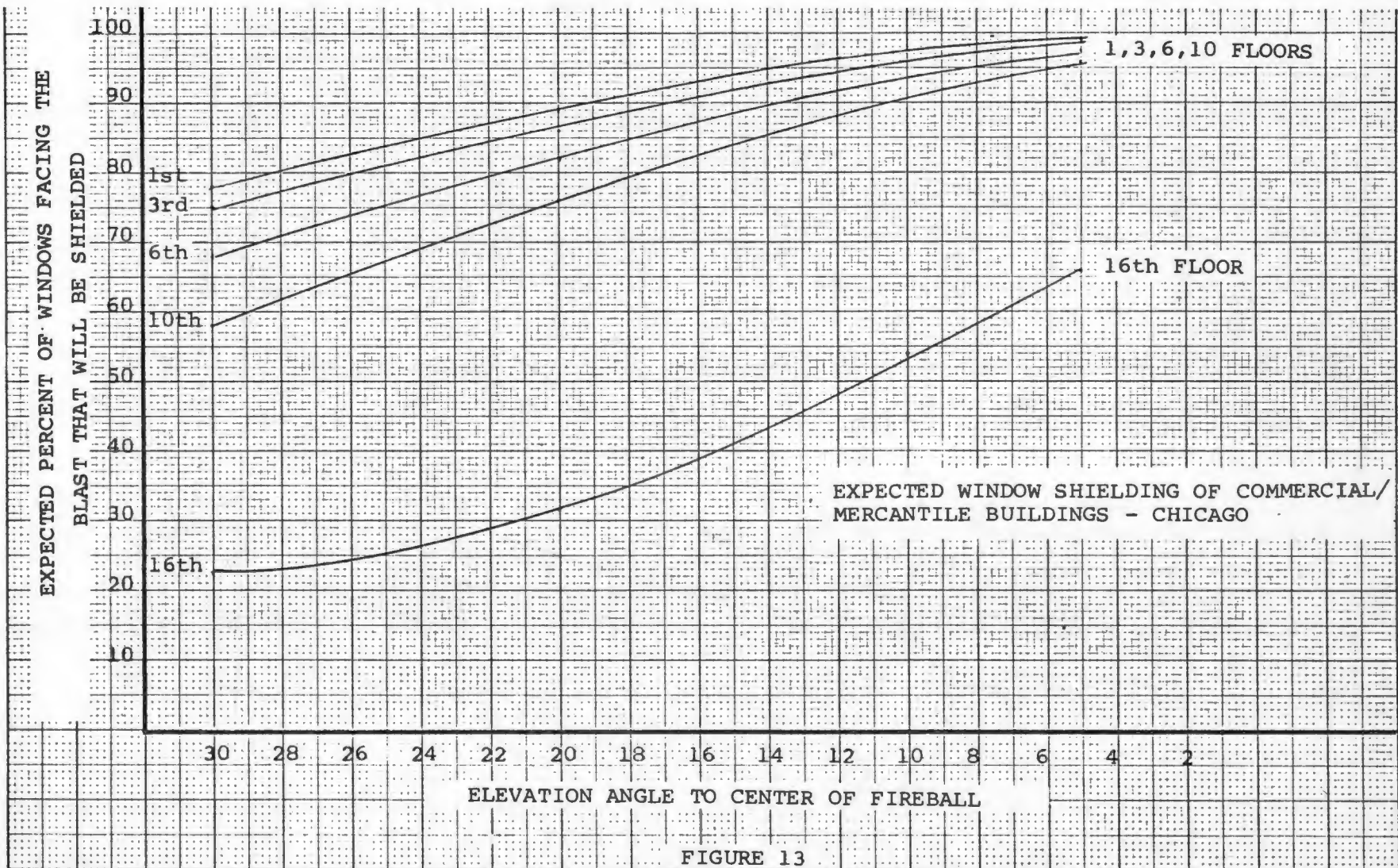


FIGURE 13

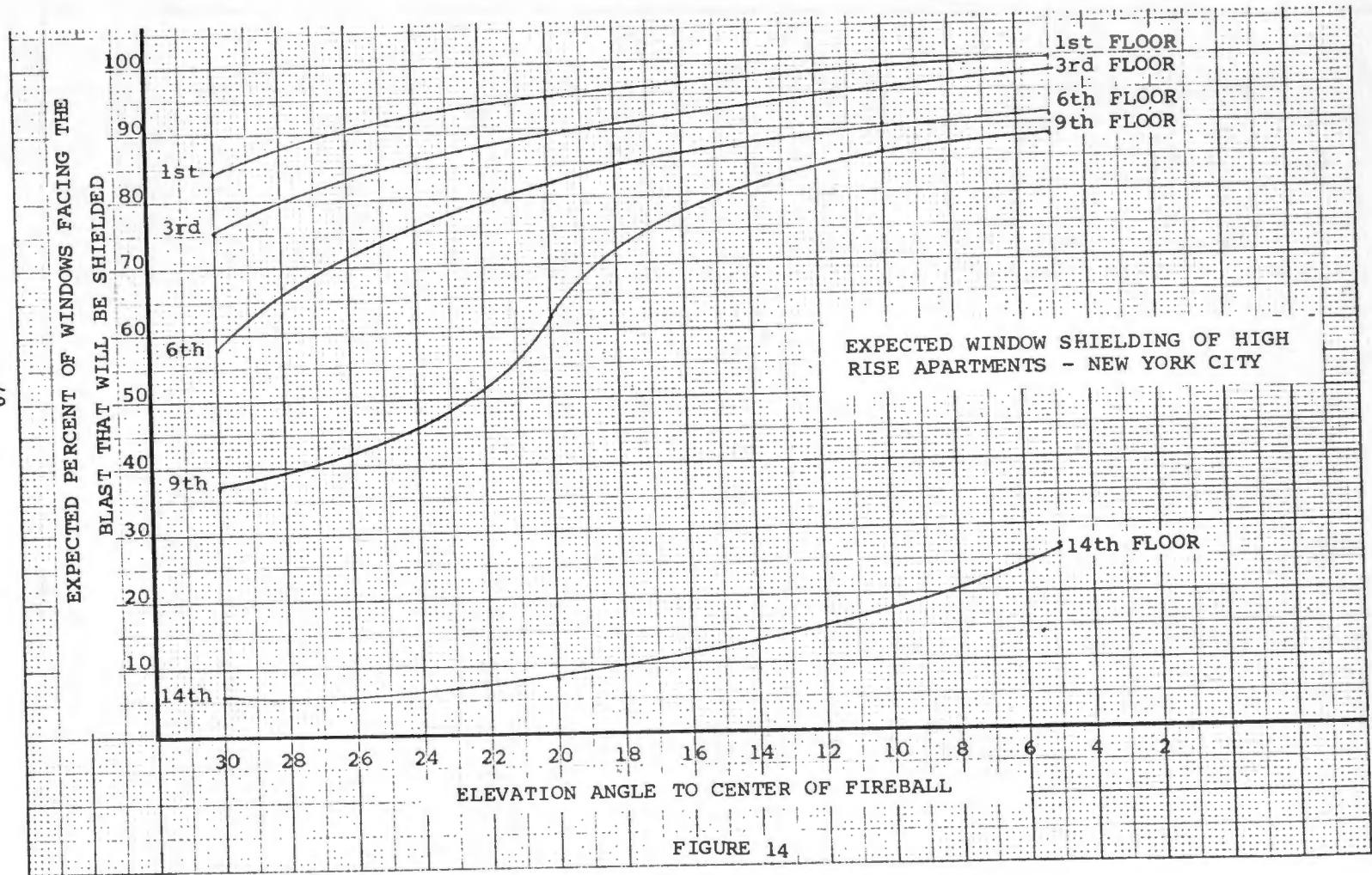


FIGURE 14

lations of ignition and spread to be more fully discussed in Section E.

To assess fire spread within a particular building, a basic quantity called p_{tp} is calculated. If a single room ignition is assumed to give rise to a fire which propagates through the entire floor of origin, the p_{tp} becomes the probability of burnout for the entire floor. Such an assumption might be reasonable for a building of typical fire-resistant construction having incombustible walls and floors, a protected frame and fire doors on the stair wells but having combustible contents. If, on the other hand, a single room ignition is assumed to give rise to a fire which propagates throughout the entire building, then p_{tp} becomes the probability of burnout of the entire building. This assumption might be reasonable for a building that is not of fire-resistant construction.

Then

$$p_{tp} = 1 - (1 - p_{r1})^N \quad (5)$$

where

N = number of ignition points.

The value for N becomes a function of the building size, the size and number of windows, and the window and geometri shading--all for one side of the building only (that side which would face the fireball).

The value for p_{tp} must be adjusted, however, for the cases involving buildings that are not perfectly fire resistant either in terms

of contents or construction. The FIREFLY model (see Section II E) calculates a quantity called p_s in which

$$p_s = \sin \left\{ \frac{[(O + w + f)h] + r}{150} \cdot \frac{\pi}{2} \right\} \quad (6)$$

where

- O = occupancy*
- w = wall construction*
- f = floor construction*
- h = height multiplier*
- r = roof construction*

The values used for O, w, f, h, and r are given in Tables 5-9.

In order that a complete internal fire spread expression may be evaluated, a new quantity p_{tpn} is defined as

$$p_{tpn} = p_{tp} p_s \quad (7)$$

The data concerning fire spread within a building is in need of extensive research. It is known, for instance, that steel doors, fireproof panels, the lack of a combustible fire load, and poor ventilation will aid in confining a room flashover to its point of origin. Further, non-flammable floors, walls and masonry connecting shafts will determine fire spread between floors. The quantification of these parameters is a problem at present. The values employed in the calculation of p_s in equation (6) need further evaluation. Recent work by IITRI, URS,

* Values taken from Reference 11

TABLE 5

OCCUPANCY FIRE LOADING

<u>Category</u>	<u>Suggested Rating</u>
Negligible	0
Light	10
Moderate	20
High	30

Examples

Negligible--vacant or essentially noncombustible contents, occupancy fire loading not exceeding 5 lbs. per square foot.

Machine shops & metalworking with negligible combustibles
Stge. of metal implements or machinery, not packed or crated

Boiler houses, power houses
Brick storage, stone crushing, etc.
Water treatment & sewage disposal plants

Light--occupancy fire loading ranging from approximately 6 to 15 lbs. per square foot.

Houses and apartments
Hotels, hospitals
Schools, laboratories
Halls, gymnasiums
Offices, court houses, jails, banks
Police and fire stations

Telephone exchanges
Libraries (metal shelving)
Funeral parlors
Coal storage
Bulk grain, salt storage
Bulk fertilizer storage

Moderate--occupancy fire loading ranging from approximately 16 to 25 lbs. per square foot.

Amusement parks, bowling alleys, theaters
Automobile service stations, repair & parking garages
Churches
Laundry & dry cleaning shops
Restaurants

Department and variety stores premises not crowded
Retail stores and shops, general
Cold storage warehouses
Drug stores
Most manufacturing plants (not involving large amounts of combustibles or flammables)
Storage of grain, fertilizer, etc. in sacks

TABLE 5 (cont.)

High--occupancy fire loading exceeding 25 lbs. per square foot.

Aircraft hangars	Department and variety stores
Petroleum refineries	premises crowded
Junk yards	Warehouses, general
Flammable liquids processing	Truck terminals
Whiskey warehouses	Plastics manufacturing
Paint factories	Cotton stocks
Asphalt mixing plants	Textiles, clothing, mattress
Rubber tire storage	manufacturing or storage
Stock yards	Woodworking and lumber yards
	Feed mills

TABLE 6

EXTERIOR WALL CONSTRUCTION

Category	Suggested Rating
Standard Masonry	0
Substandard Masonry	10
Noncombustible	10
Noncombustible on combustible supports	15
Combustible	30

Examples

Standard Masonry--not less than 12-inch brick walls or equivalent, in sound condition, with not more than an average number of openings. Equally acceptable are 8-inch brick walls on dwellings, 8-inch concrete block with 4-inch brick facing, 12-inch concrete block, 12-inch stone, 10-inch unreinforced concrete or 6-inch reinforced concrete.

Substandard Masonry--masonry walls less thick than above, or in poor condition, or with more than an average number of openings.

Noncombustible--glass store fronts on brick buildings, glass or metal curtain walls on concrete or steel supports, metal sheathing over metal supports, etc.

Noncombustible on combustible supports--glass or skeleton metal walls on wood supports, corrugated metal or cement-asbestos panels on wood supports, brick or stone veneer, etc.

Combustible--ordinary wood frame construction, wood store fronts or bay windows in brick buildings, enclosed or open wood porches; wood composition, asbestos, or metal sheathing over wood siding; exterior wood paneling, regardless of supports; plastic siding, etc.

TABLE 7

FLOOR CONSTRUCTION

Category	Suggested Rating
Fire Resistant or Non-combustible	0
One or more floors, all or partially combustible	10

Examples

Fire Resistant or Noncombustible--reinforced concrete, steel deck with or without concrete topping, concrete or other cementitious topping on formboard, etc.--all of the above supported on concrete or steel beams, girders, trusses, columns, etc. Neither wood flooring over concrete nor carpeting should affect the classification.

Combustible--ordinary wood joists with or without ceilings, mill and semimill construction, wood flooring on steel beams or joists, etc.

NOTE: Do not include basement floors.

TABLE 8

HEIGHT MULTIPLIERS

<u>Category</u>	<u>Multiplier</u>
1-2 stories	1
3-5 stories	2
Over 5 stories	3

NOTE: Count every 12 feet of building or storage height as one story whenever number of stories is not obvious.

TABLE 9

ROOF CONSTRUCTION

Category	Suggested Rating
Protected Noncombustible	0
Unprotected Noncombustible	10
Noncombustible on combustible supports	20
Combustible	30

If one-third or more of the total roof area in the block has wood shingle or wood shake roof surfacing, assign a value of 40 to the block.

Do not consider insulation or roofing materials (other than wood shingles or shakes) above the roof deck.

Examples

Protected noncombustible--reinforced concrete, precast concrete, steel construction protected by metal lath and plaster, or by "fire-rated" acoustical ceilings, etc.

Unprotected noncombustible--any concrete or gypsum roof on exposed steel supports (without metal lath and plaster or "fire-rated" acoustical ceiling), metal deck or metal on concrete supports, fire-retardant treated lumber, etc.

Noncombustible on combustible supports--metal or cement-asbestos panels on wood supports (without wood decking or combustible insulation on the inside), etc.

Combustible--ordinary wood joist construction (with or without "fire-rated" or plaster ceiling), mill construction, wood deck on metal or concrete supports, plastic panels on wood or metal supports, etc.

If the expression $\{[(o+w+f)h]+r\}$ is calculated to be greater than 150, p_s should be set equal to 1.0.

T.Y. Lin, and others, along with studies in White Plains, N. Y., may prove valuable in the future.

E. FIRE SPREAD THROUGH URBAN AREAS--THE FIREFLY MODEL

The concept of exposed room ignition giving rise to fires which may propagate through an entire floor or a whole building, possibly spreading to adjacent buildings, permits analysis of urbanized areas to assess the limits of fire damage. A computer model called FIREFLY has been developed and written to do this. Reference 12, a supplemental report, documents FIREFLY. Concurrently with the development of FIREFLY, analysis of data in standard location areas (SL's) and of U. S. Census data on urban environments was conducted to devise schemes for utilizing these data in the model. A discussion of this analysis is contained in Section V.

The basic task of FIREFLY is to perform assessments of the fire threat to an area of up to 27 city blocks with certain limitations being imposed upon the numbers and distribution of buildings within each block. Large amounts of data on a maximum of 1080 buildings may be handled. The assessed fire threat has two separate and distinct causes: the ignition by the thermal pulse of exposed rooms which may then propagate to the whole building, or the spread of fire from structure to structure. The latter cause and a discussion of the intricate workings of the FIREFLY model are presented in Reference 12. A brief outline of the procedures is given below:

1. The probability that the building will ignite and burn from the internal spread of fire (p_s as defined by equation (6), p. 42) is calculated for every building.

2. Each building is examined from the standpoint of the unobstructed radiation distance under quiescent conditions beyond which another ignition in neighboring buildings will not be initiated. The length of this path is called the "safe distance" and is a function of the magnitude of the thermal radiation source which is determined by the radiating building size, height, wall openings, and roof type.

3. Once steps (1) and (2) have been accomplished, the model is ready to begin with two parameters-- p_{ri} , the probability of room ignition which are assigned values of .1, .3, .5, .7, and .9, and the angle of elevation of the effective radiating center of the weapon fireball which are assigned values of 5° , 10° , and 30° for each p_{ri} .

4. Using one p_{ri} and one angle of elevation, p_{tp} is calculated from equation (5) in which the number of expected ignitions, N , is a function of :
 - a. The size of the building (the larger the building, the more windows are assigned to be present).
 - b. The percentage of window openings to the total wall space (ordinarily taken as 20 percent).
 - c. The average window shading (50 percent).
 - d. The average window size (3 ft. by 5 ft.).
 - e. The average expected geometric shading for the building for any randomly selected floor (unique for each angle of elevation).

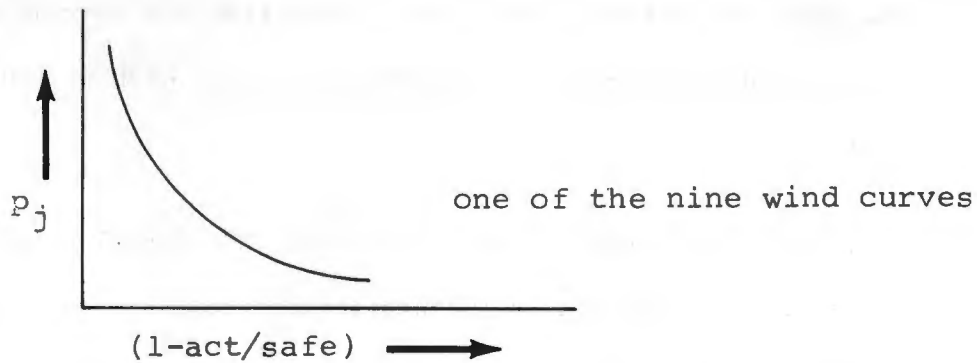
5. As explained earlier, p_s is multiplied by p_{tp} to create p_{tpn} which now embodies all the parameters relating to fire growth within the building.

6. The specific buildings which catch fire from the thermal pulse are determined by comparing random numbers to each of the values for p_{tpn} .
7. Once the buildings have been ignited by the thermal pulse, the threat to all remaining buildings is assessed.

The wind vector is divided into orthogonal components which are examined for each possibility of fire spread from a burning building to an unburned one. There are nine possible wind spreads: with, against, or perpendicular to a high, medium, or low wind (high wind is above 16 mph, medium wind is 8-16 mph, and low wind is less than 8 mph).

The actual separation distance is compared to the "safe distance." If the actual distance is zero, the probability of "jump," p_j^* , is set equal to 1.0 if no protection is afforded between buildings or to 0.95 if a firewall is present. If the actual distance is greater than the safe distance, $p_j = 0$. If the actual distance has a value between zero and the safe distance, the ratio of actual-to-safe distance is calculated and is determined from a graph of the form shown on the next page.

* The quantity called the probability of "jump" (p_j) is in actuality the measure of the probability of there being sufficient radiative energy or firebrands present at a specified distance away from a fire to cause a secondary ignition.



The probability of fire jump causing an ignition in another structure, p_j , is combined in Bayesian fashion with the probability of the subsequent internal spread of that ignition in the threatened building, p_{sj} as follows:

$$P(s/j) = p_j p_s.$$

8. All unburned buildings are assessed by comparing a random number to $p(s/j)$.
9. Results are compiled for the number of:
 - a. Buildings destroyed by thermal pulse (total and percent of total)
 - b. Buildings destroyed by spread (total and percent of total)
 - c. Buildings destroyed by both (total and percent of total).
10. This is one condition with one p_{r1} , and one angle is run 99 more times.
11. After the 100th run, a new p_{r1} is used.
12. After the 5th p_{r1} , a new angle is used.

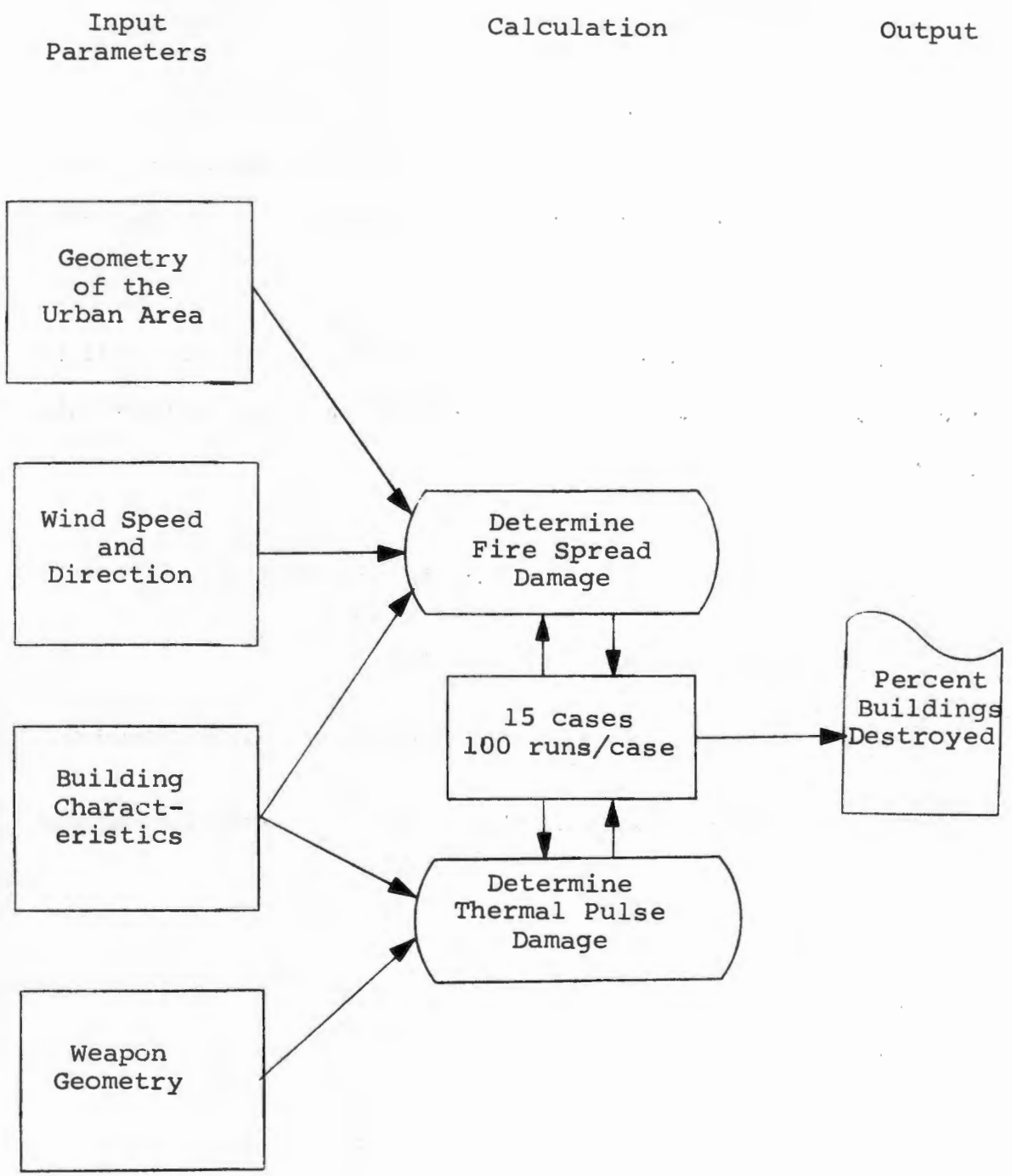
13. Standard deviations are calculated for each of the 15 cases of 100 runs each.

Figure 15 is a general schematic of the FIREFLY model. Figure 16 is a representation of fire damage to two blocks from an actual run against a medium-class residential area in N.E. Washington, D. C., using medium wind, $p_{r,1}$ of 0.3, and an angle of 10° .

One summary of the results from runs of the model is shown on Table 10. Appendix C contains summaries of runs against the following three urban area types:

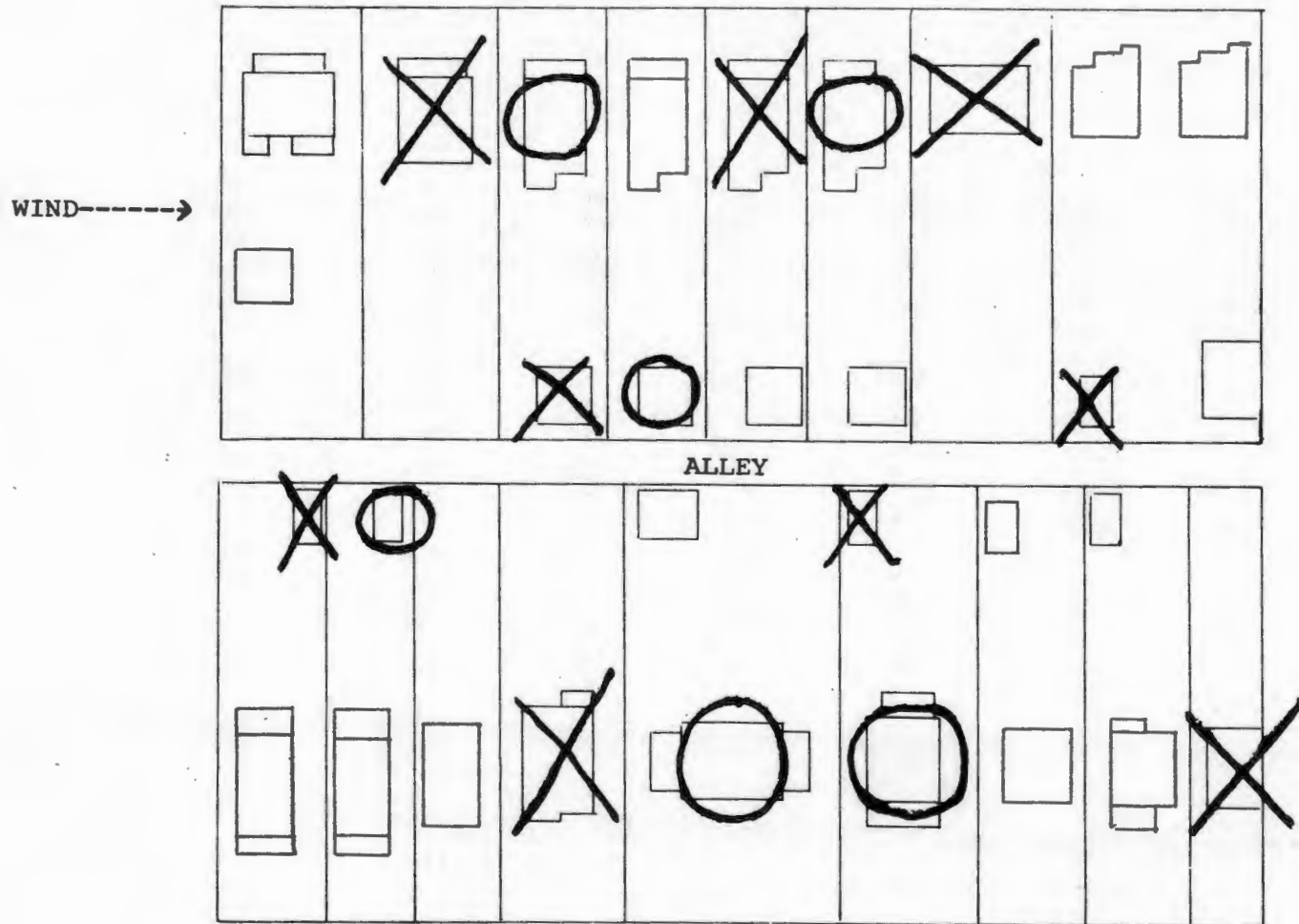
- Washington, D. C. (medium class residential)
- E. Boston, Mass. (industrial)
- Manhattan, New York (commercial/low class residential).

Figure 17 is a plot of Table 10. Similar plots are readily constructed.



THE FIREFLY MODEL

FIGURE 15



X = thermal pulse destruction
 O = fire spread destruction
 Structures are predominantly concrete brick faced, flammable interior dwellings

BUILDING DAMAGE IN ONE FIREFLY RUN

FIGURE 16

TABLE 10

EXAMPLE SUMMARY OF FIREFLY RESULTS
 SINGLE-FAMILY RESIDENTIAL - MEDIUM WIND
 (Washington, D.C.)

PROB ROOM IGNITION	ANGLE OF ELEVATION	AVG NO. OF BUILDINGS BURNT (100 CASES)			PERCENT BURNT (379 BUILDINGS)			STANDARD DEVIATION			
		THERMAL PULSE	SPREAD	TOTAL	THERMAL PULSE	SPREAD	TOTAL	THERMAL PULSE	SPREAD	TOTAL	
56	0.1	30 DEG	50	75	125	13	20	33	6.0	7.4	9.5
	0.3	30 DEG	120	51	171	32	13	45	6.6	7.0	9.6
	0.5	30 DEG	163	31	194	43	8	51	8.1	4.7	9.3
	0.7	30 DEG	190	21	211	50	6	56	7.4	3.6	8.2
	0.9	30 DEG	208	16	224	55	4	59	7.7	3.0	8.3
	0.1	10 DEG	42	75	117	11	20	31	5.6	8.3	10.0
	0.3	10 DEG	106	57	163	28	15	43	7.0	5.7	9.1
	0.5	10 DEG	148	38	186	39	10	49	7.5	4.4	8.7
	0.7	10 DEG	177	27	204	47	7	54	7.3	4.5	8.6
	0.9	10 DEG	194	20	214	51	5	56	7.9	4.2	8.9
	0.1	5 DEG	30	69	99	8	18	26	4.6	9.2	10.2
	0.3	5 DEG	80	68	148	21	18	39	7.1	7.0	9.9
	0.5	5 DEG	117	51	168	31	13	44	7.1	5.9	8.9
	0.7	5 DEG	142	40	182	37	11	48	8.0	5.8	9.9
	0.9	5 DEG	163	29	192	43	8	51	8.4	4.0	9.3

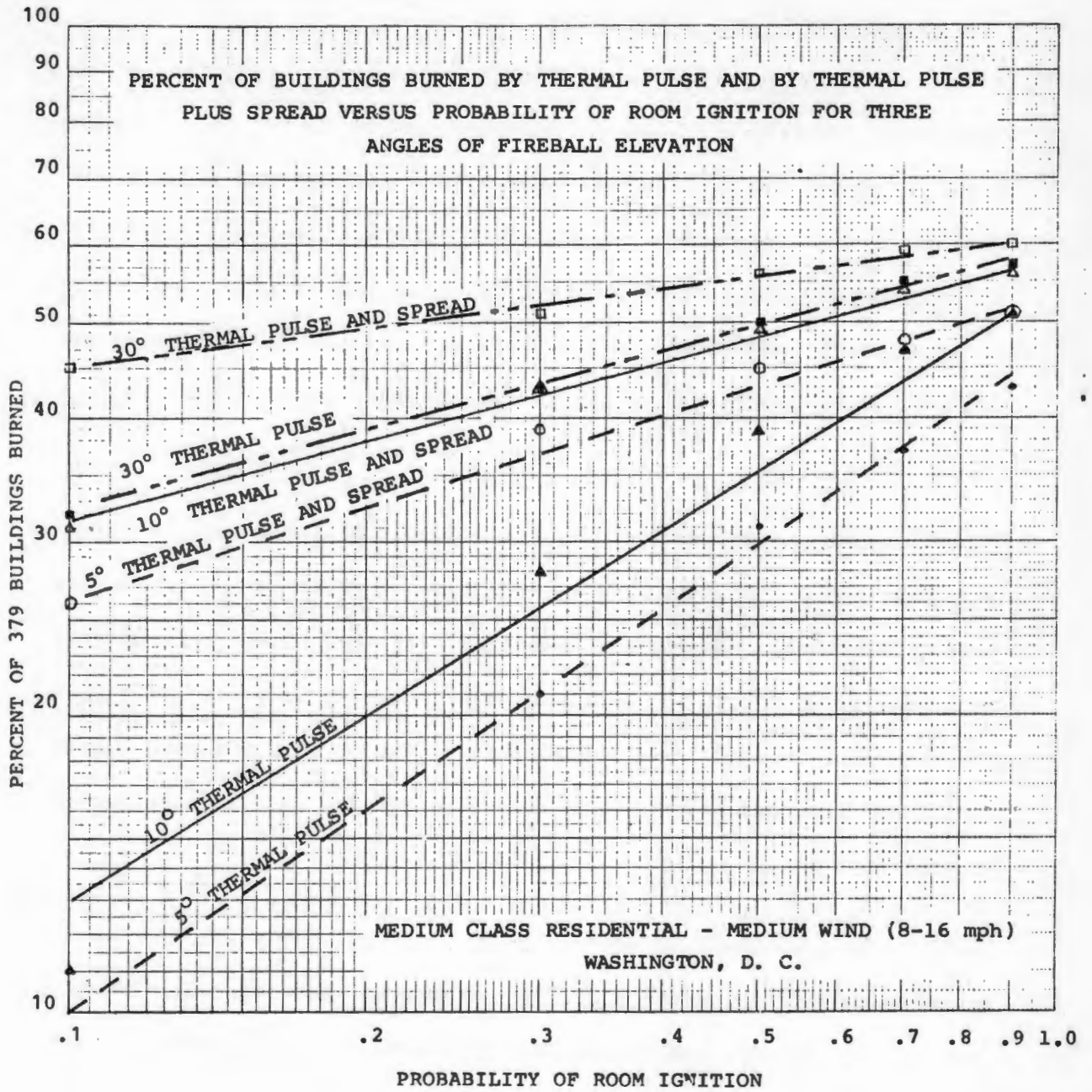


FIGURE 17

F. SYNTHESIS AND APPLICATION

Through repeated use of FIREFLY to determine ignition and fire spread for representative areas, standard tables similar to Table 10 or those in Appendix C could be produced. Then to determine the fire threat for any particular area, it would only be necessary to look up the appropriate table which had been produced from FIREFLY runs on many areas of nearly identical characteristics. Schemes for classification of urban environments by various characteristics are discussed in Section V.

Two promising approaches for classification of Standard Locations (SL's) were developed. In one approach, four factors relative to housing are averaged to obtain an index of potential fire susceptibility. For the total number of houses in an SL, the percent built before a given year, the percent deteriorating and dilapidated, the percent that are multi-family and the percent which are less than \$10,000 in value are the indicators utilized.

In the second approach, SL's are characterized by both population per square mile and the percentage of total housing units that are one-unit structures. In applications of this approach, SL's were found to group according to their basic class, e.g., single-family residential, multi-family residential, central business district and livelihood, suburbanizing, or nonurban. Experience to be gained from future applications of FIREFLY assessments may indicate the need for further subdivision of these urban environment classes.

With sufficient data accumulated from repeated application of FIREFLY to each of several classes of urban environment, the "standard" look-up tables could be incorporated into OCD DASH--A System to Provide Detailed Assessments of the Hazards of Nuclear Attack.

In addition to the eventual use of "standard" look-up tables for computer assessment of fire effects, it would be entirely feasible to produce an urban nuclear fire effects handbook of tables and graphs. Useful estimates of fire damage could then be readily calculated for situations of interest, specifying as few as the six parameters:

- Weapon yield
- Height of burst
- Ground distance of each component area from the probable ground zero
- Type and occupancy density of each component area
- Assumed wind speed
- Atmospheric visibility.

The following steps would be taken in solving a particular problem:

- Determine the angle of elevation (Figure 7 or 8, p. 32 or 36).
- Calculate Room Ignition Weapon Radius (RIWR) (equation (2), p. 26 with Table 4, p. 29)
- Calculate the standard deviation. (See Appendix B, p. 215)
- Calculate the probability of room ignition using equation (3), page 26.
- If necessary, calculate the adjusted probability of room ignition using equation (4), page 30.
- Use an appropriate table for the type of urban environment (similar to Table 10, p. 56).

A sample problem is used to illustrate. Assume the following:

- Yield is 10 MT.
- Height of burst is 640-foot scaled.
- Ground distance is 52,800 feet (10 miles).
- Atmospheric visibility is 6 miles.
- Urban area is a medium class residential, but occupancy density is high (0.9 persons per room).
- Wind speed is 20 mph (high wind).

Using Figure 8 for 640-foot scaled heights of burst, the angle of elevation is 13° for a 10 MT weapon at a distance of 52,800 feet.

RIWR is defined in equation (2) as

$$\text{RIWR} = a \left(\frac{w}{0.1} \right)^b$$

The values for a and b are 1.62 and 0.355, respectively, as shown in Table 4 for air burst weapons with a visibility of 6 miles. RIWR is then

$$\text{RIWR} = 1.62 \left(\frac{10}{.1} \right)^{0.355} = 8.30 \text{ miles.}$$

The standard deviation for air burst weapons is given by Appendix B as

$$= 0.21 \text{ RIWR} = 0.21 (8.30) = 1.74 \text{ miles.}$$

The probability of room ignition may be calculated using equation (3):

$$p = \Phi \left\{ \frac{RIWR - d}{\sigma} \right\}$$

$$p = \Phi \left\{ \frac{8.30 - 10.0}{1.74} \right\}$$

$$p = \Phi (-0.976) .$$

In this case, $\Phi(-0.976)$ is equivalent to a probability of (1.000 - 0.8355) = 0.1645. This probability of room ignition must be adjusted upwards since the dwelling occupancy is higher than the standard 0.7 persons per room. Equation (4) is

$$\begin{aligned} p_n &= \left[1.0 + \left(\frac{\text{persons/room} - 0.7}{0.2} \right) (0.232 - 0.108p) \right] p \\ &= \left[1.0 + \left(\frac{0.9 - 0.7}{0.2} \right) (0.232 - 0.108 \times 0.1645) \right] 0.1645 \\ &= [1.0 + 0.214] 0.1645 \\ p_n &= 0.20 . \end{aligned}$$

Table 10 is used here as representing a typical medium class residential area, high wind case. Interpolating within the table for 13° angle of elevation and a probability of room ignition of 0.20, one finds that the percent damage from the thermal pulse is 20 percent, the damage from fire spread is 18 percent, and thus the total expected fire damage is 38 percent.

III. BLAST VULNERABILITY

A. BLAST CASUALTY PHENOMENOLOGY

Direct blast casualties result from the action of the blast pressure upon the human body. As the shock wave engulfs the body, the rapid compression causes a sharp pressure wave to be transmitted through the body. As the shock wave encounters different densities in various internal parts (organs, tissues, bones, air spaces, etc.), the imbalance of the forces tends to rupture the interfacial surfaces of the organs and tissues, causing severe biological damage and rapid death. Air forced into the blood vessels of the brain is also a cause of rapid death, and severe hemorrhaging of the lungs may be fatal.

Impingement of the blast wave directly on the human body has lethal effects at peak overpressures above 35 psi. The steepness of the shock front also plays a role, and the more nearly instantaneous the pressure rise, the more severe are the likely biological consequences. The steepness of the shock front is degraded during the passage of the blast wave through building openings, down corridors, and through interior passageways, but this degradation is often compensated for by the amplification of the peak pressures as the blast wave is reflected off walls and other obstacles. Although they will occur, direct blast fatalities are seldom a significant assessment consideration inasmuch as they are usually overshadowed by indirect blast effects.

Indirect effects are the principal cause of blast casualties at reasonably low overpressures. These effects are caused principally by the violent impact of debris upon the body or by forceful translation of the body against hard or immovable objects. The effects of flying missiles

and debris depend upon the mass and velocity of the moving object at the moment of impact and the part of the body which it hits. The missile velocity, in turn, is governed by its side-on area per unit mass and its drag coefficient. Small light objects attain high velocities very soon after entrainment in the blast wave and may travel quite far, depending on the duration of the positive pressure, whereas large heavy objects achieve velocity more slowly and have limited displacement distances and slower speeds. Measurements at Nevada field tests of window-glass fragments and tiny stones entrained in blast waves of approximately 2 to $8\frac{1}{2}$ psi peak overpressure attained median velocities of 100 to 300 feet per second. The median mass of the broken fragments was generally less than a gram, and the number of such flying missiles ranged from a few to several hundred per square foot of shock front, the larger numbers being associated with the smaller fragments. Penetration of the abdominal cavity, with serious biological effects, is possible with a 10-gram glass fragment at 100 feet per second or by a 0.25-gram fragment moving at 200 feet per second. These criteria are achieved at 4 or 5 psi and higher overpressures, but assuming that warned personnel take shelter within interior rooms and are able to shield themselves from possible flying glass, it does not appear that tiny fragments are the principal lethal hazard.

The creation of large heavy debris by the action of the blast wave upon the walls, partitions, roof, ceilings, and floors of most types of buildings is a critical problem, however. The phenomenon in this case is not tissue penetration, necessarily, but fracturing of bones, crushing of organs, and smothering and burial of the individual. A 10-pound piece of broken

masonry, for example, traveling at 13 feet per second can fracture the skull, and a wave of moving debris caused by the breakup of walls and heavy partitions can be fatal to personnel caught in its path. Finally, with sufficient blast pressure, the principal structural members of a building may be distorted and displaced, causing collapse of the building upon its occupants.

Although blast casualties are often associated with the structural strength of the buildings they occupy (the more vulnerable the building, the more vulnerable its occupants), a direct correlation between damage and casualties does not necessarily apply in many cases. A number of factors such as size, number of windows, and location of personnel in interior rooms are involved. The immediate environment of the individual is often important, and a position under a stairway, desk, or heavy table may be relatively safe in some circumstances. The amount of structural damage to the building is also a factor. Occupants of a lightly-damaged building with concrete floors and roof may have a higher survival rate than those in a lightly-damaged frame house whereas, in the case of very severe damage or collapse, the reverse may be true. In the absence of precise data on the disposition of building occupants, however, it has been the general practice to associate the probability of blast casualties with the blast vulnerability of various structural categories of buildings.

If, however, it is desired to conduct shelter systems vulnerability analyses, casualty functions may be derived associated with particular dispositions of building occupants and/or lesser levels of structural damage to various types of structures. The last portion of Section III

synthesizes the results of the analyses of blast vulnerability of structures in terms usable as blast casualty and fatality vulnerability numbers--a transformation suitable for computer assessment.

B. LOADING OF BUILDINGS BY THE BLAST WAVE

1. Loading of the Front Face

For frontal loading, the incident blast side of the building, the usual formula is employed in which the pressure decays from reflected pressure to blast overpressure in time $t_1 = \frac{3S}{V}$ where S is the building height or half the building width--whichever is less--and V is the shock speed.

2. Loading on the Side Walls and Roof

The pressure on the sides is blast overpressure computed at the time and place of interest.

As the blast wave moves along the roof, it exerts a restoring moment on the building. This moment, however, is negligible compared to the moment of the frontal forces and may be neglected. Roof failure is a relatively slow process compared to the times of interest and may be ignored insofar as building collapse is concerned. In a later example in Section III D. 3., Failure of a Multistory Load-Bearing Building, the time to full loading on the roof is about 54 milliseconds after which at least another 40 milliseconds are required for roof failure. The building, however, would have collapsed in 90 milliseconds.

3. Loading on the Rear

The back pressure starts to build up linearly to blast over-

pressure at time $t_2 = \frac{d}{V}$ and reaches blast overpressure at time

$$t_3 = \frac{4S + d}{V} \quad \text{where } d = \text{depth of the building.}$$

4. Pressure Buildup Inside a Building

The interior buildup of pressure is of interest chiefly in the rooms on the sides. It can build up both from the overpressure on the sides entering windows and from the reflected pressure entering the front rooms. There is no good rule for computing the buildup time since interior partitions may or may not fail. However, there will be doorways and halls and perhaps as good an estimate as any of the buildup time is $\frac{2d}{V}$, which would be the proper value if there were no partitions. The maximum value of interior overpressure will depend on the percent of window openings. Load-bearing buildings will run about 20 percent window openings (which agrees with the value used in Section II, paragraph E).

As far as the deflection of the building as a whole is concerned, the pressure buildup on the inside has very little effect. It is true that the blast wave can enter a window, reflect from an interior wall and impart an impulse in the blast wave direction. It then, however, returns to the front wall and imparts an opposite impulse. Finally, it settles down to a uniform decaying pressure which acts both ways on the building as a whole. If the interior walls fail, then the building receives a few small impulses; but again the net effect is not large. Thus, interior pressure is of interest only insofar as failure of side walls is

concerned.

5. Computation of Building Loading

Later, in discussing actual buildings it will be shown that the building loading functions may be approximated adequately by

$$F(t) = A_F P_r e^{-\beta t}$$

where

- A_F = frontal area of the building less the window area,
- P_r = initial reflected overpressure,
- β = a parameter adjusted for best fit to the actual loading function.

This approximation is convenient mathematically. It must be modified for structures the failure of which also depends on drag forces.

C. ANALYTICAL PROCEDURES

Certain procedures have been found to be applicable to analysis of the response of different types of buildings to loading from the blast wave. These procedures are discussed in this section before turning to specific building types.

* See Appendix D for building loading diagrams and the determination of parameter β .

1. Dynamic Response of a Building When Treated as an Elastic Beam

The equation of motion of a building* is

$$QI \frac{\partial^4 u}{\partial x^4} + \frac{W}{gh} \frac{\partial^2 u}{\partial t^2} = a P_r e^{-\beta t} \quad (8)$$

where

Q = Young's Modulus,

W = building weight,

$a P_r e^{-\beta t}$ = force per unit length,

$\frac{W}{gh}$ = mass per unit length,

x = vertical distance above grade.

It should be stressed that the mass per unit length and the area moment of inertia, I , can vary with x significantly in many building types. In load-bearing buildings, the variation is not large and can be neglected. For steel-framed and reinforced concrete-framed buildings, a higher order of approximation may be used employing the Rayleigh-Ritz technique. For the present these quantities are kept constant. However, the accuracy and meaning of the Rayleigh-Ritz method will be examined later.

The solution of (8) follows the eigenvalue approach of mathematical physics. Solutions of the equation for free vibrations of the bar which are obtained by setting the forcing function equal to zero are looked at first. Under the boundary conditions that

* See, for example, Morse, "Vibration and Sound," McGraw-Hill, 1939.

$$\psi(0) = \frac{\partial \psi}{\partial x} \Big|_{x=0} = 0,$$

and

$$\frac{\partial^2 \psi}{\partial x^2} \Big|_{x=h} = 0$$

(moment is zero at the free end),

and

$$\frac{\partial^3 \psi}{\partial x^3} \Big|_{x=h} = 0$$

(shear is zero at the free end),

the usual allowed frequencies for the bar are obtained, i.e., ν_1, ν_2, \dots

ν_n, \dots and with each ν_j , there is a corresponding $f_j(x)$ such that

f_j 's are orthogonal, i.e.,

$$\int_0^h f_j(x) f_k(x) dx = 0 \quad j \neq k.$$

In analogy with the problem of the vibrating string, the f_j 's are usually normalized so that

$$\int_0^h f_j^2(x) dx = \frac{h}{2}.$$

The f_j 's are also complete, i.e., any function of physical interest can be expanded as a series in the f_j 's in the interval $0 \leq x \leq h$. Thus, the complete solution for free vibrations in the j th mode is

$$f_j(x) [A \cos \omega_j t + B \sin \omega_j t] \quad (9)$$

$$\text{where } \omega_j = 2\pi v_j.$$

The f_j 's satisfy the ordinary differential equation

$$\frac{d^4 f_j}{dx^4} = \lambda_j^4 f_j \quad (10)$$

$$\lambda_j^4 = \frac{\omega_j^2 w}{QIgh}. \quad (10a)$$

To solve (8) completely, set

$$\psi = \sum \alpha_j f_j(x) u_j(t)$$

where $u_j(t)$ is chosen to satisfy the initial conditions

$$u_j(0) = \frac{du_j}{dt} \Big|_{t=0} = 0,$$

as well as the inhomogeneous equation with the forcing function present.

Thus

$$u_j(t) = e^{-\beta t} - \cos \omega_j t + \beta/\omega_j \sin \omega_j t.$$

Also set

$$\frac{a P_r}{QI} = \sum \mu_j f_j(x).$$

The α_j and μ_j are to be determined. Since the f_j 's are orthogonal

$$\alpha_j \lambda_j^4 u_j(t) + \frac{\lambda_j^4 \alpha_j}{\omega_j^2} \left[\beta^2 e^{-\beta t} + \omega_j^2 \cos \omega_j t - \beta \omega_j \sin \omega_j t \right] = \mu_j e^{-\beta t}$$

or

$$\alpha_j \lambda_j^4 \left[(1 + \beta^2 / \omega_j^2) e^{-\beta t} \right] = \mu_j e^{-\beta t}.$$

So

$$\alpha_j = \frac{\mu_j}{\lambda_j^4 (1 + \beta^2 / \omega_j^2)}.$$

Further

$$\mu_j = \frac{a P_r \int_0^h f_j(x) dx}{QI \int_0^h f_j^2(x) dx}.$$

For the case of a uniform load, only α_1 is of any importance. Thus, for example, α_2 turns out to be only about 10^{-3} times α_1 , and α_3

is even smaller. This is usually the case for vibrating systems with a uniform load which decays monotonically with time. Thus, to a very good approximation

$$\psi(x,t) = \alpha f(x) \left[e^{-\beta t} - \cos \omega t + \beta/\omega \sin \omega t \right]. \quad (11)$$

Value ω_1 has been set to equal ω for simplicity, where ω_1 is the fundamental angular frequency.

The discussion of the solution of (8) has been included for clarity. Morse lists the expression for $f_j(x)$ and ω_j in his book on "Vibration and Sound," McGraw-Hill, 1939, pages 117 and 120. Thus,

$$\omega_1 = \frac{1}{h^2} \sqrt{\frac{QIgh}{w}} (\pi\beta_1)^2 = \omega \quad (11a)$$

$$\pi\beta_1 = 1.875 = h\lambda_1 \quad (11b)$$

$$f_1(x) = .707 \left[\cosh \pi\beta_1 \frac{x}{h} - \cos \pi\beta_1 \frac{x}{h} \right] - .518 \left[\sinh \pi\beta_1 \frac{x}{h} - \sin \pi\beta_1 \frac{x}{h} \right]. \quad (11c)$$

Also

$$\frac{\int_0^h f_1(x) dx}{\int_0^h f_1^2(x) dx} = 1.11$$

and thus

$$\alpha_1 = \frac{1.11}{(1 + \beta^2/\omega^2)} \frac{aP_r}{QI} \frac{1}{\lambda_1^4} = \frac{1.11 aP_r g h}{\omega^2 w (1 + \beta^2/\omega^2)} \quad (12)$$

So finally,

$$\psi(x, t) = \frac{1.11 A_F P_r g}{\omega^2 w} \frac{(\epsilon^{-\beta t} - \cos \omega t + \beta/\omega \sin \omega t)}{1 + \beta^2/\omega^2} f_1(x)$$

which can also be written

$$\psi(x, t) = \frac{1.11 a P_r}{QI} \left(\frac{h}{\pi \beta_1}\right)^4 f_1(x) \left[\frac{\epsilon^{-\beta t} - \cos \omega t + \beta/\omega \sin \omega t}{1 + \beta^2/\omega^2}\right] \quad (12a)$$

Setting

$$F(t) = \frac{\epsilon^{-\beta t} - \cos \omega t + \beta/\omega \sin \omega t}{1 + \beta^2/\omega^2}$$

The value of $\psi(x, t)$ reaches a maximum with respect to time when $F(t)$ is a maximum. Thus, the maximum of $F(t)$, for reasons to be shown later, is conveniently called the dynamic loading factor.

At this point it may be noted that the deflection at the top at any given time can be found by computing $f_1(h) = 1.41$ and so

$$\psi(x, t) = \frac{1.57 A_F P_r g}{\omega^2 w} F(t). \quad (13)$$

The maximum deflection at the top is

$$\psi(h, t)_{\max} = \frac{1.57 A_F P_r g}{\omega^2 w} [F(t)]_{\max}. \quad (14)$$

The maximum of $F(t)$ can vary from a value of 2 for β/ω very small (long loading time compared to fundamental angular frequency) to an asymptotic value of β/ω when $\beta \gg \omega$. This latter case is the case where the loading can be treated as an impulse.

Now the maximum moment at the base of the building is

$$M(0) = I A_B \left. \frac{\partial^2 \psi}{\partial x^2} \right|_{x=0} \quad F(t) = F(t)_{\max}.$$

Thus

$$M(0) = 1.57 Q I \frac{A_F P_r g}{\omega w^2} \left(\frac{\pi \beta l}{h} \right)^2 [F(t)]_{\max}. \quad (15)$$

A few useful relations may be developed when

$$M(0) = M_u$$

(ultimate*, or failure moment at the base),

$$\psi(h, t)_{\max} = x_e$$

(deflection of the top at failure). From (14) and (15)

$$\frac{M_u}{x_e} = QI \left(\frac{\pi \beta_1}{h} \right)^2 3.52 \frac{QI}{h^2} \quad (16)$$

Using the expression for ω ,

$$\frac{M_u}{x_e \omega^2} = \frac{Wh}{g} \frac{1}{3.52} \quad (17)$$

From (34), M_u may be computed; then use (16) to find x_e and (17) to calculate ω^2 . Value ω^2 can also be calculated independently.

At this point the preceding analysis of the elastic beam may be connected with two approximate analyses to show:

- The relation of the bar deflection under static load to the deflection under dynamic load and how the Rayleigh-Ritz Principle is used to verify this connection.
- Use of the Rayleigh-Ritz Principle for buildings where I and the mass per unit length vary with height, or from story to story.
- The relation of the solution for the bar to a simple one-dimensional approximation which is often used.

* In the case of a concrete bond, M_u will be the failure moment. For steel, M_u will be the point where columns go into the plastic range.

2. Deflection of a Beam under Static Load

The pertinent equation is (8) from page 69 with $\frac{\partial^2 \psi}{\partial t^2}$ set equal to zero and β set equal to zero. Then

$$\frac{d^4 \psi}{dx^4} = \frac{aP_r}{QI} \quad (18)$$

This equation integrates to

$$\psi(x) = \frac{aP_r}{24QI} (x^4 - 4x^3h + 6x^2h^2) \quad (19)$$

and

$$\psi(h) = \frac{a P_r h^4}{8QI} \quad (19a)$$

This last result may be compared with $\psi(h, t)$ as obtained from (12a) on page 74. Using (12a)

$$\psi(h, t) = \frac{1.11 a P_r h^4}{QI (\pi\beta_1)^4} f_1(h) F(t) \quad (20)$$

As seen earlier

$$f_1(h) = 1.41, \quad \pi\beta_1 = 1.875,$$

so that

$$\psi(h, t) = \frac{a P_r h^4}{7.90 QI} F(t)$$

and

$$\psi(h, t)_{\max} = \frac{a P_r h^4}{7.90 QI} [F(t)]_{\max}. \quad (20a)$$

(19a) and (20a) are virtually identical except for the term $F(t)_{\max}$ in (20a). Thus $F(t)_{\max}$ may appropriately be called the dynamic loading factor since one gets the maximum dynamic deflection from the maximum static deflection by multiplying by $F(t)_{\max}$.

Now, from (19), $M(0)$ for the static case is

$$M(0) = QI \left. \frac{d^2 \psi}{dx^2} \right|_{x=0} = \frac{a P_r h^2}{2} \quad (21)$$

and from (15), noting that

$$W\omega^2 = \left(\frac{\pi\beta_1}{h} \right)^4 QIgh,$$

$$M(0) = \frac{1.57 a P_r h^2}{(\pi/\beta_1)^2} F(t) = \frac{a P_r h^2}{2.24} F(t). \quad (22)$$

Ignoring the time factor, the dynamic moment at the base is about 12 percent less than the static moment.

This discrepancy is still not large enough for concern, considering the accuracy with which other parameters will be known. However, if a static deflection curve is used, the difference may be compensated for if desired, by reducing the computed moment at the base by a factor of $\frac{1}{1.12} = .89$.

3. The Rayleigh-Ritz Principle

The Rayleigh-Ritz Principle says, in effect, that the eigenfunction (or displacement function) which corresponds to the lowest resonant frequency is that function $f_1(x)$ which satisfies the boundary conditions and minimizes the ratio of potential energy to kinetic energy and, at the minimum,

$$\frac{V}{T} = 1.$$

If V = potential energy in the lowest mode and

T = kinetic energy in the lowest mode,

then

$$V = \frac{1}{2} QI \int_0^h \left(\frac{d^2 y_1}{dx^2} \right)^2 dx$$

and

$$T = \frac{1}{2} \frac{Ww^2}{gh} \int_0^h y_1^2 dx.$$

Thus

$$\frac{V}{T} = \frac{QIgh}{W\omega^2} \frac{\int_0^h \left(\frac{d^2 y_1}{dx^2}\right)^2 dx}{\int_0^h y_1^2 dx} .$$

At the minimum,

$$\frac{W\omega^2}{QIgh} = \frac{\int_0^h \left(\frac{d^2 y_1}{dx^2}\right)^2 dx}{\int_0^h y_1^2 dx} . \quad (23)$$

The left-hand member is, of course, λ_1^4 . In any event, the minimum of the right-hand side gives the correct value of λ_1^4 , and consequently ω^2 . If, for example, some function $g_1(x)$ satisfies boundary conditions and is an approximation to the eigenfunction, then the ratio of integrals on the right will give an approximation to ω^2 ; but the approximation must yield a higher frequency than would the correct eigenfunction. The next eigenfunction, or "first harmonic," can also be obtained from the Rayleigh-Ritz Principle. It is that function $y_2(x)$ which is orthogonal to $y_1(x)$ and which satisfies the same minimum condition, and so forth for y_3 orthogonal to both y_1 and y_2 , etc. Only the fundamental is of interest, however.

In the case of the correct eigenfunction for the bar, one might compute

$$\lambda_1^4 = \frac{\int_0^h \left(\frac{d^2 y_1}{dx^2}\right)^2 dx}{\int_0^h y_1^2 dx}$$

obtaining

$$\frac{12.4}{h^4} = \frac{(\pi\beta_1)^4}{h^4}.$$

For the static deflection function, the same result may be obtained for λ_1^4 . Thus, the resonant frequency can be found rather accurately from the static deflection functions using the Rayleigh-Ritz Principle.

It may be noted that if a function with the correct shape and which fits boundary conditions is chosen, the Rayleigh-Ritz Principle will give an accurate value of resonant frequency but that much larger errors will appear elsewhere. The 12 percent difference between moments at the base for the static and dynamic deflection functions is a good example. This type of error can be reduced by choosing an approximate function which has the shape one would expect, fits boundary conditions, but has one or more free parameters which can be adjusted to minimize the ratio of the integrals. For example, the static deflection function (19) on page 77 was essentially

$$F(x) = \frac{x}{h}^4 - 4 \frac{x}{h}^3 + 6 \frac{x}{h}^2. \quad (24)$$

The multiplying factor makes no difference in the ratio of the two integrals since it cancels out.

If $\xi = \frac{x}{h}$, then

$$F(\xi) = \xi^4 - 4 \xi^3 + 6 \xi^2.$$

To which may be added the term $\gamma \xi^2 (1 - \xi)^4$.*

Then $F(\xi) + \gamma \xi^2 (1 - \xi)^4$ fits boundary conditions for all values of γ , and γ is free to be varied to make the right-hand side of (23) a minimum. Since

$$\frac{d}{dx} = \frac{d}{d\xi} \cdot \frac{1}{h},$$

the ratio of integrals to be minimized is

$$D = \frac{1}{h^4} \frac{\int_0^h \left[\frac{d^2 F}{d\xi^2} + \gamma \frac{d^2}{d\xi^2} \xi^2 (1 - \xi)^4 \right]^2 d\xi}{\int_0^1 [F(\xi) + \gamma \xi^2 (1 - \xi)^4]^2 d\xi}. \quad (24a)$$

Evaluating the numerator and the denominator of (24a), it is found that, except for the factor in $\frac{1}{h^4}$,

$$D = \frac{24}{5} \left(6 + \frac{2\gamma}{21} + \frac{\gamma^2}{21} \right) \frac{1}{2.311 + 0.0137 \gamma}. \quad (25)$$

A term of the order γ^2 appears in the denominator of (25) but may be ignored because of a very small coefficient.

At the minimum $\gamma = -.626$ and $D = 12.43$.

This should be compared to $(\pi/\beta_1)^4 = 12.36$.

* Note that (24) is the only fourth order polynomial which satisfies boundary conditions; hence we must add a higher order polynomial must be added.

The moment at the base is proportional to

$$F''(\xi) + \gamma G''(\xi) = 12 - 2(.626) = 10.75.$$

Thus, the moment has been reduced by a factor of

$$\frac{10.75}{12} = 0.896.$$

Equation 21, page 78, may be corrected by replacing the 2 in the denominator by $\frac{2}{.896} = 2.23$. With this correction, (21) now compares very favorably with the exact results of (22). This is a simple example of the power of the Rayleigh-Ritz technique.

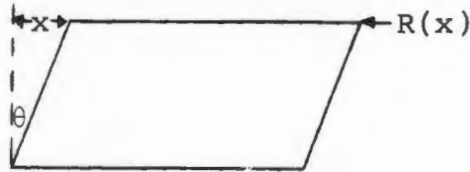
The Rayleigh-Ritz method will be very useful in the analysis of the collapse of multistory framed buildings. For in these buildings, I will vary with height above ground, x , i.e., $I = I(x)$, and the building weight per unit length ($\frac{W}{gh}$ for the homogeneous building) will also vary with x . This variation will generally not be substantial. Thus, $\rho = \rho(x)$ where $\rho(x)$ is the mass per story. With these parameters as functions of x , minimization occurs for the ratio

$$\frac{\int_0^h I(x) \left[\frac{d^2 y}{dx^2} \right]^2 dx}{\int_0^h \rho(x) y^2(x) dx}.$$

With a suitable choice of $y(x)$, the lowest resonant frequency is obtained.

4. Simple One-Dimensional Theory of Building Deflection

Finally, we wish to discuss the relation of the foregoing beam theory to a simple one degree of freedom system which is often used. Referring to the following sketch,



If the resisting moment is replaced by an equivalent resisting force applied at the top of the building, $R(x)$, as shown in the sketch, then

$$I \ddot{\theta} = \frac{hA_F}{2} P_r e^{-\beta t} - R(x)h + W \frac{x}{2} \quad \text{where} \quad (26)$$

$\frac{h}{2}$ = height of the center of pressure above grade, and

$$R(x)h = M(0).$$

The overturning moment due to the weight of the building, $W \frac{x}{2}$, is negligible for the load-bearing building. It is also negligible for any building in the elastic range. Thus, in the elastic range,

$$I \ddot{\theta} = \frac{hA_F}{2} P_r e^{-\beta t} - R(x)h. \quad (27)$$

The moment of inertia, I , is taken to be $I = \frac{Wh^2}{3g}$ since the building rotates about the base plane and not a line. Thus the depth of the building, d , does not come into the moment of inertia. Now, if the restoring moment is linear with respect to x in the elastic range (and this is a good approximation) $R(x) = R_p \frac{x}{x_e} h$ where $R_p h = M_u$. Thus, since $\theta = \frac{x}{h}$

$$\frac{Wh}{3g} \ddot{x} + R_p \frac{x}{x_e} h = \frac{h A_F}{2} P_r e^{-\beta t}$$

or

$$\ddot{x} + \omega^2 x = \frac{3g A_F P_r}{2W} t e^{-\beta t} \quad (28)$$

with

$$\omega^2 = \frac{3g R_p}{W x_e}$$

The solution of (28) is now

$$x = \frac{3g A_F P_r}{2W \omega^2} F(t) \quad (29)$$

where again

$$F(t) = \frac{e^{-\beta t} (-\cos \omega t + \beta/\omega \sin \omega t)}{1 + \beta^2/\omega^2}.$$

The only difference between (29) and the exact equation for the beam (14) from page 75 is a factor of 1.57 for (14), whereas the factor in (29) is $\frac{3}{2} = 1.50$. Also, from the formula for the beam (17), page 76,

$$\omega^2 = \frac{3.52g M_u}{Wh x_e} = \frac{3.52g R_p}{Wx_e}$$

whereas for the one degree of freedom system

$$\omega^2 = \frac{3g R_p}{W x_e}.$$

Thus, the final difference in multiplying factors for the two models is

a factor for the beam = $\frac{1.57}{3.52} = .445$, while a factor for the one

degree of freedom system = $\frac{1.5}{3} = .500$.

The change in ω has some effect on $[F(t)]_{\max}$, of course, but not much.

D. COLLAPSE VULNERABILITY, WALL-BEARING BUILDINGS

1. Structural Characteristics of Wall-Bearing Buildings

A load-bearing structure is one in which the outer walls carry the entire load. In a modern building of this type, the floor supports would be steel beams tied into the walls, and there will be support-

ing steel columns. This steel system, however, carries vertical load only and makes a negligible contribution to flexural strength. A load-bearing situation may be illustrated by Figure 18. The load-bearing walls have thickness τ , the frontal width of the building is "a" and the depth of the building is "d". For a multistory building, τ will change above the second floor from 16" to 12" (in a six-story building, for example). This does not affect deflection of the building appreciably, however. The area moment of inertia of the load-bearing section is next required. Referring to the load-bearing geometrical area as A_B , then

$$I = \int_{A_B} Z^2 ds \quad (30)$$

where Z is measured

from the neutral axis as shown in Figure 18 and I is the area moment of inertia. Thus

$$I = \frac{d^3 \tau}{6} + (a - 2\tau) \frac{d^3}{12} \left[1 - \left(1 - \frac{2\tau}{d} \right)^3 \right]. \quad (31)$$

Since τ is small compared to d, this reduces to

$$I = \frac{d^3 \tau}{6} \left[1 + \frac{3a}{d} \left(1 - \frac{2\tau}{d} \right) \right]. \quad (32)$$

If "S" is the extreme fiber stress in the section (i.e., the outer tensile stress on the front wall, if the load is applied from the front), then the restoring moment is

SCHEMATIC PLAN DRAWING OF A LOAD-BEARING STRUCTURE

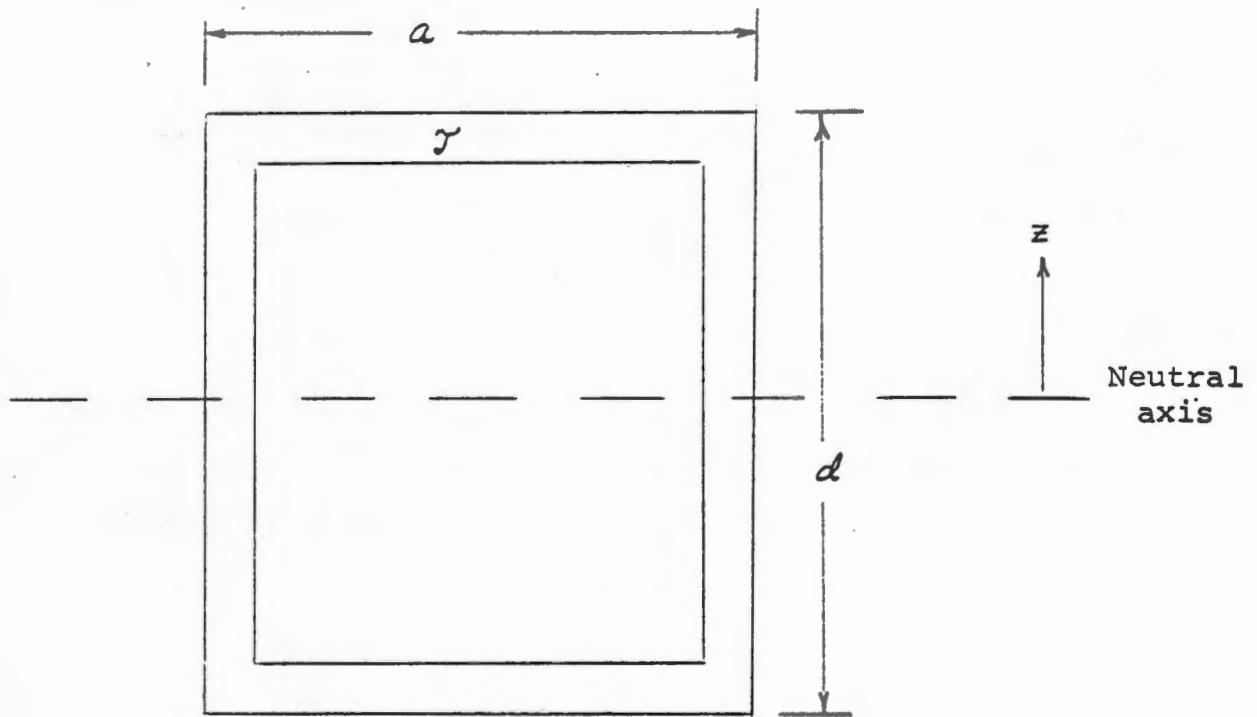


FIGURE 18

$$M = S \int_{A_B} z dz = \frac{\tau d^2}{3} \left[1 + \frac{3a}{d} \left(1 - \frac{2\tau}{a} \right) \right] S. \quad (33)$$

In a load-bearing building with brick walls, the tensile fracture value for S can vary from perhaps 50 psi to 125 psi. A good choice for any building which is not so old that it has lost all bonding of mortar to brick is 100 psi. For the ultimate elastic resisting moment, let $S = S_m$ where S_m equals the fracture stress and dead and live load stress. Thus, the ultimate elastic moment is

$$M_u = \frac{\tau d^3}{3} \left[1 + \frac{3a}{d} \left(1 - \frac{2\tau}{a} \right) \right] S_m. \quad (34)$$

In the case of a concrete bond, this will also be the failure moment.

The area of the load-bearing section is

$$A_B = 2\tau(d+a) \left[1 - \frac{2\tau}{d+a} \right]. \quad (35)$$

Finally, it is necessary to obtain the actual shearing stress distribution in the load-bearing section as a function of the vertical distance from the ground and the distance from the neutral axis. If the loading is a uniform pressure of P_0 (psi), then

$$\begin{aligned}
 x_z &= \frac{6P_0}{d^3} (h - x) (d^2/4 - z^2) \\
 &= \frac{3P_0}{2d} (h - x) (1 - 4z^2/d^2)
 \end{aligned}
 \tag{36}$$

where

h = building heights

z = distance above grade.

The shearing stress occurs in the side walls only and has the usual parabolic distribution versus distance from the neutral axis. Equation (36) is for static deflection; but, as it will be seen, static deflection formulas are adequate when the correct time behavior of the deflection is taken into account. The shearing stress can be an important consideration in load-bearing buildings since it causes bonding failure in the side walls. This shear failure does not materially affect the tensile failure point of the front wall, but it does make the side walls susceptible to being blown in or out by the blast wave.

2. Collapse of a Brick House in Nevada

This house is pictured on page 208 of Reference 9.

The parameters of the house are as follows:

$$a = 35'$$

$$d = 26'$$

$$w = 2.23 \times 10^5 \text{ lbs. (Estimated)}$$

$$\tau = 8'' \text{ (4'' brick and 4'' cinderblock)}$$

$$Q = 3 \times 10^6 \text{ psi (for concrete).}$$

Due to the presence of windows and doors, about 65 percent of the frontal, side, or back of the house may be considered to be either load-bearing or capable of taking tensile stress. Thus, it is reasonable to compute M_u , I , etc. on this basis. About 15 percent of the frontal area is open.

$$\text{Thus, } A_F = .85 \times 3.5 \times 1.8 \times 1.44 \text{ in.}^2 \times 10^4 = 7.7 \times 10^4 \text{ in.}^2.$$

The dead load stress on the bearing portion of the house is

$$\frac{W}{2(26+35)96 \times .65} = \frac{2.23 \times 10^5}{7.6 \times 10^3} = 29 \text{ psi.}$$

A good figure for the tensile strength of the brick-mortar or cinder-block mortar bond is about 100 psi. It can, of course, vary from a low value for very old masonry structures to perhaps 125 psi for the best.

The tensile yield stress may be set at

$$S_M = 100 + 29 = 129 \text{ psi.}$$

The shear yield stress is about 64 psi or

$$x_y = 64.$$

Using equation (32) from page 87,

$$I = .8d^3 \tau = 1.35 \times 10^6 \text{ ft.}^2 \text{ in.}^2$$

and from (33)

$$M \cong .65 (1.6) \tau d^2 S$$

$$M_u \cong .65 (1.6) \tau d^2 S_M = 8.7 \times 10^6 \text{ ft. lb.}$$

Then from (16) on page 76

$$x_e = 2.1 \times 10^{-4} \text{ ft.}$$

and from (17) on page 76

$$\omega^2 = 1.17 \times 10^6.$$

Referring to the loading diagram (Figure 18, p. 88), one has $\beta \cong 31$.

Thus, β/ω is small and

$$[F(t)]_{\max} \cong 1.91.$$

From (21), page 78

$$A_F P_r = \frac{W \omega^2 x_e}{[F(t)]_{\max} 1.57g} = 5.7 \times 10^5$$

or $P_r = 7.4$ psi

$P_\sigma = 3.4$ psi.

The time to tensile failure is given approximately as

$$\omega t = \pi$$

where $t = 2.9 \times 10^{-3}$ seconds.

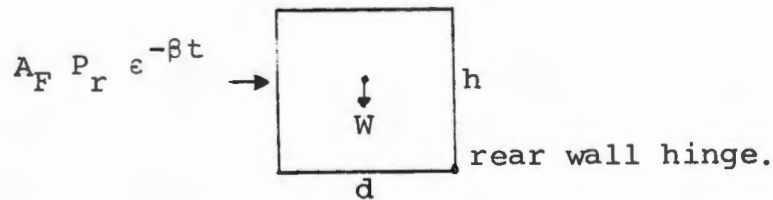
The side walls of the house can fail in shear prior to failure of the front wall in tension. First failure would normally occur at the center of the side wall at the first-floor level. The chimney on the right of the house strengthens the house in shear. Thus, a good estimate of shear failure is difficult. Further, if the front does not fail in tension, the shear failure would probably consist of hairline cracks in the masonry which would not be observable. For larger buildings shear failure in the walls can, presumably, result in the side walls being blown in or out, depending on the pressure differential. In the house, the time of maximum deflection and then recovery is so fast that any outside-inside pressure differential would be working against high compressive forces on the front or rear of the side wall at least half of the time. Incipient shear failure may be estimated at $P_\sigma \cong 2$ psi. However, in all likelihood there would be no observable effects at this overpressure level.

Since the time to front wall failure is so short, the blast wave may be expected to collapse the front wall and enter the house with little diminution from initial reflected pressure strength. Thus, the side walls would probably blow outward, and the end wall would go at about the

same time. In other words, the failure would be catastrophic.

3. Failure of a Multistory Load-Bearing Building

The large load-bearing building can fail in tension on the blast side as the house did. However, the dead weight load of the building is high, and tensile failure itself cannot be considered sufficient for building collapse. At the time of tensile failure on the blast side, there will be shear failure on the side walls to a considerable height. The dead weight will hold the building together, however, unless the blast force is sufficient to rotate the building about the rear wall enough to allow time for front wall failure. Refer to the following figure.



It is required that at the time of tensile failure

$$A_F P_r e^{-\beta t} \frac{h}{2} > W \frac{d}{2} .$$

A good criterion for massive failure is that the front walls tension long enough for the 16-inch wall near the base of the building to move 8" to 16". Eight inches is, perhaps, enough.

An example of a specific building is now taken with the following description:

$$h = 78'$$

$$a = d = 60'$$

$$\tau = \text{wall thickness} = 16'' \text{ for first two stories}$$

$$\tau = 12'' \text{ upper stories}$$

$$W = 5.1 \times 10^6 \text{ lbs.}$$

$$\% \text{ window openings} = 20\%$$

$$\% \text{ effective bearing area at grade level} = 70\%$$

$$\text{Dead weight stress on bearing area} = 160 \text{ psi}$$

$$S_M = 260 \text{ psi}$$

$$I = 2.76 \times 10^7 \text{ in.}^2 \text{ ft.}^2$$

$$M_u = 2.40 \times 10^8 \text{ ft.} \cdot \text{lbs.}$$

$$\beta = 16.7 \text{ sec.}^{-1}$$

$$Q = 3 \times 10^6 \text{ psi.}$$

Then

$$x_e = 5.0 \times 10^{-3} \text{ ft.}$$

$$\omega^2 = 1.37 \times 10^4 \text{ sec.}^{-2}$$

$$\omega = 1.17 \times 10^2 \text{ sec.}^{-1}$$

$$\beta/\omega = .143$$

$$[F(t)]_{\max} = 1.63$$

$$A_F P_r = 4.23 \times 10^6 \text{ lbs.}$$

$$A_F = .8(7.8) \cdot .60(1.44) \times 10^5 = 5.39 \times 10^5 \text{ in.}^2$$

$$P_r = 7.8 \text{ psi}$$

$$P = 3.7 \text{ psi}$$

$$\text{Time to failure} = 2.7 \times 10^{-2} \text{ sec.}$$

$$\text{At } t = t_f, P_r, e^{-\beta t_f} = 5.1 \text{ psi.}$$

The blast force at $t = t_f$ is not, however, sufficient to rotate the building. Thus, building failure in this case does not depend on tensile strength of the front wall except for the time required to reach tensile failure.

Next the time required to move a section of the front wall approximately 12" is considered. For convenience the section area is taken to be 1 ft.², and an average value for P_r of $\overline{P_r}$ is used. We have

$$W = 4/3 \times 120 = 160 \text{ lbs.}$$

$$F = \overline{P_r} \times 144.$$

Then

$$\frac{W}{g} x = 144 \overline{P_r} t^2$$

or

$$x = \frac{72g \overline{P_r}}{W} t^2.$$

Since $x = 1 \text{ ft.}$

$$t = \sqrt{\frac{W}{72g \overline{P_r}}} = \frac{.262}{\sqrt{\overline{P_r}}}$$

which yields values given below.

\overline{P}_r	$t(\text{sec})$
8	.093
10	.083
12	.076
16	.066

The equation for building rotation is

$$I \ddot{\theta} = A P'_r e^{-\beta t} \frac{h}{2} - \frac{Wd}{2}$$

$$I \ddot{\theta} = \frac{A_F P'_r h}{2\beta^2} (\epsilon^{-\beta t} + \beta t - 1) - \frac{Wd}{4} t^2.$$

The value θ starts at zero, goes to a maximum and then returns to zero again. The wall is in tension until θ reaches its second zero. Thus let

$$\frac{Wd}{4} t^2 = \frac{A_F P'_r h}{2\beta^2} (\epsilon^{-\beta t} + \beta t - 1).$$

Under the higher values of \overline{P}_r , the time to tensile failure is very short. Setting $P'_r = P_r$,

$$\beta^2 t^2 = \frac{2A_F P_r h}{Wd} (\epsilon^{-\beta t} + \beta t - 1).$$

Now

$$\overline{P_r} = \frac{P_r + P_\sigma}{2}.$$

With $\overline{P_r} = 10$, for example, $P_r = 14$, $P_\sigma = 6$.

So

$$\xi^2 = 2.70 (\epsilon^{-\xi} + \xi - 1)$$

where $\xi = \beta t$.

It is found that $\xi = 1$ or $t = 1/\beta = .06$ sec.

Since this is not quite enough time, try $\overline{P_r} = 12$ or $P_r = 17$, $P_\sigma = 7.1$.

Then

$$\xi^2 = 3.14$$

$$\xi = 1.5 \quad t = 0.09 \text{ sec.}$$

Thus, the building fails for P_σ between 6 and 7 psi. Since 7 psi is surely adequate, this value is chosen. Note that there can be pressure buildup inside the building which will act against front face pressure. However, at 7 psi interior partitions will probably go, and the shock cannot return from the rear building wall in time to affect this failure.

4. Some General Considerations on Load-Bearing Buildings

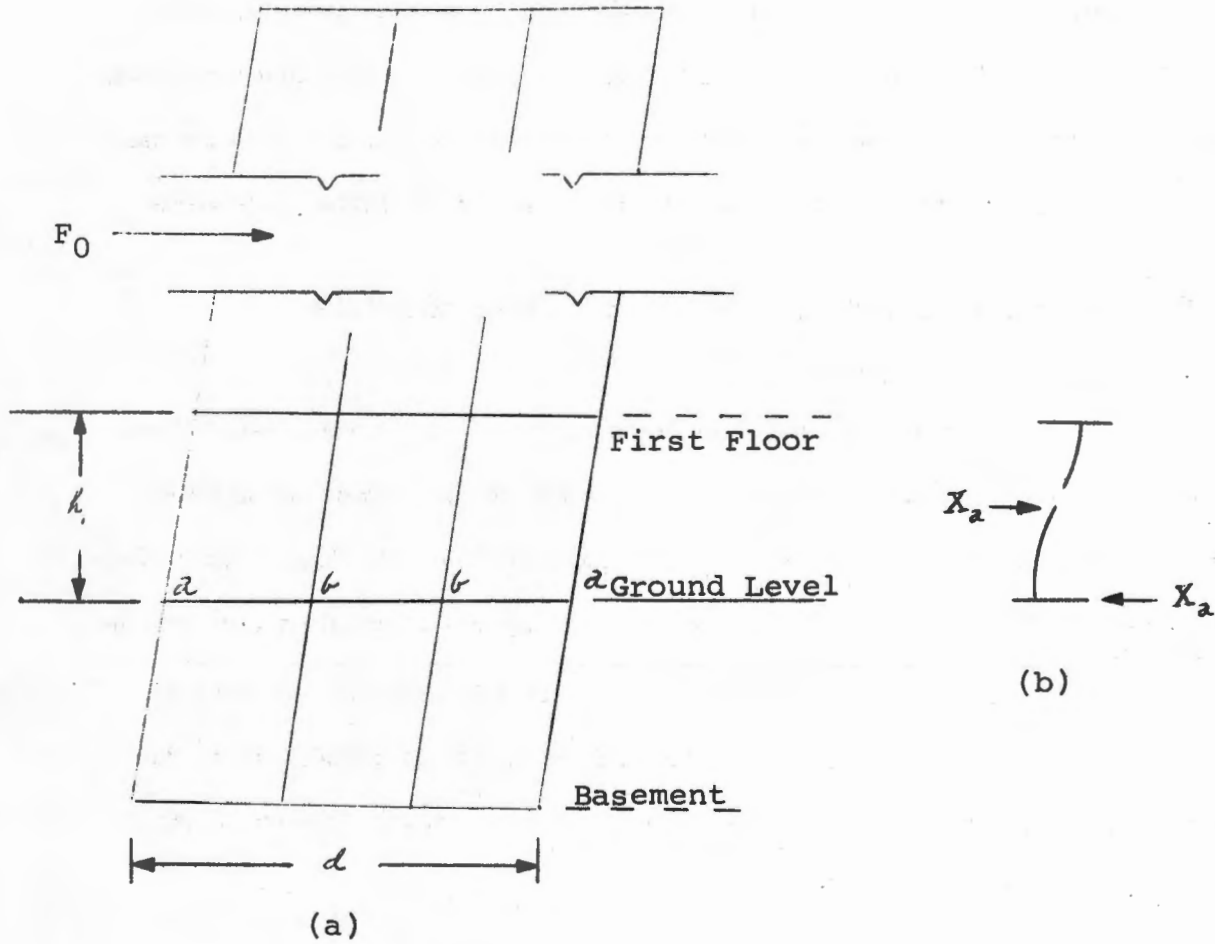
The direct failure of a wall on the blast side becomes the primary mode of failure for deep squat, load-bearing structures and also for the upper stories of high buildings without regard to the "racking" type of action we have just discussed. Wall failure in the upper stories cannot be considered as massive building failure. Such wall failure can occur, however, as the height-to-depth ratio of the building decreases.

E. COLLAPSE VULNERABILITY, MULTISTORY FRAMED BUILDINGS

1. Column Response

In the usual elastic methods of building design, each floor of the building is assumed to deflect the same amount under an applied load F_0 . This amounts to a linear deflection of the building. The value F_0 is usually a wind load, and of course, it may be assumed to act at the center of pressure which is half way up the building for a building of uniform width and open area. Now, the linear deflection model puts the columns into contraflexure at mid-height. Thus, a given ground floor column appears as shown in Figure 19.

There are, however, serious logical difficulties to this model. First, let us refer to Figure 19(a) where the building is shown with four ground floor columns illustrated. In an actual building to be discussed later, there will be 10 rows of columns laterally with each row consisting of four columns in depth. Thus, if F_1 were the total force on such a building, the force F_0 assigned to any row would be $F_1/10$. Now, the applied force F_0 corresponds to an applied moment of $F_0 h/2$. This moment cannot be balanced, however, by the bending moments in the four ground floor



COLUMN RESPONSE SCHEMATIC FOR
MULTISTORY FRAMED BUILDINGS

FIGURE 19

columns.

Let the "a" columns have area moment of inertia I_a and "b" columns I_b . Now, let the shears at the base of the columns be X_a and X_b . Then it is necessary that

$$F_0 = 2 (x_a + x_b). \quad (37)$$

All columns are assumed to have the same deflection, i.e., perfectly rigid connections between columns, so that X_a and X_b satisfy the relation

$$\frac{X_a}{X_b} = \frac{I_a}{I_b} \quad (38)$$

Equations (37) and (38) determine X_a and X_b uniquely in terms of F_0 .

Turning to Figure 19(b), an illustration of an "a" column cut at the point of contraflexure, a force X_a , as shown in the figure, will be required at the point of contraflexure to keep the lower half of the column in equilibrium. The moment about the base of X_a is $M_a = X_a \frac{h_1}{2}$ where h_1 is the first-story height. The total moment which all four columns can supply is

$$M_1 = 2 (X_a + X_b) \frac{h_1}{2} = F_0 \frac{h_1}{2}. \quad (39)$$

But the applied moment on the building is

$$M = F_0 \frac{h}{2}. \quad (40)$$

For a relatively tall building, h is very much greater than h_1 , so that $M_1 \ll M$.

The situation may be summarized as follows:

- The shears in the columns at ground level are uniquely determined by the applied force F_0 .
- The column shears uniquely determine the column moments at the base.
- The sum of the column moments, so computed, can by no means supply the required restoring moment.

The above discussion has been based entirely on the assumption that ground floor column contraflexure occurs at mid-height. The question of what the columns actually do is left for the moment to consider the source of the great bulk of the restoring moment.

To this point in considering column deflection, the shear and moment at the column base have been shown to be determined by the applied force. The other possible forces in the columns are "net" tensile and compressive forces. A "net" tensile force corresponds to a "net" stretching of a column above its equilibrium length when under compression from dead and live load. "Net" compression has the same meaning. Distributed tensile and compressive forces are shown in Figure 20.

DISTRIBUTED TENSILE AND
COMPRESSIVE FORCES ON COLUMNS

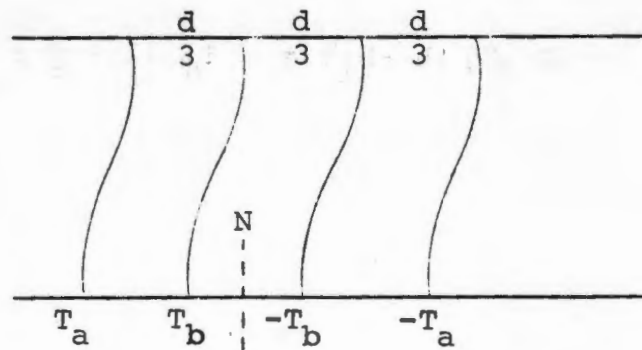


FIGURE 20

The columns are a distance $d/3$ apart. The tensile forces are T_a , T_b , while $-T_a$ and $-T_b$ are compressive forces. The distance of the "b" columns from the neutral axis N is $d/6$; the distance of the "a" columns from N is $d/2$. Tension-compression stresses vary linearly. Thus $\frac{T_b}{A_b} = \frac{1}{3} \frac{T_a}{A_a}$, and the restoring moment is

$$M_d = 2 \left[T_a \frac{d}{2} + T_b \frac{d}{6} \right] = d T_a \left[1 + \frac{1}{9} \frac{A_b}{A_a} \right]$$

A_a = area of a "a" column

A_b = area of a "b" column.

Thus, for equilibrium

$$M - M_1 = M_d \tag{41}$$

or

$$(F_0/2) (h - h_1) = d T_a \left[1 + \frac{1}{9} \frac{A_b}{A_a} \right]$$

whence

$$T_a = \frac{F_0}{2d} \frac{(h - h_1)}{1 + 1/9 A_b/A_a} \quad (42)$$

Under the tensile force, T_a , the first column will elongate by an amount

$$\frac{T_a}{A_a} = Q \frac{\Delta h_1}{h_1} \quad \text{where} \quad (43)$$

Q = Young's Modulus for steel

Δh_1 = Column elongation.

This column elongation on the windward side and similar compressions on the lee rotates the first floor through an angle θ as given by

$$\theta = \frac{\Delta h_1}{d/2} = \frac{2\Delta h_1}{d} \quad (44)$$

To summarize:

- The assumption of contraflexure at the column mid-points implies a tensile force T_a as given by (42); T_a then implies a Δh_1 , as given by (43) which, in turn, implies that the first floor rotates through an angle given by (43).

- The angle of rotation θ , as given by (44), in turn determines whether the column is or is not in contraflexure.

Calculations indicate, however, that the point of contraflexure is raised slightly; but the amount is so small that it can be neglected.

2. Calculation of Building Resistance for Steel Frame Buildings

The method of calculating maximum building resistance and the numerical result is considered important to a discussion of the collapse of steel frame buildings. This is now presented to provide additional foundation for the treatment of steel frame buildings to follow. Although the following discussion pertains to steel frame buildings, the method is equally applicable to r.c. frame buildings. The chief difference between the collapse of the two types lies not in the maximum resistance but in the behavior of the concrete under compression after the point of maximum resistance is reached in any given column.

In the discussion, the ultimate value of the column modulus, i.e., the plastic value, is taken as the value which corresponds to zero net vertical load. This might seem strange since the vertical loads on many columns will be quite high. However, this approximation is best for simplifying the calculations since, as mentioned earlier, the net distributed tensile and compressive forces account for the bulk of the restoring moment. This, in turn, affects the ultimate column moments in bending, and the two restoring moments must be self-consistent.

It was earlier noted that for relatively high buildings, the distributed first-floor column moments dominate the total restoring moment. Thus, referring to equations (39) and (40), pages 101 and 102,

$$\frac{M_1}{M} = \frac{h_1}{h} \quad \text{where}$$

M_1 = total column moment per bent for flexural bending only

M_d = distributed moment per bent

h_1 = first-story height

h = building height.

If all stories have the same height h_1 , and if there are n stories, then

$$\frac{M_1}{M} = \frac{1}{n} \quad (46)$$

and putting

$$M \left(1 - \frac{1}{n}\right) = \frac{1}{n} M_d$$

or

$$M_d = M_1 (n-1). \quad (47)$$

To show now how the maximum building resistance is calculated from the column bending moments per bent, M_1 , a specific example is used such as the twenty-story building to be discussed later commencing on page 119. The exterior columns are 14-WF-246, and the interior columns are 14-WF-426. Under a combination of net compression and bending,

these columns have an ultimate section modulus $S = I/C^*$, which we may compare with the elastic section modulus. Using the "Manual of Steel Construction," AISC, Sixth Edition, the comparison is as follows:

TABLE 11
Elastic Section Modulus Compared to Ultimate Section Modulus for Two Columns

Column Type	S_e (elastic I/C^3) in. ³	S_p (plastic or ultimate I/C^3) in. ³
14-WF-246	397	465
14-WF-426	707	869

The plastic moduli are higher by 12 percent to 17 percent.

Under a condition of no column deflection, each column will have a fixed compressive stress due to building dead and live load called S_D . It is unfortunate that the same letter S is used for section modulus (in.³) and for stress (lbs./in.²); however, the subscripts help remove confusion.

As the columns are allowed to deflect under blast loading, one of two things will happen, i.e.:

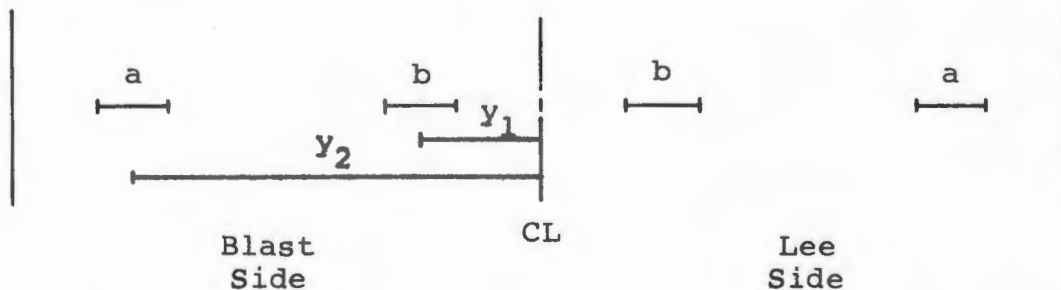
- The blast side columns will go into net tension before reaching plasticity.

* The ultimate section modulus used is the one which is correct for zero net loading on the columns.

• The blast side columns will remain in net compression until fully plastic.

The first case occurs when the building is very high compared to its depth. Since the example twenty-story building is over four times as high as it is deep, the blast side columns do, indeed, go into net tension prior to full reaching plasticity. In other words the uplift stress, S_u , due to the distributed moment M_d , exceeds the dead and live stress S_D . In this case, the tensile value of S_p should be used, and it is lower than S_p for net compression. Use of the values of S_p in Table 11 causes an error of less than 5 percent, small enough to ignore. For almost all high buildings, all columns will be in net compression until failure.

Referring to the sketch below, the calculation is carried out as follows:



Let

S_u = uplift stress in the outer blast side column

S_M = maximum elastic stress for the column steel
(plastic point)

S_{Do} = dead load stress in the outer columns

S_{Di} = dead load stress in the inner columns

M_u = ultimate value of column bending moment per bent
= M_1 (Max)

S_{po}, S_{pi} = ultimate I/C for outer and inner columns respectively.

Let us take the first case, where blast side columns go into net tension prior to failure.

In this case the effective failure stress is $S_M - (S_u - S_D)$, and first plasticity occurs on the tensile side of the column. To put this another way, if S_B is the maximum tensile stress due to bending only, then the outer fibre stress is

$$S = S_B + S_u - S_D \quad (48)$$

The column fails when $S = S_M$, and at this point $S_B = S_M - (S_u - S_D)$.

The maximum column restoring moment is determined by S_B and is equal to

$S_B S_{po}$. Thus, for the outer blast side column

$$M_u (B) = \left[S_M - (S_u - S_{Do}) \right] S_{po}$$

(B) stands for blast side.

But the identical column on the compression side has

$$M_u (L) = \left[S_M - (S_u + S_{Do}) \right] S_{po} ,$$

since it fails on the compression side, and S_u is a compressive force on the leeward side. Here (L) stands for lee side.

Thus, it is that

$$M_u (B) + M_u (L) = 2 (S_M - S_u) S_{po} \quad (49)$$

The two inner columns will always be in net compression so that their moments will be respectively

$$M_u (B) = \left[S_M - (S_{Di} - S_u) \right] S_{pi}$$

and

$$M_u (L) = \left[S_M - (S_{Di} + S_u) \right] S_{pi} \quad (50)$$

and the sum of the two is just

$$2(S_M - S_{Di}) S_{pi}.$$

Thus, the total column ultimate restoring moment is

$$M_u = 2 \left[(S_M - S_u) S_{po} + (S_M - S_{Di}) S_{pi} \right]. \quad (51)$$

The distributed moment when the column moments reach their ultimate values is

$$M_{ud} = 2(N-1) \left[(S_M - S_u) S_{po} + (S_M - S_{Di}) S_{pi} \right]$$

and this expression is in inch-pounds. Converting to foot-pounds, we have

$$M_{ud} = \frac{2(N-1)}{12} \left[(S_M - S_u) S_{po} + (S_M - S_{pi}) S_{pi} \right]. \quad (52)$$

But M_{ud} is also given by

$$M_{ud} = 2 S_u \left[A_a Y_2 + A_b Y_1 \frac{y_1}{y_2} \right] \quad (53)$$

where A_a, A_b are the areas of the respective columns and $S_u(y)$ is distributed linearly across the building, i.e.,

$$S_u(y) = S_u \frac{y}{y_2}$$

S_u is obtained by solving (52) and (53) simultaneously. The total building ultimate moment is then

$$M_{uT} = M_u + M_{ud} = hR_p = \frac{N}{N-1} M_{ud} \quad (54)$$

(This result is per bent.).

The simultaneous solution of (52) and (53) may yield a value of S_u which is smaller than S_{Do} . When this occurs (second case above), the expression for $M_u(B)$ for the outer blast side column is wrong and must be rewritten as

$$M_u(B) = \left[S_M - (S_{Do} - S_u) \quad S_{po} \right].$$

The total column bending restoring moment is now

$$M_u = 2 \left[(S_M - S_{Do}) S_{po} + (S_M - S_{Di}) S_{pi} \right]. \quad (55)$$

In other words, just replacing S_u by S_{Do} in (51) gives

$$M_{ud} = \frac{N-1}{6} \left[(S_M - S_{Do}) S_{po} + (S_M - S_{Di}) S_{pi} \right] \quad (56)$$

and

$$hR_p = \frac{N}{6} \left[(S_M - S_{Do}) S_{po} + (S_M - S_{Di}) S_{pi} \right] \quad (57)$$

(This result is also per bent.).

In the case of the twenty-story steel frame building to be described in more detail later, let

$$\begin{aligned} A_a &= 72.3 \text{ in.}^2 \\ A_b &= 125.2 \text{ in.}^2 \\ S_{Di} &= 10.0 \text{ kpsi} & S_{Do} &= 13.2 \text{ kpsi} . \end{aligned}$$

Solving (52) and (53) simultaneously, results in

$$\begin{aligned} S_u &= 22.4 \text{ kpsi} \quad (\text{This is greater than } S_{Do}.) \\ M_{ud} &= 11.6 \times 10^7 \\ M_{ut} &= 1.22 \times 10^8 \quad (\text{per bent}) . \end{aligned}$$

And, since there are 10 bents,

$$hR_p = 10 M_{ut} = 1.22 \times 10^9$$

$$R_p = \frac{1.22 \times 10^9}{240} = 5.1 \times 10^6 \text{ lbs.}$$

In this calculation of R_p , all stories are set at equal heights. Thus, the first-story height is 12', and the building height is 240'. This change has no appreciable effect on the building strength. The steel used has a static yield point of 33,000 kpsi with an increase of 25 percent allowed for dynamic effects. For deeper buildings, the calculation of building strength proceeds in an identical way. For example, with a building 100' deep, a typical design for a twenty-story building might use 14-WF-202 exterior columns and 14-WF-342 interior columns.

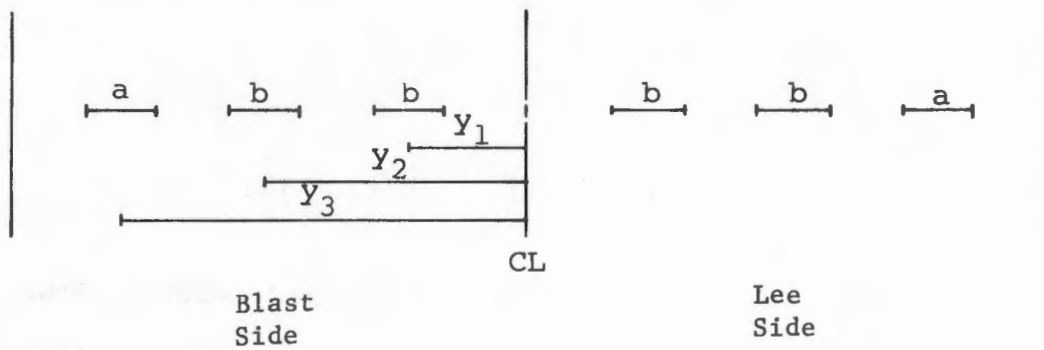
The parameters of these are:

Table 12

Column Parameters for Twenty-Story Building with 100-Foot Depth

Designation of Column	Column Type	Area (in. ²)	S_e (in. ³)	S_p (in. ³)	S_D (kpsi)
a	14-WF-246	72.3	397	465	13.2
b	14-WF-426	125.2	707	869	10.0

Using 20-foot bays as before, the building column plan looks as shown below:



Assuming $S_u > S_{Do}$ in the blast side column, then again

$$M_u = 2(S_M - S_u) S_{po} + 4 (S_M - S_{Di}) S_{pi} \quad (58)$$

and

$$M_{ud} = \frac{N-1}{12} M_u \quad (59)$$

But M_{ud} is again given by the distributed moment as

$$M_{ud} = 2 S_u \left[A_a y_3 + A_b \frac{y_2^2}{y_3} + A_b \frac{y_1^2}{y_3} \right] \quad (60)$$

$$y_3 = 50'$$

$$y_2 = 30'$$

$$y_1 = 10' .$$

Were (59) and (60) to be solved simultaneously for S_u , it might well be found that $S_u < S_{Do}$. A quick way to check this is to note that as S_u increases from zero to any given value, M_{ud} , as given by (60), increases, and M_{ud} , as given by (59), decreases. Hence, if S_u is set equal to S_{do} and if (60) is greater than (59), the solution must occur for a smaller value of S_u , i.e., some value for which $S_u < S_{Do}$. However, (59) with S_u replaced by S_{Do} is then, as shown previously, the correct value of M_{ud} . Calculating (60) gives

$$M_{ud} = 2(16.1) \times 10^3 \left\{ 59.4 (50) + 100.6 \left[\frac{900}{50} + \frac{100}{50} \right] \right\}$$

$$= 1.60 \times 10^8 .$$

From (59)

$$M_{ud} = \frac{19}{12} \left[2(41.6 - 16.1)374 + 4 (41.6 - 12.5) 673 \right] \times 10^3$$

$$= 1.46 \times 10^8 .$$

Thus, $S_u < S_{Do}$, and the building resistance is given by (59), i.e.,

$$M_{ut} = \frac{20}{19} M_{ud} = 1.62 \times 10^8$$

or

$$R_p = \frac{16.2 \times 10^7}{2.4 \times 10^2} = 6.75 \times 10^5 \text{ ft.-lbs. per bent.}$$

Again if the building has 10 bents,

$$R_p = 6.75 \times 10^6 .$$

Having discussed the calculation of maximum resistance for two buildings, the natural question which arises is, "Why has the ultimate section modulus for pure bending been used when it is clear that the net vertical loads on many columns are high?"

The easiest way to check on the accuracy of the answer is to go to the actual bending moment-vertical load reaction curves for the columns in question. If we do this, we find that the resistance, based on this presumably more accurate calculation, is about 8 percent higher for the 100-foot deep building and that the two answers are within 1 percent or 2 percent for the 60-foot deep building. However, it must be remembered that a 25 percent increase in yield stress was allowed for dynamic loading and this estimate is really not that accurate. Thus, the procedure used above is recommended as a quick way to estimate building resistance. For a wide range of height-to-depth ratios, the average error is only 5 percent.

3. Characteristics of a Twenty-Story Steel Frame Building

The particular building in question has the following parameters:

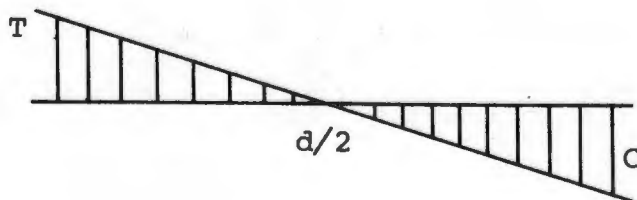
$$\begin{array}{ll}
 a = 180' \text{ (frontal width)} & \% \text{ Open Area} = 30\% \\
 d = 60' \text{ (depth)} & A_F = 4.53 \times 10^6 \text{ in.}^2 \\
 w = 4.3 \times 10^7 \text{ lbs.} & h_1 = 16' . \\
 h = 246' \text{ (height)} &
 \end{array}$$

On the ground floor there are 10 rows of columns each with the following properties:

$$\begin{array}{cccc}
 \overline{\quad a \quad} & \overline{\quad b \quad} & \overline{\quad b \quad} & \overline{\quad a \quad} \\
 A_a = 72.3 \text{ in.}^2 & & A_b = 125.3 \text{ in.}^2 & \\
 \frac{I_a}{C_a} = S_a = 397 \text{ in.}^3 & & \frac{I_b}{C_b} = S_b = 707 \text{ in.}^3 . &
 \end{array}$$

The columns are spaced 20' apart.

For this particular building $\frac{h_1}{h} = .065$; thus the column moments can supply only 6.5 percent of the restoring moment. This means that the real restoring force at the base is a distributed tension-compression force in the columns as shown below and as discussed earlier.



Even half way up the building where the story height is 12',

$$\frac{h_1}{h} = \frac{12}{123} = .09;$$

the distributed moment entirely swamps the column moments. In other words, the building behaves more like a beam than like a linearly deflected structure, which is the usually assumed deflection. It will be noted that the restoring moment of a homogeneous beam varies as $(1 - \frac{x}{h})^2$, where x is the height above ground floor. Thus, the moment half way up the building is only one-fourth that at the base. The Rayleigh-Ritz integral which determines the fundamental frequency has an integrand in the numerator which varies as $(1 - \frac{x}{h})^4$, and at mid-height the integrand is only one-sixteenth that at the base. Hence, the fundamental frequency is not very sensitive to what goes on above mid-height except for variations in area moment of inertia. The weight per unit height does not change appreciably.

Going up in the building, the area moment of inertia becomes smaller.

On the beam theory, the area moment of inertia at the bottom is

$$I_0 = 20 [A_a R_a^2 + A_b R_b^2] \quad (61)$$

$$\text{If } R_a = 30', R_b = 10' .$$

This gives

$$I_0 = 1.55 \times 10^6 \text{ in.}^2 \text{ ft.}^2$$

Note that the factor of 20 comes into (61) because there are 20 columns of type "a" and 20 of type "b".

An adequate approximation for the area moment of inertia when going up in the building is

$$I = I_0 (1 - \xi); \quad \xi = \frac{x}{h} .$$

The area moment of inertia does not, of course, go to zero at the top, but what happens above mid-height has little bearing on either the strength of the building or the fundamental frequency.

Using the assumed variation of I , the static deflection function becomes

$$y(x) = \frac{a P_r h^4}{12QI_0} \xi^2 (3 - \xi) = \frac{A_F P_r h^3}{12QI_0} \xi^2 (3 - \xi) . \quad (62)$$

Using (62) in the Rayleigh-Ritz integrals, it is found that

$$\omega = 4.65 \text{ sec.}^{-1} \quad t = 1.35 \text{ sec.}$$

Going to a higher degree of approximation by using the function

$F + \gamma G$, where

$$F(\xi) = \xi^2 (3 - \xi)$$

$$G(\xi) = \xi^2 (1 - \xi)^3$$

and γ is a parameter,

the value of which minimizes the ratio of integrals in the Rayleigh-Ritz expression, it is then found that

$$\omega = 4.57 \text{ sec.}^{-1} \quad t = 1.37 \text{ sec.}$$

All of these calculations are based, of course, on a rigidity of the footings. Ground floor motion of the footings would lead to damping which would show an apparently longer period.

4. Failure of a Twenty-Story Steel Frame Building

There are at least three end points for building failure:

- Punching of the footings on the compression side (away from the blast)
- Buckling of the columns on the compression side
- Rotation of the building about plastic hinges at the base of columns at first-floor level until the building topples.

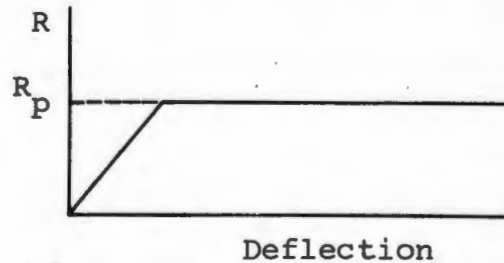
The last mode of failure can be easily investigated. The first failure mode is difficult, if not impossible, to assess since it depends on soil properties. The second mode, while not generally occurring, can be assessed. This mode might be accompanied by shearing of the footing connections on the tension side. Note here that the distributed tension-compression moment places the footings under severe tension and punching

forces. Compression is the most severe; tension only occurs with some buildup.

The following calculation of building failure is for the last listed mode. The columns on the compression side fail first with

$$R_p = 5.1 \times 10^6 \text{ lbs. at full plasticity.}$$

A value for x_e corresponding to R_p is used. In the calculation of ω , R_t is used as a compromise. This gives a period somewhat longer than the "true" period of 1.37 sec. In fact, the period used in the calculation turns out to be 1.54 sec. and $x_e = 1.22$ ft. However, some compromise is necessary to permit use of an ideal elastic-plastic curve as shown below.



With a conventional computation of loading, it is found that

$$\beta = 7.28 \text{ sec.}^{-1} \text{ and}$$

$$\omega = \frac{2\pi}{1.54} = 3.79 \text{ sec.}^{-1}$$

The one degree of freedom model outlined previously is also used.

Calculation of failure then proceeds as follows.

For any initial value of P_r , the velocity of the center of mass of the building $x = x_e$ turns out to be

$$v_0 = \frac{3g A_F P_r}{2\omega W} \sin\omega t - \beta x_e. \quad (63)$$

At the end of the elastic range, the equation of motion is

$$\ddot{x} + \frac{3g R_p}{W} \dot{x} - \frac{3g}{2h} x = \frac{3g P_r A'_F}{2W} e^{-\beta t}, \quad (64)$$

where

$$P'_r = P_r e^{-\beta t_e},$$

and t_e is the value of t when $x = x_e$. The solution of (64) is of the form

$$x = \frac{2h R_p}{W} + A e^{-\beta t} + B e^{-\sigma t} + C e^{\sigma t} \quad (65)$$

where

$$\sigma = \sqrt{\frac{3g}{2h}}$$

and at $t = 0$, $x = x_e$, and

$$\dot{x} = v_0.$$

Looking at (65), collapse just occurs when $C = 0$.

This leads to the condition

$$v_0 = \left(\frac{2h R_p}{W} - x_e \right) \sigma - \frac{\alpha}{\beta + \sigma} \quad (66)$$

where

$$\alpha = \frac{3g A_F P_r'}{2W} .$$

The problem is to select v_0 such that $C = 0$. This is done by successive approximations. In fact, P_r is related to t_e by the equation for the elastic range, i.e.,

$$x_e = \frac{3g A_F P_r}{2W \omega^2} F(t_e) . \quad (67)$$

This gives P_r versus t_e since x_e is known.

Knowing P_r versus t_e , v_0 may be calculated from (63) and from (66). At some t_e and corresponding P_r , v_0 as calculated from (63) will match v_0 as calculated from (66). This, then, gives the correct P_r .

For the twenty-story steel frame building 60 ft. deep described on page 119, it is found that

$$P_r = 35.5 \text{ psi}$$

$$P_\sigma = 13.3 \text{ psi} .$$

The overpressure required for toppling the building is then about 13 psi.

The above calculation has been made using diffractive forces only. If drag forces are added for say a 1 MT to 20 MT weapon, the calculated failure overpressure is $P_o = 10$ psi. A similar calculation was made for a twelve-story steel frame building with $a = 150'$ and $d = 60'$, with drag forces included. The result for collapse overpressure was $P_o = 14$ psi.

The really important conclusion from this analysis is that the building acts like a beam and that the distributed tension-compression force across the building governs the mode of failure.

The building has two modes of deflection: the beam type mode and the lateral deflection due to column contraflexure. This latter mode gives a substantially larger deflection but is of little interest insofar as massive failure is concerned. The beam type action gives a smaller deflection but is related to the large restoring moment across the building and hence must be considered the only deflection of interest for calculation of massive failure.

F. VULNERABILITY OF CURTAIN WALLS AND PARTITIONS

1. Introduction

The following analysis of panels and curtain walls starts with static strength data taken at the National Bureau of Standards. It is shown that the shear stress failure point is a function of A_n/A , for the type of panels considered here. A_n is the actual bearing area of a

hollow tile or concrete block, and A is the total plan area.

The static data are then used to predict panel response in the 1953 FCDA tests carried out in Nevada. Punching shear is assumed to be the important and controlling mode of failure when the failure is explosive. The static ultimate shear data are shown to fit the Nevada results as well as, or perhaps better than, one would expect.

In the application of those results to buildings, allowance will be made for the inherent variability of the strength of masonry. This variability is well illustrated by the standard deviations derived from the NBS tests.

2. Static Strength

The basic data now available for analysis of the strength of curtain walls and panels comes from two sources--static tests and the FCDA tests in Nevada in 1953. Further data are in the process of being taken in the URS facility in California. The strength of interior and exterior walls is also affected by the amount of window or open area. This effect is accounted for in data contained in References (13) and (14).

a. Effect of Wall Openings

Considering the outside wall of a room in which the area open fraction is "f", when the blast wave hits, P_o will be the over-pressure on a fraction "f" of the wall and P_r the reflected pressure on a fraction (1 -f). The average pressure on the outside will then be $(1 -f) P_r + f P_o$. This average is quickly established over the window openings since the initial low pressure (P_o) clears to the average very

rapidly. The pressure wave entering the window must expand to the room cross sectional area perpendicular to the blast direction. The ratio of window area to room area perpendicular to the blast direction is again "f". Thus the inside overpressure will be

$$P_i = f \left\{ (1 - f) P_r + f P_o \right\} .$$

If the pressure P_i is reflected from the back wall of the room, the reflected pressure will be

$$P_i^{(r)} = R f \left\{ (1 - f) P_r + f P_o \right\}$$

where R is the reflection factor, which is two or greater and varies rather slowly with incidental overpressure. These two relations may be written as follows:

$$\frac{P_i}{P_o} = f \left\{ (1 - f) \frac{P_r}{P_o} + f \right\} \quad (68)$$

$$\frac{P_i^{(r)}}{P_o} = R f \left\{ (1 - f) \frac{P_r}{P_o} + f \right\} . \quad (69)$$

Taking the reflection factor P_r/P_o to be about equal to the inside reflection factor R and choosing $R \cong 2.2$, equations (68) and (69) can be plotted versus "f". This plot is shown in Figure 21. The agreement with References 13 and 14 is excellent.

INTERIOR INITIAL AND REFLECTED OVERPRESSURE VS "f",
OUTSIDE AREA OPEN FRACTION

$$\frac{P_i}{P_\sigma} = 2.2f [(1-f) 2.2 + f]$$

$$\frac{P_i}{P_\sigma} = f [(1-f) 2.2 + f]$$

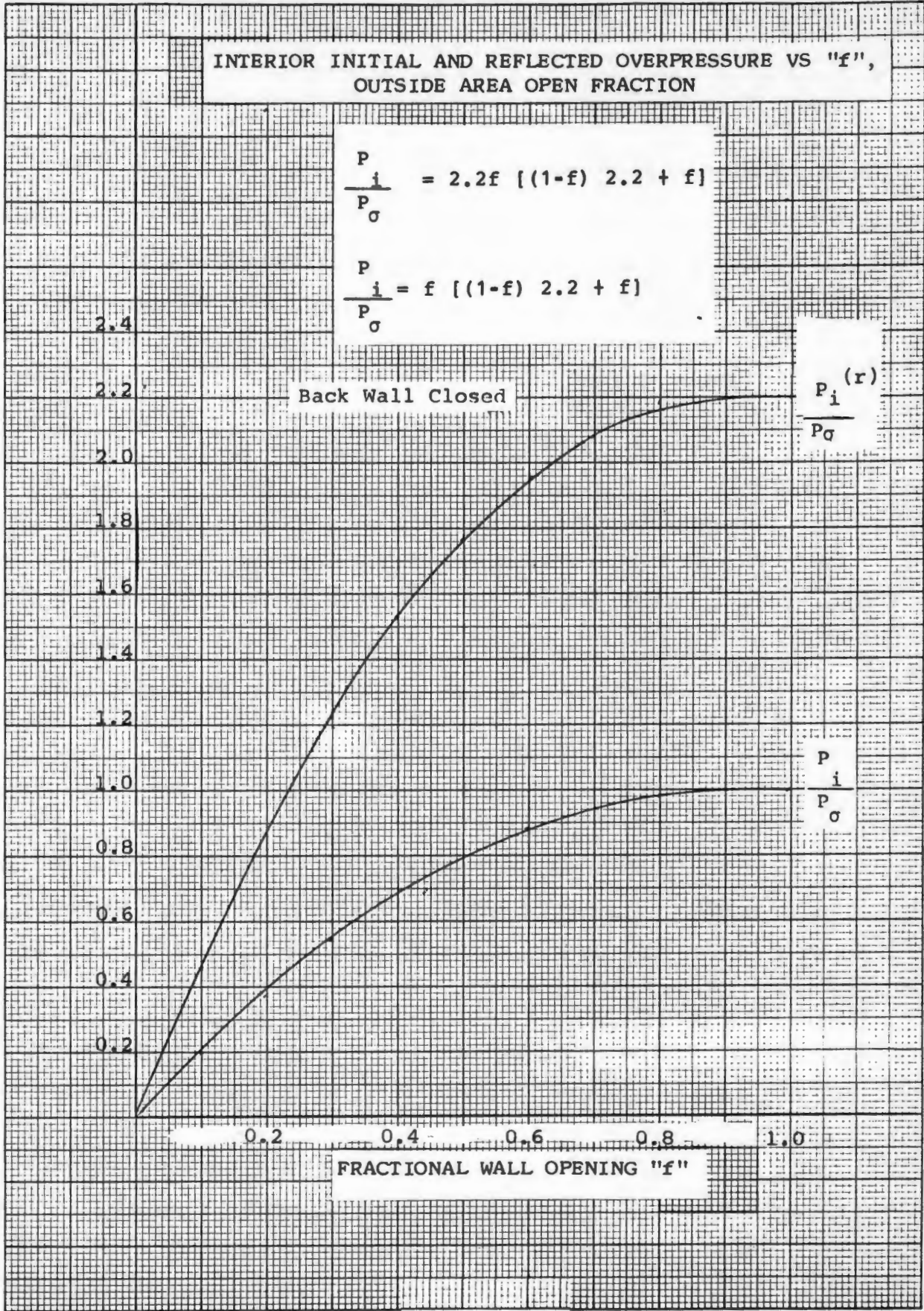


FIGURE 21
129

The loading on a partition of a room having exterior window openings may be obtained from the curves of Figure 21. The partitions in the room will experience peak pressure $P_i^{(r)}$ although the side partitions will be loaded with pressure P_i prior to reflection at the back. If the interior loading is insufficient to cause partition failure, the reflected pressure will relieve the load on the exterior wall in time $t = 2d/v$, where

d = room depth

v = shock speed.

This greatly increases exterior wall strength, depending on the value of "d". In Nevada, "d" was rather small, and hence no exterior walls (with openings) failed. This problem will be discussed in more detail later when failure times for walls are calculated.

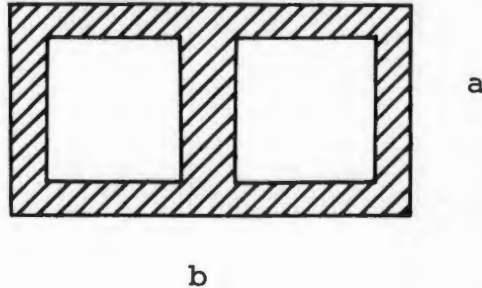
b. Static Strength Data

When a curtain wall fails explosively under blast wave loading, the failure mechanism appears to be punching shear. An explosive failure is one in which fragment speeds of at least 20 ft./sec. are attained. Available static data on shear failure of curtain walls is first reviewed and then compared with the results from the 1953 Nevada test data.

Static data are available on the racking strength of concrete masonry walls and composite masonry walls in a National Bureau of Standards report (Reference 15).

The application of racking test data to simple shear situations is none too reliable; however, the best available. Table 13, given on the following page, is extracted from Tables 17 and 18 of Reference 15.

Referring to the figure below,



the specimen wall has overall dimensions a , b . The gross area is $A = ab$, and the net area A_n is the actual bearing area or the shaded portion of the sketch.

The resultant plot of S versus A_n/A is shown in Figure 22. Since the plot is linear, passing through the origin, S is a function of A_n/A alone and does not depend upon whether or not the wall is composite or upon the nature of the materials used.

Eight-inch brick walls were also tested by the NBS, but none of these walls were tested to failure. These tests were done at an earlier date, and, apparently, the NBS equipment at that time could not supply sufficient load for failure. However, the extrapolation of Figure 22 to

Wall Type	No. Of Walls Tested	Average Compressive Strength Of Mortar (psi)	Critical Shear Stress Referred to Gross Area A	Standard Deviation Of Sample σ	$\frac{\sigma}{S}$
8-inch Cinder Concrete Block A=92.3 in. ² A _n =35.0 in. ²	12	1380	39.3	9.6	.24
Composite 4-inch Brick and 4-inch Block A=95.7 in. ² A _n =71.0 in. ²	8	1280	81.7	15.4	.19

STATIC STRENGTH OF CONCRETE MASONRY AND COMPOSITE MASONRY WALLS

TABLE 13

CRITICAL SHEAR STRESS VS RATIO OF NET
AREA TO GROSS AREA

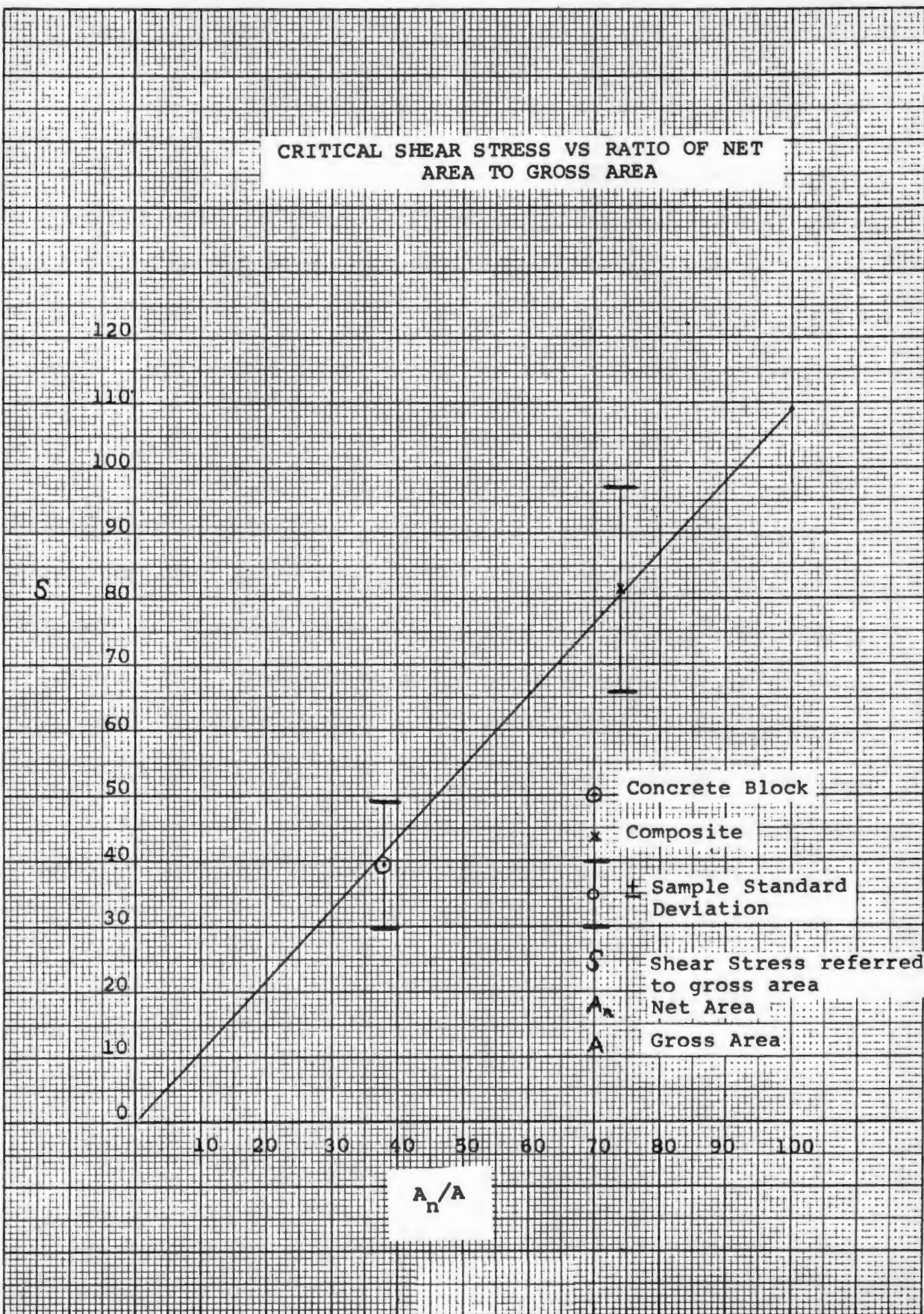


FIGURE 22

$A_n/A = 1$ shows that the failure point of a brick wall is about 110 psi (shear stress).

The results plotted in Figure 22 will not be surprising when it is recalled that the mortar and not the material is the key factor in shear failure. It is true that the Nevada data show shear of bricks as well as mortar. Once the mortar has failed, however, brick failure can occur by flexure, among other things.

c. FCDA Nevada Test Data

Before listing the Nevada test data, the use of the static data on Figure 22 will be discussed. For a given wall panel, A_n/A is computed; then the shear failure stress "S" may be obtained. For explosive wall failure, it is assumed that shear failure at the periphery occurs first. The shear stresses come into equilibrium very rapidly, whereas the time for the panel to deflect is much longer. Insofar as these shear forces are concerned, the dynamic loading factor will be two. If the actual reflected pressure is P_r , the effective pressure insofar as shear failure is concerned will be $2P_r$. For a panel height of "h", a width "w", and thickness τ , then

$$2P_r hw = 2(h + w) \tau S$$

or

$$P_r = \left(1 + \frac{w}{h}\right) \frac{\tau}{w} S. \quad (70)$$

For a solid 8-inch brick wall, this would give for a Nevada panel
($S = 100$ psi, $w = 16'$, $h = 10'$),

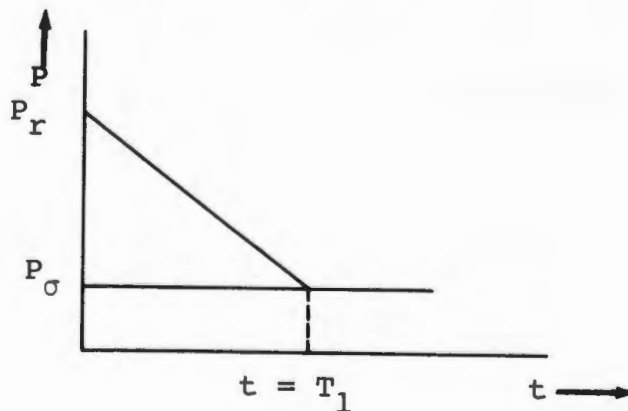
$$P_r = 12 \text{ psi.}$$

In other words, the wall will just fail at a reflected pressure of 12 psi. Table 14 shows a tabulation of the important parameters of the various Nevada wall panels; A_n/A is given for each wall, and using the listed value, "S" may be read from Figure 22.

The Nevada conditions resulted in a very small diffractive phase duration on the front face of the panel. Thus, the height of the motel structures was only 11', and with a clearing time of $3h/v$, this gives

$$T_1 = \frac{33}{1300} = 0.0254.$$

The actual front wall loading is sketched below.



Panel* No.	Size (feet)	Construction	Density (lbs./cu.ft.)	Mass (lbs.sec. ² /ft.)	S	A _n /A
1	10x16	12" brick	120	592	110	1.0
6	10x16	8" brick	120	395	110	1.0
10	10x16	4" brick, 8" block	88	435	60	.55
5	10x16	4" brick, 4" block	97	320	81	.74
8	10x16	4" brick, 4" block	97	320	81	.74
11	10x16	4" brick, 4" block	97	320	81	.74
13	10x16	4" brick, 4" tile	84	278	81	.74
7	10x16	12" block	74	366	42	.38
2	10x16	8" block	74	244	42	.38
3	10x12	4" brick, 8" block	88	326	60	.55
4	10x20	4" brick, 8" block	88	544	60	.55

* Each numbered panel is common to both front and rear wall of structures 3.29a and c.

PEAK SHEAR RESISTANCES FOR NEVADA WALL PANELS

TABLE 14

P_{σ} does not fall significantly in the time to wall failure. As shown previously, the triangular part of the pulse can be replaced by an equivalent exponential value so that

$$P = (P_r - P_{\sigma}) e^{-\beta t} + P_{\sigma} \quad (71)$$

with

$$\beta = \frac{2}{T_1} = 79 \text{ sec}^{-1}$$

For this large a value of β , it is sufficiently accurate to treat the loading as an impulse. Thus,

$$I = \int_0^{t_f} A_p P dt \quad (72)$$

where A_p is the panel area and

t_f is the time to panel failure in the sense that all diffractive loads are gone.

Drag loading was negligible in Nevada. Therefore, we have

$$I = \left\{ \frac{(P_r - P_{\sigma})}{\beta} + P_{\sigma} t_f \right\} A_p \quad (73)$$

In choosing an average wall displacement which gives a reasonable failure time, as defined above, it seems reasonable to choose a displacement x_0 equal to the wall thickness. Since wall resistance starts at some maximum value determined by the critical shear stress, "S", it is reasonable to assume that the effective value of "S", S_e , declines linearly from an initial value S to zero in the failure time t_f . Thus, the equation of motion of the wall is written

$$m\ddot{x} = A_p \left\{ (P_r - P_\sigma) e^{-\beta t} + P_\sigma \right\} - R(t) \quad (74)$$

where

$$R(t) = (h + w) \tau S(t).$$

The factor of two does not appear in this equation since a zero net force is required at $t=0$ whenever

$$A_p P_r = (h + w) \tau S$$

as required by equation (68), page 128.

Since, as discussed earlier, loading may be dealt with as an impulse, and with $A_p = hw$, then

$$\frac{mv_0}{A_p} = \frac{(P_r - P_\sigma)}{\beta} + P_\sigma t_f - \left(1 + \frac{w}{h}\right) \frac{\tau S}{w} \frac{t_f}{2} \quad (75)$$

and for displacement

$$\frac{mx_0}{A_p} = \frac{(P_r - P_\sigma)}{\beta} t_f + P_\sigma t_f^2 - \left(1 + \frac{w}{h}\right) \frac{\tau S}{w} \frac{t_f^2}{2} \quad (76)$$

where $x_0 = \tau$, the wall thickness.

From (76) t_f is calculated and then v_0 from (75).

3. Response in Tests

There were two sets of wall panels in Nevada: panels "c" (Structure 3.29c) and panels "a" (Structure 3.29a). P_r and P_σ for the two cases are listed below:

	<u>"c" panels</u>	<u>"a" panels</u>
P_r (psi)	20.4	10.5
P_σ (psi)	8.4	4.6

Taking the "c" panels first, it is possible to form Table 15 using (75) and (76).

Before hitting the ground, the top portion of the wall (top $\frac{1}{2}$) will travel a distance given by

CALCULATED VALUES OF VELOCITY AND DISPLACEMENT

FOR "c" PANELS

Panel No.	t_f (ms.)	v_o (ft./sec.)	d_m (ft.)
1	--	0	0
6	71	19	13
10	83	23	16
5	52	26	18
8	52	26	18
11	52	26	18
13	64	30	21
7	66	30	21
2	40	33	23
3	91	22	15
4	101	29	21

TABLE 15

$$d = \sqrt{\frac{2h}{g}} v_0$$

with $h \cong 8'$, before it hits the ground. This quantity, d_m , is tabulated in the last column of Table 15. The observed displacement d_m is difficult to obtain from photography since, if the rear wall does not fail, the fragments hit the rear wall in most cases. The comments of observers about these test panels are summarized in Table 16.

The 12-inch brick wall (12c) should just fail since it fails at $P_r = 18.0$ psi. This was observed in the test. Clearly the motion of the wall will indicate deflection when it is near the failure point. In any event, the criterion for failure and subsequent mass motion of fragments previously discussed appears quite reasonable in the light of actual events.

In the "c" panels of the motel structures, some of the rear panels were blown out. The time for pressure on the outside back face to build up to P_0 is about 45ms. Since this is less than any of the failure times t_f which are calculated, the initial load on the rear panels (assuming front panel failure) will be $P_r - P_0$. Here, it is assumed that the initial shock strength is not diminished by front wall failure. This is reasonable since any diminution of P_0 over a small area of the shock front would result in pressure "feed in" from the rest of the shock front. Equation (75) may thus be written as

Observed Response--FRONT Wall Panels

Structure 3.29c--1953 FCDA Tests

($P_G = 8.4, P_r = 20.4$ psi)

Panel No. Construction	Page	Response Reported in Reference 16 Quote Material
1c 12" brick 10x16	125	"The front wall was blown in with the south section rotating about the angle support and the north section rotating a lesser amount."
6c 8" brick 10x16	140	"The front wall was 85% blown into the cell."
10c 4"br.8"block 10x16	151	"The front wall was 75% blown into the back of the cell-----."
5c 4"br.4"block 10x16	137	"The front wall was blown into the cell-----."
8c 4"br.4"block 10x16	146	"The front wall was 98% blown into the back of the cell."
11c 4"br.4"block 10x16	154	"The front wall was blown into and thru the cell-----."
13c 4"br. 4"tile 10x16	159	"The front wall was 95% blown into and thru the cell."
7c 12" block 10x16	144	"The front wall was blown into and thru the cell-----."
2c 8" block 10x16	130	"The front and rear walls were blown through the rear of the cell. Rubble from the walls was found 60 ft. to the rear of the structure."
3c 4"br.8"block 10x12	133	"The front wall was blown into the cell-----."
4c 4"br.8"block 10x20	135	"The front wall was blown into the cell-----."

TABLE 16

$$\frac{mv_0}{A_p} = \frac{P_r - P_\sigma}{\beta} - \left[\left(1 + \frac{w}{h} \right) \frac{\tau S}{w} \frac{t_f}{2} \right] \quad (77)$$

and (76) as

$$\frac{mx_0}{A_p} = \frac{(P_r - P_\sigma)}{\beta} t_f - \left(1 + \frac{w}{h} \right) \frac{\tau S}{w} \frac{t_f^2}{2}. \quad (78)$$

To obtain the clearing time t_1 and hence β , the reflected shock must move from the back wall to the front before clearing can start. This distance is about 15'. Thus

$$t_1 = \frac{15 + 3h}{u} = .0370 \text{ sec.}$$

and

$$\beta = \frac{2}{t_1} = 54 \text{ sec.}^{-1}$$

Unfortunately, calculations on this basis do not show significant failure of any of the rear walls. The fact that many rear walls were hit by heavy fragments from the front wall might account for the observed failures. This is only speculation, however. Either the interior loading or the calculated value for t_f may be in error.

Table 17 shows the description of what actually happened.

Turning next to the "a" structures, which were exposed to a lesser loading, these were identical to the "c" panels listed in Table 14. The value of P_r was 10.5 psi, and P_σ was 4.6 psi. It was clear that P_σ' was insufficient for failure of either the 12-inch or the 8-inch brick walls (1a and 6a). Thus, starting with panel 10a, equations (75) and (76) from page 139 may be used to form Table 18 which is similar to Table 15.

Descriptions of what happened are given in Table 19.

The agreement of predictions with test results is quite reasonable.

Observed Response--REAR Wall Panels

Structure 3.29c--1953 FCDA Tests

($P_G = 8.4$, $P_r = 20.4$ psi)

Panel No. Construction	Page	Response Reported in Reference 16 Quote Material
1c 12" brick 10x16	125	"The rear wall was spalled, at the top, on the outside face."
6c 8" brick 10x16	140	"The rear wall was spalled, at the top, on the outside face-----."
10c 4"br.8"block 10x16	151	"The rear wall was spalled, at the top, on the outside face-----."
5c 4"br.4"block 10x16	137	"The rear wall was spalled-----and bowed out at the top center about 1" with a vertical crack halfway down the middle-----."
8c 4"br.4"block 10x16	146	"The rear wall was cracked, broken, and punched outward by the debris, but no openings were made thru it. The wall was punched outward up to 1 ft. and was on the verge of blowing thru."
11c 4"br.4"block 10x16	154	"The rear wall was 85% blown out."
13c 4"br.4"tile 10x16	159	"The rear wall was 65% blown out."
7c 12" block 10x16	144	"The rear wall was 80% blown into the rear yard. Most of the debris from both walls was in the rear yard-----."
2c 8" block 10x16	130	"The front and rear walls were blown thru the rear of the cell. Rubble from the walls was found 60 ft. to the rear of the structure."

TABLE 17

Panel No. Construction	Page	Response Reported in Reference 16 Quote Material
3c 4"br.8"block 10x12	133	"The rear wall was slightly spalled at the top -----on the outside face."
4c 4"br.8"block 10x20	135	"The rear wall was cracked down the middle of the outside face and bowed out 3" to 4" at the top center and 1" to 2" at the bottom center-----."

TABLE 17 (Continued)

CALCULATED VALUES OF VELOCITY AND DISPLACEMENT

FOR "a" PANELS

Panel	t_f (ms)	v_0 (ft./sec.)	d_m (ft.)
10	---	0	0
5	124	11	8
8	124	11	8
11	124	11	8
13	108	12	8
7	120	17	12
2	70	19	13
3	---	0	0
4	---	0	0

TABLE 18

Observed Response--FRONT Wall Panels

Structure 3.29a--1953 FCDA Tests

($P_o = 4.6$, $P_r = 10.5$ psi)

Panel No. Construction	Page	Response Reported in Reference 16 Quote Material
1a 12" brick 10x16	35	"There was no observable damage."
6a 8" brick 10x16	47	"The front wall had two small spalled spots-----. The inner wythe, on the inside face,---was knocked inward 3/8" maximum-----."
10a 4"br.8"block 10x16	58	"The front wall was slightly spalled-----with some vertical flexure cracking-----."
5a 4"br.4"block 10x16	44	"The front wall was 85% blown into the cell-----."
8a 4"br.4"block 10x16	52	"The front wall was 90% blown into the cell with debris evenly distributed."
11a 4"br.4"block 10x16	60	"The front wall was 95% blown into the cell."
13a 4"br.4"tile 10x16	64	"The front wall was 98% blown into the cell-----."
7a 12" block 10x16	49	"The front wall was 80% blown into the cell."
2a 8" block 10x16	37	"The front wall was blown into the cell-----."
3a 4"br.8"block 10x12	40	"The front wall was slightly spalled, at the top, on the outside face."
4a 4"br.8"block 10x20	42	"The front wall was displaced inward at the top 1/4" to 3/4"-----. The inside face had a slight horizon- tal crack-----."

TABLE 19

G. FIRST-FLOOR FAILURE

1. Introduction

The discussion now turns to methods and computations to establish pressures that lead to failure in typical concrete floors. The failure level sought is that which will result in casualties to unprotected personnel below. The floor systems investigated are typical reinforced concrete floor slabs, supported on reinforced concrete, steel beams or bearing walls.

2. Methods

The ultimate strength of floors can be established directly by computations using the structural properties of the beams and slabs, or indirectly by taking the design load--dead load plus the service load associated with building occupancy--and multiplying it by the applicable factor of safety. Assuming valid input data, the ultimate resistances should be the same except for the fact that design sections often have shear^{*} capacities greater than theoretically required.

Some examples and explanations are:

- Slab thickness: For practical reasons the slab thickness is often made uniform throughout a floor plan for a constant design load even though spans vary considerably.
- Steel beams are selected from available depths and weights, having at least the properties required.
- Standard beam connections are often used; they develop up to the beam's maximum capacity in shear which may be much greater than the design shear because moment governs the design.

* Shear failure is necessary for the type of collapse sought.

Therefore, results by the structural analysis method are more realistic than those obtained by the design load factor-of-safety method. Although structural analysis is preferred, the factor-of-safety method has its use wherever structural properties are lacking. Prediction by the factor-of-safety method is poor, however, and will not be discussed here.

3. Structural Analysis Method

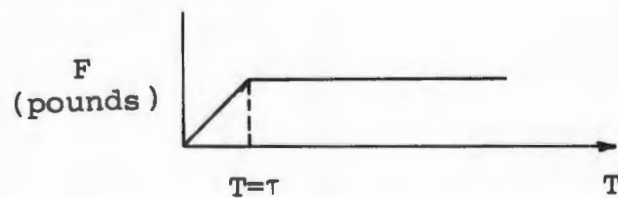
This method of computation of floor strength is based on actual structural properties and, therefore, requires that data be obtained from structural drawings or field measurements. These properties have been reported for NFSS type buildings, but the detail furnished is not adequate for our purpose. For this reason, some typical designs will be used prepared by the Portland Cement Association for guidance to the building industry to meet a range of functional requirements and alternatives. The Portland Cement slab details with associated reinforced concrete beam framing are described in Reference 17. The following designs are contained in the reference: one-way solid slab, one-way joist with 20-inch metal pans, one-way joist with 16-inch filler blocks, two-way solid slab, flat plate, flat plate waffle construction, and flat slab. Slabs, except for the flat plate and flat slab types, are equally applicable to floors supported on steel beams and concrete or masonry-bearing walls. Alternate designs using steel beam framing for the Portland Cement concrete floor slabs are described in later paragraphs.

The present investigation covers the mean of the range of panel sizes and design loads shown in Reference 17. This range includes square

panels 15, 20, 25 and 30 feet in size for superimposed loads of 50, 100 and 200 pounds per square foot, as consistent for the slab type. The concrete designs are based on a concrete ultimate, f'_c , of 3000 psi and a reinforcement working stress, f_r , of 20,000 psi. The steel beam designs are based on a f_s of 20,000 psi in tension. Design based on these stresses would be the most representative of actual construction. (See Table 20, Definition of Symbols.)

4. Response of Floor Slabs

As the blast wave sweeps across the floor slab, the net loading goes up as shown below:



where L , the length of the slab = $V\tau$

V = shock speed.

Now, to a first approximation, the slab will respond dynamically, in the elastic range, as a one degree of freedom system since only the first mode of vibration is excited. Thus,

$$m\ddot{y} + ky = F(T) \quad (79)$$

$$F(T) = F_M T/\tau \quad 0 \leq T \leq \tau$$

$$F(T) = F_M \quad T > \tau.$$

TABLE 20

DEFINITION OF SYMBOLS

A_c	floor area delivering load to section that is critical for shear failure, in. ²
b	total width or length of concrete shear section, inches
b'	average width of the rib in concrete joist slabs, inches
d	effective depth of concrete section, inches
f_c	allowable* compressive stress in concrete, psi
f'_c	compressive strength of concrete, psi
f_r	allowable tensile stress in reinforcement, psi
f'_r	ultimate* tensile strength of reinforced steel, psi
f_s	allowable tensile and compressive stress in flexure in structural beam sections, psi for top flange restrained laterally as specified by code
f'_s	ultimate tensile strength of structural steel, psi
I	moment of inertia, in. ⁴
I/c	section modulus, in. ³
I/L	stiffness factor for flexural members
Kips or K	thousand-pounds
L	span
M	bending moment
p	unit floor load, psi
plf	load per lineal foot, in pounds
psf	load per square foot, in pounds
v	allowable shear stress as a measure of diagonal tension, psi
v_u	ultimate shear strength in diagonal tension, psi
V_u	ultimate resistance of section in shear, lbs.

* allowable stress is the working stress for design
ultimate stress is the structural failure stress

Here F_M , the maximum force, equals $P_0 A$, where A is the slab area and P_0 is the shock overpressure.

Equation (79) may be solved using the Laplace transform. The result is

$$y = \frac{F_M}{k} \left[\frac{T}{\tau} - \frac{\sin \omega T}{\tau} \right] \quad 0 \leq T \leq \tau \quad (80a)$$

$$y = \frac{F_M}{k} \left[1 - \frac{2 \sin \frac{\omega T}{2} \cos [\omega(T - \tau/2)]}{\omega \tau} \right]. \quad (80b)$$

Only the case (80b) is of interest. The maximum displacement occurs when $\omega(T - \tau/2) = \pi$, at which point

$$y_m = y_s \left[1 + \frac{\sin \omega \tau/2}{\omega \tau/2} \right] \quad (81)$$

provided

$$\frac{\omega \tau}{2} \leq \pi.$$

Of course, $\frac{F_M}{k} = y_s$ is the displacement of the slab under a static load F_M and

$\omega = 2\pi f$ where "f" equals lowest resonant frequency of the slab.

Note that as $\tau \rightarrow 0$ (quick loading), $Y_M \rightarrow 2 Y_S$, which is the usual result. For a 20-by 20-foot slab, which is about the smallest bay size to be encountered, f could conceivably be as low as 30 cps and since τ will be about 15 milliseconds, $\omega\tau = 2.8$, and

$$\frac{\sin \frac{\omega\tau}{2}}{\omega\tau/2} = 1.7.$$

Thus, the dynamic loading factor may be a consideration.

For the moment the discussion will treat slabs under static loading with the idea that the dynamic loading factor can be included when slab frequencies are determined.

5. Criteria for Analyzing Response

The critical response for collapse and a comparison of working stresses and resulting designs for the 1940 and 1960 periods are discussed below:

- The critical mode of response for collapse of reinforced concrete members is generally flexure leading to diagonal tension shear failure. Generally, based upon analyses and limited observations, tensile failure in reinforcement or compression in concrete at points of maximum moment is either associated with diagonal tension shear failure or is noncritical. Pure punching failure, i.e., shear failure without flexure and diagonal tension

cracking, is presently ruled out on the basis of preliminary calculations.

- The critical responses for collapse of steel-beam floors are shear in the primary beam connection to the column, and buckling of end web members in open web joists where such construction is used. With respect to primary beams, neither beam buckling nor moment failure appear critical. However, yielding in these modes under certain conditions can occur and will contribute to beam connection failure. Yielding by web buckling would tend to occur in heavily loaded short span beams. Moment yielding leading to a plastic hinge mechanism could occur in beams in the case of small ratios of I/L . Present opinion holds that failure even in this case will occur at the connection.
- A comparison of allowable working stresses in shear for concrete for $f'_c = 3000$ psi based on the ACI codes of 1941 and 1963 is of interest from the standpoint of the relative resistance of the resulting designs. They are as follows:

	<u>1941</u>	<u>1963*</u>
1. Beams with no web reinforcement and without special anchorage of longitudinal steel	60 psi	(beams) 60 psi (joists) 66 psi
2. Same as the preceding but with special anchorage of longitudinal steel	90 psi	---
3. Beams with properly designed web reinforcement but without special anchorage of longitudinal steel	180 psi	274
4. Same as preceding but with special anchorage of longitudinal steel	360 psi	---
5. Flat slabs at distance "d" from edge of column capital or drop panel	90 psi	110 psi

The 1963 code, because of the allowable stresses and ultimate strength design provision (Ref. 18, Sec. 1504, 1506; Ref. 19, Sec. 1504) , results in somewhat smaller concrete design sections except possibly where the full benefit of the specification governing item 4 is concerned. For this reason the ultimate blast capacities for designs produced under earlier codes for equal service loads will be somewhat stronger against blast than those of the current period.

6. Ultimate Concrete Shears

The investigation will use unit ultimate diagonal shear stresses for various reinforced concrete members based on the American Concrete Institute 1963 Codes (Ref. 18, 19). These shears are developed below for collapse failure. Although some experimental data may differ,

* The values for the 1963 code are based on certain provisions related to web reinforcement, bent bars, etc. which differ some from the corresponding specifications in the 1941 code (Ref. 18, Sec. 1202-1206; Ref. 19, Sec. 801-805).

the 1963 code data are generally accepted as the best approach at present. It should be noted that collapse is a more pronounced failure than is structural failure as used by the code. By structural failure, we mean loss of members' ability to continue to carry the design loads. By collapse, we mean fracture of the member which will drop a substantial part of the floor system to the area below. The adjustment from structural failure to structural collapse will vary with the member, and may be approximated intuitively based on judgment.

- The diagonal tension shear ultimate for one-way solid and ribbed slabs, without shear reinforcement, at distance "d" from the face of the support, varies from $2\phi\sqrt{f'_c}$ to $3.5\phi\sqrt{f'_c}$, depending on the moment-shear relation at the critical section (Ref. 18, Sec. 1701 (a) (b) (c) (d) and Sec. 1707 (a) 1). The lower value is a safe design shortcut approximation; the larger value is for an optimum moment-shear relation. A value of $3\sqrt{f'_c}$ * is used. For a f'_c of 3000 psi, the ultimate value for structural failure will be 165 psi for solid slabs. A value of 182 psi will be used for ribbed slabs for a shear area equal to that of the gross rib area as allowed by the code (Ref. 18, Table 1002a) . The corresponding allowable working stresses for design are 60 and 66 psi, respectively

* Expression is based on a ϕ of unity, which infers that a theoretical ideal ultimate shear value will be realized.

(same reference). Based on these ultimates, a factor of safety of 2.75 is indicated against structural failure. The same values will be used for the collapse level for light-weight (low I/L) slabs. Others will be adjusted upward.

- The diagonal tension shear ultimate for beams with web reinforcement is $10\phi\sqrt{f'_c}$ at a distance d from the face of the support (Ref. 18 & 19, Sec. 1705 (b)). For $\phi = 1.0$ and $f'_c = 3000$ psi, the theoretical ideal ultimate shear is 550 psi. The corresponding allowable working stress for design of 274 psi (Ref. 18, Table 1002 (a)) indicates a factor of safety of 2.0 against structural failure. Since the code does not limit I/L for this stress specification, it follows that the ultimate stress was established conservatively. (I/L is used in place of I/L^3 , the significant parameter other than load influencing deflection, I/L, diagonal tension cracking and, therefore, ultimate diagonal tension shear.) A factor of safety of 2.25 is presently established for collapse failure, giving a 620 psi ultimate.
- The diagonal tension shear ultimate for slabs w/o shear reinforcement, with two-way action at the column support is $4\phi\sqrt{f'_c}$ at a distance $d/2$ from the periphery of the concentrated reaction (Ref. 18, Sec. 1707 (a)2, (b) and (c)). This gives a value of 220 psi for diagonal tension shear for $\phi = 1$ and $f'_c = 3000$ psi. The corresponding allowable working stress for design of 110 psi,

(Ref. 18, Table 1002 (a)), indicates a factor of safety of 2.0 against structural failure. A factor of safety of 2.25 is presently established for collapse failure, giving a V_u of 250 psi. The reasoning for the adjustment is the same as that given in preceding paragraphs.

The above code values are adequate for present analyses which involve the three conditions:

- (a) One-way slabs, solid and rib, without web reinforcement
- (b) Beams with web reinforcement
- (c) Slabs with two-way action at column supports (not to be confused with two-way slabs carried by beams).

The ultimate diagonal tension shears for collapse failure are 165 and 182 psi, 620 psi and 250 psi, respectively, for members a, b and c. The corresponding factors of safety against collapse are 2.75, 2.25 and 2.25.

7. Assumptions for Analyzing Steel Beam Connections

Three basic beam connections with respect to moment and shear are encountered in actual practice (rigid or fully restrained, simple or unrestrained, and semirigid)*. The problem will be simplified by the following assumptions:

- The rigid frame moment, when applicable, is taken by the couple developed by the upper and lower connection of beam flanges to the column.**

* Discussion, pp. 575, 580, and 585, Ref. 23.

** Connection Illustrations (m) and (n), p. 567, Ref. 23.

- The vertical shear from superimposed blast and dead load is taken by the connection between the beam web and column. The vertical shear from the rigid frame moments is taken by the connection of beam flanges to column.
- The moment and shear maxima occur under approximately the same blast overpressures.
- The ultimate capacity of riveted, bolted, and welded connections* are the same for a given design shear load.

8. Alternate Floor Designs

Designs for steel beam framing applicable to the slab floors shown in Reference 17, for 20-by 20-foot square panels, and a superimposed load of 100 psf, follow.

- a. Design #1: Steel Beam Alternate for One-Way Solid Slabs
(See p. 13, Ref. 17.)

Intermediate Beam Design

Weight of 4-inch slab 50 psf; superimposed load, 100 psf.

Additional weight from beam > 200 plf.

Beam load (10 ft. x 150 lbs.) + 200 lbs. = 1700 plf.

Total load for 20-foot span = 34×10^3 lbs.

Use 12" WF (Wide Flange) - 40 lbs.

Primary Beam

Concentrated load at center of span = 34×10^3 lbs.

Uniform load (additional beam wt.) 250 lbs. x 20 ft. or 5×10^3 lbs.

$$M = 182.5 \times 10^3 \text{ ft.-lbs.} \quad \frac{I}{C} = 109.5 \text{ in.}^3 \text{ @ 20,000 psi stress.}$$

Use 18" WF - 60 lbs.

* Discussion, pp. 588, 601 and 641, Ref. 23.

- b. Design #2: Steel Beam Alternate for One-Way Joists With
20-Inch Pans
(See p. 14, Ref. 17.)

Primary Beam

Wt. of 8 + 2½ ribbed slab, 60 psf; superimposed load, 100 psi.

Additional beam weight, 300 plf.

Beam load = (20 ft. x 160 lbs.) + 300 lbs. = 3500 plf.

Total load for 20-foot span = 70×10^3 lbs.

Use 18" WF - 60 lbs.

Note: Use 8" WF - 17 lbs. strut between columns in other direction.

- c. Design #3: Steel Beam Alternate for One-Way Joists With
16-Inch Filler Block
(See p. 15, Ref. 17.)

Primary Beam

Wt. of 8 + 2 ribbed slab-55 psf, and 16-inch filler block-46 psf;

total psf = 101 psf.

Superimposed load, 100 psf.

Additional beam weight, 300 plf.

Beam load = (20 ft. x 201 lbs.) + 300 lbs. = 4320 plf.

Total load for 20-foot span = 86.4×10^3 lbs.

Use 18" WF - 70 lbs.

Note: Use 8" WF - 17 lbs. strut between columns in other direction.

- d. Design #4: Steel Beam Alternate for Two-Way Solid Slab
(See p. 19, Ref. 17.)

Primary Beam

Wt. of 5-inch slab 62.5 psf, superimposed load 100 psf.

Additional beam weight, 250 plf.

Triangular beam load, $162.5 \text{ lbs.} \times 400/2 = 32.5 \times 10^3 \text{ lbs.}$

Uniform beam load $250 \text{ lbs.} \times 20 \text{ ft.} = 5.0 \times 10^3 \text{ lbs.}$

Moment = $108.3 \times 10^3 + 12.5 \times 10^3 = 120.8 \times 10^3 \text{ ft.-lbs.}$

I/C = 72.5 @ 20,000 psi stress.

Use 16' WF-45 lbs. in each direction.

9. Example: Collapse Calculations, R. C.-Framed Floors

The parameters are ultimate unit diagonal tension shear v_u , effective shear area bd , and floor area, A_c . Total shear resistance in diagonal tension V_u is equal to $v_u bd$. Calculations are based properties for one panel, the floor area carried by one column.

a. Design #1: One-Way Solid Slab, R. C. Beam Framing. Three possible locations of shear failure are investigated.

- Failure of 4-inch slab at juncture with intermediate and primary beams--

Applicable diagonal tension shear ultimate, $v_u = 165 \text{ psi.}$

Area of shear section, bd , is the effective slab depth, 3", times the shear perimeter. The perimeter is measured "d" distance inside the face of the supporting beams.
 $bd = 3816 \text{ in.}^2$

$$V_u = 165 \times 3816 = 6.30 \times 10^5 \text{ lbs.}$$

Effective floor area equals the area inside the outline of the shear section. $A_c = 4.34 \times 10^4 \text{ in.}^2$

* Equation of resistance, Ref. 18, Sec. 1701(a).

Unit load at ultimate stresses, p , is $\frac{V_u}{A_c}$ or

$$\frac{6.30 \times 10^5 \text{ lbs.}}{4.34 \times 10^4 \text{ in.}^2} = 14.6 \text{ psi}$$

- Failure of 4-inch slab and 15-by 15-inch intermediate beam at juncture with primary beams

Applicable diagonal tension shear ultimates are 165 psi for slabs and 620 psi for beams.

Area of shear sections, bd , are 1260 in.² for slabs and 780 in.² for beams, based on $d = 3''$ for the slab and 13" for the beam.

$$V_u = 165 \text{ psi} \times 1260 \text{ in.}^2 \text{ plus } 620 \text{ psi} \times 780 \text{ in.}^2 = 7.0 \times 10^5 \text{ lbs.}$$

$$\text{Effective area} = 5.25 \times 10^4 \text{ in.}^2 *$$

$$p = \frac{V_u}{A_c} \text{ or } \frac{7.0 \times 10^5}{5.25 \times 10^4} = 13.4 \text{ psi}$$

- Failure of 15- x 19-inch and 15- x 15-inch beams at juncture with columns--

$$V_u = 620 \text{ psi}$$

$$bd = 870 \text{ in.}^2$$

$$V_u = 5.40 \times 10^5 \text{ lbs.}$$

$$\text{Effective floor area} = 5.61 \times 10^4 \text{ in.}^2$$

$$p = \frac{V_u}{A_c} \text{ or } \frac{5.40 \times 10^5 \text{ lbs.}}{5.61 \times 10^4 \text{ in.}^2} = 9.6 \text{ psi.}$$

* Based on slabs and beams which constitute one 20-by 20-foot floor panel. Placing all calculations on a full panel basis facilitates direct comparison of developed values of shear area "bd" and effective floor area A_c .

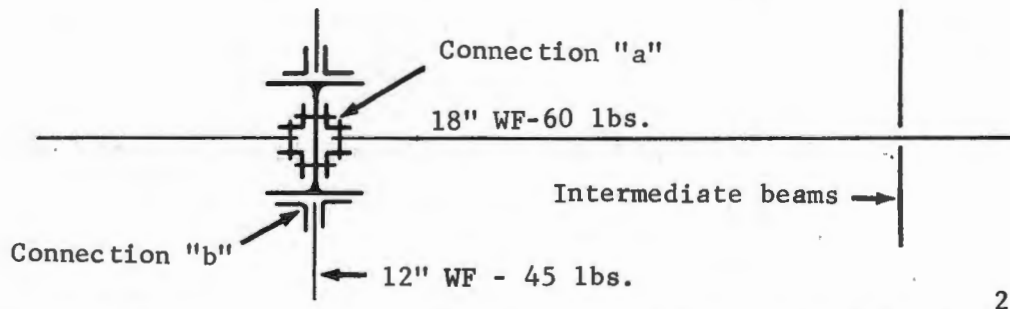
10. Examples of Collapse Calculations, Steel-Framed Floors

Two examples show the effect of supplementary beam arrangement on the resistance capacity. The comparative strength of the beam connection and beam web in shear is demonstrated. The principal parameters are the capacity of standard beam connections and the floor area that delivers load through the connection critical for collapse. The necessary steel beam properties and allowable stresses may be obtained from Reference 21. It covers the code and construction practice for the 1940's, the median period of steel construction of interest.

a. Alternate Design #1: One-Way Solid Slab.

Locations investigated for shear failure are the same as for preceding example.
*

- Failure of 18"WF and 12"WF beams at juncture with columns.



18" WF - 60 lbs. beam, web thickness 0.416", web area = 7.60in.²

12" WF - 45 lbs., web thickness 0.336", web area = 4.05 in.²

Column web thickness, assumed to be 0.44". (Column size, and therefore web thickness, depends on building loads carried; thicknesses encountered are 0.38" to 1.00" plus.)

Assume minimum standard connection series "B" and 3/4-inch rivets.
(p. 257, Ref. 21)

Allowable working stresses--beam web and rivets in shear 13,000 "

* Shear failure calculations shown are limited to connection failure at columns. Failure at edge of 4-inch slab is the same as under heading 9. Failure of slab and beam connections among primary beams do not govern.

and 15,000 psi, respectively; rivets in bearing 32,000 psi and 40,000 psi for single and double shear, respectively. (pp. 270, 286; Ref. 21)

Ultimate stresses = 3.3 times working stress.

Calculations

- (a) Capacity of rivets thru beam web, connections "a":
 (2 beams) x (4 rivets) x (12.5 kips, double shear)
 (3.3 factor of safety*) = 330 kips
- (b) Capacity of rivets thru column web, connections "a":
 (8 rivets) x (13.25 kips, double shear) x (3.3) = 350 kips
- (c) Capacity of beam webs in shear: (2 beams) (7.60 in.² x 13,000 psi) (3.3) = 650 kip

Resistances are 330, 350 and 650 kips for rivets in beam web, rivets in column web, and shear in beam web, respectively.

Note: Comparative strength of beam web in shear is nearly twice that of the connections.

$$\text{Floor area delivering to connection } (240 \text{ in.}^2) \left(\frac{1}{2}\right) = 28.8 \times 10^3 \text{ in.}^2$$

$$p = \frac{V_u}{A_c} = \frac{330 \times 10^3 \text{ lbs.}}{28.8 \times 10^3 \text{ in.}^2} = 11.4 \text{ psi}$$

- (d) Capacity of rivets thru beam web, connections "b" (2 beams) x (3 rivets)(10,0 kips)(3.3)=198 kips (governs)

$$p = \frac{198 \times 10^3 \text{ lbs.}}{28.8 \times 10^3 \text{ in.}^2} = 6.9 \text{ psi.}$$

- (e) Since connections "a" and "b" must fail simultaneously,

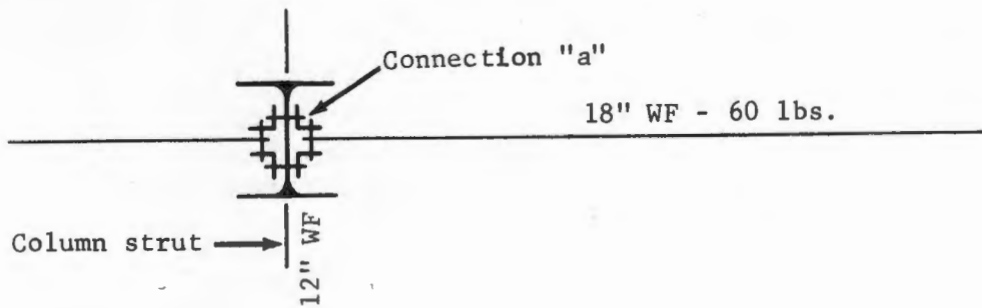
$$p = \frac{(330 + 198) 10^3}{2 \times 28.8 \times 10^3} = 9.2 \text{ psi.}$$

b. Alternate Design #2: One-Way Joists With 20-Inch Pans

Analysis of failure of beam connections at column (note that there are no secondary beams)

* Based on an average ultimate in tension of 66,300 psi developed from 4000 mill tests for period 1938-51 for structural grade steel with 20,000 psi allowable working stress--p. 5 of Ref. 22.

Data: Same as for primary beam in preceding example



Calculations

Shear resistances of primary beam, same as for preceding example.

Floor area delivering load to connection $(240 \text{ in.})^2 = 57.6 \times 10^3 \text{ in.}^2$

$$p = \frac{V_u}{A_c} = \frac{330 \times 10^3 \text{ lbs.} \times 1.15}{57.6 \times 10^3 \text{ in.}^2} = 6.5 \text{ psi.}$$

* The column strut connection must fail to drop the panel. The increased resistance is presently taken at 15 percent.

11. Structural Analysis Method Results

The collapse pressures for the concrete floors with reinforced concrete beams and the steel beam alternates are shown in Table 21. The values are for statically applied loads. They are gross loads which include the weight of the floor slab (equivalent to $\pm 0.5 \text{ psi}$) and any early debris load. The corresponding overpressure for blast will be established by multiplying the net static pressure by the appropriate dynamic load factor.

TABLE 21

COLLAPSE PRESSURES FOR CONCRETE FLOORS

<u>Design</u>	<u>Slab Type</u>	<u>Concrete Slab</u>	<u>Beam Framing</u>	
			<u>Concrete</u>	<u>Steel</u>
1.	One-way solid	14.6 psi*	9.6 psi	9.2 psi
2.	One-way joist, metal pans	3.4	6.5	6.5
3.	One-way joist, filler block	4.0	6.8	7.0
4.	Two-way solid	12.0	11.0	9.4
5.	Flat-plate solid	3.7	Not applicable	Not applicable
6.	Flat-plate, waffle	3.3**	Not applicable	Not applicable
7.	Flat-slab	8.2	Not applicable	Not applicable

* The 14.6 psi is applicable to all slabs supported on secondary beams which frame into the mid-span of primary beams. (Primary beams are members which span between columns.) Where secondary beams are not used, slab spans become longer and the members become more vulnerable. For such modification of design #1, the recorded values of 14.6, 9.6, and 9.2 psi would be reduced by about one-third.

** The 3.3 psi may range to twice this value for heavy design loads and large panels. This slab type is well suited to this design condition.

H. SYNTHESIS AND APPLICATION

The following discussion combines the results of the preceding analyses to produce a set of blast fatality functions which may be used to determine the survivability of personnel in shelter space in various locations within three types of structures.

1. Residence Shelters

For brick and wood frame buildings of not more than two stories, collapse has been shown to occur at about 3.5 psi. However, structural collapse, especially at threshold overpressures, may not be directly related to personnel fatalities. Frequent examples of fairly widespread devastation of such residential buildings by tornados with amazingly low percentages of fatalities have been noted. World War II data²⁴ support this observation. Additional force, beyond that required to collapse relatively light structures, appears necessary to produce very high fatality rates. Using data from Reference 9, it has been estimated that the displacement of a human being (in the open) at the velocity of 30 feet/second for at least 10 feet should produce widespread fatalities. Overpressures associated with such displacements are significantly greater than those required to collapse average residential structures. Thus at increasing levels of blast loading, persons on the first or second floor rapidly suffer loss of protection from dynamic pressures while the hazard of flying debris increases. The violent displacement criteria are reached at ranges that relate to overpressures of about 6 psi in the megaton range and to about 8 psi in the lower kiloton ranges.

Although residential first-story floors should collapse at the overpressures just noted, personnel previously warned and seeking shelter in areas of the basement near walls or places protected from buckling floor joists would have an increased chance of survival. However, forceful collapse of the first floor must be anticipated as overpressures reach about 10 psi. Those without specially prepared basement shelters would then have little chance of surviving.

Well constructed shelters, anchored to basement wall and floor, will provide yet further protection. However, with all structural protection above the basement removed, a buildup of reflected pressure within the basement cavity is possible. Survival appears improbable for initial overpressures greater than about 15 psi.

2. Shelters in Multistory Wall-Bearing Buildings

The massive failure of a building of this type was calculated in Section III D3 to occur at about 7 psi. Total collapse of wall-bearing buildings must be associated with almost 100 percent fatalities for personnel wherever located on floors above the basement. A relatively small percentage of the exterior of most such buildings is in window opening. Thus, the internal buildup of overpressures to fatality-producing levels is essentially precluded prior to complete failure of the structure. Therefore, the fatality criteria for persons above the basement must be directly associated with the building collapse for multistory wall-bearing buildings.

Although some first-floor collapse from rubble load is possible, the basement of a wall-bearing building will continue to provide protection

after the failure of the upper floors. However, a complexity of blast effects will act upon it as a separate structure. These include venting of overpressure into the basement through entrance ways, or through sections of floor failing with the main building. Multiple reflection buildup of pressures may produce serious effects either during the positive pressure phase or in augmentation of the negative blast wave. It is considered these effects will become critical between 15 and 20 psi.

3. Shelters in Multistory Frame Buildings

In the case of the commercial-residential twenty-story steel frame building analyzed in Section III E 4 above, the combined reflected overpressure-dynamic pressure effects caused structural failure and toppling at about the equivalent of 14 psi overpressure from lower megaton yields. This scales to about 17 psi for nominal yields for which the dynamic overpressure contribution will be relatively small. Casualty and fatality-producing overpressure levels will be created inside such a structure at incident blast levels considerably below those at which the building fails. Available data indicate that a typical multistory framed building has approximately 30 percent of its exterior surface in window area. This will convert to about 40 percent of exterior surface actually joining walls for exterior rooms. Utilizing Figure 21 (Interior Initial and Reflected Overpressure Versus "f", Outside Area Open Fraction) it may be determined that incident exterior overpressures ranging from about 8 psi for lower megaton yields to about 11 psi for lower kiloton yields will produce destructive interior overpressures. Exposed personnel will be hurled violently, and all but the sturdiest partitions will fail. Furniture and other contents of

rooms will be similarly translated.

Personnel taking shelter in internal portions of the building within compartments or corridors protected by heavy curtain walls will have an improved chance of survival, although the margin will be relatively slight. Depending upon weapon yield, external overpressures of 9-12 psi will produce sufficient force inside the building to cause the protective curtain walls to fail.

The survivability of personnel taking shelter in basements of multistory frame structures is largely independent of blast effects upon upper stories. Debris loading on the first floor, in the event of building failure, will be insufficient to collapse the floor. Collapse of the first floor into the basement will not necessarily occur with toppling of the building. Some failures of the first floor will occur at lower overpressures, and in some cases the nature of openings into the basement will permit entry of dangerous levels of overpressure. However, personnel in basements will generally be protected against outside overpressures of about 20 psi.

4. Blast Fatality Functions

Table 1 summarizes the blast fatality functions discussed above. These have been translated into the VN code discussed in Section IBl and reported separately.

By the very nature of the blast fatality functions in the table, it will be seen that above-grade stories of shelter facilities are more vulnerable than basements. The margin of increased survivability which might be obtained by strengthening above grade shelters is so small as to be

BLAST FATALITY FUNCTIONS

BUILDING TYPE	SHELTER LOCATION		
<p style="text-align: center;">Brick, wood frame not more than 2 stories</p>	<p style="text-align: center;">In above-grade rooms 6-8 psi</p>	<p style="text-align: center;">In basement without a prepared shelter ~ 10 psi</p>	<p style="text-align: center;">In basement with simple but well constructed shelter ~ 15 psi</p>
<p style="text-align: center;">Multistory wall bearing</p>	<p style="text-align: center;">Exposed rooms on above-grade floors (bldg collapse) ~ 7 psi</p>	<p style="text-align: center;">Core rooms on above-grade floors (bldg collapse) ~ 7 psi</p>	<p style="text-align: center;">In basement 15-20 psi</p>
<p style="text-align: center;">Commercial residential multistory steel frame 30-40% window area</p>	<p style="text-align: center;">Exposed rooms above grade 8-11 psi</p>	<p style="text-align: center;">Core rooms or corridor above grade 9-12 psi</p>	<p style="text-align: center;">In basement 20 psi</p>

NOTE: Where a range of psi values is shown, the lower value is associated with lower megaton yields while the high value is associated with lower kiloton yields. Stated values are approximately at the 50% fatality level.

TABLE 1

infeasible. Stronger curtain walls and partitions to provide a hard inner core would be fruitless if the building collapses, while at collapse overpressures many basements will continue to afford protection.

Upper-story blast damage generally eliminates personnel in upper-floor shelter spaces with little, if any, degradation of basement fallout protection. With building collapse, the first floor constitutes the remaining overhead fallout protection for basement shelter spaces although the protection factor rating for such a basement will still be high. In residence basement shelters, the removal of the house by the blast wave will drastically reduce the PF value of the basement shelter. Survivors may well be trapped by debris, causing difficulty in prompt movement to more adequate fallout shelter.

IV. INTERACTIVE AND COMBINED EFFECTS

A. INTERACTIVE EFFECTS

Interactive effects occur when one agent of damage indirectly causes the effects of another agent, the most common area of concern being the initiation of secondary fires by the blast wave, thus changing the fire problem. Such effects as the rupturing of natural gas lines, disruption of electrical switching equipment, overturning of petroleum and gasoline pumping equipment, and the penetration of petroleum storage tanks would undoubtedly lead to secondary fires and hence would be hazards to the population. It is nearly impossible to extrapolate from past experience (Japan, for instance) because present U. S. construction, especially residential, is vastly different.

Interactive or secondary effects will not be covered in this report.

Reliable data are extremely scarce and difficult to apply.

B. COMBINED EFFECTS

As the weapon yield increases, especially into the megaton range, the distance at which significant ignitions occur can be greater than the distance for heavy blast damage, depending upon atmospheric conditions and building type. In the lower kiloton range, blast may act at a somewhat greater distance. In any event, however, both agents of damage will be acting within a significant radius. The area so encompassed could be called a combined effects region in which buildings may be subject to either agent of damage or both.

Radiant exposure to the thermal pulse occurs over a short interval of time and is essentially complete in most instances when the blast wave

strikes a structure. The blast wave will perhaps extinguish some ignitions while intensifying others by supplying increased oxygen or by scattering burning material. The critical ignition energies for upholstery used in this study are based upon test results indicating ignition of the upholstery to depths at which the heat will be held long enough to reignite the upholstery within 15 minutes, even should the surface flame be blown out.

Figures 23-26 are identical plots of the probability of interior room ignition if exposed at various slant ranges from surface burst weapons of various yields with a 12-mile visibility. Each figure presents superimposed curves for the type of structure indicated by its title showing the range at which, for various yields:

Two percent or less of the given structure will be severely damaged by blast.

Fifty percent will be severely damaged by blast.

Ninety-eight percent or more will receive severe blast damage.*

Figure 26 assumes a range of furnishings and their dispositions in exposed rooms producing room ignition probabilities the same as in residential structures. Room ignition weapon radii (RIWR)** under 12-mile visibility conditions for various yields of surface burst weapons are presented in Table 22. For the same weapon yields the ranges for various peak overpressures are also tabulated as calculated by cube root scaling of the 1-kiloton curve presented in Figure 3.66 of Reference 9. Figure 27 is a plot of Table 22.

* At present, generally poor agreement exists as to the actual value to be used on Figures 23-26, but for any explicitly defined situation, this is the kind of plot required to permit meaningful descriptions of survival countermeasure.

** where $RIWR = 1.80 \left(\frac{W}{.1}\right)^{.286}$ miles

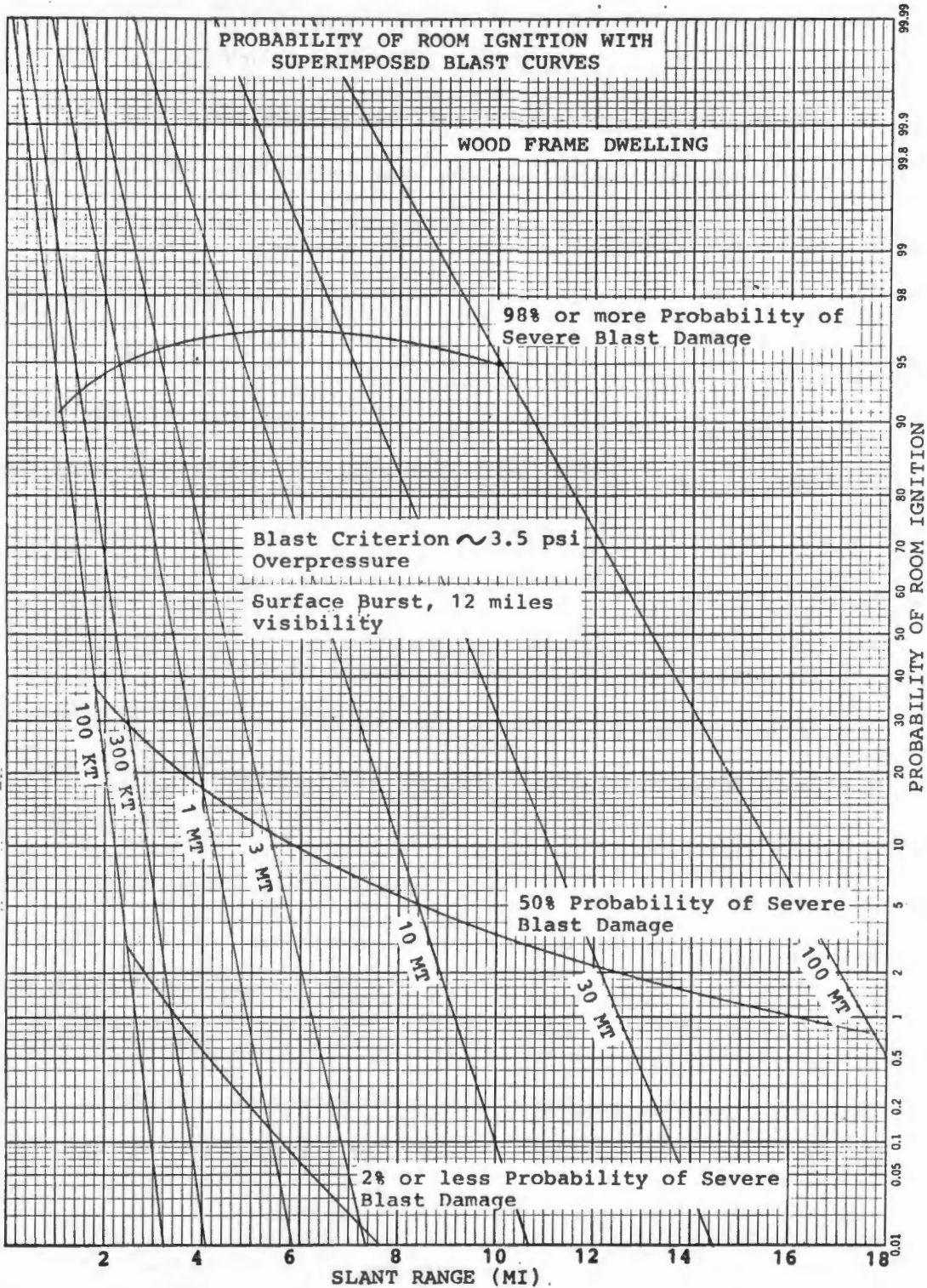


FIGURE 23

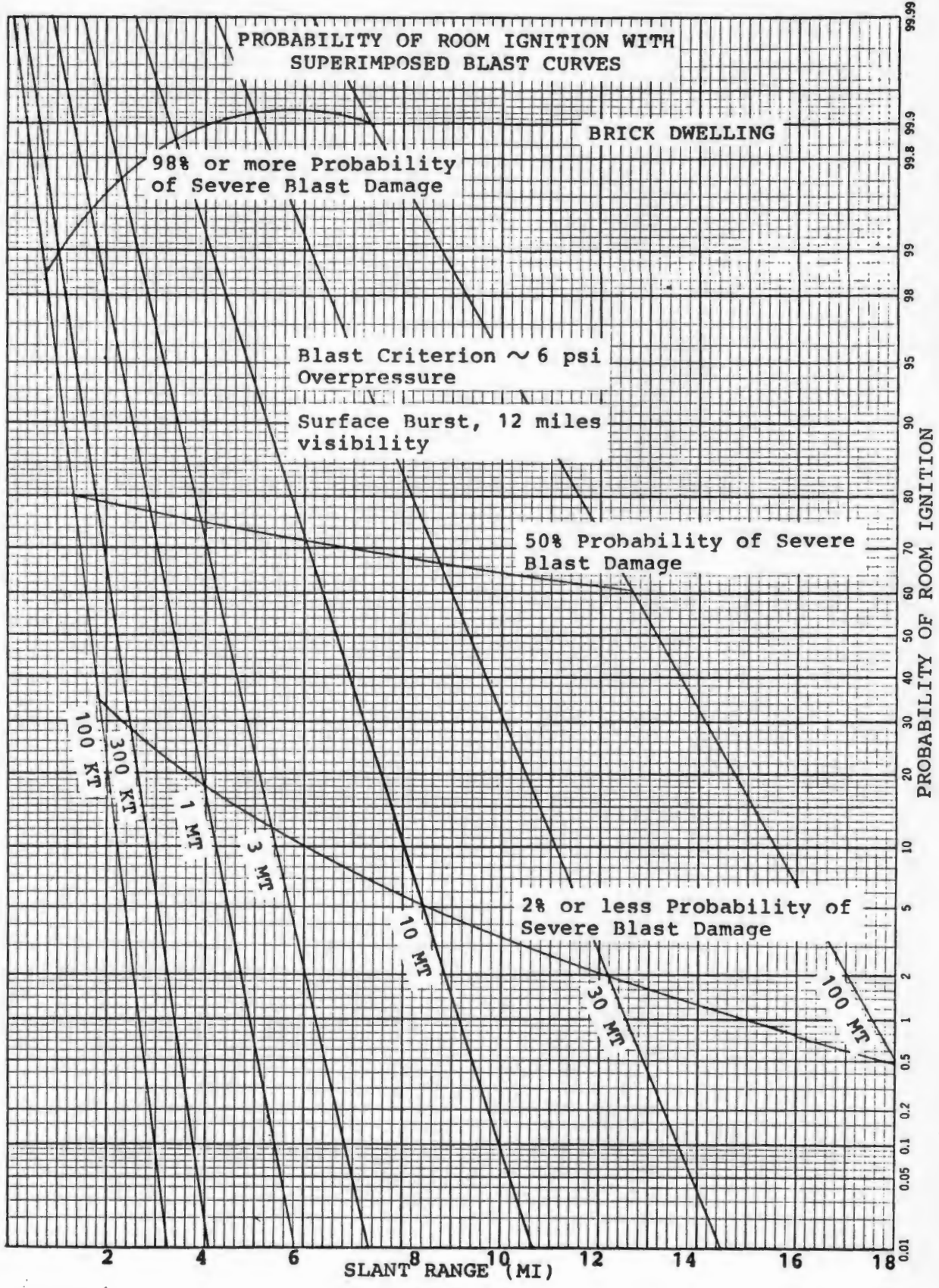


FIGURE 24

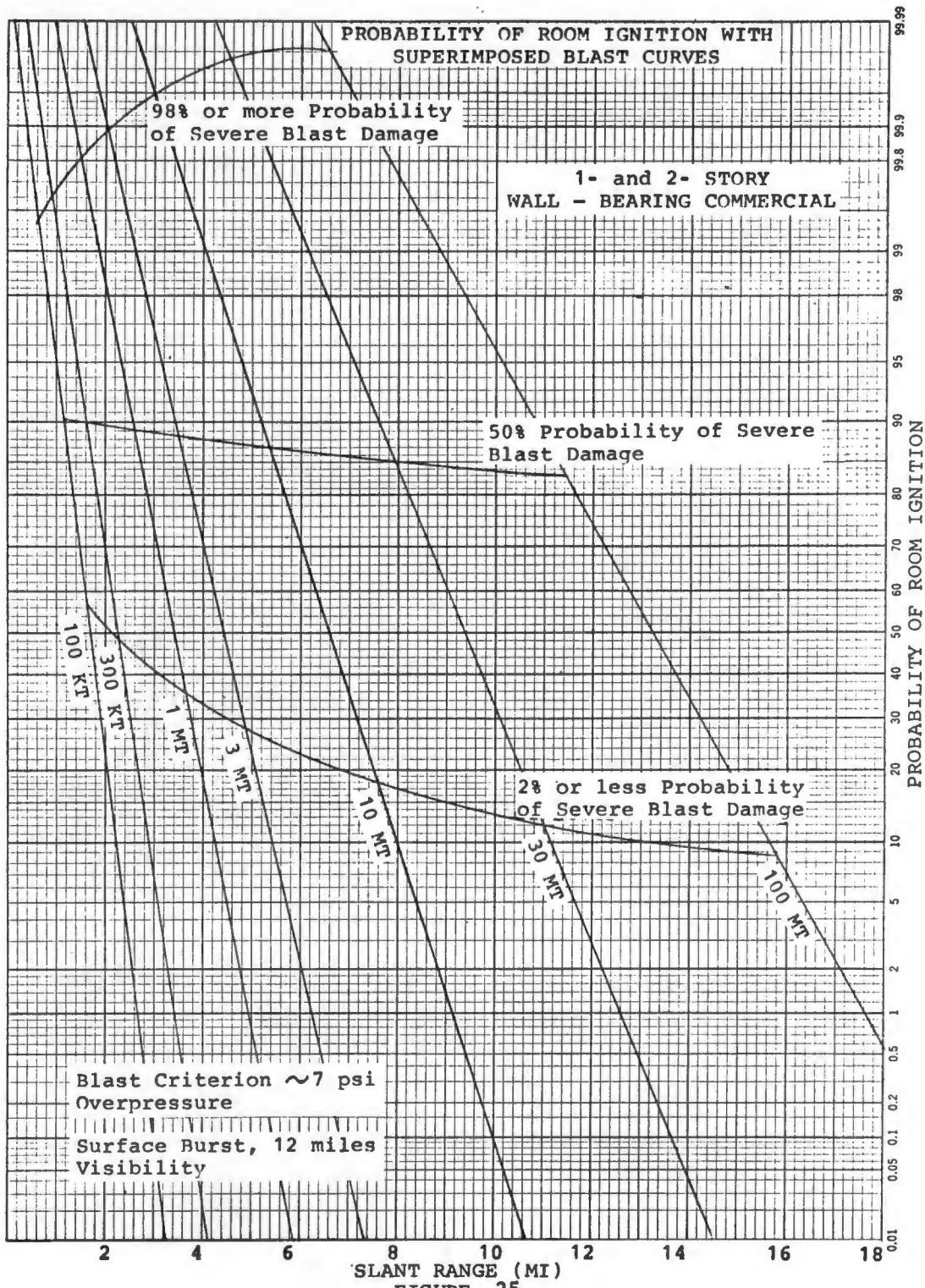


FIGURE 25

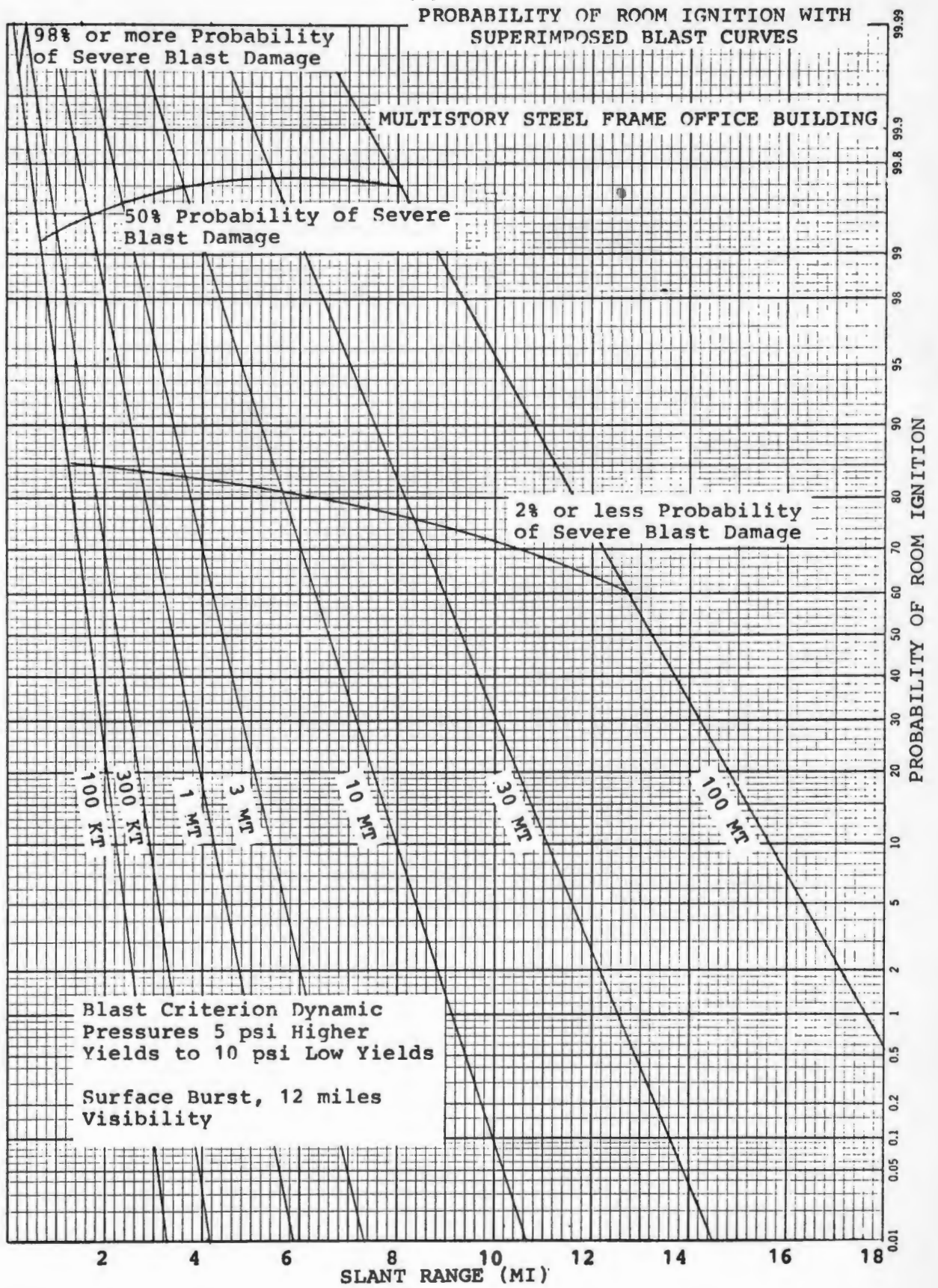


FIGURE 26

TABLE 22

RIWR VERSUS PEAK OVERPRESSURE
Surface Burst 12-Mile Visibility

YIELD (MT)	DISTANCES (miles)					
	RIWR	1 psi	2 psi	5 psi	10 psi	20 psi
.1	1.80	3.57	2.20	1.32	0.88	0.62
.3	2.46	5.09	3.17	1.91	1.27	0.89
1.0	3.47	7.58	4.73	2.84	1.89	1.33
3.0	4.76	10.94	6.82	4.10	2.74	1.92
10.0	6.73	16.39	10.21	6.13	4.08	2.86
30.0	9.18	23.6	14.7	8.83	5.90	4.12
100.0	12.97	35.7	22.0	13.2	8.80	6.17

C. SUMMARY

The blast-fire interaction may be considerable. Most of our larger cities have sizable POL storage facilities. If the blast wave ruptures these, causing them to empty their flammable contents, the probability of fire is very high. Another problem will be present in structures such as multistory apartments that have gas lines crisscrossing the entire building. Even small overpressures may flex the building sufficiently to open many of these pipes, emitting highly flammable gas through an otherwise not severely damaged building. A similar problem may exist for occupants of home basement shelters.

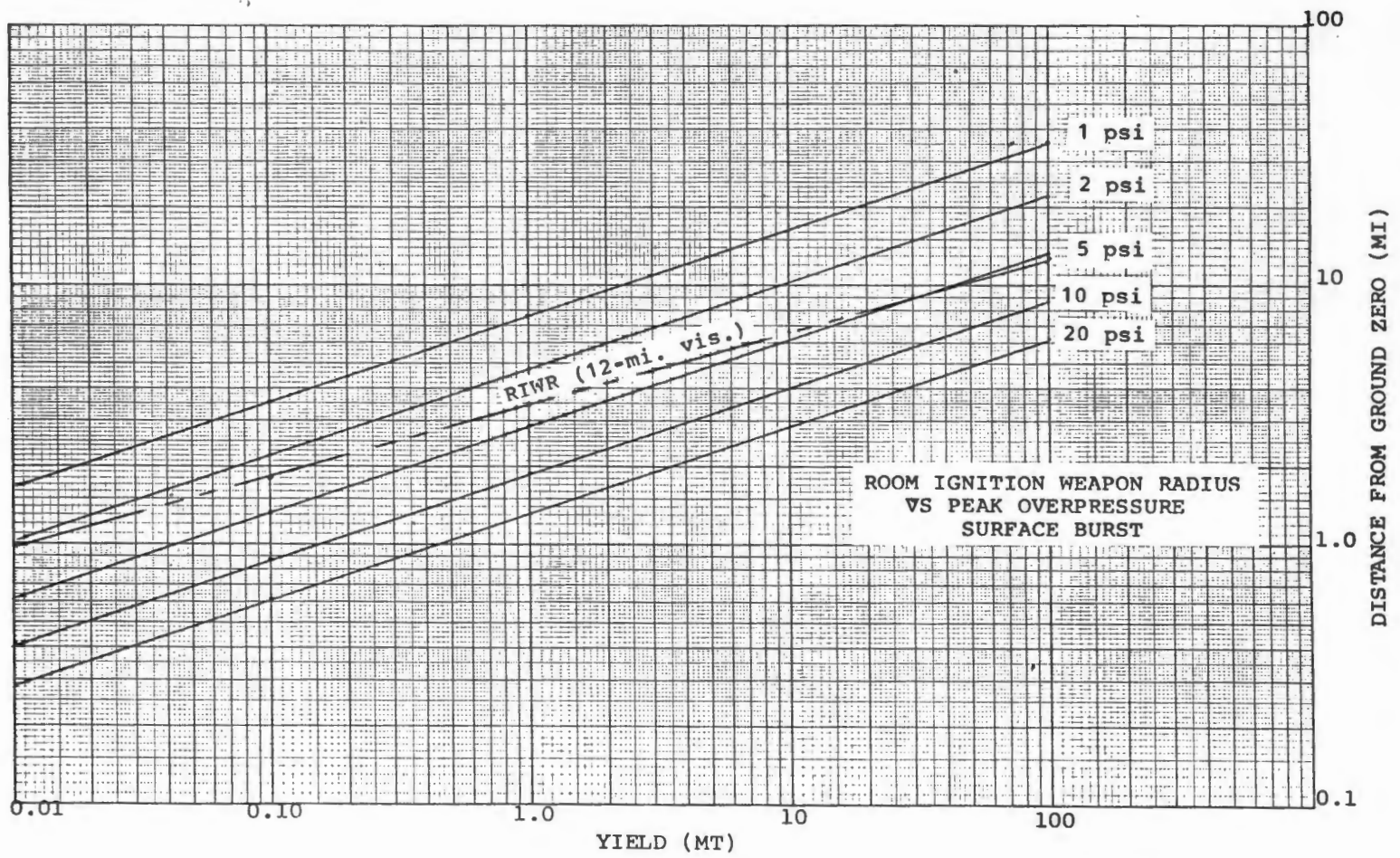


FIGURE 27

V. CLASSIFICATION OF URBAN ENVIRONMENTS

Improved methods for handling nuclear blast and fire effects are dependent upon the development of procedures and techniques for accumulating and retrieving pertinent data and statistics. This information includes data regarding individual shelter facilities, the immediate environment of shelter facilities, and the characteristics and spatial relationships of discrete portions of the urban environment. The need is particularly acute with respect to handling nuclear fire effects. Consequently, a wealth of data available in the Phase I and Phase II National Fallout Shelter Survey files and the National Resource Analysis Center housing and population files were subject to analysis to determine the significance of various parameters, possible correlations, statistical spreads, and meaningful derivable indices. Two basic approaches were pursued in analyzing the available data. For the first, data on 21 SL's selected at random from various large- and medium-size cities from all parts of the United States were compiled for study. The second approach involved detailed analysis of a single medium-size city.

A. ANALYSIS OF TWENTY-ONE SELECTED STANDARD LOCATIONS

1. Types of Data Included

Number of rooms	People per room
Number of units per structure	People per house
Year built	Numbers of shelters
Value of property	Spaces per person
Condition of property	Shelter separation
Housing density	Shelter age

In examining the data, it was difficult to determine any correlations. Certain SL's were found to have poor shelter protection while specific

shelter facilities in a few instances appeared to be questionable.

2. Indicators of Potential Fire Susceptibility

It was considered that SL's with a high potential fire susceptibility would possess one or more of the following characteristics:

- Age
- A high percentage of deteriorating or dilapidated residences
- Many multifamily dwellings
- Low property values.

Table 23 presents the total houses in each of the 21 selected SL's and the percentage built prior to 1940, deteriorating and dilapidated, multifamily and of less than \$10,000 in property value. In each SL the percentages of these four areas were averaged to form an index of fire susceptibility.

3. Shelter Assessment

From the NFSS Phase I shelter building information for the 21 selected SL's, it is possible to extract certain information that might aid in determining a relative ranking by the major types described in the previous section. Ten qualities were selected to assess each building type. The results of this assessment are shown in Table 24.

B. ANALYSIS OF PEORIA URBAN ENVIRONMENTS

1. Aim and Approach

An empirical classification of the 66 SL's comprising the Standard Metropolitan Area (SMSA) of Peoria, Illinois, was accomplished. The aim of this work was to obtain a scheme applicable to the existing nationwide SL data base which would permit a simple determination

INDICATOR CHARACTERISTICS FOR POTENTIAL FIRE SUSCEPTIBILITY

TABLE 23

TOTAL HOUSES	% Built Pre-1940	% Deteriorating & Dilapidated	% Multi-Family	% Less Than \$10,000 Value	"Index" *
1309	22	45	36	64	44
6417	56	40	11	79	46
3357	78	63	73	48	65
1296	75	36	54	91	64
5984	78	33	84	49	61
2830	0	1	1	37	10
5936	6	1	24	8	10
4440	76	5	35	4	30
2044	74	6	78	2	40
2633	26	12	2	10	13
3375	99	39	63	90	73
4291	90	32	8	95	56
3793	96	24	90	29	59
1071	98	11	78	14	50
1188	89	13	18	68	46
1345	64	10	10	72	39
1339	1	0	16	1	4
1923	6	1	1	0	1
1216	33	9	1	16	15
3123	34	4	13	11	16
1711	1	1	0	2	1

* averaged for the four characteristics

Type Of Shelter	Rank	Distribution In The Sample											Total Number		
			Total Floor Space	Useable Basement Space	Roof Mass Thickness	1st-Story Thickness	Up-Stories Exterior Wall Mass Thickness	Floor Mass Thickness	Interior Wall Mass Thickness	Street-Side Apertures	Other 3-Walls' Apertures	Interior Core Shelters	+	0	-
Schools	1	13.8%	+	-	+	+	+	0	+	-	+	+	7	1	2
Halls	2	3.4%	+	+	-	0	-	-	-	+	+	0	4	2	4
Hospitals	2	2.0%	+	0	0	0	+	0	+	-	+	0	4	5	1
Warehouses	2	6.2%	+	0	+	0	0	+	0	0	+	-	4	5	1
Offices	3	5.6%	-	0	0	0	+	+	-	0	+	-	3	4	3
Churches	4	7.0%	0	-	0	0	0	0	0	+	+	0	2	7	1
Factories	4	7.6%	+	0	0	0	0	+	-	0	0	-	2	6	2
Apartments	4	47.6%	0	0	-	0	0	-	-	+	+	0	2	5	3
Stores	5	6.5%	+	0	0	0	0	0	-	-	0	-	1	6	3

Each shelter type is evaluated as superior (+), mediocre (0), or inferior (-) in each of the 10 building parameters and ranked according to the greatest number of (+)'s. This clearly shows schools to be the best variety of shelter building and stores to be the worst, with the others ranked between.

TABLE 24
SHELTER ASSESSMENT

of the susceptibility of any urban area to fire spread and mass fires. This could then be incorporated in existing or improved detailed assessment systems. The selection of representative areas upon which to employ the FIREFLY model (described in Section II) for trial shelter system analyses was based upon this classification scheme. The Peoria SMSA was chosen for analysis because a graphic and statistical urban area study was available using early 1950 data. Among 212 SMSA's identified in 1960, Peoria's rank was 84. Its selection was prompted by this near-median position among the nation's urban centers. The median size rank provides some basis for anticipating the scope and complexity of applying any urban system analysis to both larger and smaller areas.

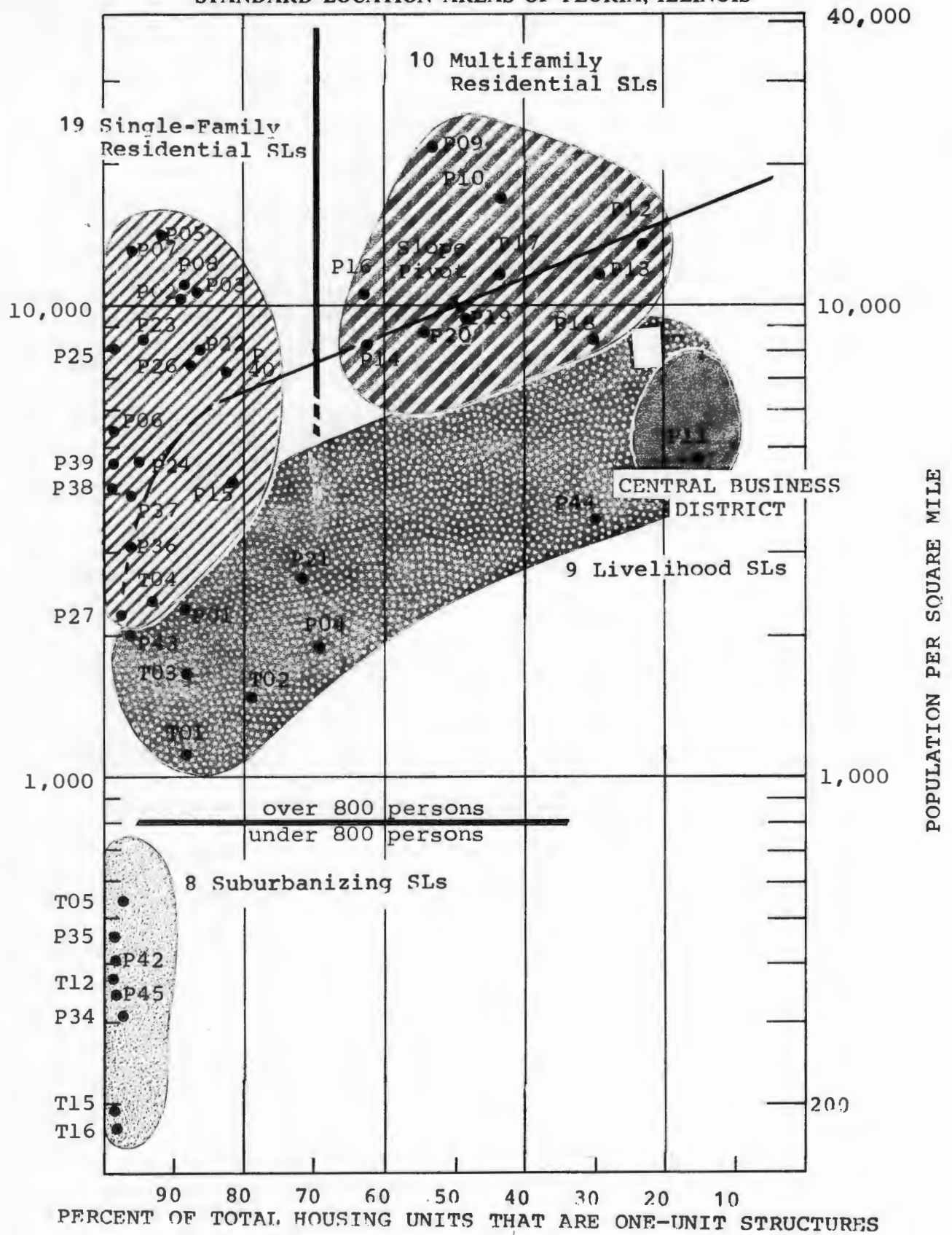
2. Basic Indicators for Classification

Two indicators were chosen to represent the urban environment: population per square mile (by place of residence) and the percentage of total housing units that are one-unit structures. A plot of the two ratios for the Peoria SL's is shown in Figure 28. In the figure each dot represents one SL. Seven SL's are omitted from the plot since they represent two smaller outlying urban centers. One SL within the SMSA has no population. Twelve nonurban SL's and one SL with no population are also omitted. SL's are grouped into five classifications:

- Central Business District (CBD) + Livelihood
- Single-family residential
- Multifamily residential

FIGURE 28

CLASSIFICATION OF THE URBAN ENVIRONMENT
OF THE
STANDARD LOCATION AREAS OF PEORIA, ILLINOIS



- Suburbanizing
- Nonurban (rural) .

These five patterns also appear on the map in Figure 29. Each pattern may be regarded as an urban environment class in terms of the two basic ratios. Detailed analysis of a sizeable portion of certain of the SL's shown on Figure 28 was accomplished as part of the trial shelter system analysis discussed in Section VI. In each case the area analyzed constituted approximately 27 blocks. The following SL's were studied:

- | | |
|--|---------|
| ● Single-family residential | P02,P03 |
| ● Multifamily residential | P09 |
| ● Livelihood (Central Business District) | P11 |

3. Sources of Data

Most of the data for obtaining the population per square mile and percentage of total housing units that are single-family units are available from the 1960 Census of Population and Housing. The total resident population of each census tract is used without modification except to relate the census tracts to the SL's. Data for the number of dwelling units by type are also available; the percentage of total housing units that are one-unit structures must be calculated for each SL, however.



The gross land area of each SL is not published with the Census Tract data. Land areas of many tracts and most minor civil divisions have been measured, and many measurements are available. None, however, are yet avail-




FIGURE 29

MAP OF
URBAN ENVIRONMENT OF
PEORIA, ILLINOIS



Environment Class


Central Urbanized Area

Livelihood:
 Central Bus. Dist. 
 Industrial, Other 

Residential:
 Multifamily 
 Single-Family 
 Suburbanizing 

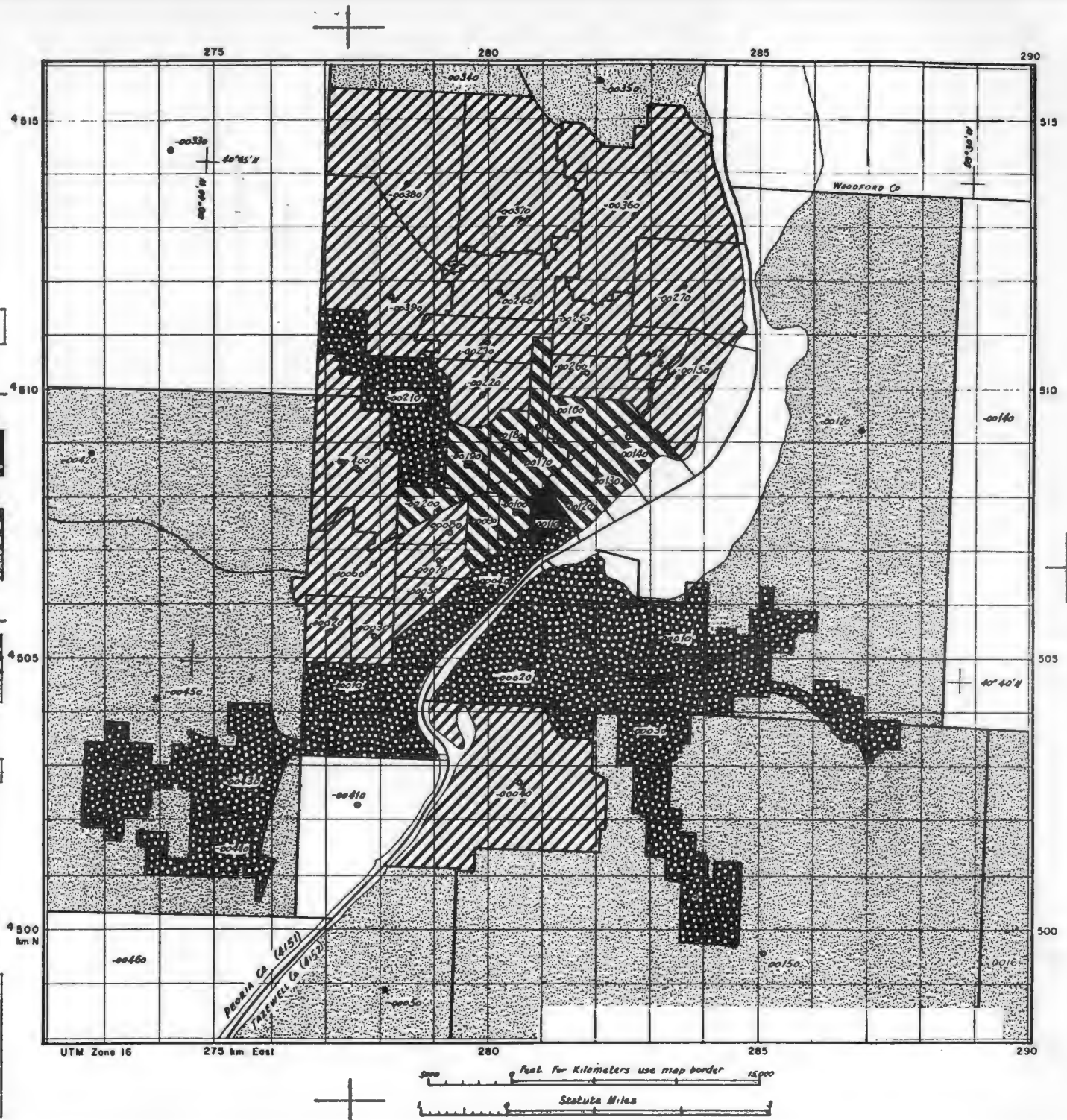
Outlying Urban Areas

Livelihood
 Residential 
 Suburbanizing 

Nonurban  no tint

Base, Standard Location Areas

SLA P14: 4151-0014
 SLA T14: 4152-0014



able on a really operational basis. The gross land areas of the Peoria SL's were measured expressly for this analysis, then adjusted to conform with published area totals. The measurement of land area excludes inland water area from consideration in computing densities of land-based phenomena. However, nonresidential land uses are not excluded in computing residential densities.

4. Discussion of Urban Classes

The SL's most clearly urban are those with population densities in excess of 800 persons per square mile (1.3 persons per acre) and which are part of the core of one contiguous urban area. The data from Peoria suggest two main environments, livelihood and residential (as shown in Figure 28), and a two-way division of each.

a. Livelihood

The job-giving livelihood area is plotted between 10 and 90 percent one-unit structures and between 1000 and 10,000 persons per square mile. The Central Business District (CBD) is a special case. The division between the single-family and multifamily is placed at 70 percent one-unit structures. In Peoria most multifamily dwellings are in structures originally built for single-family occupancy and later converted. Livelihood area SL's, excluding the CBD, are quite varied. It is necessary to examine additional data to determine what each point represents. Area P11 (SL 4151-0011) is identified by the Census as the CBD of Peoria. Area P04 is the leading riverfront industrial area and has the world's largest distillery (Hiram-Walker). Area P01 is industrial; area P21 contains Bradley University, a park, a cemetery, and the USDA Research Laboratory; area P43 has steel, wire, and grain mills; and area P44

houses the state mental hospital. No direct measure of such nonresidential areas is provided by SL in the Census of Housing and Population. The Census of Manufacturing does not provide any breakdown by SL, largely because of the nondisclosure rule. The Census of Housing reports occupation by place of residence (SL), not by place of employment. The census transportation-to-work questions do not include an identification of the SL's in a city to which people travel to work. Figure 28 does suggest, however, which SL's are probably livelihood areas, but it does not provide clues to the nature of nonresidential activities.

Likely sources for such an interpretation are maps of land use and zoning prepared by city, county, and regional planning commissions. Data about fallout shelters and industrial and administrative centers might also be used to interpret the livelihood environment.

b. Residential

Densities in single-family residential tracts range from 2000 to 15,000 persons per square mile. Those SL's exhibiting greater than 6000 persons per square mile are older residential areas, solidly built-up, with little nonresidential use except by schools, churches, parks, and a few stores. Those with lower densities are on the urban periphery. Where present, nonresidential uses include undeveloped land, large parks, or cemeteries, or modern shopping centers with offstreet parking. Densities in the multifamily residential SL's range from 8000 to 23,000 persons per square mile. Here, too, the areas with higher densities are solidly residential; the lower the density, the greater the admixture of nonresidential land uses. It should be noted that both the single-family and multifamily residential areas

exhibit densities between 8000 and 15,000. The single-family area is solidly residential. The multifamily area has more stores, warehouses, and offices, but residents are more closely packed per dwelling unit.

In Figure 28 an empirically derived curve is shown which separates at the upper density levels the clearly residential SL's from those which are otherwise classified. The data suggest a straight line with a slope as shown. There has been no inquiry as to why this should be so, but it has been found that similar lines plotted for other urban areas have nearly the same slope. Washington, D. C., has a flatter slope, reflecting a well-developed park system and a resultant drop in gross densities (computed by SL).

c. Suburbanizing

Eight SL's having population densities between 150 and 800 persons per square mile are classed as suburbanizing. These areas contain both rural and suburban land uses and represent the growing middle class suburbs which are becoming more and more prevalent around our nation's cities.

Field criteria employed by Census in determining urbanized areas use a minimum density of 1000 persons per square mile. The "suburbanizing" SL's, as shown in Figure 28, are under 800 persons per square mile; where such SL's are contiguous to the central urbanized area, it is useful to identify them as urban rather than rural because of their prospects

for a more rapid rate of growth during the planning period for which the data base will be applied.

d. Nonurban

Twelve SL's having less than 150 persons per square mile are classed as "nonurban." These include one SL having no population at all. Such SL's may be truly open, rural land, or park area and would be most easily categorized by examining a city map.

VI. TRIAL SHELTER SYSTEM ANALYSES

Using the existing shelter system of Peoria, Illinois, as the subject for comprehensive study, several analyses of the survivability of that city's projected 1975 population were conducted. These served to demonstrate the urban fire analysis model, FIREFLY, and the refined blast fatality functions. The relative value in terms of survivability of various alternative systems which might be projected for Peoria was determined. Thus the trial applications of improved methods and criteria served as pilot demonstrations for future shelter systems vulnerability analyses.

A. RELATIVE EFFECTIVENESS OF VARIOUS PEORIA SHELTER SYSTEMS

A variety of nuclear attacks with 100 percent reliable weapons were levied upon Peoria, Illinois, as indicated in the following table.

No. of Weapons	Yield	CEP	HOB	Census Tract for Aim Point
1	1 MT	3000'	640' scaled	11
1	1 MT	3000'	surface	11
1	10 MT	6000'	640' scaled	11
1	10 MT	6000'	surface	11
2	200 KT	6000'	640' scaled	11 and 4
2	200 KT	6000'	surface	11 and 4

The OCD DASH System was utilized to assess the effects of blast from the above attacks on various types of shelter which might comprise alternative shelter systems for the projected 1975 population of Peoria.

A 1975 population distribution for day and for night was produced for each of the 27 Standard Location Areas comprising Peoria proper using References 26, 27, and 28. The capability of the current existing shelter system to shelter the projected population of each SLA in above- and below-grade space was determined. Sufficient new, hypothetical below-grade spaces were then postulated for each SLA to cause the total number of spaces to

equal the projected population of the SLA. These new spaces were arbitrarily assigned as either low cost home basement prepared shelter space or as below-grade space which might be incorporated in new steel or concrete frame construction with minimum cost through design slanting. Provision was also made for determining the survivability of a certain number of persons in each SLA who took best available cover in home basements which had no previously prepared shelter.

Table 25 summarizes the effects of blast on Peoria shelter systems from various nuclear attacks. Figure 30 depicts the aim points for the attacks. It is apparent that weapon radii for damage functions from megaton weapons are such that there would be few survivors in a city the size of Peoria, even in the fallout shelters affording a measure of blast protection. Unfortunately the majority of existing fallout shelter facilities in Peoria are located in or near the Central Business District. Since Standard Location Areas away from the center of the city do not have sufficient shelter space for the population, it was primarily in these SLA's that new shelter spaces were added for the trail analysis. New below-grade shelters in the SLA's provide considerably improved chances of survivability. As may be noted from examination of Table 25, even the simple expediency of taking best cover in a home basement provides a measure of blast protection although fallout would be another matter. Separate summaries for the four outlying SLA's shown on Figure 30 are contained in Table 25. It can be seen from the table that markedly improved chances of survival exist in outlying areas. In these areas even a small additional distance from ground zero increases the effectiveness of low-cost measures. Additional analysis of the effectiveness of various shelter types when located at various ranges from different types of attacks, coupled with an analysis

of representative metropolitan areas to determine approximate percentages of urban populations which might be located sufficiently distant from potential ground zeros, are necessary to adequately evaluate shelter mix selection and allocation of shelter resources.

B. FIRE SUSCEPTIBILITY OF PEORIA

Three separate environmental areas of Peoria were analyzed for fire susceptibility using the FIREFLY model described in Section II E and in Reference 12. A description of the classification of these areas commences on page 187. Summaries of the various cases are included in Appendix C. Table 26 compares the fire susceptibility of these environments for various probabilities of room ignition when the angle of elevation to the center of the fireball is 5 degrees. FIREFLY analyses of two urban environments other than Peoria are included in Table 26 for comparison. On Figure 31 arrows point to those Peoria SL's analyzed by FIREFLY and to the two non-Peoria SL's. (Figure 31 is Figure 28 annotated.)

TYPE OF FACILITY	# OF FACILITIES	TOTAL # OF SPACES	1 MT AIR	1 MT SURFACE	10 MT AIR	10 MT SURFACE	(2) 200 KT AIR	(2) 200 KT SURFACE
<u>SUMMARY FOR 27 PEORIA SLAs</u>								
Existing Above Grade	107	77,570	.140	.235	.026	.056	.314	.491
Existing Below Grade	91	48,257	.142	.222	.032	.070	.354	.636
New Below Grade Slanted Constr.		42,400	.364	.582	.057	.177	.612	.761
Low Cost Home Basement Shelter		7,900	.338	.540	.043	.158	.548	.724
Best Cover In Home Basement		7,900	.234	.420	.015	.080	.429	.628
<u>SLA 0023</u>								
Existing Above Grade	2	70	.070	.164	.016	.039	.367	.570
Existing Below Grade	1	567	.102	.227	.023	.055	.469	.648
New Below Grade Slanted Constr.		3,000	.109	.340	.016	.063	.555	.734
Low Cost Home Basement Shelter		500	.063	.250	.008	.039	.461	.680
Best Cover In Home Basement		500	.023	.125	.000	.016	.328	.563
<u>SLA 0024</u>								
Existing Above Grade	2	998	.453	.766	.063	.141	.867	.953
Existing Below Grade	1	971	.586	.867	.036	.195	.914	.961
New Below Grade Slanted Constr.		4,500	.852	.977	.117	.360	.953	.984
<u>SLA 0025</u>								
Existing Above Grade	1	165	.070	.164	.016	.039	.406	.609
New Below Grade Slanted Constr.		4,900	.117	.344	.016	.070	.594	.758
Low Cost Home Basement Shelter		1,000	.070	.258	.003	.047	.508	.711
Best Cover In Home Basement		1,000	.023	.125	.000	.016	.359	.609
<u>SLA 0027</u>								
Existing Above Grade	2	107	.508	.813	.063	.156	.906	.969
New Below Grade Slanted Constr.		2,000	.891	.984	.141	.398	.969	.984
Low Cost Home Basement Shelter		500	.789	.977	.073	.305	.953	.984
Best Cover In Home Basement		500	.539	.906	.031	.148	.906	.969

TABLE 25

PERCENT OF PEORIA SHELTER FACILITIES SURVIVING
BLAST EFFECTS FROM VARIOUS NUCLEAR ATTACKS

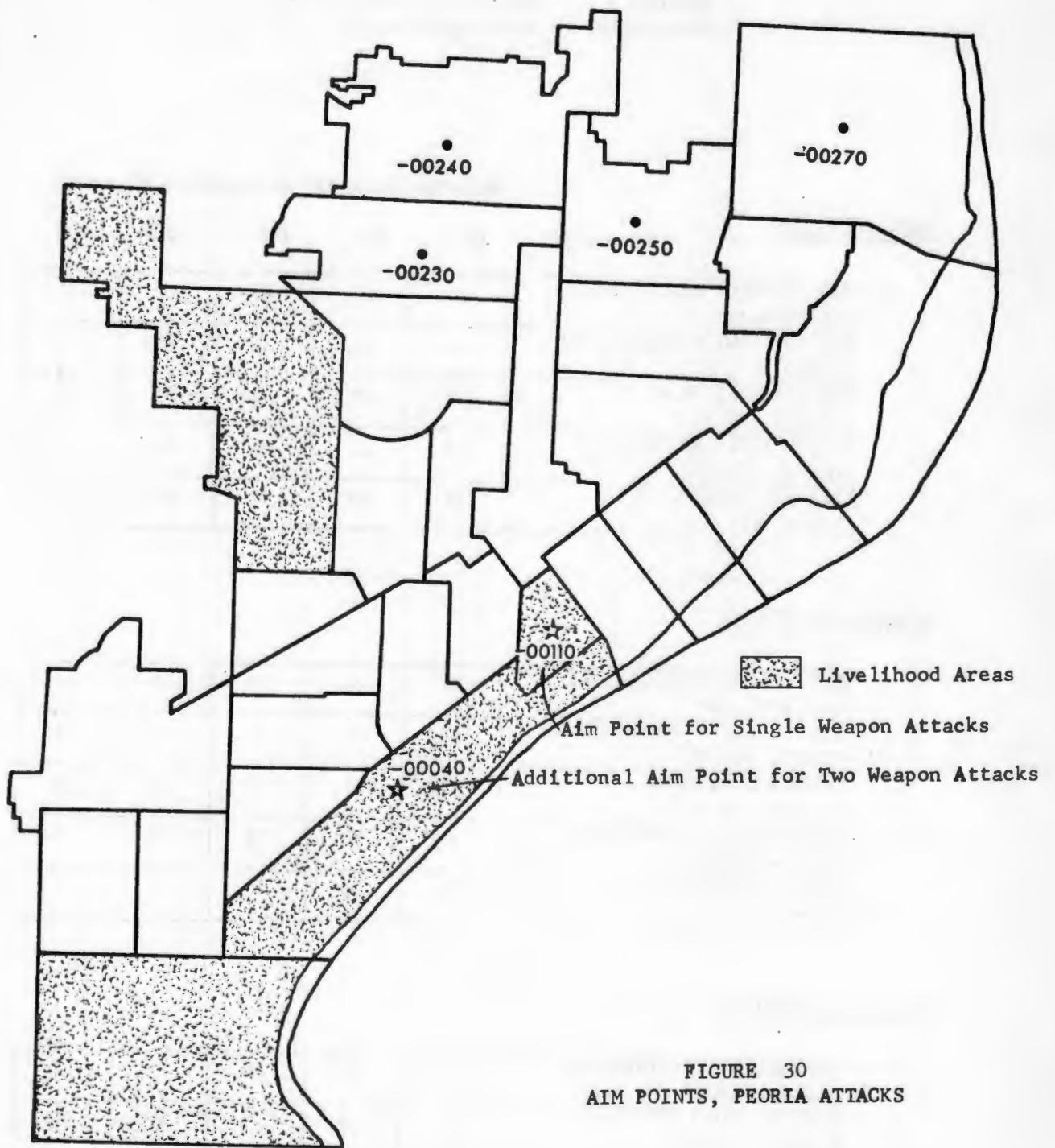


FIGURE 30
AIM POINTS, PEORIA ATTACKS



FIRE SUSCEPTIBILITY OF FIVE URBAN ENVIRONMENTS

As determined by the Percentage of Buildings
Burned when Angle of Elevation to Center of
Fireball = 5 ° with a Low Wind for Five
Probabilities of Room Ignition, P_{ri}

PERCENTAGE OF BUILDINGS BURNED

THERMAL PULSE

P_{ri} equals	0.1	0.3	0.5	0.7	0.9
MULTIFAMILY RESIDENTIAL EAST BOSTON	.01	.03	.05	.07	.09
SINGLE-FAMILY RESIDENTIAL PEORIA P02, P03	.05	.14	.20	.25	.28
MIXED RESIDENTIAL WASHINGTON, D. C.	.08	.21	.31	.38	.43
MULTIFAMILY RESIDENTIAL PEORIA P09, P10	.10	.25	.33	.38	.41
CBD + LIVELIHOOD PEORIA P11	.28	.49	.59	.65	.69

SUBSEQUENT SPREAD

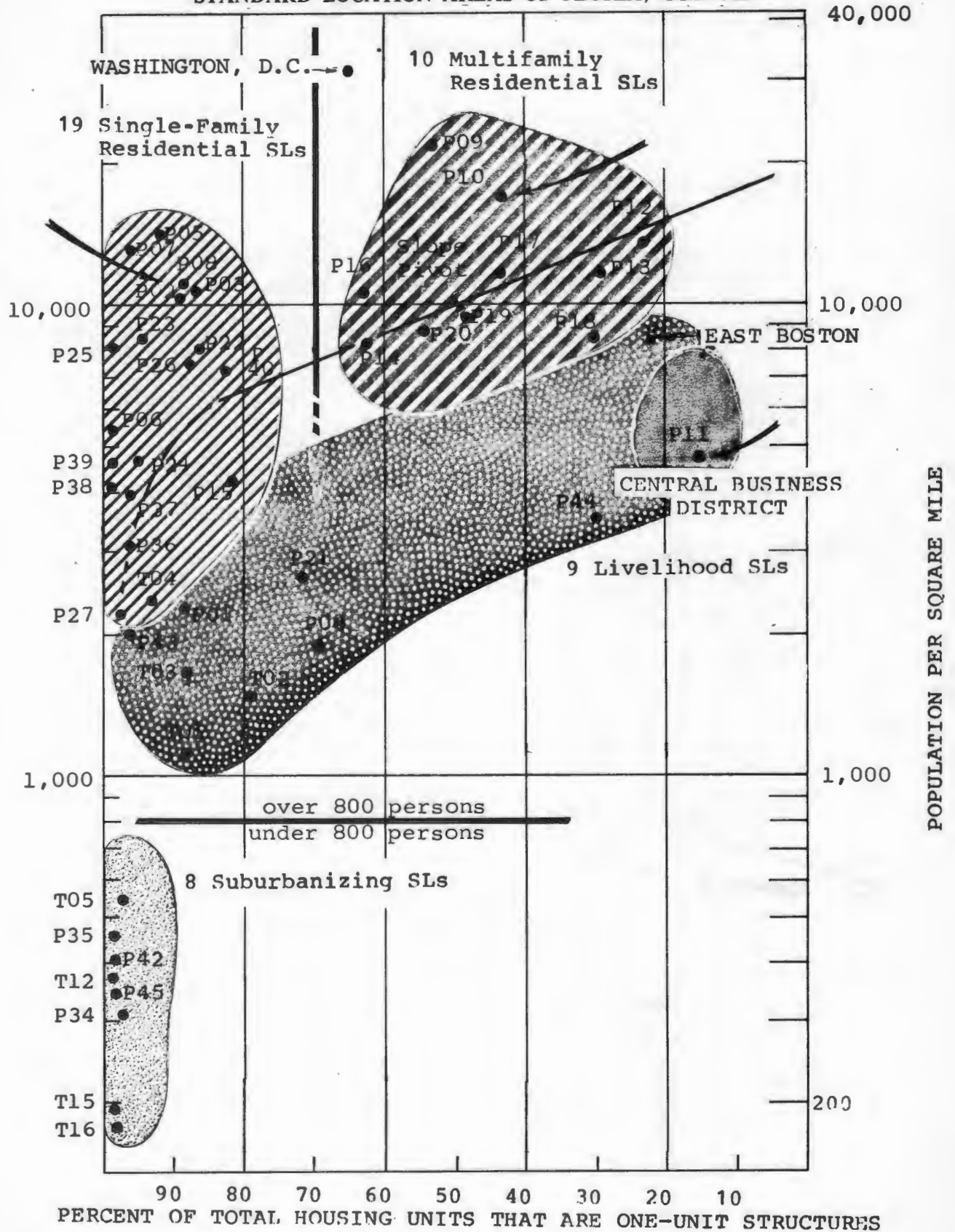
MULTIFAMILY RESIDENTIAL EAST BOSTON*	.01	.03	.04	.06	.07
SINGLE-FAMILY RESIDENTIAL PEORIA P02, P03	.03	.06	.07	.07	.08
MIXED RESIDENTIAL WASHINGTON, D. C.	.17	.17	.13	.10	.08
MULTIFAMILY RESIDENTIAL PEORIA P09, P10	.13	.16	.16	.14	.14
CBD + LIVELIHOOD PEORIA P11	.26	.20	.16	.12	.11

TOTAL DUE TO BOTH

MULTIFAMILY RESIDENTIAL EAST BOSTON*	.02	.06	.09	.13	.16
SINGLE-FAMILY RESIDENTIAL PEORIA P02, P03	.08	.20	.27	.32	.36
MIXED RESIDENTIAL WASHINGTON, D. C.	.25	.38	.44	.48	.51
MULTIFAMILY RESIDENTIAL PEORIA P09, P10	.23	.41	.49	.52	.55
CBD + LIVELIHOOD PEORIA P11	.54	.69	.75	.77	.80

FIGURE 31 Figure 28 Annotated

CLASSIFICATION OF THE URBAN ENVIRONMENT
OF THE
STANDARD LOCATION AREAS OF PEORIA, ILLINOIS



REFERENCES

1. LETTS, M., et al., "DASH--A System To Provide Detailed Assessments of the Hazards of Nuclear Attack," System Sciences, Inc., May 1967.
2. Physical Vulnerability Handbook--"Nuclear Weapons," DIA PC550/1-2, September 1963 (C).
3. STROPE, W. and CHRISTIAN, J., "Fire Aspects of Civil Defense," OCD, July 1964.
4. "Flame I Firespread Simulation Model," Special Projects Branch, University of North Carolina, January 1964.
5. CROWLEY, J. W.; LETTS, M. H.; and STAHL, F. G., "Role of the Fire Services in Nuclear War," System Sciences, Inc., April 1965.
6. SALZBERG, F.; GUTTERMAN, M. M.; and PINTAR, A. J., "Prediction of Fire Damage to Installations and Built-Up Areas from Nuclear Weapons," IITRI, Proj. No. N6001, July 1965.
7. WATERMAN, T. E. and VODVARKA, F. J., "The Ignition of Materials by High-Yield Weapons," IITRI, Proj. No. N6086, 26 March 1965.
8. BRUCE, H. D., Operation Upshot--Knothole, Proj. B.11a, "Incendiary Effects on Building and Interior Kindling Fuels," USDA, USFS, December 1953.
9. GLASSTONE, S. (ed), "The Effects of Nuclear Weapons," USDOD, USAEC, April 1962.
10. NASL, "A Report on the Investigation of Fire Starts Due to Nuclear Detonation," Physical Sciences Division, 3 April 1967.
11. COHN, B. M., et al., "A System for Local Assessment of the Conflagration Potential of Urban Areas," Gage-Babcock and Associates, March 1965.
12. CROWLEY, J. W., et al., "FIREFLY--A Computer Model to Assess the Extent of Nuclear Fire Damage in Urbanized Areas," System Sciences, Inc., 22 May, 1968.
13. WIEDERMANN, A. H., et al., "Experimental Observations of Pressures in Hollow Models," Final Test Report No. 5, ARF M069, Armour Research Foundation, 12 March, 1956. (U)
14. SCHIFFMAN, T. H., et al., "Experimental Observations of Pressures in Hollow Models," Part II, Final Test Report No. 7, ARF D087, Armour Research Foundation, July 1956. (C)

15. FISHBURN, C. C., "Effects of Mortar Properties on Strength of Masonry," NBS Monograph 36, November 1961.
16. TAYLOR, B. C., "Blast Effects of Atomic Weapons Upon Curtain Walls and Partitions of Masonry and other Materials," FCDA, August 1956.
17. "Reinforced Concrete Floor Systems," Portland Cement Association, 1956.
18. ACI Committee 318, "Building Code Requirements for Reinforced Concrete," (ACI 318-63), June 1963.
19. ACI Committee 318, "Commentary on Building Code Requirements for Reinforced Concrete," (ACI 318-63), September 1965.
20. ACI Committee 318, "Building Regulations for Reinforced Concrete," (ACI 318-41), 1941.
21. "Steel Construction Manual," American Institute of Steel Construction, Fifth Edition 1949.
22. NORRIS, HANSEN, HOLLEY, et al., "Structural Design for Dynamic Loads," McGraw-Hill Book Co., New York, 1959.
23. BEEDLE, et al., "Structural Steel Design," Fritz Engineering Laboratory, Lehigh University, The Ronald Press Co., New York, 1964.
24. "Capabilities of Nuclear Weapons," Defense Atomic Support Agency, 1964. (C)
25. WRAY, J. R., "Photo Interpretation in Urban Area Analysis," Manual of Photographic Interpretation, Washington, D. C., 1960.
26. Tri-County Regional Planning Commission, "Peoria Area Traffic Study," March 27, 1968.
27. _____, "Population Projections," February 28, 1968.
28. U. S. Bureau of the Census, "U. S. Census of Population: 1960, Subject Reports, Journey to Work," Final Report PC(2)-6B, 1963.
29. GIBBONS, M. G., "Transmissivity of the Atmosphere for Thermal Radiation from Nuclear Weapons," USNRDL-TR-1060, 12 August 1966.
30. MARTIN, S. B. and HOLTON, S., "Preliminary Program for Estimating Primary Ignition Ranges for Nuclear Weapons," USNRDL-TR-866, 3 June, 1965.

APPENDIX A

THERMAL PULSE AND ATMOSPHERIC TRANSMISSION

Gibbons²⁹ and Martin³⁰ have developed relationships which permit the calculation of radiant exposure intensity in calories per square centimeter versus slant range as a function of:

- Weapon yield (100 KT to 100 MT)
- Height of burst (ground and 640-foot scaled)
- Visibility within the atmosphere (less than 0.5 to 12 miles).

The radius of the fireball, R, in miles is given by

$$R = KW^{0.35} e^{0.0465h} \quad (82)$$

where

K = 0.53 for surface
0.41 for air burst

W = yield in megatons

h = height of burst in
statute miles.

The incident thermal energy, Q, in calories per square centimeter is

$$Q = \left(\frac{98.4}{S} \right)^2 \frac{FWT}{\pi} \quad (83)$$

S = slant range to burst point
in miles minus 0.6R

F = fraction of total energy
radiated as thermal energy
(0.21 for surface, 0.33 for
air burst)

T = atmospheric transmittance.

H is defined as the effective height of the radiation source (in miles) and equals the actual HOB for air bursts and 0.4R for surface bursts.

For H < 0.25

$$T = e^{-\frac{2S}{v}} \left(1 + \frac{1.4S}{v} \right) \quad (84)$$

where v = surface visibility in miles.

For H \cong 0.25

$$T = e^{-\frac{T(H)}{S/H}} \quad (85)$$

$T(H)$ is the optical thickness of the relatively clear atmosphere for a vertical path from the surface to altitude H , taken from Reference 29 and reproduced in Table A 1.

The transmittance is further modified for various atmospheric conditions as given in Reference 30 and shown in Table A 2.

Curves of thermal energy versus range for surface bursts and 640-foot scaled height of burst for various yields and atmospheric conditions are given as Figures A 1 through A 12.

The rather abrupt transition in slope between the 1MT and 3MT surface burst thermal energy curves for visibilities below 3 miles (see Figures A 7 - A 10) results from changing the mode of calculating transmittance from equation (84) to equation (85). Equation (85) is used with yields over 1MT for which the size of the fireball will be sufficiently large that an appreciable part of the thermal radiation will traverse a significant fraction of its course in the thin upper atmosphere. Although the discontinuity created by two modes of calculation appears abrupt, no efforts toward further refinement have been attempted since the most pronounced divergence between the 1MT and 3MT curves occurs below the thermal energy ranges that are of importance in causing ignitions. The data from these curves become the basis for determining potential ignitions.

OPTICAL THICKNESS OF A CLEAR ATMOSPHERE

TABLE A 1

<u>H (miles)</u>	<u>T (H)</u>
0.25	0.0310
0.35	0.0443
0.50	0.0603
0.70	0.0777
1.0	0.0952
1.5	0.1130
2	0.1239
3	0.1341
5	0.1426
10	0.1531
20	0.1662
30	0.1680

EFFECTS OF ATMOSPHERIC
CONDITIONS ON TRANSMITTANCE

TABLE A 2

<u>Condition</u>	<u>Transmission modifying factor</u>
Clear or very clear, $v \approx 12$ miles	1.0
Light haze, $v \approx 6$ miles	0.7
Medium haze, $v \approx 3$ miles	0.5
Thin fog, $v \approx 1.2$ miles or light clouds between fireball and target	0.3
Light fog, $v \approx 0.6$ miles or medium clouds between fireball and target	0.2
Medium to heavy fog, $v < 0.5$ miles or heavy clouds between fireball and target	0.1

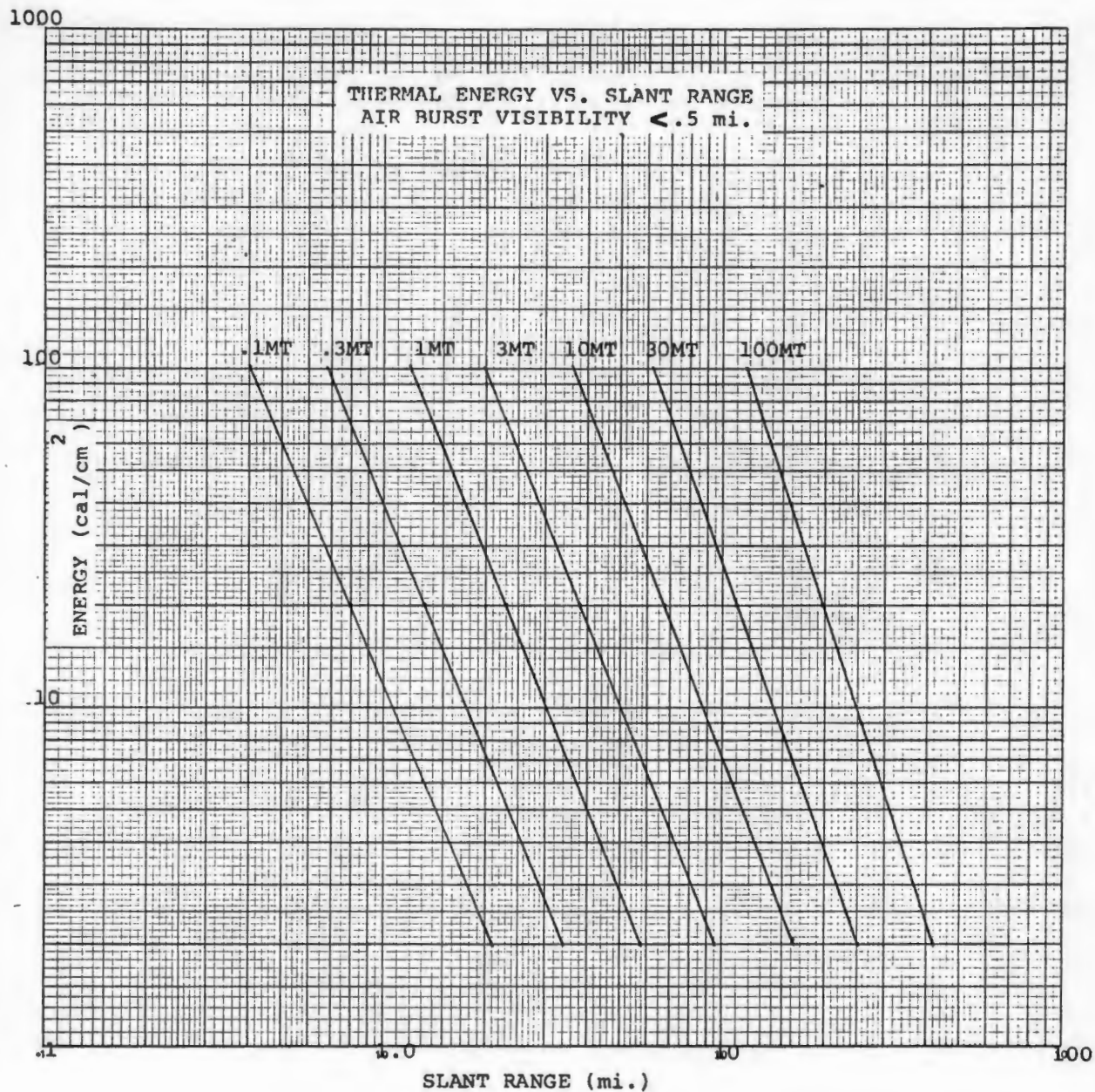


FIGURE A1

1000

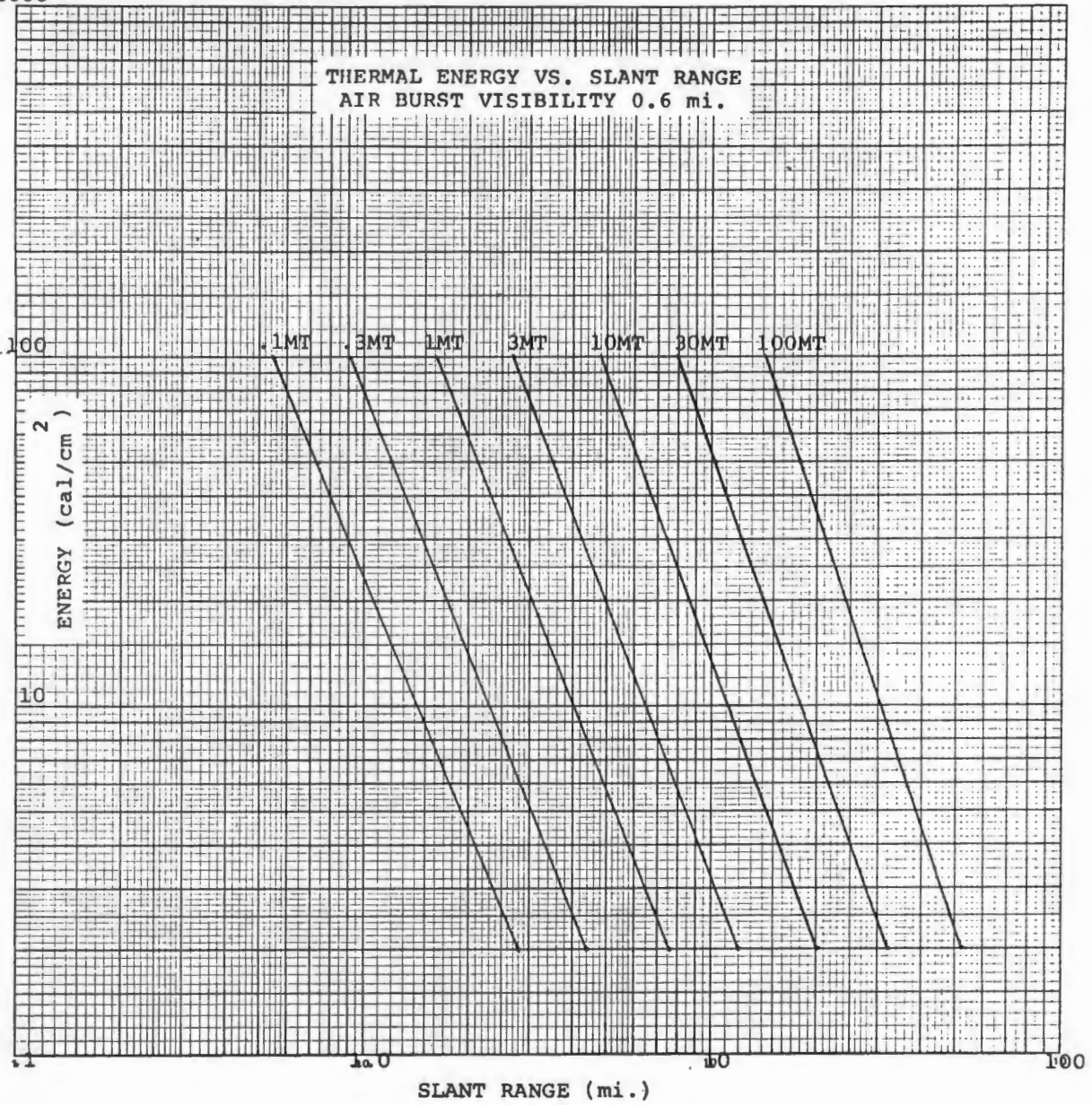


FIGURE A2

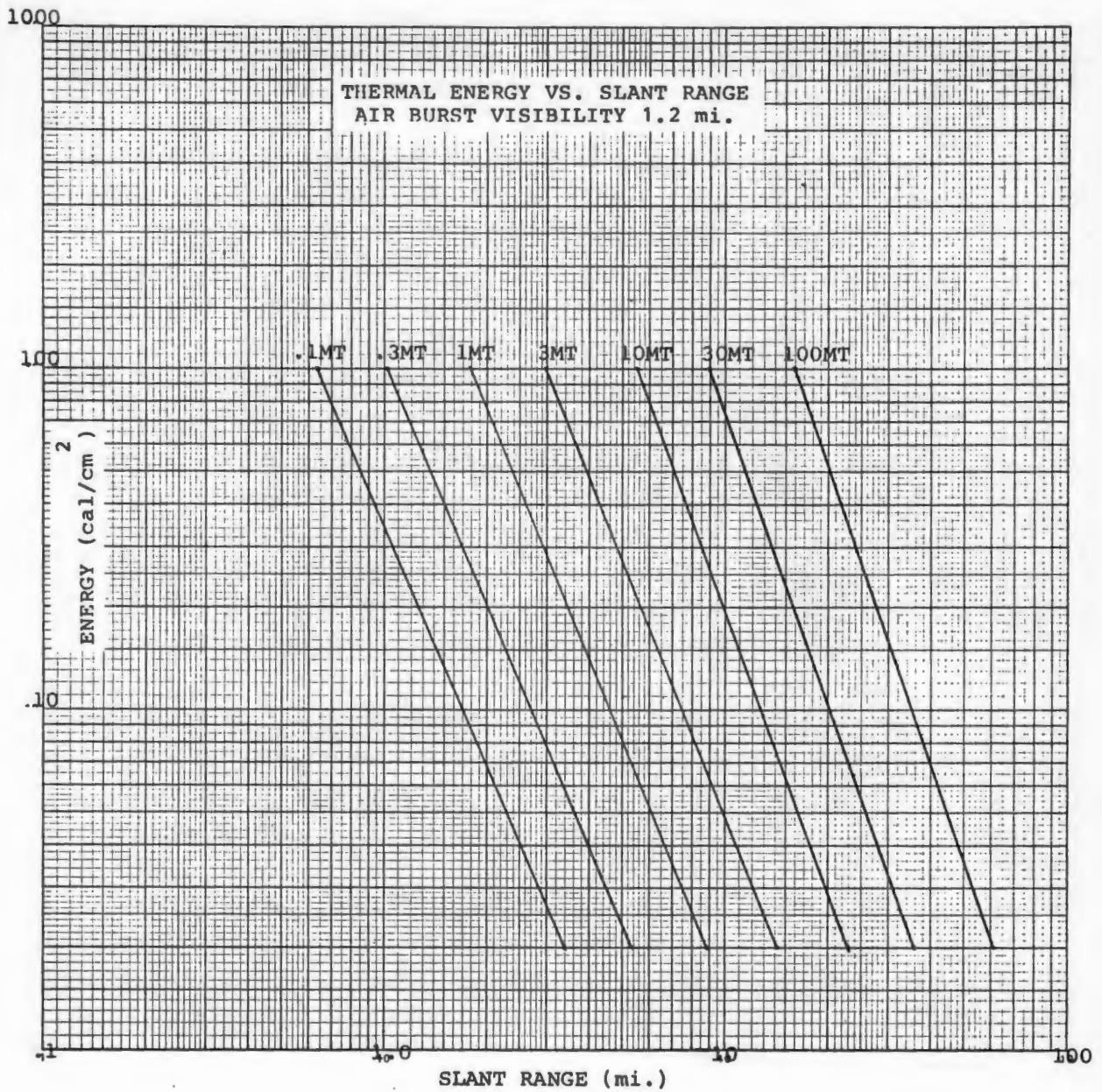


FIGURE A3

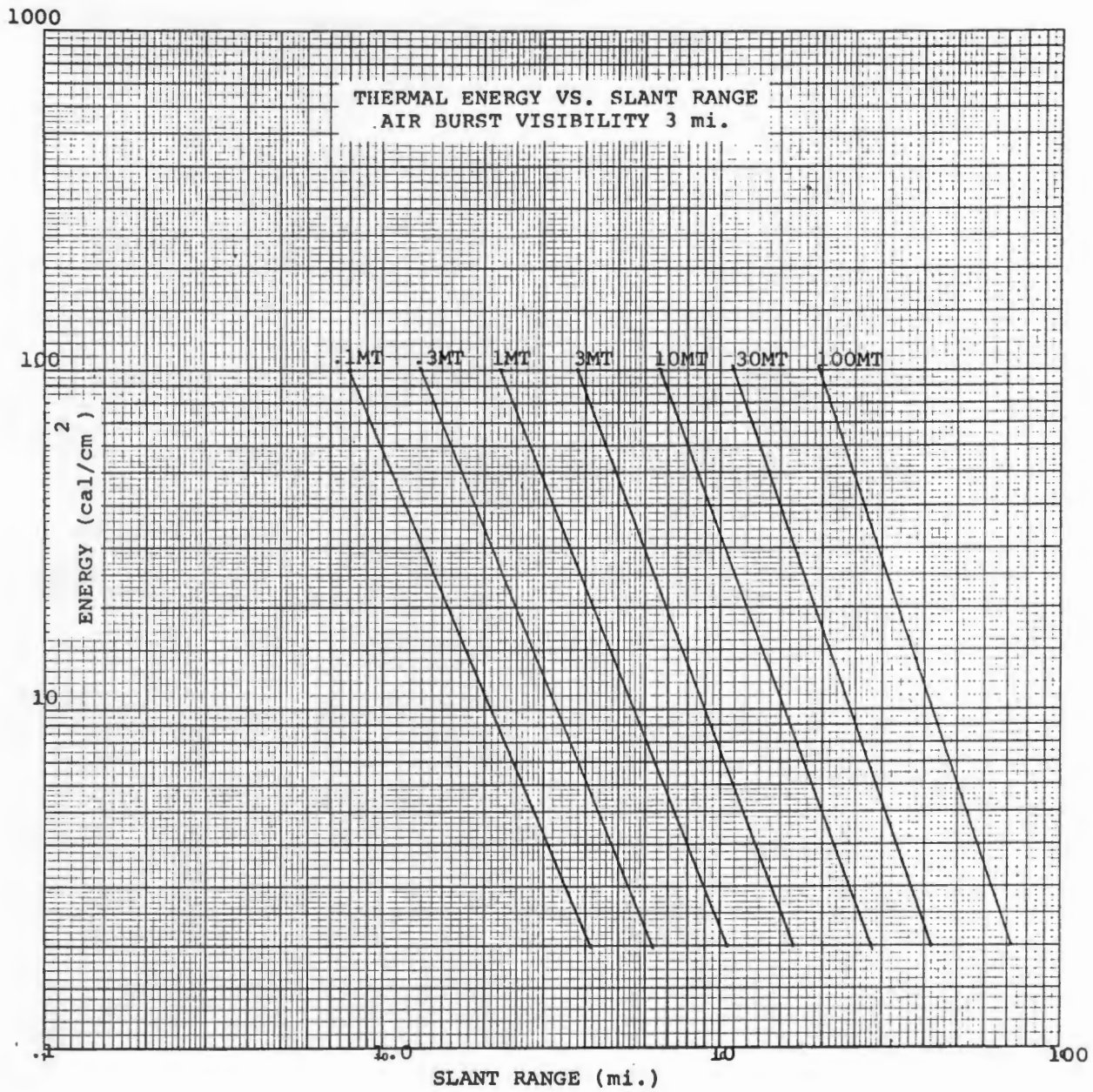


FIGURE A4

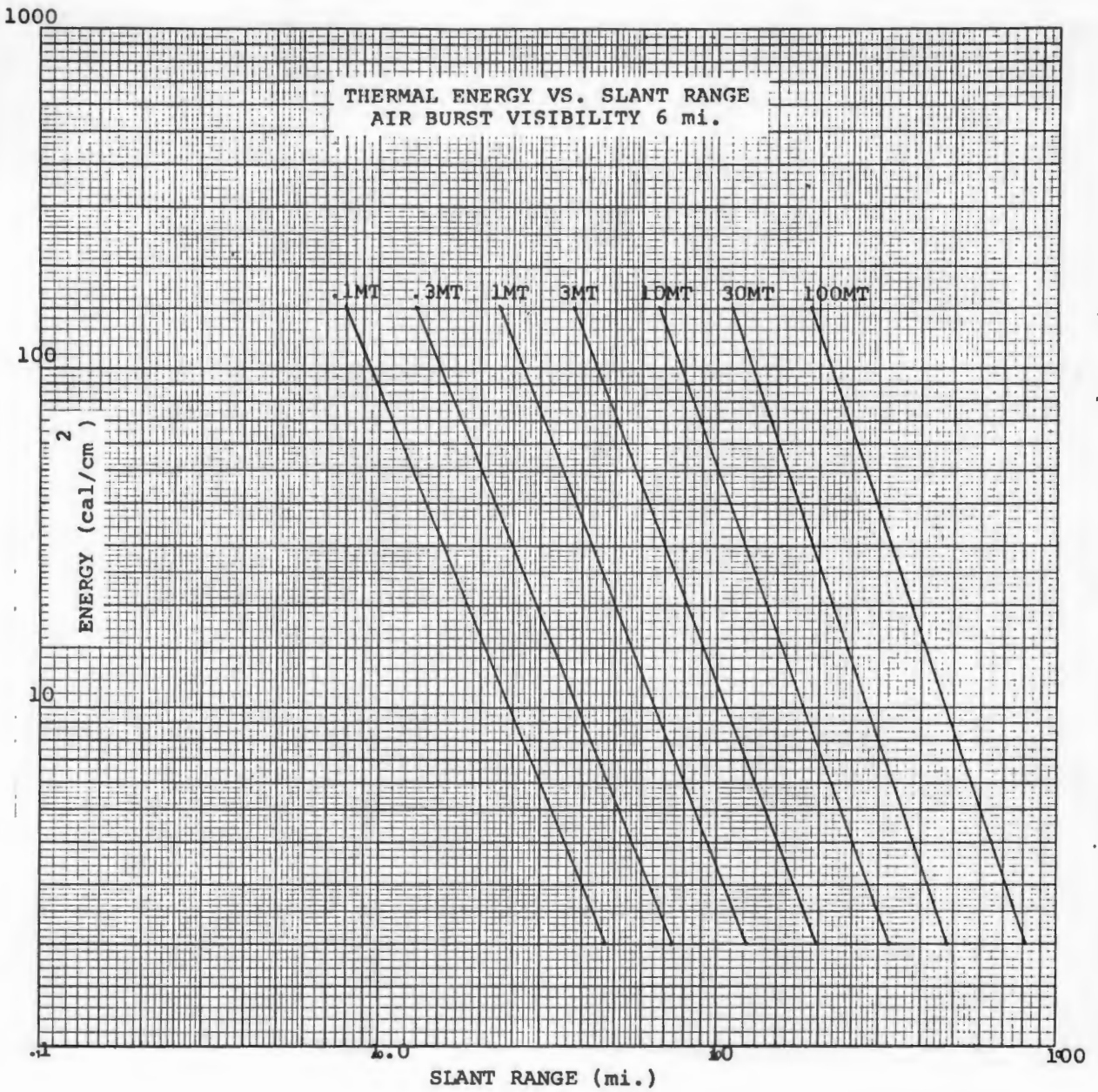


FIGURE A5

1000

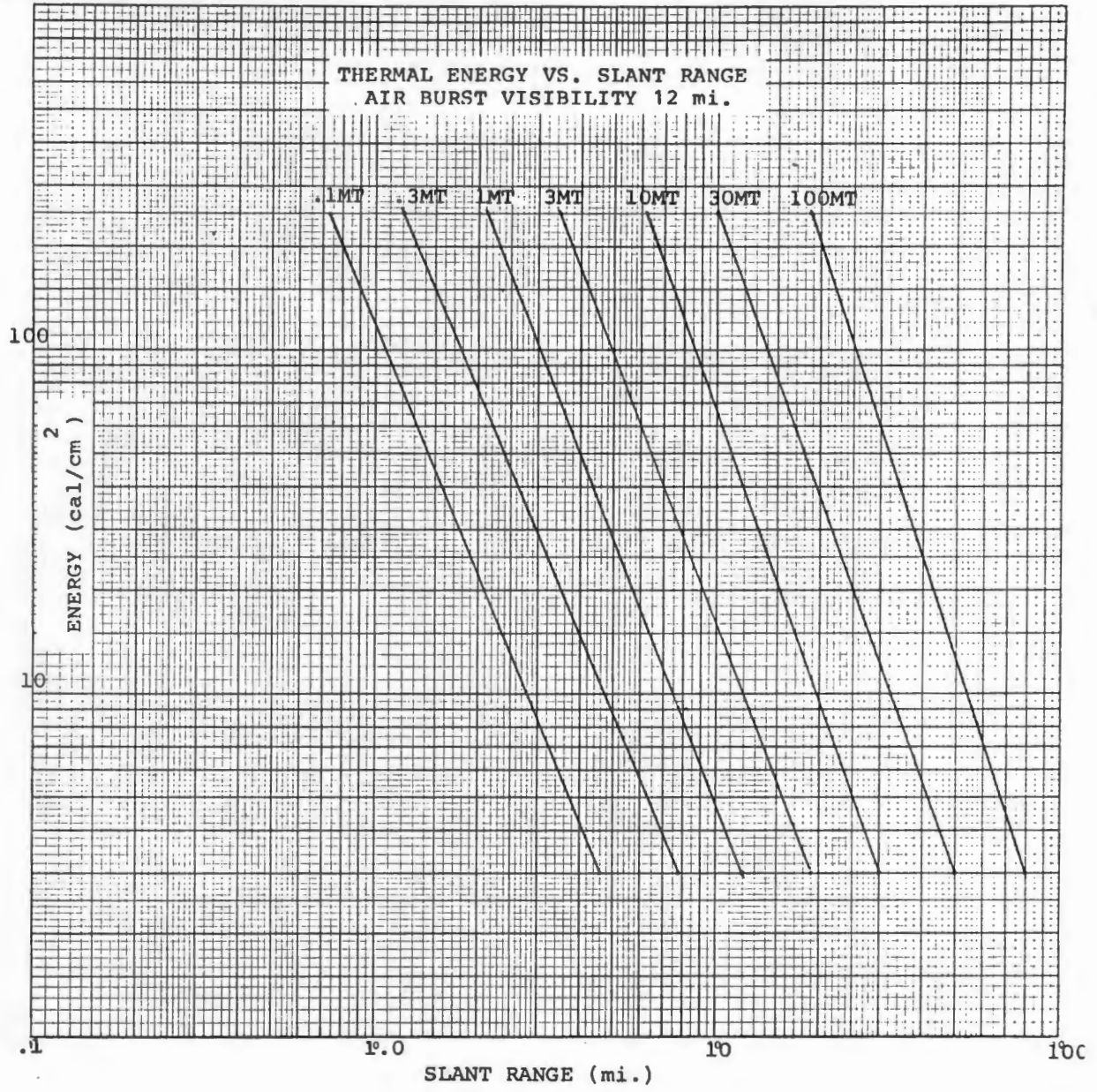


FIGURE A6

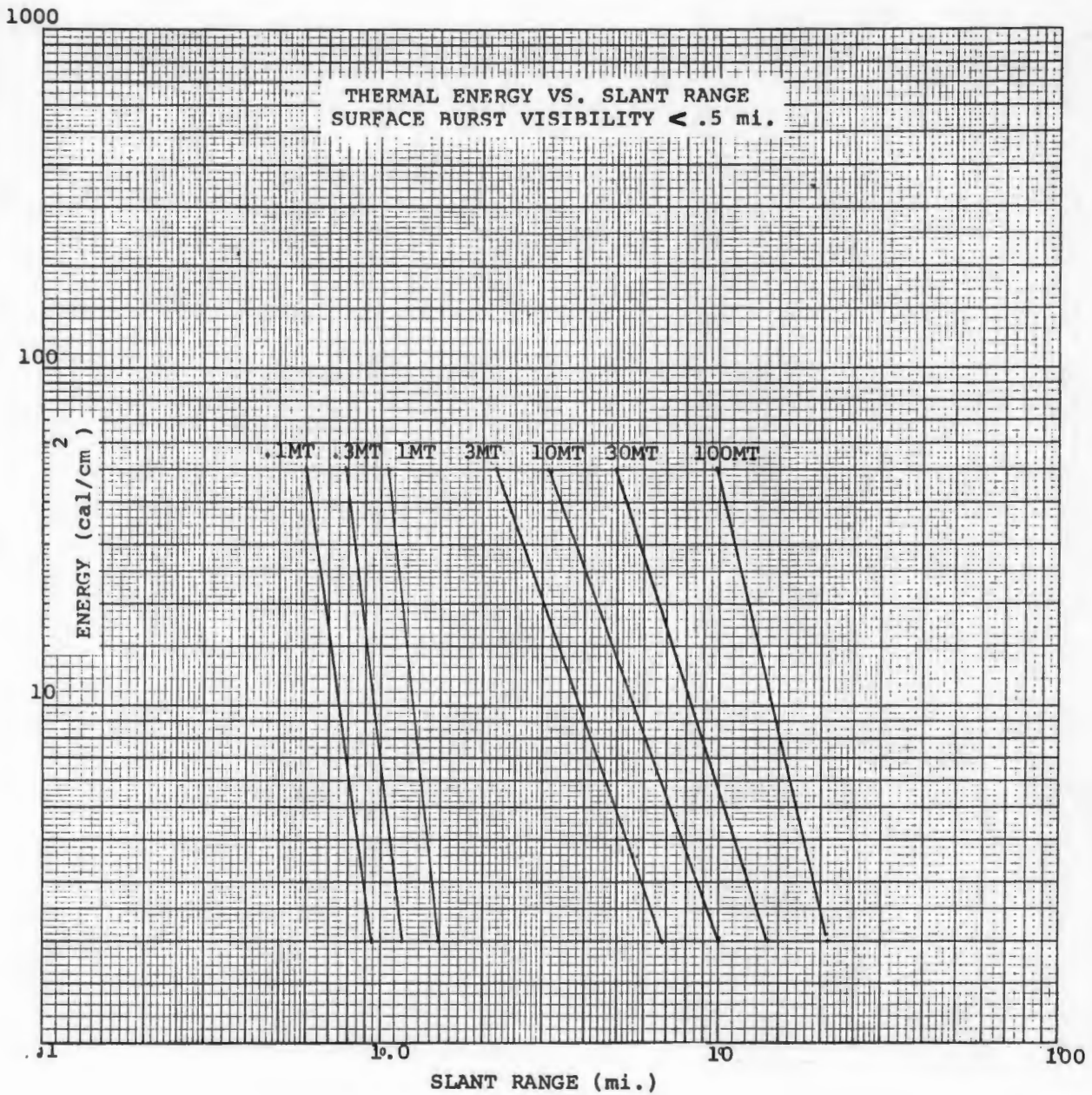


FIGURE A7

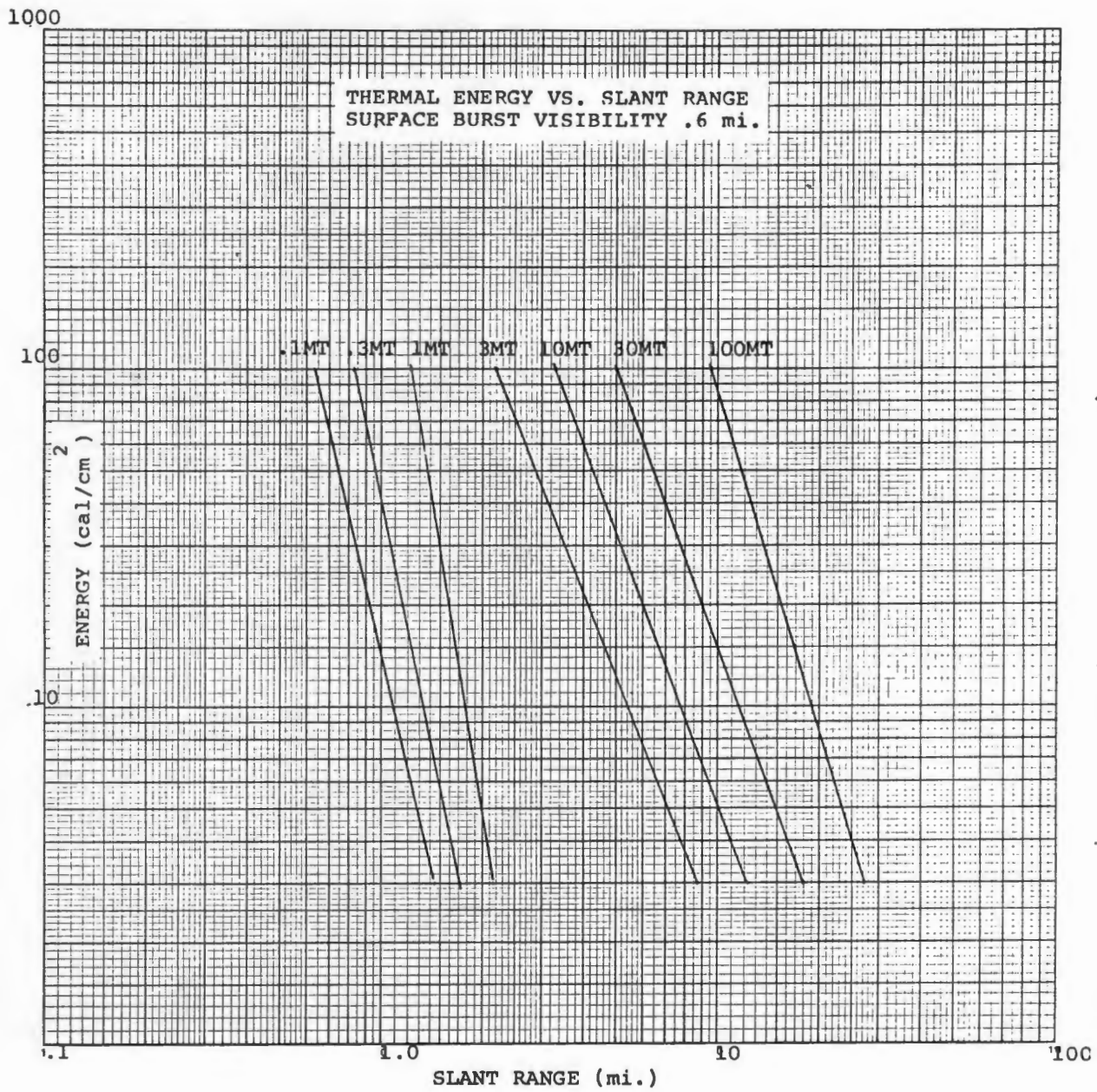


FIGURE A8

1000

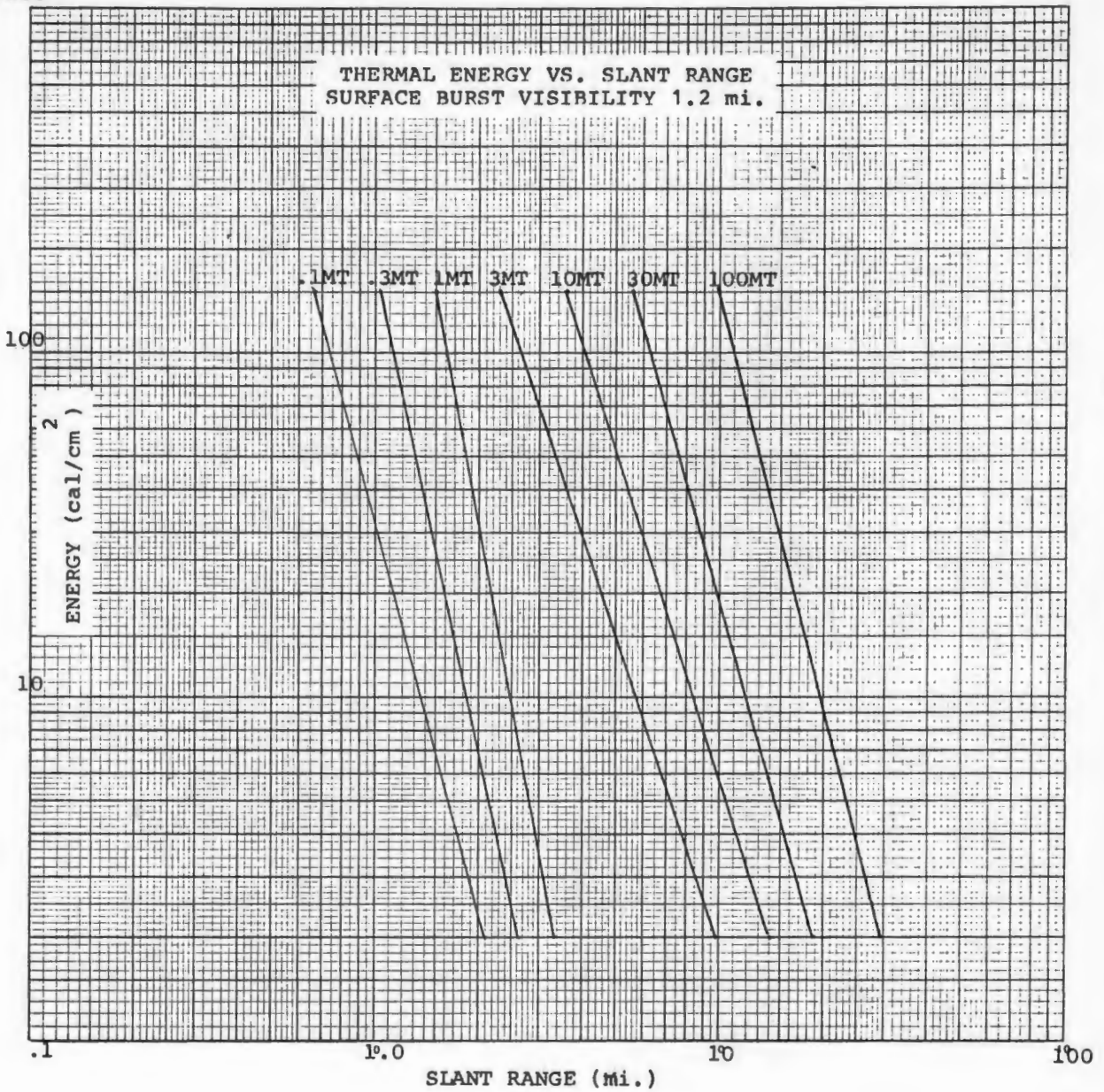


FIGURE A9

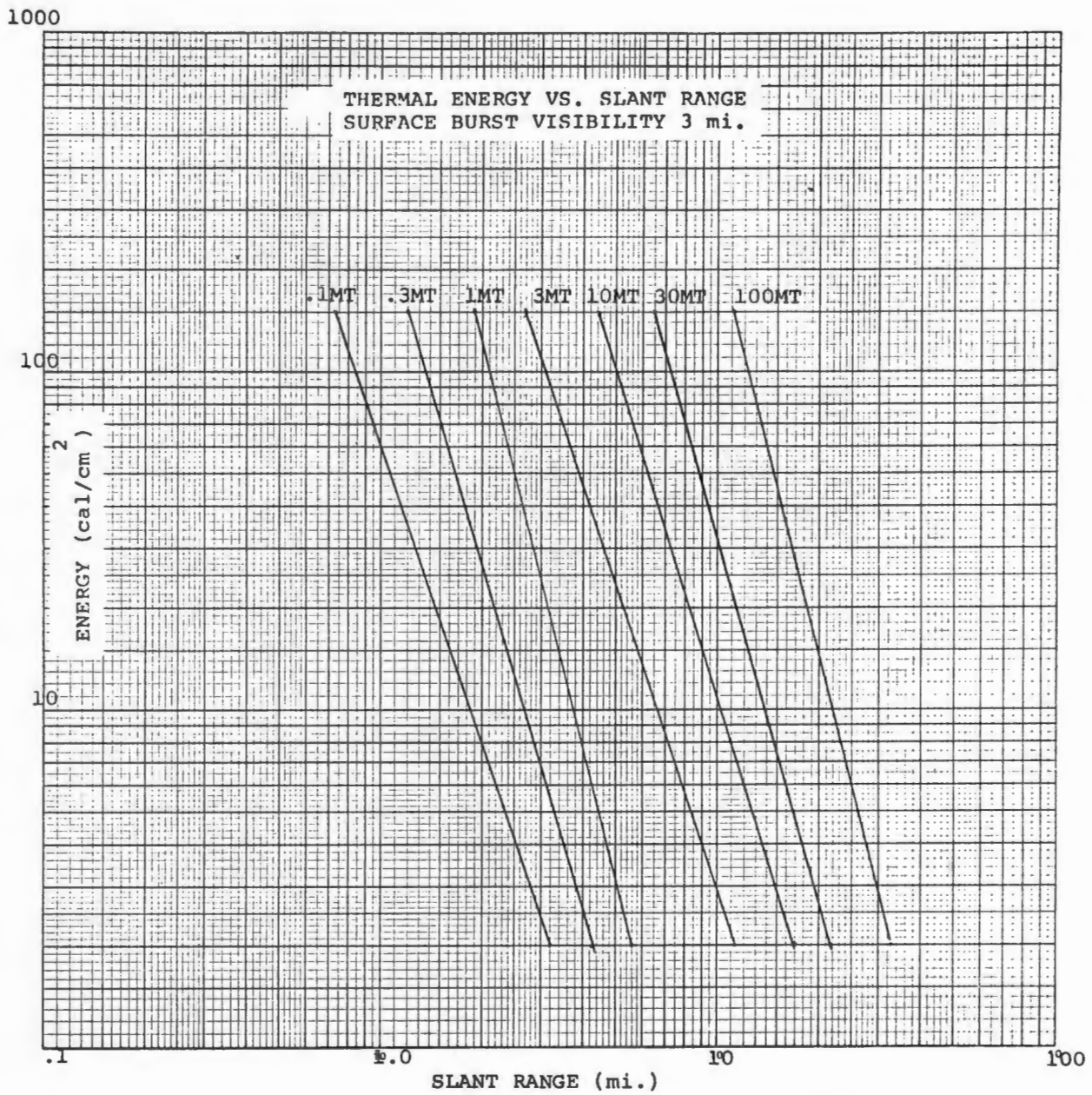


FIGURE A10

1000

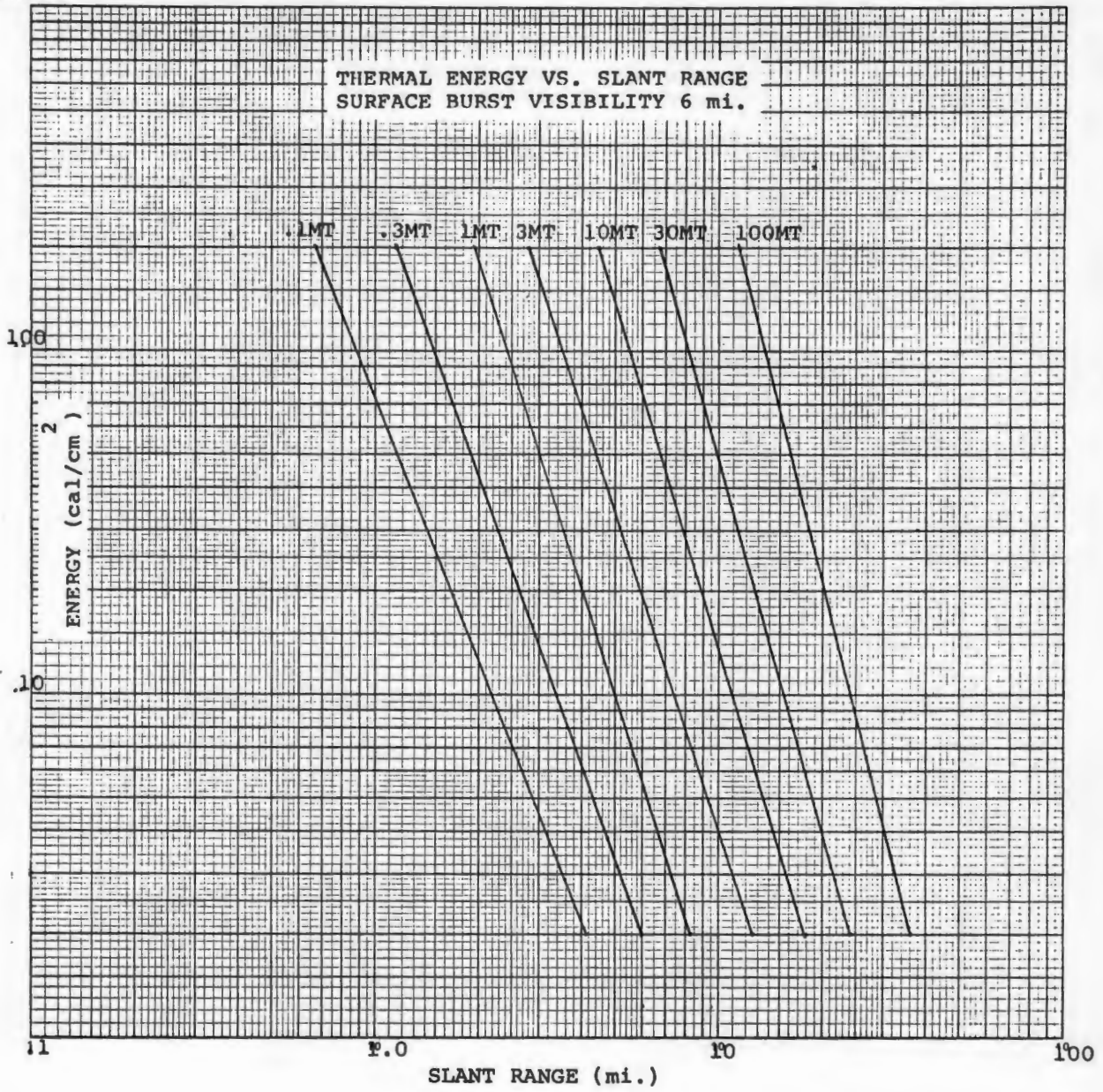


FIGURE A11

1000

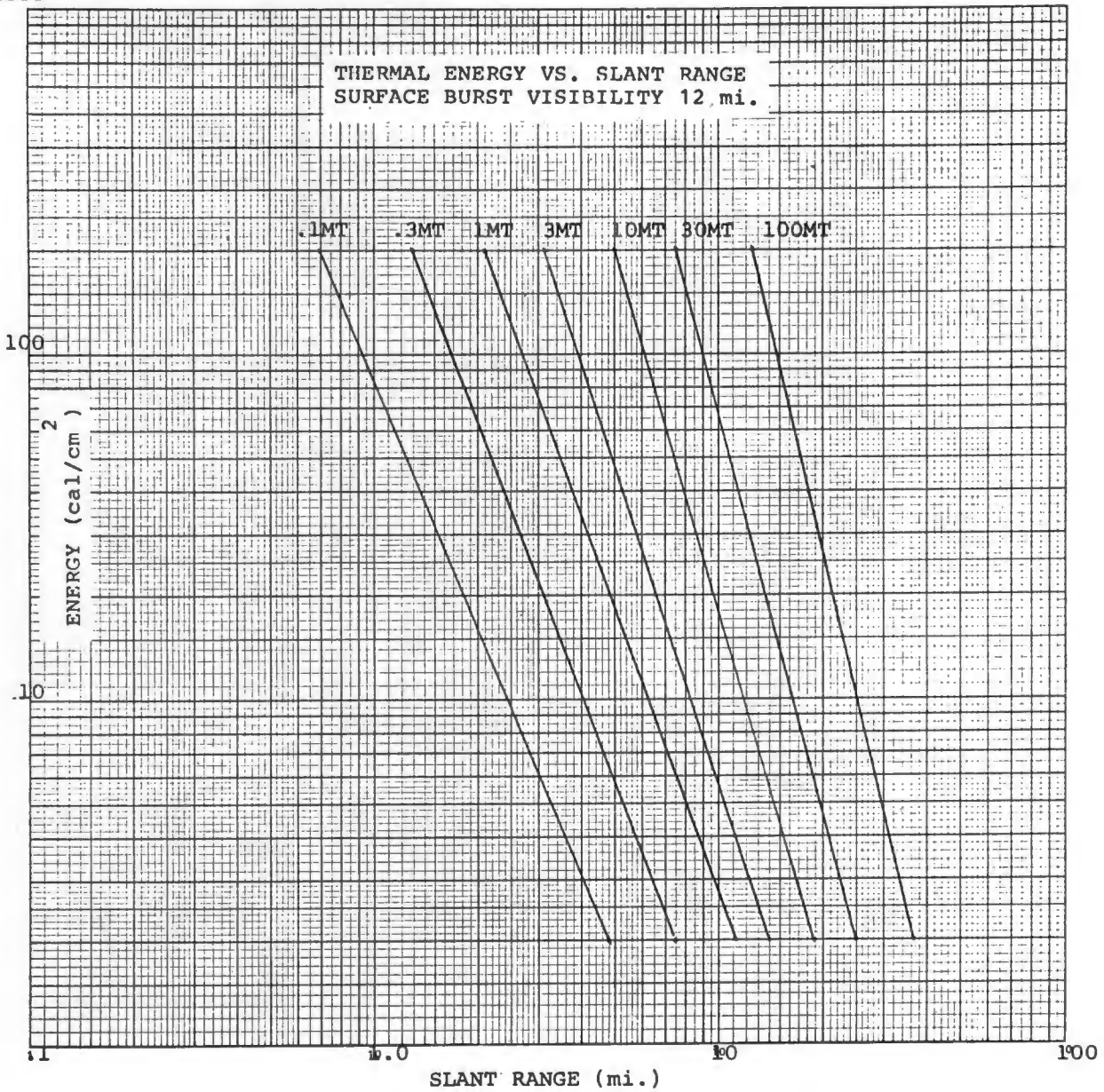


FIGURE A12

APPENDIX B

PROBABILITY CHARTS FOR EXPOSED ROOM IGNITION

Figure B1 is a graph of the probability of exposed room ignition for surface burst weapons in the clear atmosphere. Figures B2-B4 present selected weapon yields (surface burst) plotted at various visibilities. The slopes in Figures B2-B4 may be reasonably estimated in terms of standard deviations (in miles) for surface burst weapons of 3 megatons or greater by

$$\sigma = 0.16 \text{ RIWR} .$$

For yields less than three megatons, σ may be derived from Table B1. To calculate standard deviations for all air burst weapons, use

$$\sigma = 0.21 \text{ RIWR} .$$

Figures B5 and B6 present typical plots of two air burst weapons.

PROBABILITY OF ROOM IGNITION
Surface burst, 12-mile visibility

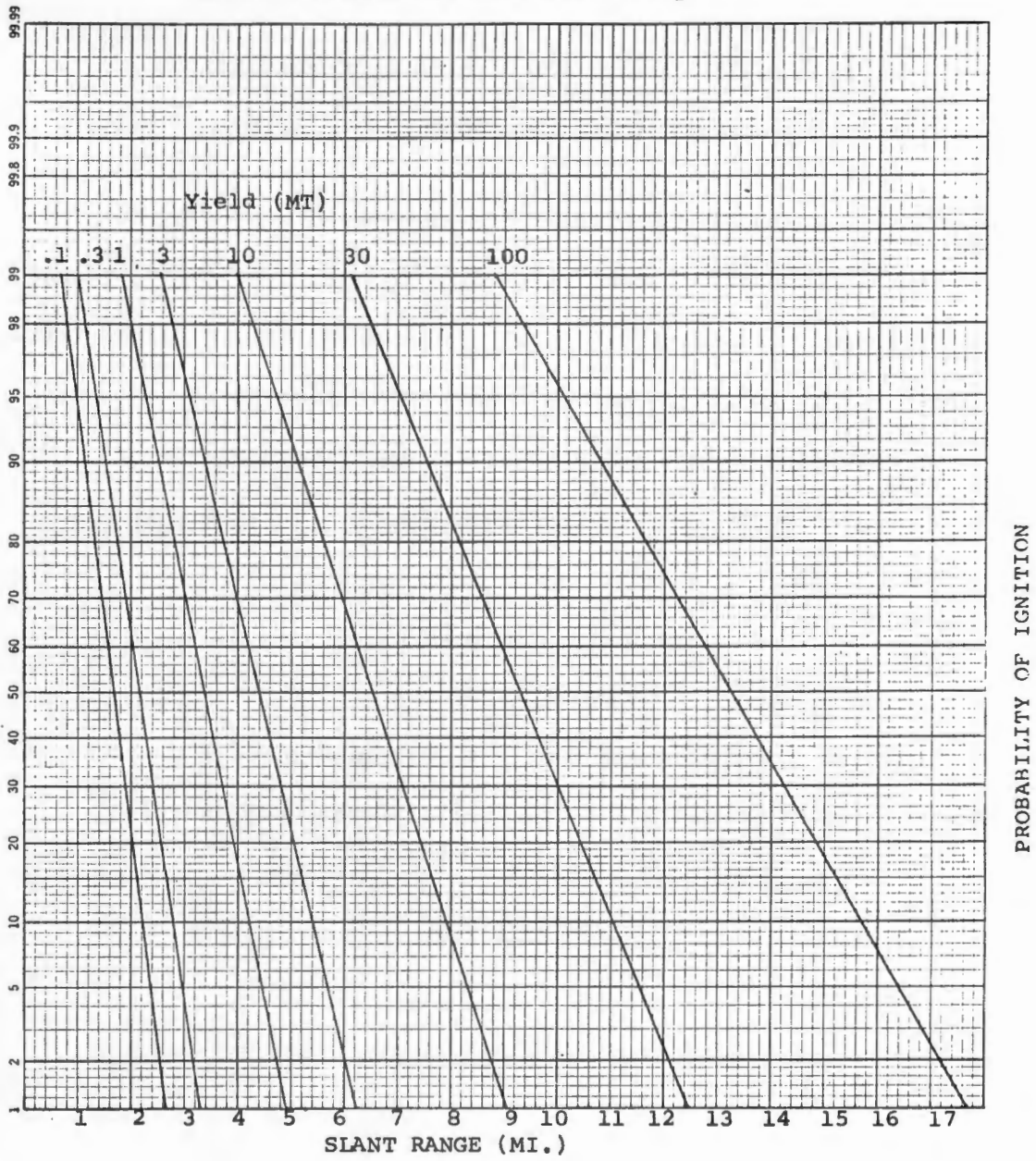


FIGURE B1

PROBABILITY OF ROOM IGNITION
1.0 megaton, surface burst

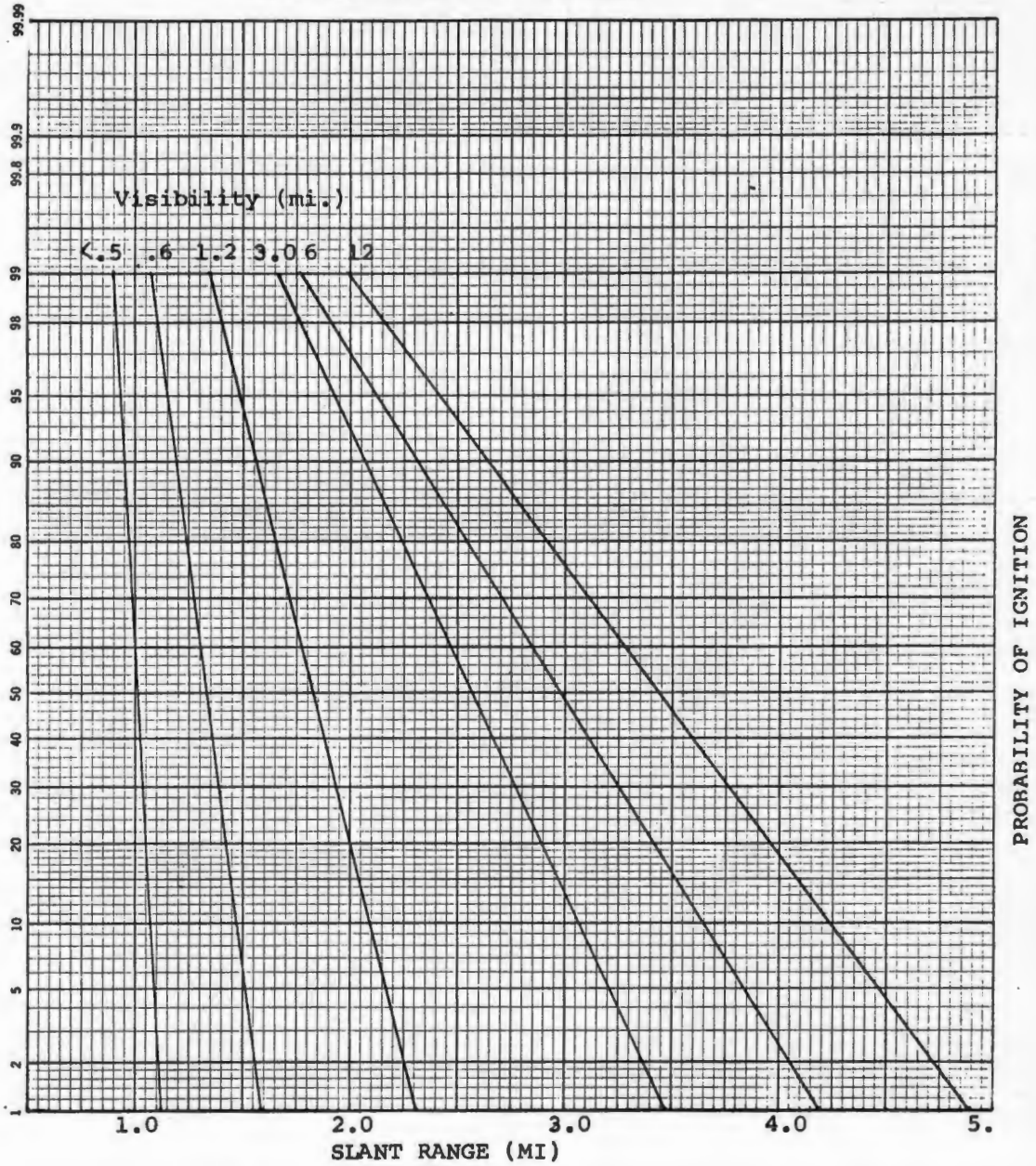
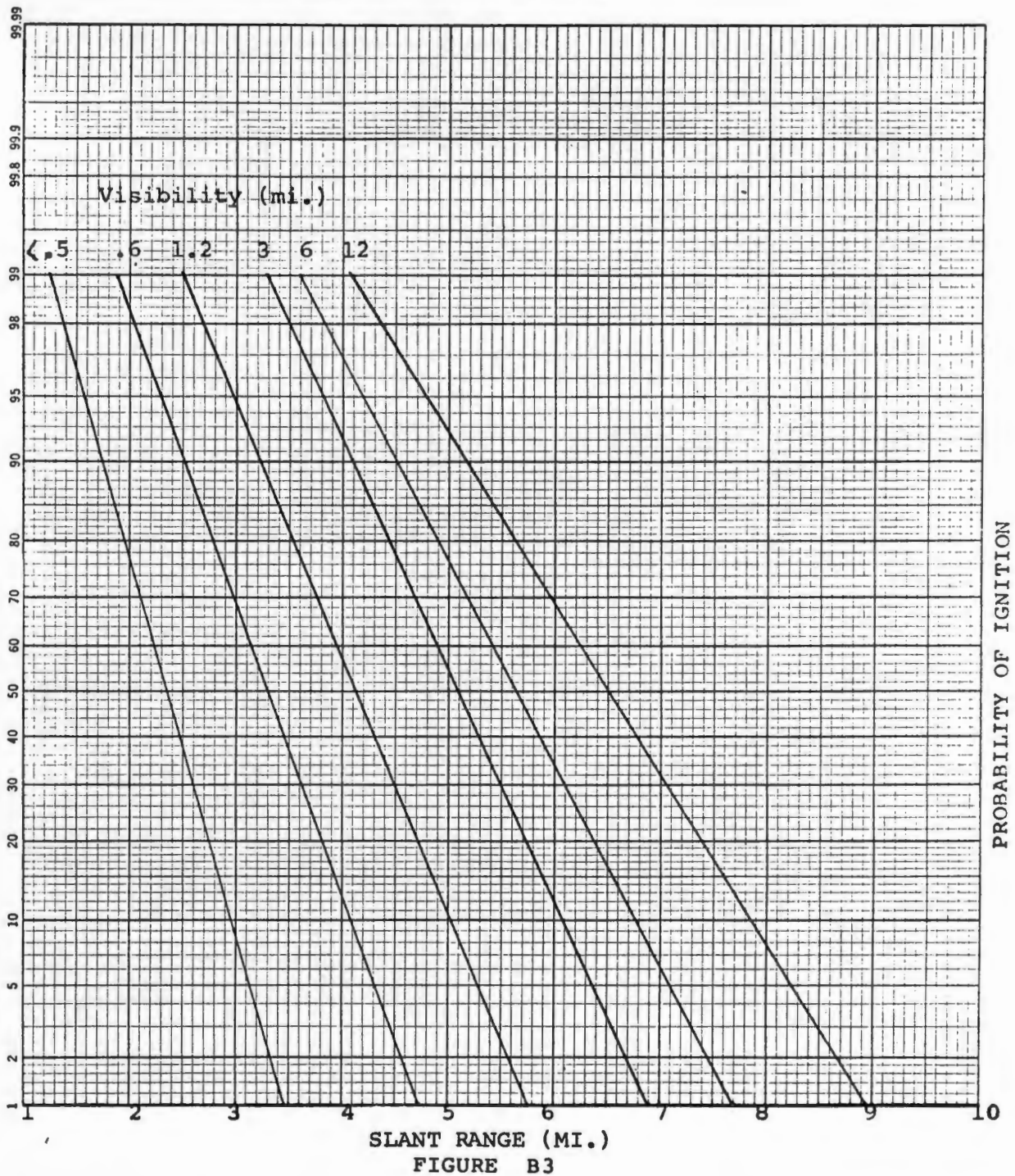


FIGURE B2

PROBABILITY OF ROOM IGNITION
 10 megaton, surface burst



PROBABILITY OF ROOM IGNITION
30 megaton, surface burst

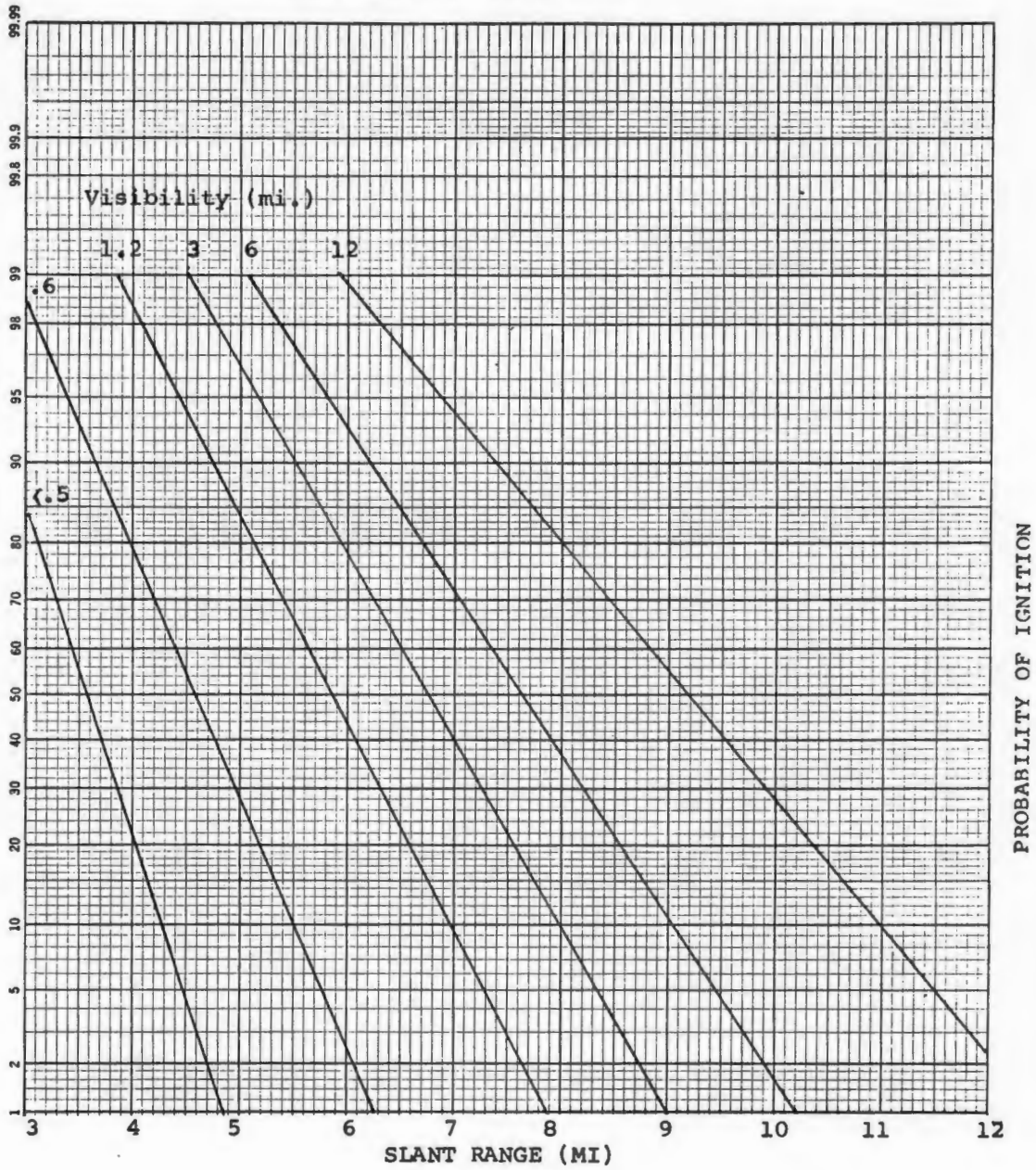


FIGURE B4

PROBABILITY OF ROOM IGNITION
1.0 megaton, air burst

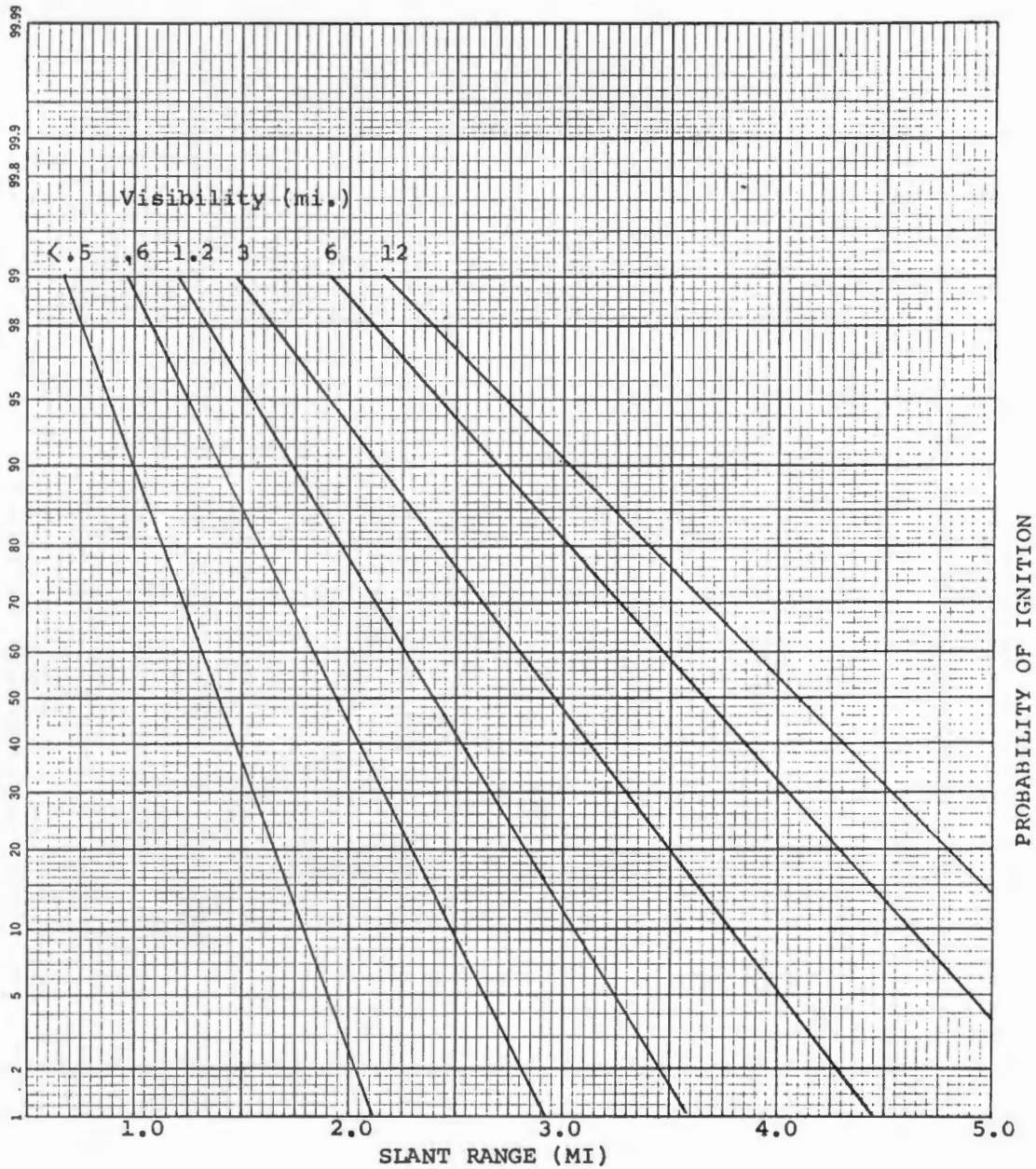


FIGURE B5

PROBABILITY OF ROOM IGNITION
100 megaton, air burst

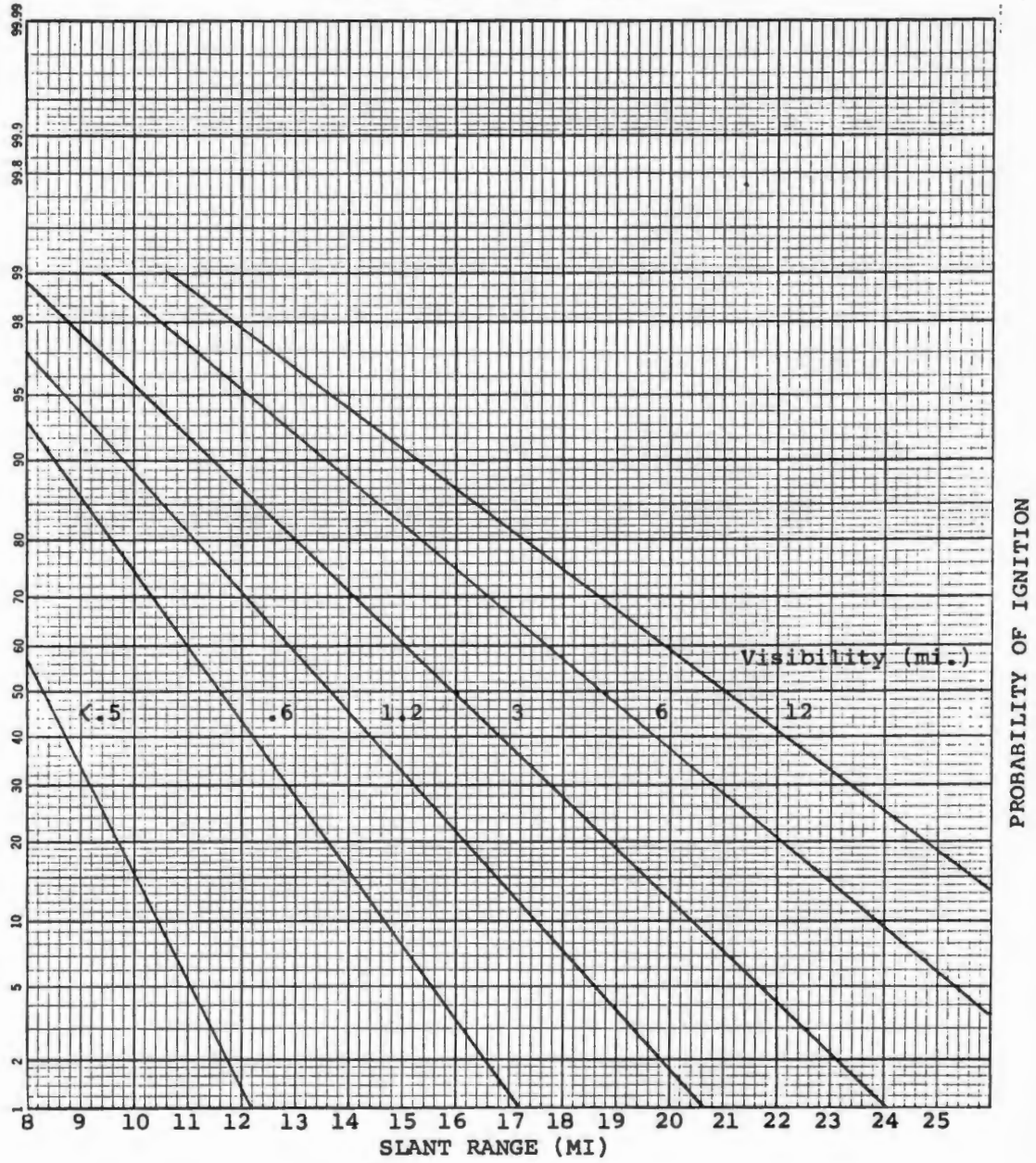


FIGURE B6

TABLE B 1

Standard Deviation, (in miles)

W	Visibility (miles)					
	<.5	.6	1.2	3.0	6.0	12.0
3MT	.24	.33	.43	.56	.66	.74
1MT	.06	.13	.20	.38	.50	.62
.1MT	.05	.10	.15	.30	.35	.40

APPENDIX C

FIREFLY SUMMARIES

Summaries of all FIREFLY runs are contained on the following pages of this appendix.

MIXED RESIDENTIAL - LOW WIND
(WASHINGTON, D. C., SL 22110021)

PROB. ROOM IGNITION	ANGLE OF ELEVATION	AVG NO. OF BUILDINGS BURNT (100 CASES)			PERCENT BURNT (379 BUILDINGS)			STANDARD DEVIATION		
		THERMAL PULSE	SPREAD	TOTAL	THERMAL PULSE	SPREAD	TOTAL	THERMAL PULSE	SPREAD	TOTAL
0.1	30 DEG	51	73	124	13	19	32	6.3	7.3	9.6
0.3	30 DEG	120	50	170	32	13	45	8.1	6.3	10.3
0.5	30 DEG	164	30	194	43	8	51	7.4	4.5	8.7
0.7	30 DEG	190	20	210	50	5	55	7.2	4.1	8.3
0.9	30 DEG	208	15	223	55	4	59	7.3	3.3	8.0
230 0.1	10 DEG	43	70	113	11	18	29	5.2	8.1	9.6
0.3	10 DEG	107	56	163	28	15	43	7.1	6.0	9.3
0.5	10 DEG	148	37	185	39	10	49	6.8	5.1	8.5
0.7	10 DEG	177	24	201	47	6	53	7.5	4.5	8.8
0.9	10 DEG	195	17	212	51	4	55	7.4	3.9	8.4
0.1	5 DEG	30	65	95	8	17	25	5.0	9.9	11.1
0.3	5 DEG	80	66	146	21	17	38	6.2	6.7	9.1
0.5	5 DEG	116	48	164	31	13	44	7.9	6.1	10.0
0.7	5 DEG	143	38	181	38	10	48	7.9	5.4	9.5
0.9	5 DEG	163	29	192	43	8	51	7.5	4.9	9.0

SINGLE-FAMILY RESIDENTIAL - LOW WIND
 (PEORIA, ILLINOIS, PART OF SL's 41510002 and 41510003)

PROB ROOM IGNITION	ANGLE OF ELEVATION	AVG NO. OF BUILDINGS BURNT (100 CASES)			PERCENT BURNT (518 BUILDINGS)			STANDARD DEVIATION		
		THERMAL PULSE	SPREAD	TOTAL	THERMAL PULSE	SPREAD	TOTAL	THERMAL PULSE	SPREAD	TOTAL
0,1	30 DFG	54	28	82	10	5	15	6,6	6,6	9,3
0,3	30 DEG	138	40	178	27	8	35	10,1	6,2	11,9
0,5	30 DEG	198	39	237	38	8	46	9,3	5,7	10,9
0,7	30 DEG	244	35	279	47	7	54	11,1	5,1	12,2
0,9	30 DEG	278	31	309	54	6	60	10,4	5,1	11,6
0,1	10 DEG	48	25	73	9	5	14	7,0	6,2	9,4
0,3	10 DFG	124	39	163	24	8	32	9,5	5,9	11,2
0,5	10 DFG	181	40	221	35	8	43	9,6	6,5	11,6
0,7	10 DEG	222	36	258	43	7	50	10,6	5,7	12,0
0,9	10 DEG	258	33	291	50	6	56	11,5	5,5	12,7
0,1	5 DEG	28	16	44	5	3	8	4,4	5,2	6,8
0,3	5 DFG	72	32	104	14	6	20	6,2	5,8	8,5
0,5	5 DFG	104	36	140	20	7	27	8,5	6,1	10,4
0,7	5 DEG	127	37	164	25	7	32	9,5	6,2	11,4
0,9	5 DEG	145	40	185	28	8	36	9,2	6,3	11,1

MIXED RESIDENTIAL - MEDIUM WIND
(WASHINGTON, D. C., SL 22110021)

PROB ROOM IGNITION	ANGLE OF ELEVATION	AVG NO. OF BUILDINGS BURNT (100 CASES)			PERCENT BURNT (379 BUILDINGS)			STANDARD DEVIATION			
		THERMAL PULSE	SPREAD	TOTAL	THERMAL PULSE	SPREAD	TOTAL	THERMAL PULSE	SPREAD	TOTAL	
	0.1	30 DEG	50	75	125	13	20	33	6.0	7.4	9.5
	0.3	30 DEG	120	51	171	32	13	45	6.6	7.0	9.6
	0.5	30 DEG	163	31	194	43	8	51	8.1	4.7	9.3
	0.7	30 DEG	190	21	211	50	6	56	7.4	3.6	8.2
	0.9	30 DEG	208	16	224	55	4	59	7.7	3.0	8.3
232	0.1	10 DEG	42	75	117	11	20	31	5.6	8.3	10.0
	0.3	10 DEG	106	57	163	28	15	43	7.0	5.7	9.1
	0.5	10 DEG	148	38	186	39	10	49	7.5	4.4	8.7
	0.7	10 DEG	177	27	204	47	7	54	7.3	4.5	8.6
	0.9	10 DEG	194	20	214	51	5	56	7.9	4.2	8.9
	0.1	5 DEG	30	69	99	8	18	26	4.6	9.2	10.2
	0.3	5 DEG	80	68	148	21	18	39	7.1	7.0	9.9
	0.5	5 DEG	117	51	168	31	13	44	7.1	5.5	8.9
	0.7	5 DEG	142	40	182	37	11	48	8.0	5.8	9.9
	0.9	5 DEG	163	29	192	43	8	51	8.4	4.0	9.3

SINGLE-FAMILY RESIDENTIAL - MEDIUM WIND
(PEORIA, ILLINOIS, PART OF SL's 41510002 and 41510003)

PROB ROOM IGNITION	ANGLE OF ELEVATION	AVG NO, OF BUILDINGS BURNT (100 CASES)			PERCENT BURNT (518 BUILDINGS)			STANDARD DEVIATION		
		THERMAL PULSE	SPREAD	TOTAL	THERMAL PULSE	SPREAD	TOTAL	THERMAL PULSE	SPREAD	TOTAL
0,1	30 DEG	55	30	85	11	6	17	6,8	7,3	10,0
0,3	30 DEG	137	43	180	26	8	34	8,7	7,0	11,1
0,5	30 DEG	199	41	240	38	8	46	11,4	6,9	13,4
0,7	30 DEG	244	38	282	47	7	54	10,0	5,7	11,5
0,9	30 DEG	276	33	309	53	6	59	11,4	5,5	12,6
0,1	10 DEG	47	29	76	9	6	15	6,0	7,0	9,2
0,3	10 DEG	123	43	166	24	8	32	8,9	6,5	11,0
0,5	10 DEG	181	43	224	35	8	43	11,0	6,4	12,7
0,7	10 DEG	222	40	262	43	8	51	10,1	5,7	11,6
0,9	10 DEG	258	37	295	50	7	57	11,2	5,7	12,6
0,1	5 DEG	28	17	45	5	3	8	4,5	5,8	7,3
0,3	5 DEG	71	32	103	14	6	20	7,7	7,4	10,7
0,5	5 DEG	102	40	142	20	8	28	7,2	7,2	10,2
0,7	5 DEG	127	41	168	25	8	33	7,1	6,9	9,8
0,9	5 DEG	146	43	189	28	8	36	9,6	7,3	12,1

MIYED RESIDENTIAL - HIGH WIND
(WASHINGTON, D. C., SL 22110021)

PROB ROOM IGNITION	ANGLE OF ELEVATION	AVG NO. OF BUILDINGS BURNT (100 CASES)			PERCENT BURNT (379 BUILDINGS)			STANDARD DEVIATION		
		THERMAL PULSE	SPREAD	TOTAL	THERMAL PULSE	SPREAD	TOTAL	THERMAL PULSE	SPREAD	TOTAL
0.1	30 DEG	49	78	127	13	21	34	5.7	7.5	9.5
0.3	30 DEG	120	54	174	32	14	46	6.9	5.7	9.0
0.5	30 DEG	163	35	198	43	9	52	8.9	4.9	10.1
0.7	30 DEG	191	23	214	50	6	56	8.6	5.0	9.9
0.9	30 DEG	206	19	225	54	5	59	7.5	4.5	8.7
234 0.1	10 DEG	42	76	118	11	20	31	6.0	7.2	9.4
0.3	10 DEG	105	60	165	28	16	44	8.1	6.6	10.4
0.5	10 DEG	149	40	189	39	11	50	6.8	5.4	8.7
0.7	10 DEG	176	28	204	46	7	53	7.1	5.2	8.8
0.9	10 DEG	194	22	216	51	6	57	8.0	4.7	9.3
0.1	5 DEG	31	72	103	8	19	27	5.5	9.8	11.2
0.3	5 DEG	80	69	149	21	18	39	7.3	6.9	10.0
0.5	5 DEG	116	54	170	31	14	45	8.7	6.1	10.6
0.7	5 DEG	143	41	184	38	11	49	8.8	5.7	10.4
0.9	5 DEG	164	32	196	43	8	51	7.7	5.7	9.5

SINGLE-FAMILY RESIDENTIAL - HIGH WIND
(PEORIA, ILLINOIS, PART OF SL's 41510002 and 41510003)

235

PROP ROOM IGNITION	ANGLE OF ELEVATION	AVG NO. OF BUILDINGS BURNT (100 CASES)			PERCENT BURNT (518 BUILDINGS)			STANDARD DEVIATION		
		THERMAL PULSE	SPREAD	TOTAL	THERMAL PULSE	SPREAD	TOTAL	THERMAL PULSE	SPREAD	TOTAL
0,1	30 DEG	55	33	88	11	6	17	6,6	7,3	9,8
0,3	30 DEG	139	46	185	27	9	36	9,1	6,9	11,4
0,5	30 DEG	197	44	241	38	8	46	11,3	6,4	13,0
0,7	30 DEG	244	39	283	47	8	55	11,0	6,0	12,5
0,9	30 DEG	277	34	311	53	7	60	10,1	5,0	11,3
0,1	10 DEG	48	31	79	9	6	15	6,2	7,0	9,3
0,3	10 DEG	123	45	168	24	9	33	9,6	6,3	11,5
0,5	10 DEG	180	44	224	35	8	43	10,1	6,6	12,0
0,7	10 DEG	224	41	265	43	8	51	11,4	6,0	12,9
0,9	10 DEG	257	39	296	50	8	58	10,4	6,1	12,0
0,1	5 DEG	29	19	48	6	4	10	5,4	6,2	8,2
0,3	5 DEG	71	35	106	14	7	21	7,4	7,3	10,4
0,5	5 DEG	103	39	142	20	8	28	7,6	7,0	10,3
0,7	5 DEG	127	44	171	25	8	33	9,8	6,9	12,0
0,9	5 DEG	147	45	192	28	9	37	10,0	5,8	11,6

MULTIFAMILY RESIDENTIAL/COMMERCIAL - LOW WIND
(E. BOSTON, MASSACHUSETTS, SL 13150001)

PROB ROOM IGNITION	ANGLE OF ELEVATION	AVG NO. OF BUILDINGS BURNT (100 CASES)			PERCENT BURNT (200 BUILDINGS)			STANDARD DEVIATION		
		THERMAL PULSE	SPREAD	TOTAL	THERMAL PULSE	SPREAD	TOTAL	THERMAL PULSE	SPREAD	TOTAL
0.1	30 DEG	14	12	26	7	6	13	3.3	4.8	5.8
0.3	30 DEG	38	19	57	19	10	29	4.9	3.7	6.2
0.5	30 DEG	55	20	75	28	10	38	5.9	4.1	7.2
0.7	30 DEG	68	20	88	34	10	44	5.7	4.4	7.2
0.9	30 DEG	79	18	97	40	9	49	5.6	4.1	6.9
236 0.1	10 DEG	3	3	6	2	2	4	1.7	3.3	3.7
0.3	10 DEG	8	9	17	4	5	9	2.6	4.4	5.1
0.5	10 DEG	15	12	27	8	6	14	3.0	4.5	5.4
0.7	10 DEG	20	14	34	10	7	17	3.6	4.4	5.7
0.9	10 DEG	24	17	41	12	9	21	3.9	4.5	5.9
0.1	5 DEG	1	2	3	1	1	2	1.4	2.6	3.0
0.3	5 DEG	6	5	11	3	3	6	2.2	3.7	4.4
0.5	5 DEG	10	8	18	5	4	9	3.5	4.2	5.5
0.7	5 DEG	14	11	25	7	6	13	3.3	4.5	5.6
0.9	5 DEG	17	14	31	9	7	16	3.9	4.1	5.7

MULTIFAMILY RESIDENTIAL - LOW WIND
 (PEORIA, ILLINOIS, PART OF SL's 41510009 and 41510010)

PROB ROOM IGNITION	ANGLE OF ELEVATION	AVG NO. OF BUILDINGS BURNT (100 CASES)			PERCENT BURNT (431 BUILDINGS)			STANDARD DEVIATION		
		THERMAL PULSE	SPREAD	TOTAL	THERMAL PULSE	SPREAD	TOTAL	THERMAL PULSE	SPREAD	TOTAL
0.1	30 DEG	64	69	133	15	16	31	7,3	9,1	11,6
0.3	30 DEG	150	67	217	35	16	51	9,1	7,2	11,6
0.5	30 DEG	196	59	255	45	14	59	8,8	6,6	11,0
0.7	30 DEG	225	50	275	52	12	64	9,1	6,9	11,4
0.9	30 DEG	244	47	291	57	11	68	9,5	5,6	11,0
0.1	10 DEG	57	67	124	13	16	29	6,7	10,2	12,2
0.3	10 DEG	138	72	210	32	17	49	8,9	8,2	12,1
0.5	10 DEG	184	60	244	43	14	57	9,4	5,7	11,0
0.7	10 DEG	216	51	267	50	12	62	10,4	5,4	11,7
0.9	10 DEG	231	48	279	54	11	65	10,5	5,8	12,0
0.1	5 DEG	44	56	100	10	13	23	6,9	11,3	13,2
0.3	5 DEG	106	70	176	25	16	41	6,9	8,4	10,8
0.5	5 DEG	142	68	210	33	16	49	7,1	7,1	10,0
0.7	5 DEG	164	62	226	38	14	52	8,8	6,9	11,1
0.9	5 DEG	176	60	236	41	14	55	9,2	6,2	11,1

MULTIFAMILY RESIDENTIAL/COMMERCIAL - MEDIUM WIND
(E. BOSTON, MASSACHUSETTS, SL 13150001)

PROB ROOM IGNITION	ANGLE OF ELEVATION	AVG NO. OF BUILDINGS BURNT (100 CASES)			PERCENT BURNT (200 BUILDINGS)			STANDARD DEVIATION			
		THERMAL PULSE	SPREAD	TOTAL	THERMAL PULSE	SPREAD	TOTAL	THERMAL PULSE	SPREAD	TOTAL	
	0.1	30 DEG	14	13	27	7	6	13	3.3	4.8	5.8
	0.3	30 DEG	38	22	60	19	11	30	5.1	4.6	6.9
	0.5	30 DEG	54	23	77	27	12	39	6.0	4.6	7.5
	0.7	30 DEG	67	21	88	34	11	45	5.6	4.5	7.1
	0.9	30 DEG	79	21	100	40	11	51	5.4	4.1	6.8
238	0.1	10 DEG	3	4	7	2	2	4	1.4	3.3	3.6
	0.3	10 DEG	9	10	19	5	5	10	3.0	4.7	5.6
	0.5	10 DEG	14	13	27	7	6	13	3.9	5.0	6.3
	0.7	10 DEG	20	16	36	10	8	18	3.9	4.7	6.1
	0.9	10 DEG	24	18	42	12	9	21	4.5	4.5	6.3
	0.1	5 DEG	2	2	4	1	1	2	1.0	2.8	3.0
	0.3	5 DEG	6	7	13	3	4	7	2.2	4.9	5.4
	0.5	5 DEG	9	10	19	5	5	10	2.8	4.5	5.3
	0.7	5 DEG	14	14	28	7	7	14	3.5	4.7	5.8
	0.9	5 DEG	17	15	32	9	8	17	3.6	5.1	6.2

MULTIFAMILY RESIDENTIAL - MEDIUM WIND
 (PEORIA, ILLINOIS, PART OF SL's 41510009 and 41510010)

PROB ROOM IGNITION	ANGLE OF ELEVATION	AVG NO. OF BUILDINGS BURNT (100 CASES)			PERCENT BURNT (431 BUILDINGS)			STANDARD DEVIATION		
		THERMAL PULSE	SPREAD	TOTAL	THERMAL PULSE	SPREAD	TOTAL	THERMAL PULSE	SPREAD	TOTAL
0.1	30 DEG	64	73	137	15	17	32	6.2	10.0	11.8
0.3	30 DEG	150	70	220	35	16	51	9.1	7.0	11.4
0.5	30 DEG	198	59	257	46	14	60	9.0	6.2	11.0
0.7	30 DEG	226	52	278	52	12	64	8.4	6.1	10.3
0.9	30 DEG	244	49	293	57	11	68	9.3	6.3	11.2
0.1	10 DEG	59	69	128	14	16	30	6.9	11.4	13.4
0.3	10 DEG	140	73	213	32	17	49	9.5	7.3	12.0
0.5	10 DEG	186	62	248	43	14	57	9.8	7.0	12.0
0.7	10 DEG	215	53	268	50	12	62	9.7	6.2	11.5
0.9	10 DEG	232	50	282	54	12	66	9.7	6.1	11.5
0.1	5 DEG	44	64	108	10	15	25	5.6	11.5	12.8
0.3	5 DEG	106	75	181	25	17	42	7.9	8.4	11.6
0.5	5 DEG	143	68	211	33	16	49	8.8	7.3	11.4
0.7	5 DEG	164	64	228	38	15	53	8.7	6.7	11.0
0.9	5 DEG	177	62	239	41	14	55	8.9	5.7	10.6

MULTIFAMILY RESIDENTIAL/COMMERCIAL - HIGH WIND
(E. BOSTON, MASSACHUSETTS, SL 13150001)

PROB ROOM IGNITION	ANGLE OF ELEVATION	AVG NO. OF BUILDINGS BURNT (100 CASES)			PERCENT BURNT (200 BUILDINGS)			STANDARD DEVIATION			
		THERMAL PULSE	SPREAD	TOTAL	THERMAL PULSE	SPREAD	TOTAL	THERMAL PULSE	SPREAD	TOTAL	
0.1	30 DEG	14	15	29	7	8	15	3.5	5.0	6.1	
0.3	30 DEG	38	23	61	19	12	31	5.2	5.2	7.3	
0.5	30 DEG	54	24	78	27	12	39	5.0	4.6	6.8	
0.7	30 DEG	69	24	93	35	12	47	5.5	4.7	7.2	
0.9	30 DEG	80	22	102	40	11	51	5.3	4.0	6.6	
240	0.1	10 DEG	3	4	7	2	2	4	1.4	3.6	3.9
	0.3	10 DEG	9	11	20	5	6	11	3.0	5.4	6.2
	0.5	10 DEG	15	16	31	8	8	16	3.7	4.9	6.2
	0.7	10 DEG	19	17	36	10	9	19	3.3	4.6	5.7
	0.9	10 DEG	24	21	45	12	11	23	4.7	5.2	7.0
0.1	5 DEG	2	2	4	1	1	2	1.7	3.3	3.7	
0.3	5 DEG	6	7	13	3	4	7	2.0	4.5	4.9	
0.5	5 DEG	9	11	20	5	6	11	2.6	5.1	5.7	
0.7	5 DEG	14	16	30	7	8	15	3.7	5.3	6.5	
0.9	5 DEG	18	17	35	9	9	18	4.0	4.7	6.2	

MULTIFAMILY RESIDENTIAL - HIGH WIND
 (PEORIA, ILLINOIS, PART OF SL's 41510009 and 41510010)

PROB ROOM IGNITION	ANGLE OF ELEVATION	AVG NO. OF BUILDINGS BURNT (100 CASES)			PERCENT BURNT (431 BUILDINGS)			STANDARD DEVIATION		
		THERMAL PULSE	SPREAD	TOTAL	THERMAL PULSE	SPREAD	TOTAL	THERMAL PULSE	SPREAD	TOTAL
0.1	30 DEG	64	77	141	15	18	33	6,3	11,7	13,3
0.3	30 DEG	149	75	224	35	17	52	8,6	7,6	11,5
0.5	30 DEG	196	63	259	45	15	60	9,5	6,9	11,7
0.7	30 DEG	225	53	278	52	12	64	9,8	6,1	11,5
0.9	30 DEG	244	51	295	57	12	69	10,2	5,4	11,6
0.1	10 DEG	58	76	134	13	18	31	6,4	11,3	13,0
0.3	10 DEG	137	78	215	32	18	50	9,5	7,7	12,2
0.5	10 DEG	185	66	251	43	15	58	9,8	7,3	12,2
0.7	10 DEG	214	57	271	50	13	63	10,0	6,8	12,1
0.9	10 DEG	232	51	283	54	12	66	10,3	5,7	11,8
0.1	5 DEG	44	70	114	10	16	26	5,7	10,8	12,2
0.3	5 DEG	106	78	184	25	18	43	7,4	8,8	11,5
0.5	5 DEG	141	74	215	33	17	50	8,7	7,1	11,2
0.7	5 DEG	162	68	230	38	16	54	9,8	6,5	11,8
0.9	5 DEG	178	65	243	41	15	56	8,8	7,3	11,4

CENTRAL BUSINESS DISTRICT & LIVELIHOOD - LOW WIND
 (PEORIA, ILLINOIS, PART OF SL's 41510010, 41510011 and 4150017)

242

PROB ROOM IGNITION	ANGLE OF ELEVATION	AVG NO. OF BUILDINGS BURNT (100 CASES)			PERCENT BURNT (250 BUILDINGS)			STANDARD DEVIATION		
		THERMAL PULSE	SPREAD	TOTAL	THERMAL PULSE	SPREAD	TOTAL	THERMAL PULSE	SPREAD	TOTAL
0.1	30 DEG	92	67	159	36	26	62	6.3	5.6	8.4
0.3	30 DEG	156	38	194	60	15	75	6.3	4.7	7.9
0.5	30 DEG	180	27	207	70	10	80	5.5	4.1	6.9
0.7	30 DEG	191	21	212	74	8	82	5.7	3.6	6.8
0.9	30 DEG	196	18	214	76	7	83	5.6	3.7	6.7
0.1	10 DEG	87	66	153	34	26	60	7.1	5.9	9.2
0.3	10 DEG	150	40	190	58	16	74	7.2	5.3	8.9
0.5	10 DEG	174	30	204	67	12	79	6.6	4.7	8.1
0.7	10 DEG	187	24	211	72	9	81	4.9	3.7	6.2
0.9	10 DEG	195	19	214	76	7	83	5.4	3.6	6.5
0.1	5 DEG	73	68	141	28	26	54	6.6	7.7	10.1
0.3	5 DEG	127	52	179	49	20	69	6.4	5.7	8.5
0.5	5 DEG	152	40	192	59	16	75	6.6	4.8	8.2
0.7	5 DEG	168	32	200	65	12	77	5.5	4.2	6.9
0.9	5 DEG	177	29	206	69	11	80	5.1	4.1	6.6

CENTRAL BUSINESS DISTRICT & LIVELIHOOD - MEDIUM WIND
 (PEORIA, ILLINOIS, PART OF SL's 41510010, 41510011 and 4150017)

PROB ROOM IGNITION	ANGLE OF ELEVATION	AVG NO. OF BUILDINGS BURNT (100 CASES)			PERCENT BURNT (258 BUILDINGS)			STANDARD DEVIATION		
		THERMAL PULSE	SPREAD	TOTAL	THERMAL PULSE	SPREAD	TOTAL	THERMAL PULSE	SPREAD	TOTAL
0,1	30 DEG	93	66	159	36	26	62	6,5	6,2	9,0
0,3	30 DEG	156	39	195	60	15	75	7,1	5,1	8,7
0,5	30 DEG	180	27	207	70	10	80	5,7	4,8	7,5
0,7	30 DEG	192	21	213	74	8	82	4,8	3,9	6,2
0,9	30 DEG	196	19	215	76	7	83	5,1	3,6	6,2
0,1	10 DEG	87	70	157	34	27	61	6,3	7,5	9,8
0,3	10 DEG	150	43	193	58	17	75	6,2	5,1	8,1
0,5	10 DEG	174	30	204	67	12	79	6,1	4,2	7,4
0,7	10 DEG	187	24	211	72	9	81	5,4	4,2	6,9
0,9	10 DEG	193	20	213	75	8	83	5,6	3,9	6,8
0,1	5 DEG	74	70	144	29	27	56	6,8	8,1	10,6
0,3	5 DEG	128	52	180	50	20	70	6,4	6,2	8,9
0,5	5 DEG	154	40	194	60	16	76	7,1	5,6	9,0
0,7	5 DEG	168	34	202	65	13	78	6,5	4,6	7,9
0,9	5 DEG	177	29	206	69	11	80	5,7	4,1	7,1

CENTRAL BUSINESS DISTRICT & LIVELIHOOD - HIGH WIND
 (PEORIA, ILLINOIS, PART OF SL's 41510010, 41510011 and 4150017)

244

PROB ROOM IGNITION	ANGLE OF ELEVATION	AVG NO. OF BUILDINGS BURNT (100 CASES)			PERCENT BURNT (258 BUILDINGS)			STANDARD DEVIATION		
		THERMAL PULSE	SPREAD	TOTAL	THERMAL PULSE	SPREAD	TOTAL	THERMAL PULSE	SPREAD	TOTAL
0.1	30 DEG	93	68	161	36	26	62	7.1	7.9	10.6
0.3	30 DEG	156	42	198	60	16	76	6.7	5.8	8.9
0.5	30 DEG	180	28	208	70	11	81	6.0	5.1	7.9
0.7	30 DEG	191	22	213	74	9	83	5.7	4.1	7.1
0.9	30 DEG	196	20	216	76	8	84	5.6	3.6	6.6
0.1	10 DEG	87	70	157	34	27	61	6.8	8.5	10.9
0.3	10 DEG	150	44	194	58	17	75	6.5	5.1	8.2
0.5	10 DEG	173	33	206	67	13	80	6.7	4.8	8.2
0.7	10 DEG	186	25	211	72	10	82	5.4	4.4	6.9
0.9	10 DEG	193	22	215	75	9	84	5.5	3.5	6.5
0.1	5 DEG	73	73	146	28	28	56	5.6	8.6	10.2
0.3	5 DEG	128	55	183	50	21	71	7.8	6.2	9.9
0.5	5 DEG	153	43	196	59	17	76	5.7	5.1	7.6
0.7	5 DEG	168	35	203	65	14	79	5.8	4.5	7.3
0.9	5 DEG	177	31	208	69	12	81	5.7	4.4	7.1

APPENDIX D

BUILDING LOADING

In developing loading diagrams, the procedure in which reflected pressure P_r decays to overpressure P_σ in time has been followed where

$$T_0 = \frac{3S}{U}$$

where

- S = building height or half the building width, whichever is less
- U = short velocity.

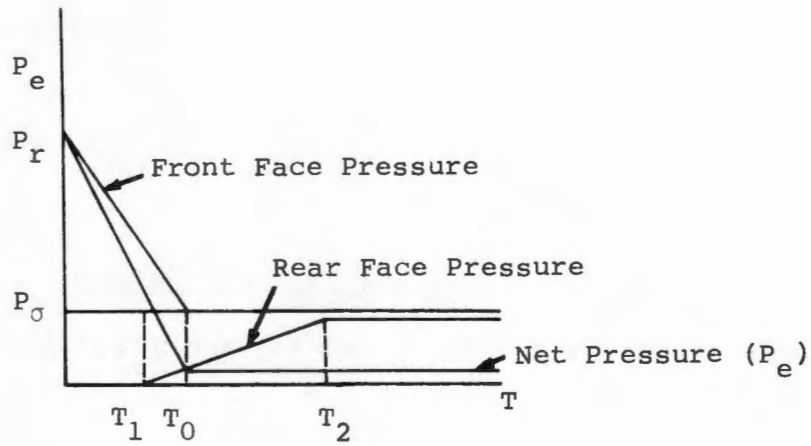
Overpressure P_σ starts to build up on the rear of the building at time

$$T_1 = \frac{d}{U}, \quad d = \text{building depth}$$

and radius P_σ at time

$$T_2 = \frac{d}{U} + \frac{4S}{u} .$$

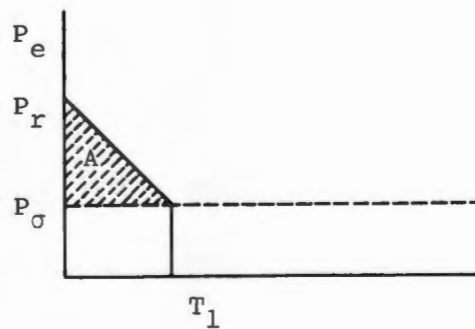
The resultant loading is the diagram as shown on the following page.



To determine β , the area under the net pressure curve is set equal to

$$P_r \int_0^{\infty} e^{-\beta t} dt = \frac{P_r}{\beta} .$$

For obtaining net pressure on the front face only, a β based on the shaded triangular area shown below is determined.



Thus

$$A = (P_r - P_\sigma) \int_0^{\infty} e^{-\beta t} dt = \frac{P_r - P_\sigma}{\beta}.$$

The front wall loading is then

$$P_e = (P_r - P_\sigma) e^{-\beta t} + P_\sigma.$$

If the building has a fraction f of openings, then to be correct P_r on the front face should be replaced everywhere by $(1-f) P_r + f P_\sigma$. The rear pressure would be $(1-f) P_\sigma$ at maximum. Calculations thus far have used $(1-f) P_r$ as the net initial pressure on the front wall and $(1-f) P_\sigma$ as the maximum on the rear wall.

DISTRIBUTION LIST

<u>Addressees</u>	<u>No. of Copies</u>
Defense Documentation Center Cameron Station, Alexandria, Virginia	20
Dr. James O. Buchanan, Director Shelter Research Division, OSA/OCD Washington, D. C. 20310	1
Assistant Secretary of the Army (R&D) Attention: Assistant for Research Washington, D. C. 20310	1
Army Library, TAGO, Civil Defense Unit The Pentagon, Washington, D. C. 20310	1
Chief of Engineers, Department of the Army Attention: ENGTE-E, Washington, D. C. 20310	1
Mr. Edward R. Saunders, Office of Emergency Planning Executive Office of the President Washington, D. C. 20504	1
Mr. Charles F. Coffin, Planning Officer Technical Analysis Division Office of Emergency Planning Executive Office of the President Washington, D. C. 20504	1
Director, Defense Atomic Support Agency Attention: Technical Library Washington, D. C. 20301	1
U.S. Naval Radiological Defense Laboratory Attention: Technical Library (Code 222A) San Francisco, California 94135	1
Civil Defense Technical Office Attention: Mr. William L. White Stanford Research Institute Menlo Park, California 94025	1
Director, Civil Effects Branch Division of Biology and Medicine Atomic Energy Commission Attention: Mr. L. J. Deal Washington, D. C. 20545	1

<u>Addressees</u>	<u>No. of Copies</u>
Advisory Committee on Civil Defense National Academy of Sciences, Attention: Mr. Richard Park 2101 Constitution Avenue, N.W. Washington, D. C. 20418	1
The RAND Corporation 1700 Main Street Attention: Dr. Harold Brode Santa Monica, California	1
Dr. A. Sachs, Institute of Defense Analysis 400 Army-Navy Drive Arlington, Virginia 22202	1
Sandia Corporation Attention: Mr. Luke Vortman, Division 5412 Box 5800, Sandia Base Albuquerque, New Mexico 87115	1
University of Washington Attention: Mr. Bill Miller Department of Civil Engineering 307 More Hall Seattle, Washington	1
San Jose State College Attention: Mr. Franklin J. Agardy Department of Civil Engineering San Jose, California	1
Worcester Polytechnic Institute Attention: Mr. Carl Koontz Department of Civil Engineering Worcester, Massachusetts	1
Purdue University Attention: Mr. M. B. Scott School of Engineering Lafayette, Indiana	1
University of Colorado Attention: Mr. C. K. Vetter School of Architecture Boulder, Colorado	1
Texas A&M University Attention: Mr. Charles H. Samson, Jr., Head Civil Engineering Department College Station, Texas	1

<u>Addressees</u>	<u>No. of Copies</u>
IIT Research Institute Attention: Dr. Eugene Sevin 10 W. 35th Street Chicago, Illinois 60616	1
OSA/OCD Attention: Mr. Henry Dorsett The Pentagon, Room 1E543 Washington, D. C. 20310	1
U.S. Naval Radiological Defense Laboratory Attention: Dr. M. G. Gibbons San Francisco, California 94135	1
IIT Research Institute Attention: Dr. William Christian Technology Center Chicago, Illinois 60616	1
U.S. Naval Applied Science Laboratory Flusing and Washington Avenue Attention: Mr. J. Bracciaventi Brooklyn, New York 11251	1
The Dikewood Corporation Attention: Mr. T. E. Lommasson University Research Park 1009 Bradbury Drive, S.E. Albuquerque, New Mexico 87106	1
Southwest Research Institute Attention: Mr. Lester Eggleston Fire Research Section Department of Structural Research San Antonia, Texas	1
Gage-Babcock & Associates, Inc. Attention: Mr. B. M. Cohn 9836 W. Roosevelt Road West Chester, Illinois 60153	1
URS Corporation Attention: Mr. Stan Martin Radiation Technology Division 1811 Trusdale Drive Burlingame, California 94010	1

<u>Addressees</u>	<u>No. of Copies</u>
Stanford Research Institute, Attention: Mr. Kendall Moll R&D Studies Menlo Park, California 94025	1
Applied Physics Laboratory Attention: Dr. Robert Fristrom, Editor Fire Research Abstracts and Reviews The Johns Hopkins Laboratory 8621 Georgia Avenue Silber Spring, Maryland 20910	1
National Bureau of Standards Attention: Dr. A. F. Robertson Washington, D. C. 20234	1
Chief, NMCSSC Attention: Mr. R. Epperson The Pentagon, Room BE685 Washington, D. C.	1
Assistant Director of Civil Defense (Research) Office of Civil Defense Department of the Army-OSA Washington, D. C. 20310	47

UNCLASSIFIED

Security Classification

DOCUMENT CONTROL DATA - R & D		
<i>(Security classification of title, body of abstract and indexing annotation must be entered when the overall report is classified)</i>		
1. ORIGINATING ACTIVITY (Corporate author) System Sciences, Inc. 4720 Montgomery Lane Bethesda, Maryland		2a. REPORT SECURITY CLASSIFICATION UNCLASSIFIED
		2b. GROUP
3. REPORT TITLE DEVELOPMENT OF ANALYTICAL RELATIONSHIPS AND CRITERIA FOR BLAST AND FIRE VULNERABILITY OF FALLOUT SHELTER OCCUPANTS		
4. DESCRIPTIVE NOTES (Type of report and inclusive dates) Final		
5. AUTHOR(S) (First name, middle initial, last name) John W. Crowley, Raymond H. Hogue, Herbert J. Avise, Edward H. Smith, Walter G. Hiner		
6. REPORT DATE October 1, 1968	7a. TOTAL NO. OF PAGES 250	7b. NO. OF REFS 30
8a. CONTRACT OR GRANT NO. DAHC20-67-C-0147	9a. ORIGINATOR'S REPORT NUMBER(S)	
b. PROJECT NO.		
c. WORK UNIT NO. 1614B	9b. OTHER REPORT NO(S) (Any other numbers that may be assigned this report)	
d.		
10. DISTRIBUTION STATEMENT Each transmittal of this document outside the agencies of the U S. Government must have prior approval of THE OFFICE OF THE SECRETARY OF THE ARMY, OFFICE OF CIVIL DEFENSE, RESEARCH, The Pentagon, Washington, D. C. 20310		
11. SUPPLEMENTARY NOTES	12. SPONSORING MILITARY ACTIVITY Office of Civil Defense Pentagon Washington, D. C.	
13. ABSTRACT The objective of this study is the development of improved methods and criteria for estimating blast casualties and for handling nuclear fire effects in order to determine means for improving survivability and injury avoidance for shelter occupants. The urban fire analysis model, FIREFLY, was developed to provide an automated method for assessing the potential damage to shelter buildings from fires which occur as a result of ignition from the thermal pulse of a nuclear weapon or fire spread from nearby buildings. Two promising approaches for classification of urban environments with regard to potential fire susceptibility were developed. Upon the basis of blast vulnerability analyses of structures including interior floors, walls and partitions, a set of blast fatality functions was produced which may be used to determine the survivability of personnel in shelters in various locations within three principal types of structures. Trial applications of improved methods and criteria served as a pilot sensitivity analysis for future shelter systems vulnerability analyses.		

DD FORM 1473
1 NOV 65

REPLACES DD FORM 1473, 1 JAN 64, WHICH IS OBSOLETE FOR ARMY USE.

UNCLASSIFIED

Security Classification

UNCLASSIFIED

Security Classification

14	KEY WORDS	LINK A		LINK B		LINK C	
		ROLE	WT	ROLE	WT	ROLE	WT
	Urban fire analysis model Classification of urban environments Blast vulnerability analyses Blast fatality functions Shelter systems vulnerability analyses						

UNCLASSIFIED

Security Classification